Regulation of somatosensory cortex development downstream of glutamate

Anne Petrie

PhD

The University of Edinburgh

2008

Declaration

I declare that the composition of thesis and all experiments, analyses and generation of figures have been carried out by myself with a few exceptions.

The histochemistry performed on tissue in the figures listed below was carried out with Adam James, an honours student working in Dr. Kind's laboratory under my supervision.

Figure 1.3 a, b & c
Figure 1.4 a, b & c
Figure 1.8
Figure 1.13
Figure 1.17

The statistical analyses carried out in the figures listed below were carried out with the help of Alex Crocker-Buque, a PhD student in Dr. Kind's laboratory.

Figure 2.8
Figure 3.6
Figure 3.7
Section 5.2.3

None of the work presented in this thesis has been submitted for any other degree or professional qualification.

Anne Petrie

Acknowledgements

I would like to thank the following for their help and support in reaching this point of submitting my thesis.

My supervisors
Dr. Peter Kind and Dr. Phillip Larkman

Past and present members of Dr. Kind's laboratory
Dr. Mark Barnett, Dr. Ruth Deighton, Dr. Sally Till, Dr Mark Hillen, Dr. Alison Begg, Lasani Wijetunge, Aoife McMahon, Alex Croqer-Buque, Louise Dunn, & Adam James.

Collaborators at the Sanger Institute, Cambridge
Prof. Seth Grant, Karen Strathdee, Dr. Peter Cuthbert, Georgina Berry, Jane Robinson & Dr. Noboru Komiyama.

Technical assistants
Linda Sharp, Dr. Trudi Gillespie, Vivian Allison, Grace Grant and all technicians at BRR

All members of Development and Biology group at Edinburgh University

For funding
The Medical Research Council and Edinburgh University

And finally, Derek and my family.

Thank you all so much.

Table of Contents

List of Diagrams

List of Tables

Abstract
Development of the rodent somatosensory cortex is well characterised and involves activity-dependent mechanisms that occur during the first postnatal week. Glutamate is a key neurotransmitter responsible for signalling events that result in formation of cortical barrels - aggregates of cells in the cortex corresponding to whiskers on the face pad. The molecular mechanisms that occur downstream of glutamate signalling are not fully understood and data here contributes to the unveiling of some of these mechanisms. Transgenic mice with deletions of genes that encode members of the post-synaptic complex associated with NMDARs were used to understand the role of individual genes in the formation of barrels. SynGAP, a ras GTPase activating protein (GAP) that negatively regulates the ERK-MAPK pathway downstream of NMDARs is required for the formation of barrels and data here agrees with other findings that the ras GAP NF1 has a similar role. Examination of RICS, a RhoGAP and Dusp6 - a phosphatase that inactivates ERK reveals that neither are necessary for the formation of barrels. This finding adds to previous data postulating that barrels form in an ERK-independent manner (Watson et al., 2006, Barnett et al., 2006). MAGUKs are important scaffolding molecules in the PSD and bind NMDARs to downstream signalling molecules such as SynGAP. Two of these MAGUKs SAP102 and PSD-95 have roles in hippocampal plasticity, and learning and memory and *Sap102* mutations result in a form of X-linked human retardation (Tarpey et al., 2004). Deletion of either gene does not cause defects in the development of barrels, perhaps due to compensation mechanisms already described in hippocampus (Vickers et al., 2006 Cuthbert et al., 2007). Double knockout mice die by P3 and analysis of all other mutants revealed a defect in the formation of barrels and segregation of TCAs in *Sap102*$^{-/y}$ *Psd-95*$^{+/-}$. Surprisingly this defect was not seen in *Sap102*$^{+/-}$ *Psd-95*$^{-/-}$ mice, agreeing with previous findings that SAP102 is better able to compensate for loss of PSD-95 (is up-regulated) than PSD-95 is for SAP102. An explanation for this effect may lie with the fact that *Sap102* is X-linked and therefore females that are heterozygote for *Sap102* are mosaic with a population of cells expressing SAP102 and a population not expressing SAP102. Using β-Galactosidase antibody to label one population of cells, female mice that had two populations of cells were examined. In these mice one population of cells were *Sap102*$^{-}$*Psd-95*$^{+/-}$,

and did not previously segregate into normal barrels and the other population were *Sap102*$^{+}$*Psd-95*$^{+/-}$ and should segregate normally. Both populations of cells segregated normally, indicating that the cells expressing SAP102 were rescuing the cells not expressing SAP102 by a cell non-autonomous mechanism.

The final part of this thesis focuses on the role of glutamate-dependent signalling pathways in the regulation of CSPGs- key extracellular matrix proteoglycans that regulate the termination of the sensitive period. Analysis of 3 overlapping but distinct subsets of chondroitin-sulphate proteoglycans (CSPGs) reveals that expression of each of the three is different throughout development. After 2-3 weeks perineuronal nets (PNNs) labelled with Cat-315 and Cat-316 are visible and locate to specific regions within the cortical barrel-field. To determine whether the formation of PNNs is regulated by proteins involved in glutamate signalling, expression of the three CSPG subsets was analysed in mice with barrel defects due to mutations of *Plcβ1*, *Mglur5*, *Syngap* and *Prkar2b*. Interestingly, *Prkar2b* mutant adults but no other mutants have reduced Cat-315-PNNs, indicating that PKARIIβ regulates pathways that lead to formation of Cat-315-PNNs in adulthood. Cat-315 has previously been found to be regulated in the cortex of visually deprived cats and the cortex of whisker-trimmed mice, indicating that specific subsets of CSPGs are regulated by neuronal activity. Molecular pathways that lead to expression of Cat-315 positive PNNs involve PKARIIβ and the formation of PNNs may be an important step in the plasticity of circuits in barrels.

Taken together, these results demonstrate that an important part of molecular signalling downstream of glutamate enabling barrels to form is played by molecules that maintain structure inside the synapse and outside the cell.

1 Introduction

Establishment of the correct connectivity and physiology at each stage of development is essential for the formation of a mature mammalian brain. At early embryonic stages development occurs according to genetic instruction. Late embryonically and postnatally development is shaped by experience. Experience refines the processes that have begun in early embryonic development, but both genetic factors and experience contribute to formation of correct connectivity and physiology. Autonomous (cell-intrinsic) properties allow each cell to behave based on instruction from its own genetic code. In non-autonomous (cell-extrinsic) processes a cell relies on cues from and interactions between surrounding cells and tissues, often responding to concentration factors of secreted morphogens that attract/stimulate or repel/inhibit. Cells in the developing brain utilise both autonomous and non-autonomous mechanisms to migrate, multiply and signal effectively.

Neurons perform the major roles of communication and information processing and are responsible for transmission of action potentials, the mechanism by which signals are rapidly relayed around the nervous system. The brain also contains multifunctional non-neuronal cells such as glia, which are essential in their modulatory and supportive roles. Surrounding neurons and glia is the extra-cellular matrix (ECM), containing a range of molecules and substances necessary for neurons to perform correctly. While some neural connections (synapses) remain plastic throughout life, constantly responding to activity and sensory experience, others go through a critical or sensitive period during which circuitry and structure is correctly established. Brain disorders such as mental retardation (Chechlacz et al., 2003), autism spectrum disorders (Garber, 2007), schizophrenia and depression (numerous publications from Meador-Woodruff lab: Kristiansen et al., 2005, Gupta et al., 2005, Torrey et al., 2005, Beneyto et al., 2005, McCullumsmith et al., 2007) often correlate with results showing malfunction of synaptic activity from early in development which may be visible as altered anatomy or measured as electrophysiological abnormalities. In some cases mutations to a single gene result in both synaptic plasticity abnormalities and mental retardation disorders. Examples being mutations to FMR1 which result in loss or severe reduction of the protein FMRP, causing fragile X mental retardation (Penagarikano et al., 2007) and mutations to SAP102 which result in moderate to severe mental retardation (Tarpey et al., 2004). Therefore it is essential that the processes and mechanisms that are involved in regulating synaptic activity in the brain from early in development are understood if realistic medical advances in treating these disorders are to be made.

The form that activity takes and the role it plays changes during development. The types of activity can be separated into three main types; random spontaneous activity independent of any stimuli, patterned spontaneous activity independent of sensory experience and finally sensory driven activity, necessary for refinement and maturation of the system. The formation of sensory maps in the cortex provides a good model to study the different forms of activity and the associated plasticity mechanisms. Plasticity is defined as the ability of a synapse or group of synapses to undergo alterations in strength or connectivity in response to activity. Development of the cortex demonstrates the interplay of both genetic factors and the environment, with the rodent somatosensory system providing a good model to study genetic factors and the role of spontaneous activity, and the visual system of small mammals providing an example of the role of different types of activity. Both systems demonstrate experience-dependent plasticity at various stages of development.

1.1 Development of the cortex

1.1.1 Cortical neurogenesis and gliogenesis

In the mammalian embryo the nervous system begins in the form of the neural plate, which invaginates to form the neural tube. The most anterior region of the neural plate becomes the forebrain, consisting of the diencephalon and the telencephalon. The wall of the anterior/rostral neural tube is composed of neuroepithelial stem cells that form the ventricular zone (VZ), which eventually becomes the mature forebrain (Sidman and Rakic, 1973). Cortical neurons are generated during the final week of rodent gestation, and during the last few months in human gestation. The first mitotic divisions of neuroepithelial progenitor cells that take place in the ventricular zone result in a population of cells to maintain the progenitor population and radial glial cells (RGCs). RGSs undergo further proliferation, and serve as migratory guides for subsequent neurons (Parnavelas and Nadarajah, 2001). Glia, the non-neuronal cells of the brain are generated late during embryonic corticogenesis and perinatally (Privat, 1975). They originate largely from the sub ventricular zone (SVZ), which appears later in development and lies beneath the ventricular zone. The VZ and SVZ generate the majority of cortical neurons and glia, and are together described as the germinal zone (GZ).

1.1.2 Cortical Differentiation & Lamination

Neurons, astrocytes and oligodendrocytes of the adult nervous system primarily originate in the ventricular zone of the embryonic neural tube, specifically the telencephalon, and migrate to their destination (Angevine and Sidman, 1961).
Some progenitors in the cortical ventricular zone of the embryonic telencephalon are multipotent stem cells that give rise to both cortical projection (pyramidal) neurons and astrocytes (Davis and Temple, 1994, Williams and Price, 1995, Temple, 2001). These stem cells undergo symmetric divisions to begin with, followed by generation of progenitors that are largely astrocyte- or neuronal-restricted (Luskin et al., 1988, Price et al., 1995, Reid et al., 1995, Williams and Price, 1995, Nieto et al., 2001, Temple, 2001). Due to the order in which precursors are generated, cortical neurons are born and differentiate before cortical astrocytes (Bayer et al., 1991, Qian et al., 2000). Progenitors outside the cortex in the ventral telencephalon give rise to cortical interneurons, which migrate tangentially from the ganglionic eminence to reach their positions in the developing cortex (Marin and Rubenstein, 2001, Gorski et al., 2002). Recent evidence suggests that some GABAergic interneurons are also generated in the cortex (Letinic et al., 2002).
Cortical oligodendrocytes are thought to be produced from stem cells in the ventral telencephalon, which also generates interneurons (He et al., 2001, Ross et al., 2003). Oligodendrocyte precursors then migrate tangentially into the cortex in a similar way to interneurons (Thomas et al., 2000, Tekki-Kessaris et al., 2001). There is evidence in the mouse to suggest that some oligodendrocytes (those becoming glia) originate from cortical progenitors in the subventricular zone (Gorski et al., 2002), perhaps

produced in a ‘second wave’ that are born postnatally (Marshall et al., 2003, Ivanova et al., 2003).

Post mitotic neurons migrate laterally and accumulate under the pial surface of the dorsal telencephalon, forming the layers of the cerebral cortex. The first cortical cells prior to lamination are called either the ‘preplate’ (Stewart and Pearlman, 1987), ‘early marginal zone’ (Rickman et al., 1977, Raedler and Raedler, 1978) or ‘primordial plexiform layer (PPL)’ (Marin-Padilla, 1971, Meyer et al., 1998), before emergence of the cortical plate. The developing cortical plate is divided into the deep subplate (SP) and the superficial marginal zone (MZ), which becomes layer 1 (Marin-Padilla, 1971, Luskin and Shatz, 1985). The cortical plate forms in an ordered sequence with younger neurons migrating past their older counterparts forming the cortical layers 5-2 with deeper layers forming first (Angevine and Sidman, 1961, Berry and Rogers, 1965). In mammals the cortex undergoes laminar expansion into six layers and tangential expansion (Abdel-Mannan et al., 2007). A greater tangential expansion and the formation of gyri are associated with higher mammals.

During embryonic corticogenesis genes play a key role in arrangement by regulating morphogenesis and axonal growth and guidance. For example, transcription factors and growth factors play a major part in early stages of development by their selective expression in specific cell types, in specific regions and at specific stages. Two experimental approaches to studying the role of genes are 1.) by the use of mutant mice that have defects in morphogenesis or axon growth/pathfinding or 2.) by the use of chimeras, where the embryo consists of a mixture of wildtype and mutant cells (Pratt and Price, 2006, article in Erzurumlu et al., 2006). Chimeras have advantages because alterations in brain shape that might complicate the analysis can be minimised by the presence of wildtype cells. Price and colleagues have used both these approaches to understand the role of various transcription factors in the developing cortex. Expression of each transcription factor is specifically organised in regions forming gradients that are key for correct migration, proliferation and innervation (see diagram 1). These gradients are disrupted in the PAX6 mutant mouse - cortical markers are down-regulated and patterning at the LGE/MGE boundaries is found more dorsally (Manuel and Price, 2005).

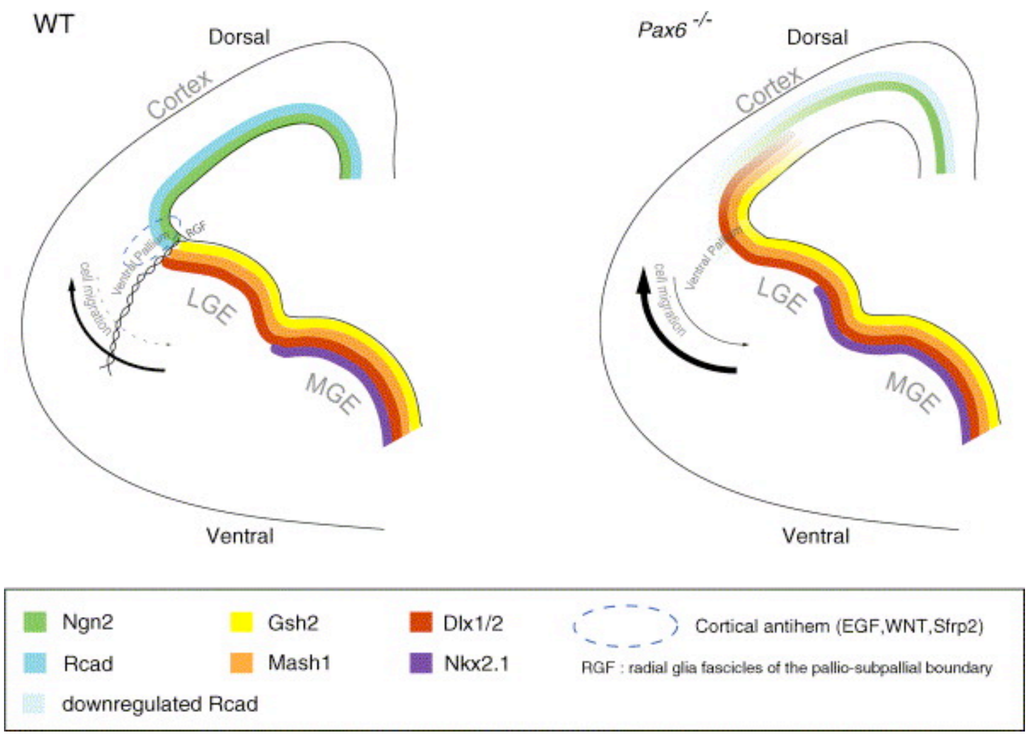

Diagram 1 Schematic representation of left telencephalic vesicle at E14.5

Taken from Manuel and Price, 2005

Expression of region specific markers in Wildtype and Pax6-/- are indicated with colours. Intensity of colour indicates gradient of marker. Arrows indicate cell migration patterns.

1.1.3 Cortical specification

In order for sensory processing to occur the cortex is organised into sense-specific regions or cortical maps. These regions are characteristically both structurally and functionally specialised with innervation from particular thalamic nuclei (Jones et al., 1997, Jones and Hendry, 1980, Duffy et al., 1998). It is proposed that thalamocortical projections play an important role in the differentiation of cortical fields (O'Leary, 1989, Krubitzer, 1995). Co-culture experiments carried out by Molnar and Blakemore with explants from different regions of the rat thalamus and cortex showed that regional specificity of the cortex was lost despite some thalamo-cortical and cortico-thalamic connections appearing to form normally. They concluded that thalamo-cortical and cortico-thalamic outgrowth of axons is synchronised, with each pioneering its pathway through its own brain segment as an organised array of axons, not relying on any chemotropic factors from the target region. The two groups of axons meet each other near the primitive internal capsule, and provide contact guidance for the other over the remainder of the trajectory. It is thought that regionalisation of the cortex requires selective afferent innervation and that this must then depend on the extracellular environment between thalamus and cortex (Molnar and Blakemore, 1991). Fibroblast growth factor 8 (FGF8) is secreted into the extracellular environment and regulates cortical innervation. Mis-expression of FGF8 results in rearrangement of the area map of the cortex. Changes in FGF8/17 signalling can shift the somatosensory map in the anterior/posterior direction and thalamic axons responding to an additional ectopic source of FGF8 innervated duplicate somatosensory fields, indicating that thalamic axons respond to positional information within the cortex (Fukuchi-Shimogori and Grove, 2001, 2003, Shimogori and Grove, 2005). Similarly, over-expression of the transcription factor *Emx2* in the neuroepithelium causes the somatosensory map to shift anteriorly in the cortex (Hamasaki et al., 2004). Expression of markers in an E14.5 *Pax6-/-* brain indicate that the area of cortex is reduced (see diagram 1) – in knockouts the area of caudo-medial areas is enlarged while rostro-lateral areas are reduced (Bishop et al., 2000, Bishop et al., 2002, Muzio et al., 2002). Over-expressing Pax6 results in a decreased thickness of layers 2-4 in rostral and central cortex, but arealization is not affected; innervation of both somatosensory and visual cortex from thalamus at E17.5 is normal (Manuel et al., 2007). Reducing the size of the immature neocortex of *monodelphis domestica* (opossums) by up to three quarters before thalamocortical connections are established results in normal spatial relationships between visual, somatosensory and auditory cortical fields on the remaining cortical sheet (Huffman et al., 1999). This shows that the neuroepithelium can accommodate different cortical fields early in development while maintaining order in the antero-posterior and medio-lateral distribution of regions. Ephrins may help in the positional location of the sensory representation. Ephrin A5 is expressed in a medial to lateral gradient across S1 while the receptor EphA4 is in a similar pattern in ventrobasal (VB) region of thalamus providing the input. Disrupting *Ephrin-A5* gene causes a topographical distortion to the S1 map with a change of up to 50% of relative areas. Medial regions become contracted and lateral regions expanded (Vanderhaeghen et al., 2000). As well as ephrins, netrins and Slits aid the pathfinding of RGC axons to the target. The molecular mechanisms of guidance are not yet fully understood and future progress may lie in understanding the precise regulation of receptor expression in growth cones (Erskine & Herrera, 2007). Neuronal migration is key to the formation of neuronal circuits and eventually behaviour. If migration is disrupted or slowed during embryonic development, subtle or gross abnormalities can have major effects later in development (Rakic et al., 2007). Axon outgrowth, axon pathfinding and selection of appropriate targets are processes that occur independently of action potentials and synaptic transmission (Goodman and Shatz, 1993). The processes establish relatively accurate (albeit crude) connectivity based on detection of molecular cues such as cell surface markers, extracellular matrix or diffusion of growth factors by growth cones. This is the pre-critical period (Hooks and Chen, 2007), formation of the cortex to this stage is dependent on genetic instruction and neural activity has little if any influence. Evidence for this comes from mice that have the synaptic vesicle protein SNAP25 deleted. While these mice do not survive beyond birth, at E18.5 axonal growth appears normal, as does cortical lamination and early indications of topographical maps, despite no action-potential mediated neurotransmitter being released (Molnar et al., 2002 & 2003). However, constitutive spontaneous release of neurotransmitter can still occur in the absence of synaptic vesicle exocytosis (Washbourne et al., 2002).

1.2 Activity-dependent development

After lamination, specification and innervation of the cortex have occurred, neural connections are often not accurate and need refining by neural activity. The role of genes and the influence of neural activity in establishing the correct connectivity and anatomy can be well studied in two sensory systems, the visual system and the somatosensory system (see diagram 2). In this section the normal development of the mammalian visual system and the rodent somatosensory system will be described, then the forms that activity takes will be explained using examples from the two systems.

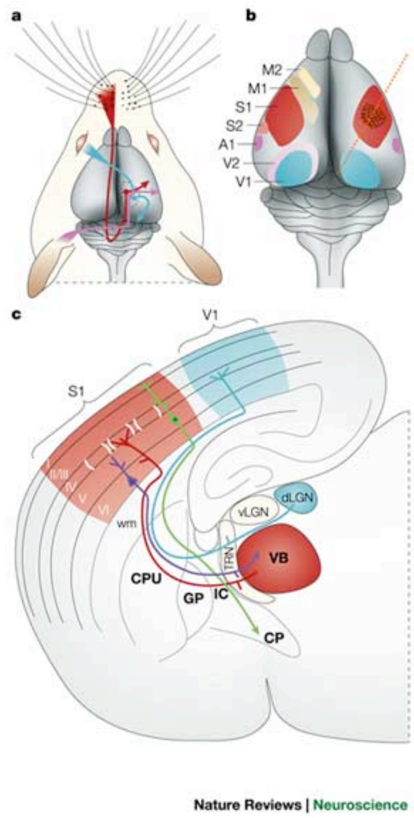

Diagram 2 **Schematic to show thalamocortical innervation of V1 and S1 cortex**

Visual input from the retina (blue line) is relayed via dLGN to primary visual cortex (V1)
Somatosensory information from the whiskers (red line) reach ventrobasal complex (VB) through brainstem and reaches primary somatosensory cortex (S1).
Taken from Lopez-Bendito and Molnar, 2003.

1.2.1 Visual System

The visual system is the most studied sensory system for examining the role of activity in cortical development and plasticity. In Nobel prize – winning experiments in the 1960s Hubel and Wiesel showed that a cat's early visual experience can modify physiological and anatomical development of the visual system (Wiesel and Hubel, 1963a & 1963b). Since then the visual system has remained as one of the most easy-to manipulate sensory systems, due to the fact that visual experience can be instantly restored after deprivation. In comparison, in the somatosensory system it takes time for whiskers to re-grow after trimming. There are three main connections in the visual system that undergo activity-dependent modifications; the retinocollicular, the retinogeniculate and the geniculocortical system.

1.2.1.1 Retinocollicular System

The retinocollicular system in mammals (retinotectal in non-mammal vertebrates) is the projections from retinal ganglion cells to the superior colliculus (SC). Retinal axons navigate along the appropriate pathway with the help of guidance cues. Chondroitin and heparan sulphate proteoglycans are involved in steering along the route (Ichijo, 2004). In the SC axons from RGCs innervate forming a topographical map of visual space (McLaughlin and O'Leary, 2005). The initial projections are coarsely arranged and become refined to target precise topographical regions. In mice the refinement occurs in the first postnatal week prior to eye opening.

1.2.1.2 Retinogeniculate System

Retinal ganglion cells also project afferents to the lateral geniculate nucleus (LGN) of the dorsal thalamus during embryonic and early postnatal development. In mouse at P3 the retinal afferents from each eye largely overlap in the LGN and converge onto single neurons. Even after eye-specific zones are formed in mouse, one LGN neuron can be innervated by up to 20 RGCs (Chen and Regehr, 2000). Analysis at P9 in mouse found that convergence onto a single LGN neuron is dramatically reduced in this period spanning eye-opening (Torberg and Feller, 2005, reviewed in Shatz, 1996). Investigations to determine the mechanism by which remaining synapses are strengthened found that at the end of the first three postnatal weeks there are 1-3 RGCs innervating each LGN neuron. These remaining synapses are strengthened by up to 50% by increases in quantal size and number of neurotransmitter release sites within the synapse (Chen and Regehr, 2000). During this period the extensive axon remodelling resulting in inputs from the two eyes segregating into eye-specific territories (Reese, 1988, Sefton et al., 1991). The axon terminals then branch abundantly within the distinctive terminal field of the LGN. Anterograde labelling of RGCs shows that in rodents the LGN has regions that contain cells specifically responsive to one eye. In carnivores and primates, the LGN has cytoarchitectural boundaries separating the projections into eye-specific laminae.

1.2.1.3 Geniculocortical System

The cat primary visual cortex is organised into ocular dominance (OD) bands or columns where one band responds preferentially to visual activity from one eye.

Cells in the neighbouring band respond to the other eye. OD columns in the cat form during the first few months of life. Initial studies reported that geniculocortical afferents from the two eyes initially overlap and innervate wide areas within area 17 of the cortex. Through processes of activity dependent competition for synaptic space, the inputs segregate into OD columns (Le Vay et al., 1978, Stryker and Harris, 1986, Antonini and Stryker, 1993). However, these studies used tracing agents that may have leaked into the extracellular environment. More recent studies from Katz and colleagues indicate that retinogeniculate axons may segregate as they innervate prior to eye opening (Katz and Crowley, 2002).

1.2.2 Somatosensory System

All mammals except humans have tactile hairs on the face known as whiskers or vibrissae that are used to sense the environment (Munger and Ide, 1988). Development of the rodent somatosensory system has been well characterised and is influenced by neuronal activity. Somatosensory system development can be disrupted by both genetic manipulation and interventions of experience. Therefore it provides a useful model in which the role of activity can be studied in development and plasticity, and the contribution made by specific molecules that are responsible for transducing the neuronal activity can be identified. The trigeminal neuraxis consists of several neural relay stations between whiskers and cortex (see diagram 3). The pattern of whiskers on the face is topographically represented at each station where cells form modules with a single module corresponding to a single whisker (Ma, 1993, Killackey, 1973, Van der Loos, 1976, Woolsey and Van der Loos, 1970). Initial studies discovered that when follicles of row C were ablated, in the cortex surrounding modules (‘barrels’) in rows B and D expanded leaving a thin stripe of innervating axons and a ‘megabarrel’ of cortical cells corresponding to row C (Van der Loos and Woolsey, 1973).

1.2.2.1 Facepad, Brainstem and Thalamus

Whiskers and sinus hairs are embedded in the mouse facepad in an ordered pattern of rows, and are innervated by bundles of axons from trigeminal ganglion cells (TGCs) that form branches of the infra-orbital nerve (ION). TGCs project to the brainstem where they form synapses in four ipsilateral nuclei (Hayashi et al., 1980) (principal

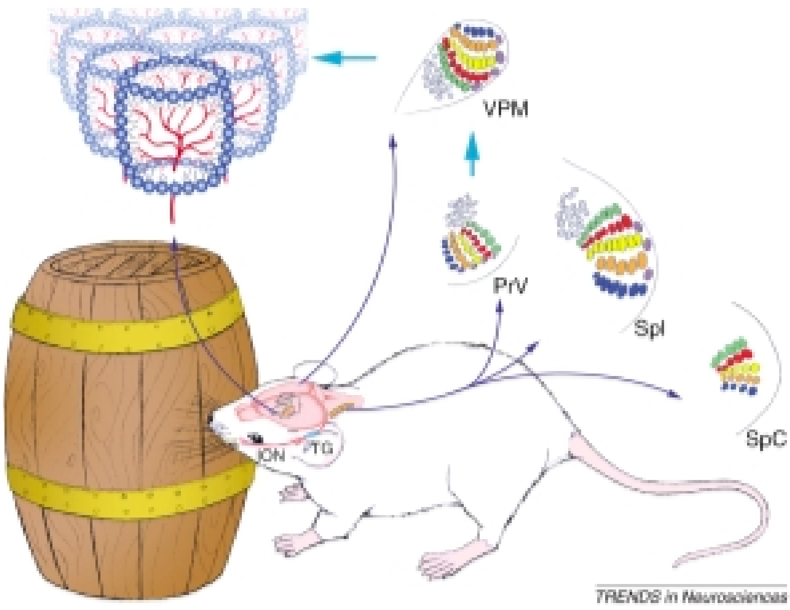

Diagram 3 **The whisker-barrel pathway of mice**

Taken from Erzurumlu and Kind, 2001

At each level there is a topographical representation of the whiskers in the form of axonal bundles and cellular aggregates.

nuclei or (nVp), sub-nuclei interpolaris (nVi), sub-nuclei caudalis (nVc) and sub-nuclei oralis (nVo)). Three of the four trigeminal nuclei (nVp, nVi & nVc) recapitulate the pattern of whiskers on the facepad in a display of cytoarchitectural arrangements known as barrelettes (Bates and Killackey, 1985, Ma and Woolsey, 1984) The axons innervating barrelettes are first visible at P0 in mice by cytochrome oxidase (CO) histochemistry and the cellular aggregates in the nVp, nVi and nVc nuclei visible by Nissl stain at P4 (Ma, 1993). Cells primarily from nVp but also nVi, nVc and nVo project axons up to the contralateral ventro-posterior medial (VpM) thalamus, where they form synapses on dendrites of thalamic nuclei. Both axons from brainstem and cells of the VpM replicate the whisker facepad pattern of ordered rows. Patterns in nVp but not other nVs are required for the recapitulation of the pattern in VpM. In VpM the whisker representations are called barreloids (Van der Loos, 1976). Brainstem axons in VpM are visible by CO histochemistry in mice at P3 (Yamakado, 1985) but can be best seen at P5.

1.2.2.2 Thalamocortical Axons and Cortex

Thalamic nuclei of the VpM project their thalamo-cortical afferents (TCAs) to cortex. At P0 in mice axons invade layer 6 and 5 with very little branching. By P2 branches in a lower tier are seen at the border of layer 6 and 5. By P4 an upper tier of branches are visible in layer 4 and consist of periodic clusters of dense terminal arborisations. It appears that there are clusters of radially extending axons through lower layers indicating that tangential organisation is reached upon reaching layer 6 (Agmon et al., 1993). The largest density of arborisations are found in layer 4, where initially axons are evenly distributed tangentially with each axon extending over twice the diameter of a patch, then during the first three postnatal days axons segregate into whisker-related patches (Senft and Woolsey, 1991, Agmon et al., 1995, Rebsam et al., 2002). The ordering of TCAs is modulated by serotonin signalling within TCAs (Gaspar et al., 2003) and involves the retraction of inappropriate arbours and the elaboration of appropriate arbours (Rebsam et al., 2002). The role of serotonin will be discussed further in section 1.5.1.1. In a normal mouse, cells within layer 4 redistribute to form a dense ring called a barrel (Woolsey and Van der Loos, 1970) surrounding each TCA bundle that represents a single whisker (Miller et al., 2001). By P7, TCA arbours are exclusively located to a single barrel. There is some confusion over the extent to which TCAs initially branch. Studies using liphophilic tracers of TCAs in rat revealed that TCA arbours do not exceed the width of a cluster. By P7 axons within a cluster (barrel) overlap but remain spatially restricted to a single barrel (Catalano et al., 1996). Placement of two different coloured fluorescent dyes in neighbouring mouse barrels at P0 revealed only a negligible number of double-labelled thalamic nuclei indicating that TCAs do not overlap. However, quantitative analysis of the terminal arbours revealed that at P0 TCAs were within 1.3 presumptive barrel diameters from their target (Agmon et al., 1995). Similarly, there is confusion over the segregation of retinal afferents into eye-specific territories in the LGN of the visual system. Recent evidence suggests that axons are correctly targeted initially and refinement takes place later (Katz and Crowley, 2002). It is possible that in somatosensory cortex there may be differences in the extent of branches of TCAs innervating barrels within same row compared to barrels between separate rows. Therefore the angle at which the slice is cut is key to understanding the direction of initial elaboration.

At the same stage that layer 4 cells relocate to form barrels, dendrites of layer 4 cells re-orientate towards the sparsely populated barrel hollow where TCAs form synapses (Woolsey and Van der Loos, 1970, Woolsey et al., 1975, Killackey, 1973). Whisker trimming does not effect the segregation of cells into a whisker-related pattern, but it does alter the magnitude of single neuron responses in the barrel corresponding to the trimmed whisker (Armstrong-James et al., 1992, Fox, 1992). In mice cells in layer 4 start to form barrels at P4 as soon as TCAs initiate a pattern. Cell-sparse regions between barrels are called septae and are first visible at P6 (Rice and Van der Loos, 1977). Cell-dense walls and cell-sparse walls can first be seen at P6. However, cells continue to segregate into dense walls after P6, and barrels are best segregated at P10 or later (Kind et al., unpublished observations).

1.2.2.3 Cellular mechanisms of barrel formation

Barrels do not form in layer 4 of cortex unless TCAs are innervating and segregating into whisker-related patches. The exact cellular mechanism by which TCAs instruct the formation of barrels is not known but a number of suggestions have been proposed (Barnett et al., 2006 - Article in Erzurumlu et al., 2006).

- 1.) Selective cell death

  The elaboration of TCAs in a patch may trigger cell death in the barrel hollow but not the barrel wall, resulting in a higher cell density in the wall with respect to the hollow. To date, there is no evidence to support this theory. Analyses of cell death in S1 cortex find the majority of cell death occurs uniformly across S1(Miller, 1995) and after barrels form in the second or third postnatal week (Heumann and Leuba, 1983, Heumann et al., 1978, Al-Ghoul and Miller, 1989). Similarly in the brainstem there is evidence to suggest that while there is extensive cell death, it does not account for absence of patterning in mutants of the transcription factor DRG11 (Jacquin et al., 2008).
- 2.) Passive displacement

  Due to the extensive elaboration of dendrites and axons within the barrel hollow it is possible that the increased density of neuropil results in the displacement of hollow cells into the wall. However, in *Plcβ-1* mutant mice where cells do not relocate to form dense walls, TCA patches are normal and cells that occupy the wall region still orientate dendrites towards the hollow (Hannan et al., 2001). This mutation provides evidence suggesting that dendritic orientation of layer 4 cells does not cause cellular segregation and it shows that the mechanisms of cell segregation into barrels and reorientation of dendrites require different molecules. However it does not rule out that passive displacement is occurring. TCAs are extensively branching at this time, leading to an elaboration of neuropil.

- 3.) Active migration away from TCAs
  It is difficult to imagine how evidence could prove that passive displacement was not actually active migration of an unknown mechanism. Cortical neurons certainly have the ability to migrate in response to neurotransmitter or growth factors.
- 4) Selective adhesion and expansion
  Adhesion molecules are expressed in cortex during postnatal development. If innervating TCAs cause a localised decreased in adhesion molecules, between P3 and P7 natural brain growth and associated increase in cortical size could result in barrel walls remaining dense while barrel hollows become enlarged. An approach to testing this theory could involve adding enzyme that degrades adhesion molecules to the developing cortex. So far, no barrel defects have been found in mice that have mutations to adhesion molecules.

1.3 Activity-dependent Plasticity

Experimentally there are numerous advantages of using the somatosensory system in mice to examine the role of activity in development. Mice can be genetically altered to dissect the function of each molecule. It is still unclear what form of activity and to what extent activity is necessary for the formation of somatotopic maps. In an attempt to bring clarity to the role of activity in organisation of maps, different types of activity need to be defined and explained using the previously described visual and somatosensory systems as examples.

In each system activity may play a different role (instructive/selective/permissive), and these descriptions are often used to explain it. Activity is described as '*instructive*' if it is necessary to establish or modify a neuronal structure or function, and the nature of the activity directly regulates the structure or function (Sengpiel and Kind, 2002). The alternative interpretation would be activity plays a *'selective'* role, in that in an early situation where equal numbers of cells are responsive to each orientation, a certain threshold of activity causes cells designated to the experienced orientation to survive at the expense of cells not receiving the required threshold of activity corresponding to other orientations. If activity is *'permissive'* then there is a threshold of activity required beyond which no changes in responses or plasticity are detectable.

1.3.1 Manipulation of experience in visual system

1.3.1.1 Random Spontaneous activity

Neurons fire action potentials embryonically, and the first action potentials are spontaneous, without any correlation or pattern. Also, synapses spontaneously release neurotransmitter independently of action potentials. All cells are thought to undergo random spontaneous activity, before synapses become functional. This type of activity is best visualised by the addition of voltage-sensitive dyes along with optical imaging.

Example from somatosensory system:

The drug tetrodotoxin (TTX) blocks sodium channels responsible for transmission of action potentials along the membrane, and so is often used to block all forms of action-potential-driven neural activity, including spontaneous activity which cannot be blocked by receptor-specific drugs. TTX applied to primary somatosensory cortex (S1) at P0 does not block segregation of TCAs into patches (Chiaia et al., 1992) neither do N-methyl-D-aspartate Receptor (NMDAR) inhibitors APV and MK801 (Henderson et al., 1992, Schlaggar et al., 1993) indicating TCAs and therefore barrels form independently of any type of action potential driven neural activity, even spontaneous activity. However, glutamate can be spontaneously released independently of action potentials. TCAs reach the subplate embryonically and may have already received the signal necessary to segregate into patches (TTX and APV also prevent the rearrangement in cortical representation of row C that is seen when row C whiskers are ablated (Schlaggar et al., 1993). This result indicates that while spontaneous activity after P0 is not *necessary* for TCAs to segregate into barrel-specific patches, activity after P0 can be *instructive* in determining which axons may be at a disadvantage or an advantage in innervating the greatest cortical area. This also suggests that activity between axons permits *competition* for an innervating target to take place.

1.3.1.2 Patterned Spontaneous activity

Patterned spontaneous activity occurs in many developing circuits, spinal cord, hippocampus, auditory nuclei and retina (O'Donovan, 1999, Wong, 1999). It is defined as the rhythmic bursting of action potentials that are temporarily synchronised between neighbouring cells. These events may drive competition, enabling maintenance of synaptic contacts while contacts undergoing asynchronous firing are weakened.

Investigations in lower vertebrates such as frogs and fish suggested that topographical projections in optic tectum form as a combination of 1) highly correlated patterns in RGCs and 2) activity-independent mechanisms. Activity independent mechanisms may be for example, a gradient of cell surface molecule on axons of RGCs and surrounding tectal neurons. The concentration of surface molecules (such as extra-cellular matrix molecules) are detected and allow crude alignment of axons, which is later refined by patterned activity to give a precise representation of the visual environment (Cline et al., 1991).

Example from visual system:

A well studied example of synchronised activity in seen in the form of retinal waves in the visual system. Retinal waves are bursts of correlated action potentials that spread across the retina in mice during the first postnatal week (Bansal et al., 2000) prior to eye opening at P13, making studying retinogeniculate map development in mice ideal. The waves occur independently in the two eyes, so are clearly not responding to light that may be detected through the closed lid. The correlated waves are initiated by synchronised calcium bursting of cholinergic starburst amacrine cells in retina (Feller et al., 1996, Zhou, 1998) and can be detected by calcium imaging or electrophysiology. Physiology shows that waves are transmitted from retinal ganglion cells in the retina across synapses to drive target LGN neurons (Shatz, 1996). Waves are seen prior to appearance of photoreceptors in the retina, and then they disappear. The detection of waves indicates that there are neural circuits forming between cells in the retina, and their synchronised firing coincides with formation of eye-specific retinotopic maps in the dorso-lateral geniculate nucleus (dLGN) (Penn et al., 1998, Wong, 1999). The formation of eye-specific bands is disrupted by TTX application to the retina (Shatz, 1996, Wong, 1999, Katz and Crowley, 2002, Shatz and Stryker, 1988), leading to suggestions that retinal waves drive the segregation (Galli and Maffei, 1988, Meister et al., 1991, Penn et al., 1998). Applying TTX to one eye during the period of retinal waves results in a reduced territory representing that eye in the dLGN (Penn et al., 1998). When retinal axons reach their target, the synapses undergo a period of refinement with some synapses being strengthened and some eliminated (Chen and Regehr, 2000, Jaubert-Miazza et al., 2005). This period of refinement is claimed to be driven by spontaneous activity, not vision (Hooks and Chen, 2006), as dark rearing does not affect synapse maturation in dLGN. However it is not yet proven that it is specifically waves that are responsible for the refinement of maps. Artificially altering the degree of synchronous firing without abolishing activity altogether is an obvious approach (Weliky and Katz, 1997), either by stimulating the optic nerves, by introducing a drug to the eye or by manipulating genes responsible for wave transmission. Advances are being made in finding the neurotransmitters responsible in order that an appropriate drug can be selected. Mice lacking the β2 subunit of nicotinic acetyl choline (ACh) receptors have an absence of correlated retinal waves in the first postnatal week. This delay disrupts retinotopic map formation in SC and SC synapses are immature (Shah and Crair, 2008). There are also defects in this mouse in retinogeniculate projections (Grubb et al., 2003) and defects in visual cortex while retina remains normal (Rossi et al., 2001). Similar results are found when the enzyme producing ACh is deleted (ChAT) selectively in retinal regions of mice, or when acetyl choline antagonists are applied to wild type retinas. Again, there is a delay in onset of correlated retinal waves until P5 (Stacy et al., 2005, Cang et al., 2005). Prior to synapse formation, retinal waves are propagated by gap junctions (Wong et al., 1998). Cholinergic synapses are believed to be responsible for retinal waves in the first postnatal week and glutamatergic synapses drive waves in the second week (Wong et al., 2000). As well as cholinergic, adenosine and GABAergic transmission (Stellwagen, 1999 neuron) have all been investigated and adenosine acting via the cAMP-PKA pathway forms a major role in controlling the width, speed and frequency of retinal waves. Increasing or reducing correlated firing among neighbouring retinal cells provides a future target for interfering with retinal waves, but since cAMP may play other roles in the developing eye as well as regulating retinal waves it may be difficult to interpret if any abnormalities in dLGN segregation are seen.

All these findings indicate that retinal waves play an *instructive* role in the formation of eye-specific bands in the dLGN. That is, waves must be present in order for bands to form in dLGN. However, a review of recent findings casts doubt on the 'instructional' properties of waves (Chalupa, 2007). Chalupa concedes that retinal activity *is involved* in formation of eye-specific projections, but highlights differences between correlated retinal waves and retinal activity. Most of the experimental approaches to abolishing or disrupting waves also affect the overall discharge of RGCs, making attributing outcomes to retinal waves inaccurate. In ferrets eye-specific bands still develop despite treatment with an immunotoxin targeting amacrine cells that decorrelates bursting without affecting discharge rates. While this result shows that correlated waves are not necessary for formation of dLGN bands, retinal activity in some form is necessary (Huberman et al., 2003). Similar findings were reported using Elvax embedded with TTX placed in either one or both neonatal ferret eyes (Prusky and Ramoa, 1999). This treatment has the advantage over intraocular injections of TTX every second day in that it slowly releases TTX for up to 25 days. TTX injections also have a detrimental effect on maturation of circuits within the LGN. Elvax TTX treatment removed retinal activity altogether but to a certain extent eye-specific bands still formed, indicating that spontaneous retinal activity *modulates* the time course of binocular segregation, but doesn't block it altogether (Cook et al., 1999). Together, these results show that there is still controversy on whether the LGN segregates independently of retinal waves.

1.3.1.3 Sensory driven activity

Sensory driven activity is neural activity that is driven by sensory stimulation. For example, after eye opening retinal ganglion cells fire in response to light and can detect orientation and in some species, colour.

Sensory experience forms and modifies neuronal circuits in the brain during early postnatal 'critical periods' (reviewed in Hensch, 2005). The terms sensitive and critical periods are used in the same way in many publications. A definition of a critical period is the 'Onset of robust plasticity in response to experience when initially formed circuits can be modified by experience' (Hooks and Chen, 2007). Closure of the critical period is the period at which the same visual experience no longer elicits the same degree of plasticity. There are multiple critical and sensitive periods in many brain systems, with specific beginnings, latencies and terminations depending on which system is being studied (reviewed in Sengpiel and Kind, 2002). For example, in visual system there are critical periods for plasticity in OD, orientation selectivity and direction selectivity. Each period is activated by different mechanisms and occurs at different times (for review, see Hensch, 2004).

Example from visual system:

The visual system provides many opportunities for studying the role of sensory driven experience due to ease in which vision can be disrupted and manipulated. Visual deprivation in one eye (monocular deprivation; MD) in kittens shortly after eye opening at P10 for the first few months of life (when the connectivity is extremely plastic) results in a majority of cortical cells that are physiologically responsive to input from the non-deprived eye and fewer cells responding to the deprived eye (Hubel and Wiesel, 1963, Shatz and Stryker, 1978, LeVay et al., 1980). These findings first resulted in the introduction of the term 'critical period' (defined in previous paragraph). In this case the 'critical period of OD plasticity' is most robust during early postnatal development and diminishes with maturity (Hubel and Wiesel, 1970). Restoring visual activity before 8 weeks deprivation to the deprived eye results in restoration of the balance in the cortex, but after 8 weeks plasticity is reduced (Hubel and Wiesel, 1970, Wiesel and Hubel, 1963). Prolonged MD leads to shifts in OD in mice (Sawtell et al., 2003), and a similar plasticity has been recently detected in adults, except the threshold is higher in adults (duration of MD needs to be greater for OD to occur). Blocking vision by dark rearing is best known for its influence on OD as described above, but dark rearing also delays physiological *functional* maturation of the visual cortex (Cynader et al., 1976, Fagiolini et al., 1994, Mower, 1991) and anatomical maturation of intra-cortical circuitry (Fox and Wong, 2005). Many investigations into functional plasticity record from single neurons in the cortex, or measure visually evoked potentials (VEPS), with more recent techniques of imaging.

In certain regions of the mature mouse visual cortex, cells are responsive to a single eye but do not group together to form columns in the same way as in the cat visual cortex. Part of the mouse visual cortex is ‘binocular’, in this region cells respond to both eyes and innervation of this region can be modulated by visual experience. The mouse visual cortex does undergo OD shifts that are dependent upon differences in experience between two eyes (Gordon and Stryker, 1996). Other mammals also undergo OD shifts in response to MD; sheep (Kennedy et al., 1980), rabbits (Van Sluyters and Stewart, 1974), rats (Maffei et al., 1992, Fagiolini et al., 1994) hamsters (Emerson et al., 1982) and mice (Drager, 1978).

Visual experience drives neurons in the visual cortex to be responsive to shapes of particular orientations, cortical cells are said to have ‘orientation selectivity’. Kittens were raised in an environment where black and white stripes in a particular orientation occupy the surrounding walls (Blakemore and Cooper, 1970). Optical imaging of the visual cortex revealed that there is a bias in the area that responds to stripes of the experienced orientation compared to other orientations (Sengpiel et al., 1999). Sengpiel concluded that activity plays an *instructive* role in determining the orientation preference of a particular cell (Sengpiel et al., 1999, Sengpiel and Kind, 2002).

Recent research has revealed sub-cortical development roles for visual experience. In retina vision plays a role in development of circuits by instructing specificity of connectivity. RGCs dendrites undergo a refinement into ON and OFF regions of the inner plexiform layer of the retina, and this refinement can be blocked by dark rearing (Tian and Copenhagen, 2003). While dark rearing does not affect segregation of axons into eye-specific bands in dLGN, visual experience is necessary for circuit development and maintenance (Hooks and Chen, 2006) and to trigger experience-dependent plasticity in thalamus (Hooks and Chen, 2008). In SC visual experience influences maintenance but not development of circuitry (Carrasco et al., 2005).

Example from somatosensory system:

In the somatosensory system sensory driven activity can be blocked by follicle ablation. The first investigations into plasticity in the rodent somatosensory system involved follicle ablation of row C, and resulted in a narrow band of TCAs corresponding to row C surrounded by two enlarged rows of patches in rows B and D in layer 4 of cortex. Cortical cells in row C form a megabarrel (a row of fused barrels) (Van der Loos and Woolsey, 1973) with dendrites of cortical cells orienting towards the centre of the long axis of the megabarrel (Steffen and Van der Loos, 1980). For plasticity to occur, ablation must occur before P5, indicating that sensory activity that is uncorrelated between neighbouring whiskers is necessary for formation of individual barrels. It is important to note that experiments in rats found that lesioning of the ION causes 24% more cell loss in the contralateral VB than the 27% normal cell death occurring between E19 to P8 (Waite et al., 1992). Interestingly this loss can be rescued by application of nerve growth factor (NGF) or brain derived growth factor (BDNF) to the ION stump (Baldi et al., 2000). Therefore the alterations in cortex, especially the reduction in size of the area taken up by the megabarrel may be due to cell death and/or absence of activity in ablated follicles. Whisker trimming in a row does not alter barrel structure but changes the balance of activity measured in individual cortical cells (Simons and Land, 1987), enabling the study of experience dependent physiological plasticity, an approach used by K Fox and colleagues (Fox, 1992, Fox, 1994). Advantages of this approach are that whiskers can be allowed to re-grow, and functional studies performed as they re-grow.

1.4 Cellular mechanisms of experience dependent plasticity

During periods of plasticity, specifically in systems that undergo a critical period, there are a number of cellular mechanisms that are occurring. These mechanisms may change the intercellular or extracellular environment so that plasticity is able to occur or they may be mechanisms by which activity is translated into anatomical or physiological alterations. Understanding these mechanisms is key to identifying the molecules that are involved in activity-dependent development and plasticity. In this section a number of mechanisms will be described and their role explained in plasticity and development of the visual and somatosensory systems.

1.4.1 Long-term potentiation (LTP) and Long-term depression (LTD)

The mechanisms of LTP and LTD have been implicated in anatomical and physiological development. They have been implicated in the formation of OD bands, as well as being a model for learning and memory. The Hebbian mechanism of synaptic plasticity is when synapses become stronger due to a repeated persistent stimulation of the postsynaptic cell (Hebb, 1949). This can be demonstrated by artificially inducing LTP using an electrode to give high frequency pulses of stimulation, in order to initiate a long-lasting increase in strength of output. Inducing LTD involves giving 15 minutes of low frequency stimulation, in order to reduce the strength of response. These methods can be applied to single cells or groups of fibres and are frequently used to measure plasticity in hippocampus and other brain circuits. These mechanisms dictate plasticity as they force it to occur, but it is unclear to what extent LTP and LTD mimic physiological events. There are many advantages to these techniques in identifying the molecules involved in plasticity, especially if used alongside molecular genetics and with pharmacological blockade. Experience-dependent plasticity in the barrel cortex requires autophosphorylation of the post-synaptic protein α-CAMKII, indicating that excitatory synapses are involved in this type of plasticity (Malinow, 1989, Silva et al., 1992). α-CAMKII mutant mice also have deficient plasticity in primary visual cortex (Gordon et al., 1996). This, along with findings from CREB mutant mice raised the possibility that LTP-like mechanisms are involved in experience-dependent plasticity in barrels (Fox, 2002). LTP and LTD can both be induced in TCA-cortex synapses in rat S1 slices between

P3 and P7 indicating a critical period of physiological plasticity exists (Crair and Malenka, 1995, Lu et al., 2001). LTP can also be induced in septal and barrel wall regions in layers 2/3 by stimulating layer 4, but less so in barrel hollows (Glazewski et al., 1998). It is quite possible that LTP-like mechanisms are responsible for plasticity during critical periods in local cortical circuits of S1 (Fox, 2002), however, these mechanisms do not explain how barrels form. In visual cortex the link between LTD and plasticity is stronger. An interesting paper by Heynen and colleagues found that MD induces the same molecular mechanisms as LTD and that MD occludes any subsequent attempts to induce LTD (Heynen et al., 2003).

Two of the key molecular mechanisms that form the basis of strengthening and weakening of synapses such that seen in LTP and LTD are the insertion/removal and (de)phosphorylation of AMPARs (α-Amino-3-hydroxy-5-Methyl-4-isoxazolePropionic Acid Receptors) (Lee et al., 1998 neuron, Bear and Abraham, 1996) and the developmental switch of NR2B to NR2A. Such mechanisms as this can take place relatively quickly compared to anatomical alterations, which require more time. For example, in MD cortical cells that undergo a shift in OD initially undergo synaptic depression (Wiesel and Hubel, 1963). Further studies have found that as little as 8 hours of MD can produce synaptic depression in visual cortex (Freeman and Olson, 1982). Alterations in branching patterns of geniculocortical axonal arbours serving the deprived eye are noticeable after 4 days of MD (Antonini and Stryker, 1993). Retraction of geniculate terminals associated with the deprived eye occurs before expansion of terminals associated with the non-deprived eye (Antonini and Stryker, 1996). It is thought that cells responding to the non-deprived eye are experiencing LTP, but the relationship is complex and genetic mutants which have abnormalities in combinations of LTP, LTD and OD plasticity do not provide an easy interpretation (reviewed in Daw et al., 2004)

Some interesting experiments have been carried out investigating the role of the NR2B/A switch in experience-dependent plasticity. NMDARs have a total of 4 subunits which consist of one obligatory NR1 subunits and combinations of NR2A-D subunits (Hollmann and Heinemann, 1994, Stephenson, 2006). During the first few weeks of early development there is a switch in expression of NMDARs that are predominantly NR2B-containing to those which predominantly contain NR2A. The currents associated with activation of NMDARs containing particular subunits have been well documented (Carmignoto and Vicini, 1992, Shi et al., 1997), and contribute significantly to the function of NMDARs. The maturation of the activity dependent ON/OFF pathways in the retina may be regulated by this mechanism. Immunolabelling revealed that NR1/NR2A and NR1/NR2B containing NMDARs are localised to dendrites of RGCs (Fletcher et al., 2000, Pourcho et al., 2001). The expression of NR2A in RGCs changes with age and is decreased in rats if dark-reared from P12-P19 (Xue and Cooper, 2001). The electrophysiological properties of RGC light-evoked excitatory post-synaptic currents (EPSCs) are consistent throughout development with a switch from NR2B to NR2A (Xu and Tian, 2004). NR2A insertion shortens NMDAR currents in layer 4 neurons in adults but not young rats and may account for the age-dependent decline in visual cortical plasticity (Carmignoto and Vicini, 1992). Surprisingly mice with genetic deletions of *Nr2A* do not have extended critical periods even though NMDAR kinetics remain in the immature 'NR2B' state (Lu et al., 2001, Fagiolini et al., 2003). Also, barrel cortex critical period plasticity occurs independently of critical period plasticity. The critical period for LTP at thalamocortical synapses also occurs independently of NMDAR kinetics, even though there is strong correlation between the NR2B/2A switch and the loss of ability to generate LTP in thalamocortical synapses (Barth and Malenka, 2001). Scaffolding molecule PSD-95 preferentially binds NR2A to downstream signalling molecules, enabling signalling to occur. While OD plasticity is unaffected in mice with a deletion of the scaffolding molecule PSD-95 (Migaud et al., 1998), these mice do show defects in natural maturation of orientation preference, indicating that each form of plasticity requires specific cellular mechanisms (Fagiolini et al., 2003). Key to the effects of the NR2B to NR2A switch are the downstream mechanisms which also change as a consequence. There is a huge potential for scaffolding molecules SAP102 and PSD-95 to be significant in other mechanisms affected by this switch and two chapters of this thesis will address their role in somatosensory system development.

1.4.2 Neurotrophins

Neurotrophins and their receptors are expressed in cortex during the critical period for visual cortical plasticity. Neurotrophin release is regulated by electrical activity and modulates neurotransmission and neural connectivity (Caleo and Maffei, 2002). Nerve growth factor (NGF) and brain derived growth factor (BDNF) are both known to increase neurotransmitter release in rat visual cortex (Sala et al., 1998). In mouse visual cortex BDNF overexpression brings forward the critical period by promoting the rapid maturation of GABAergic interneurons (Tian et al., 1999, Hanover et al., 1999). BDNF may play a role via its expression in subplate neurons in the formation of OD columns (Lein et al., 1999, McAllister, 1999), a mechanism not yet fully understood. It is likely that growth factors function as retrograde signals and it seems that they play an instructive role in plasticity. However, growth factors have such wide ranging functions and modifying them can dramatically alter cell growth and death in all systems making it difficult to assess the particular affect on plasticity mechanisms.

1.4.3 GABAergic system

GABAergic cells migrate into the cortex from the ganglionic eminence after lamination has occurred. This occurs postnatally in mice at around the time that barrels are forming, and alters an environment where neurotransmission was largely glutamatergic. Inhibitory synapses are seen at P4 in all layers of PMBSF (De Felipe et al., 1997). Between P4-P8 there is almost an equal amount of excitatory and inhibitory synapses, then correlating with the onset of whisking there is a large increase in the amount of excitatory synapses (White et al., 1997). It is thought that the introduction of inhibitory cells alters the environment making it more permissive to plasticity, especially if activity is synchronised, for example (Galarreta and Hestrin, 2001, Galameta and Hestrin, 2001, Hensch and Fagiolini, 2005). GABAergic circuits have also been implicated in determining the column spacing from an initial overlapping mosaic, such as in the formation of OD columns. This model was tested in vivo in kittens by using agents to modify $GABA_A$ currents during the critical period (Willshaw and von der Malsberg, 1976, Miller et al., 1989, Hensch and Stryker, 2004, Sieghart, 1995). The onset of OD plasticity in mice can be delayed by preventing the maturation of GABA transmission by deletion of *Gad65*, similar results are seen if the mouse is dark-reared from birth (Hensch et al., 1998, Morales et al., 2002, Chen et al., 2001, Mower, 1991). Drugs that enhance GABA transmission can bring forward the critical period (Fagiolini and Hensch, 2000, Iwai et al., 2003, Fagiolini et al., 2004).

1.4.4 **Proteoglycans of the extracellular matrix (ECM)**

The ECM performs functions related to many biological processes. For example, the ECM maintains hydration of cells due to their negative charge, it strengthens tissues such as tendons, ligaments, blood vessels and bones and enables blood coagulation and cell adhesion. In the CNS the ECM is crucial for functions involved in development such as providing the substrate for nerve outgrowth and growth cone guidance and regulating synapse formation and stabilisation (Ruegg, 2001). The ECM in adults has functions in normal physiological processes such as synaptic plasticity (reviewed in Dityatev & Schachner, 2003) and malfunctions in neuropathological conditions such as MS, glioma, & Alzheimers (Knott et al., 1998, Bruckner et al., 1999, Gutowski et al., 1999, Sobel and Ahmed, 2001).
Proteoglycans, a family of molecules that contribute to the ECM have roles in regulating growth and plasticity. They perform their functions by modifying the environment to make it permissive to growth and plasticity. This may be by their proteolytic removal during critical periods, permitting reorganisation of circuits (Hensch et al., 2005).
There are four direct mechanisms by which proteoglycans may modulate neuronal development and plasticity in response to activity (first 3; Pavlov et al., 2004)

1.) By regulating motility and morphology or cells, resulting in structural alterations such as spine number or shape.
2.) By signalling between cells via cell surface receptors.
3.) By defining the extent of the extracellular space regulating the diffusion of soluble signalling molecules (i.e. neurotransmitters) (Nicholson & Sykova, 1998).
4.) By regulating receptor expression and composition at a synapse. A recent publication has shown that reelin, a component of the ECM regulates NMDAR subunit composition and trafficking during development (Groc et al., 2007).

One type of proteoglycan, chondroitin-sulphate proteoglycans (CSPGs) has been implicated in promoting the termination of plasticity (Hockfield et al., 1990). There is a correlation between closure of the critical period and CSPG maturation (Sur et al., 1988), indicating that CSPGs inhibit OD plasticity (Hockfield et al., 1990). Removal of CSPGs with the enzyme Chondroitinase ABC reactivates OD plasticity in MD rats (Pizzorusso et al., 2002, Berardi et al., 2003).

1.4.5 Neuromodulatory systems

Glutamate is the major excitatory neurotransmitter in the brain. Other neurotransmitters such as acetylcholine (ACh) and monoamines are often referred to as 'modulatory' due to their role of exciting or inhibiting depending on the receptor subtypes. These neurotransmitters are the basis of arousal, attention and motivation and can function as modulators of plasticity in cortex (Gu, 2002). The source may be sub-cortical but long projection axons reach into cortex. For example, ACh is released in cortex by inputs from the basal forebrain. In S1 cortex ACh is required for plasticity of the barrelfield map. Applying ACh at the same time as whisker stimulation drives plasticity of the receptive field (Shulz et al., 2003). Cholinergic transmission is required in the first postnatal week for retinal waves to occur. Initial studies of the β2 KO mouse indicates that when correlated firing in RGCs is lowered in these mice retinotopic maps are less precise (McLaughlin et al., 2003, Grubb et al., 2003). Even after 3-4 weeks when cholinergic transmission is no longer required the retinotopic map is still less precise, indicating there may be a critical period during the first postnatal week when retinotopic maps are refined by ACh (McLaughlin et al., 2003). Serotonin is described at a modulating neurotransmitter, however presynaptic mechanisms involving serotonin are probably just as important as post-synaptic mechanisms for the refinement of retinogeniculate and thalamocortical connections during development (Rebsam and Gaspar, 2006 - article in Erzurumlu et al., 2006). The role of serotonin will be discussed in more depth in the next section 'molecules and mechanisms'. Noradrenaline, dopamine and histamine also appear to modulate the excitability of cortical neurons (Gu, 2002).

1.5 Molecular basis of activity-dependent plasticity

Our group aims to understand the role that individual genes play in the activity-dependent development and refinement of these two systems. The mouse barrel-cortex provides a useful tool (and will be used in findings described in this thesis) to understand the molecules and mechanisms involved, since proteins in the molecular pathways can be genetically deleted, revealing the role of each protein. Next an overview will be given of the experiments that led to identification of the neurotransmitters and receptors that are involved in formation of sensory maps, in particular the formation of barrels. Then the proteins downstream of these receptors and the molecular pathways that are implicated will be discussed. This leads to the introduction of the purpose of this thesis and the aims of each chapter.

1.5.1 Neurotransmitters and Receptors

1.5.1.1 Serotonin

Serotonin (5-hydroxytryptamine or 5-HT) was the first neurotransmitter that was suspected to have a role in development of brain circuits. Neurons that release serotonin are some of the first to generated and serotonin release is detected prior to synapse development. There is a large family of serotonin receptors, each with roles at different stages and different brain regions. Initial studies to decipher the function of serotonin involved genetic deletion of serotonin receptors or proteins involved in metabolism of serotonin (such as monoamineoxidase A (MAOA), 5-HT1B and serotonin transporter (SERT)). Defects were found in neurogenesis, axonal connectivity, dendritic maturation, synaptic plasticity, cell survival and apoptosis (reviewed in Gaspar et al., 2003). The ordering of TCAs into barrel-related patterns is also modulated by serotonin signalling within TCAs (Gaspar et al., 2003). MAOA and SERT knockout mice both have problems with serotonin release. TCAs do not segregate into whisker-related patches in layer 4 of cortex and have fewer branches (Cases et al., 1996, Salichon et al., 2001, Persico et al., 2001) and retinal axons do not segregate in the dLGN (Upton et al., 1999, Upton et al., 2002). Interestingly knocking out both 5-HT1b and MAOA rescues the MAOA phenotype in both visual system (Salichon et al., 2001) and somatosensory cortex (Rebsam et al., 2002, Salichon et al., 2001). The vesicular monoamine transporter (VMAT2) is important for packaging monoamines into synaptic vesicles. Loss of VMAT2 results in severe depletion of serotonin, dopamine and adrenaline (Fon et al., 1997, Wang et al., 1997, Takahashi et al., 1997). VMAT2 knockout mice die shortly after birth with the occasional pup surviving to P6. TCA innervation is delayed by 1 day and cells do not form barrels in layer 4 (Alvarez, 2002), but it is likely that barrels would form a day later too, and so at P6 barrels are barely be visible. Also VMAT2 KO brains have reduced thickness of upper cortical layers making it difficult to see layer 4. In mice where VMAT2 and MAOA were deleted, serotonin is increased while dopamine and adrenaline are depleted (Perisco et al., 2003, Lipton and Kater, 1989). Conclusions from analyses of these mutants revealed that monoamines are required for modulation of late maturation processes (Perisco et al., 2003, Gaspar et al., 2003) rather than formation of retinogeniculate or thalamocortical connections (Fon et al., 1997, Perisco et al., 2003, Alvarez et al., 2002).

1.5.1.2 Glutamate

Cline and colleagues first found that NMDARs were involved in patterning of developing sensory projections. They injected NMDAR inhibitor APV into retina of three-eyed tadpoles and found that retinal inputs did not segregate (Cline et al., 1987). This led to a whole host of findings in patterning in other species. APV prevents OD plasticity in the cat visual cortex (Kleinschmidt et al., 1987, Bear et al., 1990) and segregation in ferret thalamus of retino-geniculate afferents into ON/OFF sublaminae (Hahm et al., 1991). In rat visual cortex APV blocks refinement of retinal projections to the SC (Simon et al., 1992). In mice visual cortex plasticity in the binocular region after depriving the dominant contralateral input is NMDAR-dependent (Sawtell el al., 2003), providing evidence that mouse visual cortex is a viable model for studying experience-dependent plasticity. Initial studies using APV in postnatal rat whisker-barrel cortex did not detect any alterations to the somatotopic map, even when manipulations are made to the sensory periphery (Chiaia et al., 1992, 1994a, Henderson et al., 1992, Schlaggar et al., 1993) but the timing, specificity of agent and method of application are crucial to detecting alterations (Chiaia et al., 1992, Schlaggar and O'Leary, 1994). Later studies found that function and organization are also affected by NMDAR blockade, in addition to anatomy (Fox et al., 1996, Mitrovic et al., 1996).

Following confirmation that there are good models of experience-dependent plasticity in mice, an obvious approach to understanding the significance of NMDARs is to use mouse genetics to delete genes encoding NMDAR subunits. At least three independent laboratories generated mice with deletions of the NMDAR subunit 1 (*Nr1)* gene (Li et al., 1994, Forrest et al., 1994, Tokita et al., 1996), encoding the protein of the essential NR1. Unfortunately *Nr1-/-* mice die at birth, making analysis of only patterning in brainstem possible. When birth was delayed by one day and mice were maintained in an incubator with stimulation to their respiration with CO2, they reached an equivalent stage to P2. There were no barrelettes in *Nr1-/-* brainstem, despite trigeminal afferents reaching brainstem and branched normally (Li et al., 1994). *Nr2B* mutants have a similar phenotype. When handfed they survive until P2 but also fail to form barrelettes (Kutsuwada et al., 1996). Nr2D mutants survive and form normal patterns of barrelettes, barreloids and barrels (Ikeda et al., 1995). In order to investigate the role of NR1 in cortical development targeted mutations were generated with NR1 deleted in cortical cells (*CxNr1*) (under expression control of the *emx1* promoter) (Iwasato et al., 2000). NR1 is deleted from excitatory cortical cells, hippocampus and olfactory bulb but is present in brainstem, thalamus and striatum and cerebellum. These mice have segregated but smaller rudimentary TCA patches in layer 4, with less axon terminal branching. TCAs undergo critical period plasticity as in wildtypes. Layer 4 cortical cells do not relocate to form barrels in *CxNr1* KO mice and interestingly, the dendrites of layer 4 cells do not reorientate towards the TCA patches. Instead they radiate in all directions covering large areas with increased elaboration and spine density (Datwani et al., 2002). This indicates that TCAs segregate independently of post-synaptic NMDARs but that postsynaptic NMDARs are required for the elaboration of TCA axons into the correct space and layer 4 cell dendrite reorientation. However Datwani and colleagues did not pay attention to the location of the layer 4 cells which had dendrites traced with respect to TCA patches, so it is not possible to tell in *CxNr1* KO if cells are in the would-be barrel wall, hollow or septae. It is important to note that GABAergic cells escaped the deletion due to their source being extra-cortical and may contain NMDARs that help to regulate TCA segregation.

At around the same time that NMDARs were being implicated in barrel formation, other groups found that reduced glutamate release from TCAs resulted in absence of barrels in layer 4. The spontaneous mutation resulting in ‘barrelless’ mice was discovered to be due to a mutation in *adenylate cyclase type 1* (*adcy1*) which causes modifications to PKA/cAMP signalling resulting in reduced glutamate release from TCAs (Welker et al., 1996, Abdel-Majid et al., 1998).

Glutamate signalling leads to barrel formation

The previous section presented evidence that the formation of barrels in mice is dependent upon 1) Segregation of TCAs into barrel-related patches via mechanisms that require serotonin (Gaspar et al., 2003), 2) Adequate release of glutamate from TCAs (Welker et al., 1996, Abdel-Majid et al., 1998, Laurent et al., 2002, Iwasato et al., 2000), 3) Intact glutamate signalling via the NMDAR (Iwasato et al., 2000, Erzurumlu and Kind, 2001, Kind and Neumann, 2001).
Knowing that glutamate is required for activity-dependent development of the somatosensory cortex, the next step is to further elucidate the molecular signalling pathways involved. This began with investigating the role of other glutamate receptors, along with molecules downstream of glutamate neurotransmission. Some of these investigations have been carried out by Dr Kind and colleagues and have provided interesting findings.

The metabotropic glutamate receptor 5 (mGluR5) is expressed in S1 cortex and is involved in activity-dependent development. Both mGluR5 and its downstream activating target phospho-lipase β-1 (PLCβ-1) are necessary for formation of normal barrels (Hannan et al., 1998, Hannan et al., 2001). TCAs in *Mglur5-/-* mice segregate into rows but not patches, however layer 4 cells do not form barrels (Hannan et al., 2001). Mice lacking PLC-β1 have no segregation of cells into barrels in layer 4, despite TCAs segregating into patches representing the whisker pattern. PLC-β1 hydrolyses phosphoinisitol (PI) into IP3 and DAG, and when mGluR5 is absent, PI hydrolysis is reduced, indicating that PI hydrolysis may be the mechanism of action necessary for barrel formation (Hannan et al., 2001).

Downstream of NMDARs, interacting molecules are also essential to the normal formation of barrels. SynGAP, a GTPase activating protein acting on Ras and Rap GTPase is bound to NMDARs via scaffolding molecule PSD-95 and is activated by calcium entering via the NMDAR. SynGAP also plays a key role in plasticity in the hippocampus and has been implicated in regulating synaptic development (Komiyama et al., 2002, Kim et al., 2003, Vazquez et al., 2004). *Syngap*$^{-/-}$ mice do not form barrels and die by P7, while *Syngap*$^{+/-}$ mice survive, breed and have small but significant defects in segregation of cells into barrels (Barnett et al., 2006). SynGAP negatively regulates the extracellular regulated kinase (ERK) cascade, also implicated in OD plasticity. In rodents MD enhances ERK signalling (Takamura et al., 2007) and pharmacological blockade of ERK pathways prevent the OD shift (Di Cristo et al., 2001).

In response to the finding from 'barrelless' mice that cAMP/PKA signalling is involved in barrel formation (Welker et al., 1996, Abdel-Majid et al., 1998), it was hypothesised that PKA is also necessary for the formation of barrels. Investigations were made to determine which subunit of the PKA heterodimer is responsible for this signalling. Out of all the subunits investigated, the second regulatory subunit of PKA (PKARIIβ) was the only one found to be involved (Watson et al., 2006). Cells in layer 4 do not segregate fully into dense walls and sparse hollows, despite TCAs forming normal whisker-related patches (Watson et al., 2006). Surprisingly, PKARIIβ was found to be post-synaptic in excitatory synapses in layer 4, indicating that its role is downstream of glutamate receptors rather than regulating glutamate release (Watson et al., 2006). *Prkar2b* KOs also do not undergo OD plasticity (Fischer et al., 2004).

Other regulators of glutamate activity

As discussed earlier, release of neurotransmitter be it spontaneous or evoked is necessary for the refinement of circuitry. Glutamate and serotonin have been found to play a key role in development of the somatosensory system. NMDARs are activated by glutamate in the presence of glycine, and the open channel allows calcium to pass through, activating intercellular mechanisms. NMDARs also play key roles in modulating activity as they can bind numerous intercellular proteins with varying specificity depending on the combination of subunits that contribute to the receptor. Calcium signals regulate the branching and growth of dendritic trees and are regulated by two main signalling targets, mitogen-activated kinase (MAPK) and calcium/calmodulin-dependent protein kinases (CaMKs) (Konur and Ghosh, 2005).

Calmodulin binds calcium and activates various intercellular cascades. Understanding the mechanisms and cascades that perform the functions associated with regulation and refinement is key if the role of activity is to be fully understood. The first step in an approach using targeted mutations in mice is to identify candidate molecules that act downstream of glutamate receptors. This approach was used by the Grant group at Sanger Institute to identify new genes that affect cognition.

1.6 Identification of NRC/MASC components

Most of the molecules and pathways described above are members of the 185-member complex known as the NMDAR/MAGUK (membrane associated guanylate kinase)-associated signalling complex (NRC/MASC) (Husi et al., 2000, Collins et al., 2006). The complex is embedded within the post-synaptic density (PSD) and provides an ideal spatially-restricted microenvironment for signalling to occur. Members of the complex were first identified by performing immunoblot and mass spectrometry on whole brain homogenate purified by NMDAR immuno-precipitation (Husi et al., 2000). This initial complex consisted of 77 proteins falling into the categories of receptors, adaptors, signalling molecules, cytoskeletal and novel molecules. Since then more have been added to the group by affinity isolation of MAGUKs, which directly bind NMDARs (Collins et al., 2006). Many of the proteins in the NRC/MASC complex have been implicated in human psychiatric disorders such as mental retardation, schizophrenia, bipolar & other depressive illnesses, (for review, Laumonnier et al., 2007) indicating that correct arrangement of the complex is essential for normal brain function as well as anatomy. New categories have been added so that all 185 members of the NRC/MASC are categorised according to function. The 10 categories will be outlined in the next section. Understanding the role of individual members of the complex is possible using the knock-out approach. In 2004 a team was set up to pursue this in the Sanger Institute, Cambridge under the direction of Prof. Seth Grant. ‘Genes to Cognition’ investigate brain function in these mice by carrying spatial learning and cue/context conditioning tasks, they measure electrophysiological plasticity in the hippocampus and through collaboration with our group in Edinburgh brains are examined for somatosensory system development defects. So far over 30 different mutants have been examined by our group, revealing a defect in barrel development in *Syngap* mutants (Barnett et al., 2006).

1.7 Classification of PSD components

In this thesis, findings from investigations of a new mutant *Rics* are presented, along with double mutants *Syngap* & *Dusp6*, *Syngap* & *Nf1*, *Dusp6* & *Nf1*, and *Sap102 & Psd-95*. Each of the mutants to be presented in this thesis are briefly described in the appropriate category along with key reasons as to why they are candidates in the pathways to barrel development. More detailed information about each protein can be found in the results chapters. The remaining categories as identified by Collins and colleagues are briefly introduced (Collins et al., 2006).

1.7.1 Categories of NRC/MASCs containing molecules investigated in this thesis:

1.7.1.1 G- proteins and Modulators

There are 13 G-proteins in this category from subclasses of Rabs, GNBs, and also H-Ras, Ral-A, Ran, Rap2, Rac1. Best known of the 6 modulators are SynGAP and NF1 both GTPase activating proteins already described in the literature. *Syngap* knockouts die in the first post-natal week and *Nf1* knockouts die embryonically (Brannan et al., 1994, Jacks et al., 1994). Knocking out *Syngap* globally and cortex-specific *Nf1*results in lack of barrels (Barnett et al., 2006, Lush et al., 2008), and while *Nf1* heterozygotes have not been described, *Syngap* heterozygotes exhibit a milder form of the *Syngap*$^{-/-}$ phenotype. This thesis will address the interaction between the two GAPs to see whether there is any compensation or additional effects of mutating both GAPs at once. It will also analyse the formation of barrels in mice carrying either a *Nf1*$^{+/-}$ *or Syngap*$^{+/-}$ mutation as the background strain of these mice is different from previous publications.
The RhoGAP RICS was not identified to be a member of the NRC/MASC but is known to regulate RhoA and Rac1 and neurite extension (Nakamura et al., 2002) and spine width (Nakazawa et al., 2008). It is associated with NMDARs (Nakazawa et al., 2003) and PSD-95 (Okabe et al., 2003) and relocates in vitro to the PSD in response to NMDAR activation (Zhao et al., 2003). RICS is therefore a good

candidate for regulating the processes known to be associated with barrel formation. Its role in barrel formation will be investigated in this thesis.

1.7.1.2 MAGUKS/Adaptors/Scaffolders

The subcategories of this category are 14-3-3s, and those with or without PDZ-domains. PDZ-domain containing and non-PDZ-domain containing are listed in full in table 3 in Appendix I. Most important for this thesis are the MAGUKs PSD-95 and SAP102 which are PDZ-domain containing proteins. Both have been implicated in synaptic plasticity (Migaud et al., 1998, Cuthbert et al., 2007), and are known to bind NMDARs to maintain associations between NMDARs with many other signalling molecules. Importantly, both have been found to link SynGAP to the NMDAR, making them candidates for having roles in the formation of barrels. This role will be addressed in this thesis, and to fully investigate the possible compensation roles double mutants will be generated and analysed.

1.7.1.3 Protein Phosphatases

This is a small category containing 8 protein phosphatases, none of which have yet been implicated in the development of the somatosensory system. Dusp6, a dual specificity phosphatase of the protein tyrosine phosphatase superfamily was not isolated in the NRC/MASC (nor the original 77 NRC components (Husi et al., 2000). Dusp6 inactivates MAPK and so is in a unique position to mediate events that occur in response to NMDAR activation. *Dusp6* mutants will be analysed along with double mutants *Dusp6* with *Nf1* and *Syngap* (which both act on the MAPK cascade) to reveal any additional or rescue of the defect in barrel formation.

1.7.2 The remaining NRC/MASC categories:

1.7.2.1 Channels and Receptors

Falling into this category are glutamate receptors NMDARs, mGluRs, kainite and AMPARs and their subunits, voltage sensitive calcium channels and ATP channels.

1.7.2.2 Cell Adhesion and Cytoskeletal

Falling into this category are actins, actinins, myelins, β-catenin, cadherins, and others. So far no molecules from this category have been implicated in barrel formation.

1.7.2.3 Kinases

Kinases can be further segregated into two types, Ser/Thr kinases such as CaMKIIs, ERKs, MEKs, MKK7 and other MAPKs, PKA, PKC, Raf and Rsk. Also Tyr kinases such as Src.

1.7.2.4 Signalling Molecules and Enzymes

In this category are the calcium signalling molecules calmodulin and calretinin. Also stargazing, PLCβ (mutant described above) and PLCχ, enzymes involved in mitochondrial processes, ATP synthesis and other house-keeping processes.

1.7.2.5 Synaptic vesicles/Protein Transport

Falling into this category are clathrin, motor proteins, and machinery associated with vesicle exocytosis. Protein transporters make up the remainder.

1.7.2.6 Transcription and Translation

This category contains ribosomal proteins and transcriptional elements.

1.7.2.7 Uncharacterised/Novel

This category contains 3 previously uncharacterised or hypothetical proteins.

1.8 Summary

This thesis uses the mouse barrel cortex as a model to investigate the role that members of the NRC/MASC complex have on regulating glutamate activity pathways involved in anatomical development. It attempts to decipher some of the compensation mechanisms that occur between molecules that perform similar functions, and determine whether any molecules act on the same molecular pathways.

The first three results chapters focus on proteins in the pathways leading to barrel development. These are proteins expressed during early post-natal stages when spontaneous release of neurotransmitter is the main form of activity that drives the cellular rearrangement resulting in cytoarchitectural barrels. The proteins studied are involved in NMDAR signalling via the ERK/MAPK pathway and may regulate pathways that have been previously shown to be necessary for barrel formation. There is a particular focus on MAGUK scaffolding molecules as an interesting interaction is revealed between X-linked *Sap102* and *Psd-95*. Methods are developed to analyse whether SAP102 has a cell-autonomous role or non-autonomous role as it compensates for the loss of PSD-95. The fourth results chapter is investigating the role that CSPGs play in later stages of development as experience-dependent plasticity dissipates. These events are at the close of the critical period when sensory activity is more influential than spontaneous release of neurotransmitter. A subset of CSPG-expressing cells are studied throughout development to investigate their role in formation of barrels in mice that have previously been published to have poorly formed barrels due to genetic defects in glutamate signalling (Hannan et al., 2001, Barnett et al., 2006, Watson et al., 2006). Any alteration in expression of CSPGs between mutants and wildtypes would indicate that expression is regulated by NMDAR-dependent signalling pathways.

1.8.1 Specific aims of thesis

1. To examine mice with NRC/MASC-component mutations that have previously undescribed roles in somatosensory system development to determine whether they are necessary for formation of barrels in layer 4 somatosensory cortex.

2. To determine whether scaffolding molecules SAP102 and PSD-95 together are necessary for formation of normal barrels.

3. To determine whether cells containing SAP102 act autonomously or non-autonomously on surrounding cells not containing SAP102 in the formation of normal barrels.

4. To determine whether expression of subsets of CSPGs are regulated by NMDAR-dependent signalling pathways necessary for formation of normal barrels.

2 Methods

2.1 *Mice*

2.1.1 NRC/MASC component mutants

Rics, *Dusp6*/ *Nf1*, *Syngap/Nf1*, *Syngap*/*Dusp6* mutants were generated by Prof. S G Grant's laboratory. The generation of *Rics* and *Dusp6* mutants has not yet been published and is explained in diagram 4 A, B & C. For each mutant, genomic DNA was replaced with flanking DNA and a selection marker into targeting vectors. Those in which homologous recombination had occurred were selected by Southern blotting. The vector was then inserted into 129p2 embryonic stem (ES) cells, and injected into a C57 Bl/6 blastocyst. The resulting chimeras born were crossed to C57 Bl/6 (F1 generation), some litters were used for experiments, and some offspring crossed again to C57 Bl/6 to provide more pups. Pups were therefore 25% or 12.5% 129 background, and the rest Bl/6. The generation of *Syngap* and *Nf1* mutants has been previously described (Komiyama et al., 2002, Brannan et al., 1994) (see diagram 4 D). *Syngap* and *Nf1* mutants were maintained on Bl/6 129background, similar to the background of *Rics* and *Dusp6* mutants. Litters were anaesthetised and perfused at 7 or 8 days after birth with PBS followed by 4% paraformaldehyde in 0.1M PB (PFA/PB). Brains were removed and placed in 4% PFA/PB and posted from Sanger Institute, Cambridge to Edinburgh. Upon arrival they were stored at 4°C and divided into batches for analysis. Hemispheres were dissected and one hemisphere sectioned coronally for measurements of lamination. The other hemisphere was dissected to leave a cortex which can be sectioned tangential to pia, so that barrels in layer 4 can be labelled and density of cells in wall: hollow can be calculated. Detail on preparation of tissue and immunohistochemistry are described later.

The *Rics* mutation involved adding a LacZ reporter to the target for deletion. LacZ gene product is then expressed when the *Rics* gene should be expressed. This allows analysis of expression of RICS by labelling with α-β-Gal antibody. The procedures for this are described later.

Diagram 4: The nature of the targeted mutations

A: Rics mutation

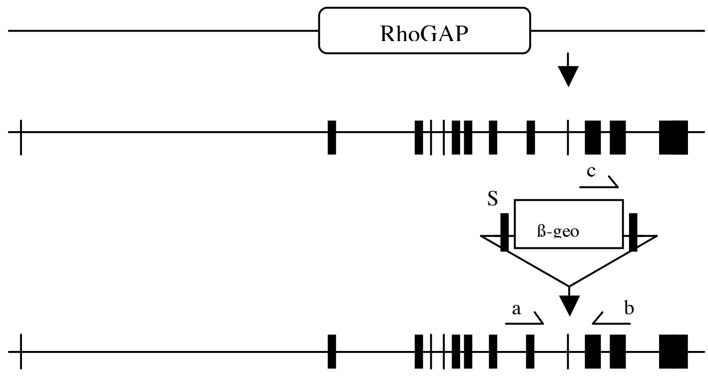

Targeting of Rics mutation by gene trap. Top line indicates gemonic DNA and position of RhoGAP domain. Exons are drawn as blank bands in middle line. The targeting cassette to be inserted is indicated along with the location of insert (lower line). There are 368 amino acids before the trap was inserted. a, b, c location of genotyping primers (Diagram created by David Fricker, Grant Lab)

B: Dusp6 mutation

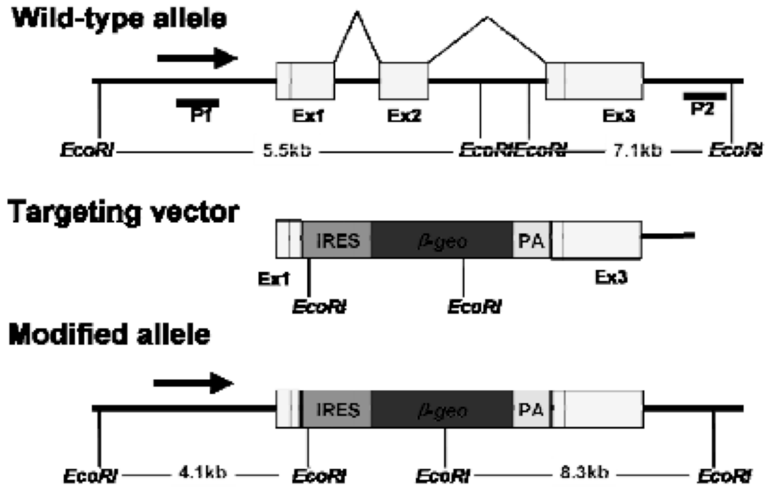

Targeted disruption of Dusp6 gene. The top line indicates the wildtype Dusp6 gene containing exons 1-3. The middle line indicates the targeting vector containing an IRES and β-geo site, which replaces exon 2. The modified segment is indicated in the lower line. (Diagram created by Douglas Strathdee, Grant lab)

C: Nf1 mutation

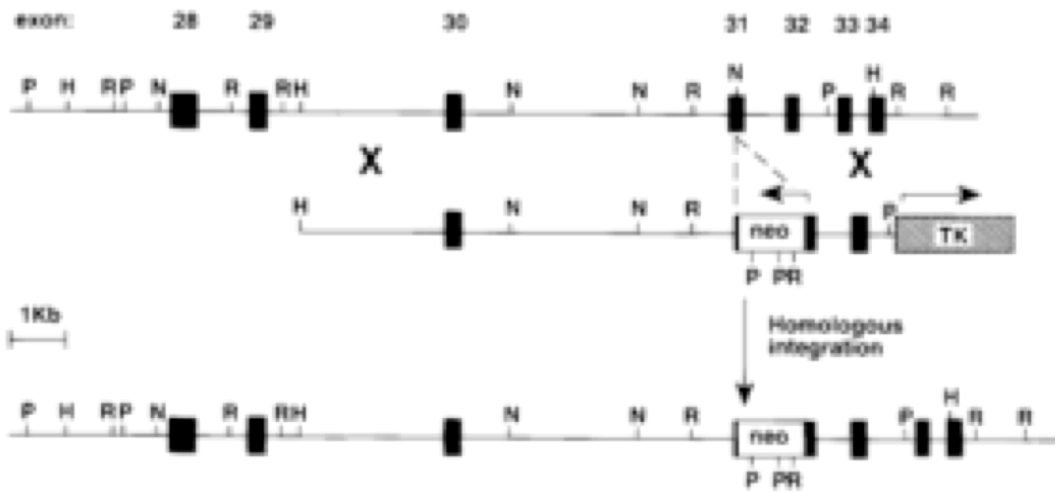

Homologous recombination at the *Nfl* locus. The *top* line represents the structure of the region of the *Nfl* gene containing exons 28-34. Exons are shown as black boxes. The middle line represents the targeting vector in which the 1.1-kb pMClneo/poly(A) + cassette has been inserted into the *NcoI* site of exon 31 and a viral thymidine gene, under the control of the pMC1 promoter, which has been placed at the 3' end. Arrows indicate the direction of transcription of the *neo* ~ and *tk* genes. In the *bottom* line is the predicted structure of the locus following targeted integration of the replacement vector. Homologous recombination events were confirmed by probing Southern blots of ES cell clones with probes A, a 4-kb *HindIII* fragment. Exon 31 was chosen because several point mutations exist at this site in human NF1 patients. This mutation is a null allele, no RNA or protein is made from this mutated allele. (Diagram and legend taken from Brannan et al., 1994).

D: SynGAP mutation

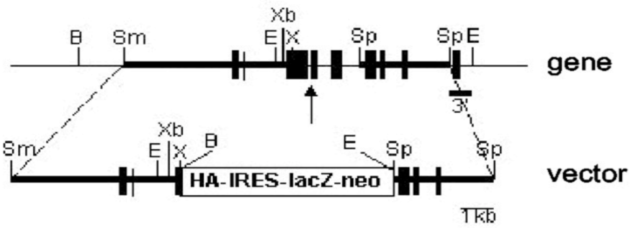

Targeted disruption of SynGAP gene. *Top*, SynGAP gene with restriction enzyme sites (*B*, *Bgl*II; *E*, *Eco*RI; *Sm*, *Sma*I; *Sp*, *Spe*I; *X*, *Xho*I; *Xb*, *Xba*I); *black boxes*, exon; *thick horizontal lines*, homologous regions used in the targeting vector; Southern blot probes are indicated (3'). *Bottom*, SynGAP targeting vector. *HA*, Hemagglutinin sequence; *IRES*, internal ribosomal entry site; *lac*Z, -galactosidase gene; *neo*, neomycin-resistance gene. The *arrow* below the SynGAP gene indicates arginine 312 (or 470) (Chen et al., 1998; Kim et al., 1998), which is highly conserved in RasGAP proteins and necessary for GAP activity and was deleted in the targeting vector. (Diagram and legend taken from Komiyama et al., 2002)

E: SAP102 mutation

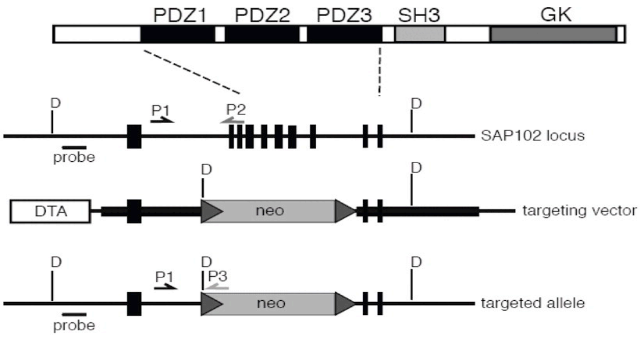

SAP102 has three PDZ, a SH3, and a GK domain (top). SAP102 exons 2–8 were replaced with a selection cassette in targeted mice, deleting the majority of the PDZ-coding sequence and creating a frame-shift mutation between exons 1 and 9 (middle and bottom). The 5' probe outside the targeting region and primers P1–P3, used for Southern blot and PCR genotyping respectively, are shown. D, *Dra*I restriction sites. (Diagram and legend taken from Cuthbert et al., 2007)

F: PSD-95 mutation

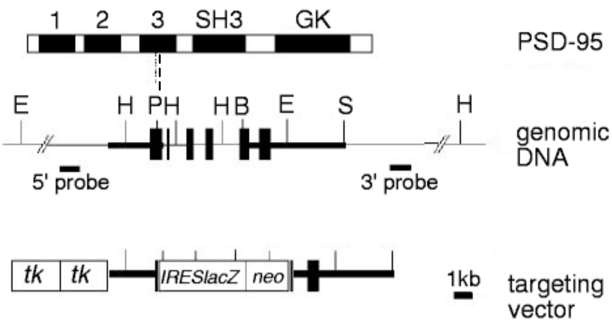

Top: PSD-95 protein with three PDZ domains (labelled 1, 2, 3), a SH3 domain and a GK homology region. Middle: PSD-95 gene with restriction-enzyme cutting sites (E, *Eco*RI; H, *Hin*dIII; P, *Pvu*II; B, *Bam*H1; S, *Sac*I); black boxes, exons, thick horizontal lines, homology regions used in the targeting vector; Southern blot probes are indicated. Bottom: targeting vector. *tk*, thymidine kinase gene; *IRES*, internal ribosome-entry sequence; *lacZ*, -galactosidase gene; *neo*, neomycin-resistance gene. The dotted vertical line from the PDZ3 domain (upper) to the *Pvu*II site (middle) represents the position of the stop codon inserted into PDZ3. (Diagram and legend taken from Migaud et al., 1998)

2.1.2 MAGUK mutants

Psd-95 and *Sap102* mutant mice were generated by Prof. S G Grant's lab (Migaud et al., 1998, Cuthbert et al., 2007) (see diagram 4 E & F). To generate *Sap102* mutant mice, HM1 mouse ES cells were targeted with a vector containing a neomycin selectable marker with 3.6 and 4.5kb flanking fragments, replacing 4kb of SAP102 genomic DNA (Cuthbert et al., 2007). To generate *Psd-95* mutant mice, a stop codon was introduced into the PDZ3 domain replacing downstream sequences with an IRES that drives a β-galactosidase reporter gene. The targeting construct was incorporated into ES cells and clones were selected by Southern blot in which homologous recombination had occurred (Migaud et al., 1998). Both *Sap102* and *Psd-95* mutant mice were maintained on a 50/50 MF1/129 background strain. Initial analysis of somatosensory system development was performed on this background. Unfortunately after contracting MHV this colony were culled and all subsequent analysis was carried out on Bl/6 129 mixed background. Numerous breeding pairs were arranged to give a variety of mutants, taking care to avoid using neglecting *Psd-95*$^{-/-}$ mothers. PCR reactions were carried out on *Psd*-95 mutant mice using primers designed to amplify a wild type sequence upstream of the *PvuII* site in the 3rd PDZ domain. Primers were AAC CAA GGC GGA TCG TGA TCC A (forward) and TCT CTT TGG TGG GCA GTG (reverse) identifying a 220bp fragment. The mutant allele (a 2kb product) was identified with forward primer CAT TCG ACC ACC AAG CGA AAG ATC and a reverse primer CAG GGA GCG GGG ACG GAT GA identifying a strand of the neo gene (Migaud et al., 1998). PCR reactions were carried out on *Sap102* mutant mice using a forward primer GGT CTC TGA TGA AGC AGT GAT TTT T and reverse primers TGA TGA CCC ATA GAC AGT AGG ATC A and CTA AAG CGC ATG CTC CAG AC amplifying a 535bp wild type fragment and a 215bp KO fragment respectively (Cuthbert et al., 2007).

2.1.3 X-linked Hmg CoA Reductase *LacZ* mutants

Mice carrying the X-linked *LacZ* transgene linked to a nuclear localisation sequence were obtained from Dr J West at the University of Edinburgh. They were originally made by S S Tan and colleagues (Tan et al., 1993) and maintained at Edinburgh on a C57Bl/6 – DBA/2 mixed background. Identification of mice carrying the transgene was carried out in two different ways. Ear or tail tissue left for a few hours in X-Gal stain turned blue if carrying the transgene. However, while this method was reliable for determining whether a male was carrying the transgene or not, it could not differentiate between whether a female was expressing *LacZ* on either one or both X-chromosomes. QPCR was carried out using primers that recognised LacZ but it was difficult to be sure of some tissue that did not obviously have twice as much *LacZ* DNA as single-copy controls. Unfortunately the *LacZ* primers also amplified the LacZ reporter DNA which was inserted into the genome when *Psd-95* mutants were being generated. Therefore qPCR was not reliable if the *Psd-95* mutation was present. While a new method of genotyping females was being developed, the issue was resolved by only breeding from females where genotype was known due to only one parent carrying the transgene. It took multiple generations to create mice that carried all 3 mutations necessary for analysis. A significant amount of time was taken to ensure breeding produced the required mutants in as few generations as possible but some mice proved difficult to generate ($Xb^{-}Y$ $Psd\text{-}95^{+/-}$), despite the probabilities of their production being reasonable.

2.1.4 Mutants for CSPG analysis

Mice were anaesthetised and perfused transcardially with PBS followed by a 0.1M PB solution containing 4% PFA according to Home Office (HO) licence and regulations and brains removed and placed in 4% PFA in PB at 4°C. Genotyping by PCR was carried out as previously described (PLBβ-1 & MGluR5: Hannan et al., 2001, SynGAP: Barnett et al., 2006, PKARIIβ: Watson et al., 2006) and at least 3 wildtype and 3 KO brains were selected at each age; P14, P21, & Adult for each transgenic line (except *Syngap* where heterozygotes were used instead of KOs). In some cases only 2 brains were available at a particular age and genotype. Different transgenic lines are on different backgrounds, *Plc*β-1 & *Mglur5* are on Bl/6 129, *Syngap* and *Prkar2b* are on Bl/6. *Plcβ-1* mutant adults are 5 months old. *Prkar2b* mutant adults are 6-13 months old. *Mglur5* mutant adults are 6-7 months old. *Syngap* mutant adults are 3-6 months old. To establish the wild-type expression profile Bl/6 mice were used at P7, P14, P21 & Adult (C57 Bl/6 J Ola Hsd).

2.2 Analysing Cortical Lamination

2.2.1 Preparation of Tissue

Mice were anaesthetised and perfused transcardially with PBS followed by a 0.1M PB solution containing 4% PFA according to HO licence and regulations and brains removed and placed in 4% PFA in PB at 4°C.

P7 and P14 brains were taken and one hemisphere placed in a cryoprotective solution of PBS containing 30% sucrose overnight to clear PFA. Each hemisphere was dissected using a pair of FST fine tip no. 7 Forceps to remove hindbrain, midbrain including striatum and archicortex, to preserve the area of the neocortex containing S1 region (fig M1.1 a-g). The remaining fragment can be flattened allowing the cortex to be sectioned tangentially through the layers where each histological section should contain cells from in most cases only one cortical layer. When coronal sections were required one hemisphere was dissected and sectioned as described in fig M1.2. 48μM coronal cortical sections were taken on the freezing microtome and placed serially into 4 wells containing PBS. Sections were incubated overnight at RT in D-MEM containing 5% FCS and sodium azide with a polyclonal antibody recognising a specific layer of the cortex (Barnett et al., 2006).

2.2.2 Staining Tissue for Cortical Lamination Analysis

2.2.2.1 For Layer 4 thickness:

An antibody raised in rabbit against PKARIIβ (1:600, Santa Cruz Biotechnology) precisely labels layer 4 since PKARIIβ is found to be postsynaptic (Watson et al., 2006) in cortical neurons. This allows definition of the area of layer 4 and part of layer 5 which provides the target for much of the TCAs. However, for the purposes of comparisons made in this study the thickness of layer 4 and part of 5 is referred to as 'layer 4 thickness'.

2.2.2.2 Defining the boundary of layer 4&5

An antibody raised against calretinin (1:3000; Swant, Bellinzona, Switzerland) was used to labels cells in the outermost band of layer 5. This enables the boundary of layer 4 and 5 to be very clearly defined, and so measurements of thickness of layers 1-4 & 5-6 can be made.

2.2.2.3 Performing the immunohistochemical reaction:

One quarter of sections from a coronally sliced hemisphere were incubated overnight in each of the primary antibodies, diluted in DMEM (Invitrogen) containing 5% fetal calf serum (FCS) (Sigma) and 0.2-0.5% triton X-100 (Sigma). After washing, sections were incubated in the same media as primary antibodies, containing biotinylated goat anti-rabbit (1:200-250) (DAKO) for at least 90 minutes. Sections were washed and antibodies were visualised using a Vectastain ABC kit (Vector Laboratories) with DAB (Sigma) as the chromagen. After a final wash sections were mounted, dried, dehydrated and coverslipped in DPX.

2.2.2.4 Labelling all cell bodies to measure layer 1-6

One quarter of sections from each coronally sectioned hemisphere were mounted and dried on microscope slides in preparation for Nissl stain. Nissl substance was first described by Franz Nissl over 100 years ago. It is composed of rough endoplasmic reticulum and ribosomes (primarily RNA) outside the nucleus, unique to neuronal cells bodies and dendrites. A number of stains have been developed which stain Nissl substance, in this case the conventional purple dye thionin is used which also stains nuclear DNA and turns to blue following alcohol dehydration. The specificity of thionin for staining nucleic acids in DNA and cytoplasmic RNA or 'Nissl substance', is determined by the final pH of the staining solution. Stock dye solutions were prepared in advance allowing fresh staining solutions to be created when required. Stock solution A contains 1g thionin crystals in 100mls ddH2O.
Stock Solution B is 0.1M glacial acetic acid. (6mls in 1 litre ddH20)
Stock Solution C is 0.1M Sodium acetate (13.6g in 1 litre ddH20)
For a pH 3.7 working staining solution 10 mls of solution C and 2.5 mls of solution A was added to 90 mls of solution B. Mounted sections were submerged in the staining solution for 20 minutes or longer. The working solution is replenished or replaced when 30 minute stains fail to produce adequate staining intensity. To de-stain and increase the background sections were dipped in 70% ethanol followed by 95% ethanol with 1:1000 acetic acid. Sections were then dehydrated through an

alcohol series (starting at 95%) and coverslipped in DPX. Nissl staining allows identification of different layers in the cortex by their cell morphology. Measurements can be made of total cortical thickness (layers 1-6).

2.2.3 Cortical measurements

Images were captured using a Leica DLMB microscope and Leica 480 digital camera, using 5x objective. In analysis of coronal sections, 2 sections were chosen. One that includes barrels from the anterior snout region (AS) and one that includes barrels from the posterior medial barrel subfield (PMBSF). This enables defects to be measured in two regions of the cortex. Images were opened and measurements made using the freely available Image J software (http://rsb.info.nih.gov/ij/). From each section chosen, 3 measurements were made, one through the most medial part of the barrel field visible, one from the most lateral part of the barrel field and one in between (see fig M2). The average of AS and PMBSF was calculated for each brain, and data combined by age and genotype.

In summary, the measurements taken were

1.) Total cortical thickness in AS and PMBSF

2.) Thickness of layers 5 & 6 in AS and PMBSF

3.) Thickness of layers 1-4 in AS and PMBSF

4.) Thickness of layer 4 in AS and PMBSF

5.) Area of individual SERT patches (in some cases)

6.) Area of serotonin transporter – labelled (SERT) TCA patches B, C & D 2-3

2.3 Analysing cell segregation into barrel walls and hollows

2.3.1 Preparation of Tissue

Mice were anaesthetised and perfused transcardially with PBS followed by a 0.1M PB solution containing 4% PFA according to HO licence and regulations and brains removed and placed in 4% PFA in PB at 4°C.

P7 and P14 brains were taken and one hemisphere placed in the cryoprotective solution 30%sucrose /PBS solution overnight to clear PFA. Hemispheres were bisected with a razor blade (fig M1.1 a) and the cerebellum was removed (fig M1.1 c). A pair of FST 7 forceps were used to remove hindbrain, midbrain including

striatum and archicortex, to preserve the area of the neocortex containing S1 region (fig M1.1 d-f). The remaining fragment can be flattened allowing the cortex to be sectioned tangentially through the layers where each histological section should contain cells from in most cases only one cortical layer (fig M1.1 g).
48uM transverse cortical sections were taken on the freezing microtome and placed serially into wells containing PBS.

2.3.2 Labelling TCAs and nuclei for barrel segregation analysis

Sections were incubated overnight at RT in D-MEM containing 5%FCS and sodium azide and a poly-clonal antibody recognising the pre-synaptic serotonin transporter 'SERT' (Calbiochem 1:3000). Sections were washed and incubated in the same DMEM solution with biotinylated anti-rabbit immunoglobins for 1 hr. After washing sections were incubated with a streptavidin-conjugated Fluorescent marker (Molecular Probes) fluorescing at 488λ. After washing sections were left in a 90% glycerol 10%PBS solution containing nuclei stain To-Pro-3 (T3; Molecular Probes), which fluoresces at 647λ.

2.3.3 Labelling β-Galactosidase and nuclei in barrels

Preparation of tissue was carried out as described above for 'analysis of cell segregation'. Sections of flattened cortices were transferred from PBS to a blocking solution containing 20% heat inactivated goat serum (HINGS, Sigma), triton, and $MgCl_2$ for 1 hour. Sections were rinsed and placed into a similar solution containing rabbit anti-β-Galactosidase antibody (Molecular Probes, 1:500) overnight. This antibody will label any nuclei expressing the X-linked *LacZ* transgene. The next day, sections were removed, rinsed twice in PBS with 0.1% triton and transferred to a PBS/0.5% Triton solution containing goat anti-rabbit biotinylated secondary antibody for 90 minutes. Sections were rinsed twice with PBS/0.1% triton and placed in a solution containing streptavidin-conjugated Alexa fluor 488λ or 568λ. After two final rinses with PBS/0.1%Triton sections were left to clear overnight in 9:1 glycerol/PBS containing 1:2000 To-Pro-3 (T3; Molecular Probes), a nuclear stain that fluoresces at 647λ.

2.3.4 Obtaining an image

After mounting in MOWIOL, a glycerol based hard-drying fluoro-protectant, sections were coverslipped and left to dry overnight in a dark place. A Leica DMR confocal microscope with a TCS-NT laser was used to capture a series of images of the section found to display barrels in Layer 4. Usually 2 or 3 sections will display part of the barrel field so the section containing the majority of the field and showing cells segregated into barrel walls and hollows to the largest degree was chosen. A series of images were captured by lasers picking up To-Pro-3 at 647λ (blue) and either SERT at 488λ (green) or β–Gal at 568λ using objectives 5x, 10x, and 20x, maintaining barrel C2 in the centre of all images (fig M5.1 a-c). At, 20x Barrel C2 can be enlarged using an optical zoom to enhance the detail of that particular barrel (fig M5.1 d). A series of 1024x1024 pixel images were captured 7uM apart in z-plane providing approximately 5-6 images that can be viewed as a stack if necessary. All cells in barrel C2 should be captured in one or two of the optical sections. The optical image providing the best indication of barrel C2 where there is the most cell segregation into dense walls and sparse hollows was chosen for analysis (fig M5.1 e & f). This image is made up of 2 channels capturing 488λ or 568λ and 647λ. It is with this image that further methods of analysing cell density ratio between wall and hollow were carried out.

2.4 Analysis of the barrel

Different methods were tested in order to find the most accurate and reproducible method for determining the extent to which cells in layer 4 segregate into cell-dense barrel walls and cell-sparse barrel hollows.

2.4.1 Method 1 ‘Pixel density analysis through a rectangle’

Using freely available image analysis software ‘Image J’ (http://rsb.info.nih.gov/ij/) images of the two channels were opened and adjusted as follows. The two channels are detecting the two separate fluorophores at 647 (To-Pro-3) and 568nm (SERT) wavelength. The optical zoom image using, 20x objective showing most cell segregation was selected (fig M3.1 a &b). The image taken on the channel capturing 488λ containing SERT staining (green) was converted to grey scale, and contrast was adjusted up to +80 to enhance the definition of the barrel hollow (fig M3.1 c & d).

Immuno positive areas then appear to be white. The image is rotated arbitrarily so that barrel walls are vertical on the screen. This may take a few minor adjustments using Image J /rotate/arbitrarily. When the correct angle had been chosen, the T3 image was rotated by the same no of degrees. Using the SERT image as a guide a rectangle was drawn over the 2 parallel edges of the barrel, cutting off the top and bottom and including the two long edges of the barrel wall (fig M3.1 g - h). A macro was designed to carry out a number of editing tasks described below. Image is converted to greyscale (8-bit), contrast is enhanced, image is resized to 350 pixels width and a density plot is carried out. The density plot calculates the average intensity of light across the rectangle and every pixel (350 points) (fig M3.1 i). It then plots the 350 points on a graph representing the width of the barrel and provides a list of the data points (fig M3.1 j). Data points were then collected and copied into Microsoft excel where data was combined for mice of the same age and genotype and comparative analysis carried out (fig M3.2).

NB

This method produces a line graph for each data set, rather than a single number representing ratio of wall: hollow. It therefore contains more information about the density change across a barrel in different genotypes. This method was developed because it takes into account variation in wall thickness and hollow size, rather than assuming that this never varies. However it may not be as accurate as counting because the number is falsely increased if there is high background T3 staining. The image editing process attempts to reduce the background by increasing contrast but it is not always possible to entirely remove it.

2.4.2 Method 2 'Pixel density analysis along lines placed in wall and hollow'

The advantage of this method is predicted to be that it provides a similar analysis to the one above, but that it includes analysis of the top and bottom of the barrel. Using Image J, the same editing of the image was performed as described above, up until the point where the rectangle is drawn (fig M4.1 a-f). At this point, instead of a rectangle, a freehand line is drawn on the image showing SERT along the perimeter of the immuno-positive patch illuminated by white at this stage (fig M4.1 g-h yellow line). This shape is then transferred onto the image showing T3-stained cells. The shape should appear to include the barrel wall and a small section of the barrel hollow.

A macro was designed to draw concentric circles on the T3 image using the initial 'SERT boundary' as a guide. The first line drawn reduces the whole image by 50 pixels and then redraws the SERT boundary on the reduced image (fig M4.1 h red line). The result of this is that the line length is the same, but it appears nearer the edge of the image. The macro was designed so that by reducing the image by 50 pixels the new line drawn is highly likely to be almost completely through the barrel wall. The macro then takes a measurement of pixel intensity along this line. The result is a single number, described as W1. The macro then reopens the original image, and this time enlarges it by 100 pixels and redraws the shape defining the perimeter of the SERT patch (fig M4.1 h white line). The result is that the new line is drawn inside the original perimeter of the SERT patch. The macro calculated the pixel intensity, and the number is named H1. A repeat of this step is calculated so that there is a line even closer to the centre of the barrel (fig M4.1 h green line). This number is H2. Analysis can then be carried out by comparing pixel intensity along the line going through barrel wall (W1) to an average of pixel intensity along 2 lines going through hollow (H1 and 2). The ratio of W1:(H1+H2)/2 should be representative of the extent of cell segregation where a higher number means the barrel has more cells in wall relative to hollow. Data can be grouped by age and genotype and statistical analysis performed.

NB

This analysis relies on the assumption that a more cell-dense area of an image will produce a higher measurement of pixel intensity, as the cells stained with T3 appear white and background is black. It is limiting when an image has a particularly high background, perhaps as a result of incomplete clearing of T3. In this case the pixel intensity will be higher as it is taking into account pixels which appear white due to background (fig M4.2 b) rather than the presence of a T3-stained cell (fig M4.2 a).

2.4.3 Method 3 'Stereological counting of a sample of cells within wall and hollow'

This method uses the software Adobe Photoshop 7.0 for image editing and for counting. Confocal images are collected from the section best representing the barrel field, ensuring that C2 shows good segregation of To-Pro-3 cells. Images are collected using 5x objective, 10 x objective and 20x objective, taking care to have barrel C2 in the centre of the image at all times. C2 can be identified using a barrel map (fig M5.2 b). C2 is one of the easiest barrels to consistently identify due to its location in relation to barrels α, β, χ, and δ. If the tangential section does not contain all barrels due to the plane of section then it is usually possible to identify the greek-lettered barrels and then locate C2. In choosing one barrel I am assuming that the segregation of cells in C2 is representative of all other barrels. This assumption has been tested in other mutant mice examined previously in Dr. Kind's lab when sometimes C3 was analysed, and the same results were found when C2 was analysed. However a comprehensive study comparing the segregation of cells in all barrels has never been carried out.

The optical section of the, 20x zoom showing the best cell segregation is selected for analysis (fig M5.1 e & f). A line is drawn defining the perimeter of the SERT stained area (Fig M5.1 e). This enables 4 x 7 μm rectangles to be placed on the image both in the wall and in the hollow. When placed on the image 4μm should be less than the thickness of the barrel wall so that all cells inside the wall rectangles are part of the wall and not the hollow. The 'wall' rectangles are placed slightly overlapping the SERT border line so that they are positioned in the best place to include cells in the barrel wall.

Approximately 10 rectangles were placed in the barrel wall, and approx 7 in the barrel hollow. The rectangles placed in the wall need to be positioned with the long side closest to the centre of the barrel. Once positioned, rectangles are transferred to the image containing To-Pro-3 labelled cells (fig 5.1 f), and cells are marked with a red dot and counted if they overlap 2 sides of the rectangle or if contained within the rectangle (see fig M5.2).

The number of cells per rectangle and rectangles per hollow and per wall is noted for each barrel analysed. This enables the ratio to be calculated of cells in wall:hollow for each barrel. Numbers can be grouped by genotype and age and statistical analyses such as ANOVA with post-hoc Tukey Test performed using either Microsoft Excel or SPSS.

2.4.4 Method 4 'Counting cells in 3D using voxel analysis software Volocity'

This method uses data from the whole histological section rather than relying on choosing the optical section with the 'best segregation'.
Using the Leica confocal microscope images are captured at, 20x with an optimal number of optical stacks. This gives the best chance of being able to identify a cell while keeping the background fluorescence to a minimum. Optical images can be viewed in series allowing elimination of optical stacks that contain data beyond what is considered layer 4. The remaining optical stacks are imported into software programme 'Volocity' (www.improvision.com) and a 3D image can be constructed using data from the selected optical stacks. Volocity is a piece of software developed by biologists in Warwick to analyse images captured on confocal microscopes. It can perform many basic skills such as counting cells and making measurements of biological objects stained with fluorescence but its major advantage is its ability to analyse voxels (3D pixels). This means that a stack of optical images taken with a confocal microscope can be re-constructed to make a 3D image and instructions given to identify cells, shapes and tissues.

2.4.4.1 Preparation of tissue

Mice were perfused as described in section 2.3.1 and immunofluorescence carried out as previously described in section 2.3.2.

2.4.4.2 Image acquisition

The optimum method of capturing images in preparation for software analysis using Leica microscope was determined to allow accurate cell identification in the minimum of time. The images captured were an overall view of the barrel field using 5x objective scanning for 2 channels; wavelength 488 or 568 (β-Gal) and wavelength 647 (To-Pro-3). An image identifying the location of a particular barrel using 10x objective, a, 20x image of the barrel of interest and a 1.44zoom using, 20x to enlarge the barrel of interest and maximise data colleted from that barrel (Fig M6). For image analysis it is important that the same level of 'zoom' is used for each barrel.

2.4.4.3 Setting up software

A series of instructions is listed and saved as a 'protocol'. This protocol is optimised to enable identification of 'objects' in this case objects are cells labelled with To-Pro-3 and also cells labelled with β-Gal. It searches for groups of voxels in a particular colour touching one another and identifies them as a single 'object'. The protocol includes instructions to exclude objects smaller than 75um3, a figure determined to be the size of the smallest nuclei. It separates touching objects, reduces background fluorescence and lists the data in rows and columns. The protocol can measure 2 channels; To-Pro-3 in blue and β-Gal in green, and label 'objects' from each channel in different colours. Data from each object identified is listed in rows and columns and can be linked back to the original image, allowing visualisation of individual objects when clicking on the row of data associated. The data can also be viewed in the format of a histogram. The population of objects appears to be dispersed over 3 peaks in the histogram, and was found to be relating to single cells (peak 1), 2 cells together (peak 2) 3 cells together (peak3) etc. The mean volume of all objects within the first peak refers to the 'average cell volume' and this value is used to calculate the total number of cells in the image. There is some variation in the volume of a single nucleus, but this should be minimal when lots of cells are counted.

2.4.4.4 Image Analysis

First, the region of interest (ROI) is defined. This ROI is defined using a tool to draw around and select the area containing cells seen to be within a barrel. Figure M7 is a movie contructed using all voxel information. A barrel can be seen in the centre of the 3D image, and indicates where the boundaries lie between barrel wall and hollow. Drawing a further ROI along the boundary of the barrel wall and hollow allows the creation of 2 images, one containing the barrel hollow and the other containing cells in a ring, the barrel wall. Using the saved protocol, it can be applied to each image of a single barrel. Data displaying statistics on each object identified is saved as a 'Measurement Item' and exported into Microscope Excel for further

analysis. Once in excel, using the histogram the mean nuclei volume is determined and the volume of each object is divided by the mean volume. This gives a total number of cells identified in each channel.
Calculating a % of β-Gal positive neurons is achieved by this simple sum performed in excel.

$$\% = \frac{\text{No. of cells identified in channel 1(}\beta\text{-Gal)}}{\text{No. of cells identified in channel 2(To-Pro-3)}} \times 100$$

NB
While Volocity is useful in analysing small volumes of data, when it comes to analysing a whole barrel it's limitations are revealed. It is incredibly difficult to optimise the setting so that the software identified a cell correctly. While the human eye can often tell whether an object is two cells very close together, the programme needs to be able detect an invagination between the two objects. The programme relies on an accurate cell volume being entered, and cell volume varies to a huge extent within a barrel, due to the variety of cell types and shapes. When a large area of the barrel was analysed it was possible to easily see how cells had been mis-identified. The analysis software also took a long time to process a whole barrel and so optimising the software was a lengthy process. In conclusion, this method is useful in analysing small regions of the barrel but its accuracy cannot be relied upon for whole barrel.
Using volocity did identify defects in labelling with To-Pro and Fluorescent secondary 488λ. The collection of visual information is not exactly the same between the fluorophores and so it appears that To-Pro-3 stain is more superficial in the slice to fluor 488λ (fig M6 b). This effect is reduced if β-Gal is labelled with fluor 568λ, since the wavelength is closer to that of To-Pro-3 (647λ). A high power image with optical sections taken 0.8μm apart can be reconstructed to show this effect on a single cell (fig M8). This figure shows a cross section taken through the stack of images (fig M8 a). Separate images show a single cell inside a yellow square (fig M8 b, c & d). When the image is enlarged, the 'top-hat' effect of To-Pro-3 can be seen (fig M8 e, f & g). Analysis of this enlarged cell shows that depth in z-plane of cell is 12.23μm when labelled with To-Pro-3 and 11.38μm when labelled with β-Gal. A

difference in depth of cells will result in fewer β-Gal cells being counted when only a single optical slice is used for counting (as in counting method 3).

2.5 Why do the images of a nucleus labelled with two fluorophores not overlap?

The 'top-hat' effect described in the previous paragraph causes problems when a cell is at the top or the bottom of the z-plane of the collected data, as it may appear in one optical slice in one colour (and be counted) but not the other. An explanation for the difference in apparent optical slice thickness can be explained by the physics of microscopy. The thickness of the optical slice is influenced by numerous parameters of the microscope; pinhole size, refractive index, and the wavelength of the fluorophore. In the microscope used, a Leica TCS the pinhole changes depending on the objective used. Optical sections do not have well defined edges and the z-intensity profile is shaped like a bell. The thickness of an optical section is defined as the full width half maximum of this bell-shaped profile. The exact profile depends on

- correction of the optical components
- lens type
- refractive index
- matching of indices.

There are three explanations related to the parameters of the microscope that result in this effect. 1.) the thickness of the tissue that is illuminated by the laser in z-plane varies depending on which wavelength of fluorophore is being excited. 2.) Chromatic aberration 3.) A mis-match in refractive index due to light passing through air before it enters the lens.

2.5.1 Illumination thickness

The empirical section thickness can deviate from theoretical section thickness by 1/3 or more. An estimation for the illuminated section thickness can be obtained by the following formula. Note that this is the illuminated thickness, not the thickness of the collected information. The dz number is related to the wavelength of light, and is defined by parameters of the microscope.

$$dz = \sqrt{\left(\frac{0.88 \times \lambda}{n - \sqrt{n^2 - NA^2}}\right)^2 + \left(\frac{1.4 \times n \times PH}{NA}\right)^2}$$

n= refractive index of object =1

PH =This is the back-projected pinhole diameter and is calculated from pinhole diameter (r Phys=0.5) ÷ total magnification factor (Magnification of objective (20) x magnification of the system (4.5 for Leica TCS NT)) = 0.00555. However this is for a circular pinhole, but the leica TCS NT has a square pinhole. To convert circle to square, (when areas are equal) divide by 1.128.

NA = numerical aperture of objective which is 0.5 for a 20x objective

λ= emission wavelength in nm

green excited at 488, emission at 520nm

red excited at 568, emission at 600nm

blue excited at 647, emission at 670nm.

After entering the above parameters, the Zeiss microscope, for example gives

Fluorophore	Optical Slice
488nm	0.7µm
548nm	0.8µm
633nm	1.0µm

Therefore fluorophore 568 was used to reduce the differences in illuminated thickness between the 2 images.

This formula is based on theory and is only an estimate of the optical slice thickness. Therefore in this thesis data was presented as originally counted, with no alteration carried out. In the second last figure of chapter 3, an alternative histogram is presented to indicate the alteration in the spread of data that is predicted if the difference in optical slice thicknesses is causing less red nuclei than blue nuclei being counted.

2.5.2 Chromatic aberration

Different wavelengths of light focus at different distances from the lens creating a blur in the z-plane of an image. This is commonly demonstrated by passing light through a prism, and light is seen as a spectrum. For fluorescence this causes a lack of registration between channels in X, Y and in Z planes. Different types of lenses take this into account and correct for it. For example, a 'plan apochromat' can correct for 4-5 colours and field curvature, but is very expensive.

2.5.3 Refractive index

Since the objective used in imaging barrels was a 20x, the light must pass through air before entering the lens. Each wavelength is bent to different extents as it passes through air, increasing the difference seen due to chromatic aberration. This effect can be overcome by the use of an oil immersion lens, and since carrying out my experiments, the use of an oil immersion 20x has become normal procedure when imaging barrels for analysis.

2.5.4 Summary & Conclusions

As a result of investigating different models for analysing the density of cells in a barrel wall and hollow, the most accurate method has been revealed. Method 1 is useful as it provides information relating to the thickness of the wall. Method 2 has the advantage of being able to measure a barrel no matter how symmetrical it is. Both of these two methods cannot identify individual cells. Method 4 attempts to identify individual cells, but is time-consuming and inaccurate. However, using method 4 did reveal the inconsistency of the microscope in detecting optical thickness between the two fluorophores. It is clear that counting method 3 is the most reliable since it uses human judgement to decide the exact location of the barrel wall, and to determine exactly what is a cell. After consulting with other members of the Lab, we came up with a list of criteria that should be applied whenever a barrel is being analysed, to maintain consistency in technique.

1.) Nucleus must be labelled with To-Pro-3 so that either the whole nucleus is densely labelled or there are at least 2 'freckles'. Freckles are dense patches of blue labelling within the cell and are where To-Pro-3 binds chromatin in nuclei.
2.) Nucleus must be roughly spherical in appearance.
3.) Nucleus must be of similar size to other surrounding nuclei (approx 10μm diameter).

4.) Nucleus can be counted if it falls entirely within the counting rectangle.
5.) Nucleus can be counted if it touches either of the two walls that are decided to be ‘counting walls’ or either of the two corners that are decided to be ‘counting corners’.
6.) Nucleus must NOT be counted if it touches any of the 2 ‘non-counting-walls’ or 2 ‘non-counting-corners’.

However, some of these criteria require a judgement that is subjective, and so the method is not perfect.

2.6 Counting perineuronal nets in layer 4 of cortex

2.6.1 Histology

One hemisphere was dissected to produce a tangential flattened cortex as described in general methods, and the other hemisphere was prepared for coronal sections. Each piece of tissue was left for at least 24 hours in 30% sucrose in PBS solution for cryoprotection. For coronal sections, 48μM sections were taken using the freezing microtome and every 4^{th} section was collected for each of the 4 treatments. One quarter of sections were mounted onto gelatin-coated slides and stained for Nissl, while the other 3 quarters were incubated in primary monoclonal antibodies Cat-301 (1:80), Cat-315 (1:40), & Cat-316 (1:200) diluted in DMEM with 5% FCS and 2% Triton overnight. For details on Nissl staining technique and immunohistochemistry procedure see general methods. After staining, the sections were mounted on gelatin-coated slides, dehydrated and coverslipped in DPX. Cortices that were dissected for tangential flats were sectioned on freezing microtome at 48μM. Each section was placed serially in wells containing PBS and incubated in Cat-3XX antibody overnight. Primary antibodies were labelled as described in general methods and sections were mounted on gelatin coated slides, dehydrated and coverslipped in DPX. Sections containing the somatosensory cortex were photographed using a leica microscope with digital camera. Sections were photographed using a 1.6X, 5X, & 10X objective and cells were counted using a 40X objective. Sections labelled for parvalbumin and Cat-315 were placed in primary antibodies overnight (PVA 1:500) and Cat-315 (1:40) with 0.5% Triton, and primary antibodies were labelled with fluorescent secondaries Alexa fluor anti-mouse 488 and Alexa fluor anti-rabbit 568, and placed in 90% glycerol 10% PBS containing nuclear marker To-Pro-3 to clear overnight and label nuclei. Images were captured on Leica Confocal (Leica Microsystems, Heidelberg GmbH)

2.6.2 Analysis

Procedures for choosing the section to analyse and placement of counting rectangles in S1 are described in general methods. In order to be able to count a PNN the following criteria must be met.
(a) There must be a dense area of immuno stain in the shape of a peri-neuronal net (PNN), a mesh – like formation surrounding the nucleus and proximal dendrites.
(b) A cell body shape must be seen within the area of immuno stain, most easily seen when focal plane is altered.
(c) Immuno stain must fall within the counting rectangle, with the location of the centre of the PNN determining whether it was 'in' or 'out'.
Raw data consists of number of counting rectangles used, and number of PNNs counted per section. Using Microsoft excel an average density of PNNs in adult S1 in each genotype was presented in a bar chart with standard error bars, and student's t-test were performed on the mean density.

Adult sections that have been immunostained for Cat-315 & Cat-316 have perineuronal nets (PNNs) in layer 4 of cortex. For analysis, the density of PNNs is counted. Coronal sections are chosen that contain PMBSF and where barrels are clearly visible in the corresponding Nissl section. Under 40x objective on the microscope, the section is positioned so that the eyepiece graticule covers PNNs in layer 4 (fig M9). The focus needs to be constantly altered so that PNNs in all depths of field can be counted. The number of PNNs is recorded, along with a number of graticule 'rectangles' that are used to count in each section. This enables a density to be calculated per mm^2. Data is entered into Microsoft excel and mean, standard error and t-test can be carried out comparing wild-type to mutant. Data is presented in bar charts for each antibody and mouse line.

2.7 Methods Figures

Figure M1.1

Dissection of brain to produce flattened cortex for tangential sections.

A: Dorsal view of brain. Red line indicates cut for bisection of hemispheres

B: Lateral view of left hemisphere

C: Red line indicates cut for removal of cerebellum

D: Red line indicates cut for removal of archicortex and midbrain

E: Ventral view of left hemisphere. Using curved forceps hippocampus and any remaining striatum are removed

F: Cortex ready for flattening

G: Using light pressure applied through a microscope slide the piece of cortex is flattened onto the freezing microtome stage, the surface of which is prepared with a piece of blotting paper and fixed in position using 30% sucrose/PBS.

Figure M1.2

Dissection of brain to produce a hemisphere for coronal sections

A: Dorsal view of brain. Red line indicates cut for bisection of hemispheres

B: Lateral view of left hemisphere

C: Red line indicates cut for removal of cerebellum

D: Red line indicates removal of olfactory bulbs

E: Left hemisphere ready for mounting on stage

F: Using a microscope slide to keep brain upright, left hemisphere is placed caudal-side down onto the freezing microtome stage, the surface of which is prepared with a piece of blotting paper and fixed in position using 30% sucrose/PBS.

Figure M2

Coronal sections used to take measurements of lamination of cortex.

A: Section from AS region of barrel cortex stained for Nissl. 3 measurements are taken of whole cortical thickness (layer 1-6) through region where barrels are visible.

B: Section from PMBSF region of barrel cortex stained for Nissl. 3 measurements are taken of whole cortical thickness (layer 1-6) through region where barrels are visible.

C: Section from AS region of barrel cortex stained for calretinin. 3 measurements are taken of layers 1-4 and of layer 5-6 through region where barrels are visible.

D: Section from PMBSF snout region of barrel cortex stained for calretinin. 3 measurements are taken of layers 1-4 and of layer 5-6 through region where barrels are visible.

E: Section from AS region of barrel cortex stained for PKARIIβ. 3 measurements are taken of thickness of layer 4 through region where barrels are visible.

D: Section from PMBSF snout region of barrel cortex stained for PKARIIβ. 3 measurements are taken of thickness of layer 4 through region where barrels are visible.

Figure M3.1

Example of Image J editing process to produce images that can be analysed by rectangles method.

A: SERT labelling of TCAs in barrel C2

B: To-Pro-3 labelling of nuclei in barrel C2

C & D: Images are rotated so that long side of C2 is vertical and converted to 8-bit (black and white)

E & F: Images are cropped and re-sized so that barrels width is always 500 pixels & normalised for intensity of white/black.

G: Rectangle is drawn on SERT image through region of C2 that does not contain short sides of barrel.

H: Rectangle is transferred to image of To-Pro-3 cells.

I: Pixel intensity analysis is performed across width of rectangle

Figure M3.2

Summary of data from normalised pixel intensity plot profiles across width of barrel C2.

A: Data from *Sap102/Psd-95* mutants at P7/8. Orange line (*Sap102KO Psd-95 HET*) does not dip in central region of graph (hollow) indicating there is a more uniform distribution of pixels across the width of a barrel in these mice (corresponding to a less-well segregated barrel).

B: Data from Sap102/Psd-95 mutants at P14/15. Orange line (*Sap102KO Psd-95 HET)* does dip in the hollow region of this graph but dips further away from barrel walls, indicating barrel walls are thicker in these mice.

Figure M4.1

Example of Image J editing process for producing images which can be analysed by concentric circles method.

A: SERT labelling of TCAs in barrel C2

B: To-Pro-3 labelling of nuclei in barrel C2

C & D: Images are rotated so that long side of C2 is vertical and converted to 8-bit (black and white)

E & F: Images are cropped and re-sized so that barrels width is always 500 pixels & normalised for intensity of white/black.

G: A line is drawn on edges of SERT patch

H: SERT boundary line is transferred to image containing To-Pro-3 labelled cells, and macro is performed.

Figure M4.2

Example of 2 images of layer 4 cells labelled with To-Pro-3 from litter-mates processed together. Variation in background leads to pixel intensity analysis being inaccurate for determining cell density.

A: Background is low and pixel analysis will be accurate.

B: Background is high and pixel analysis will not be accurate.

Figure M4.3

Graph to show ratio of pixel density in wall:hollow of *Sap102/Psd-95* mutants when analysed by method 'pixel density along lines placed through barrel wall and hollow'. *Sap102 KO Psd-95 Het* ratio is significantly different from WT (t-test black bars p=0.0035, grey bars p=0.03). Similar results are seen when either one or two hollow measurements are taken.

Black bars: ratio of wall:one hollow measurement

Grey bars: ratio of wall:average of 2 hollow measurements

Figure M5.1

Example of process of identifying barrel C2 and collecting images in preparation for counting cells.

A: Image taken using 5x objective to show PMBSF labelled with SERT and To-Pro-3. Scale:, 200μM

B: Image taken using 10x objective to show barrel C2 in centre. Scale bar: 100μM

C: Image taken using, 20x objective to show barrel C2 in centre. Scale bar: 50μM

D: Image taken using digital zoom on, 20x to capture whole of C2 in image. Scale bar:

E: SERT-labelled image of C2 showing placement of rectangles in barrel wall and hollow.

F: To-Pro-3 labelled image of C2 showing placement of rectangles in wall and hollow and yellow dots identifying cells which fall into criteria of size, shape, brightness and location in rectangle.

Figure M5.2

Barrel C2 stereological counting techniques

A: Schematic showing position of rectangle and red dots on cells which are to be counted. Cells positioned under rectangle line are counted only if they fall under 2 lower sides and 2 corners anti-clockwise from lower sides.

B: Schematic of PMBSF showing position of barrel C2 (red)

Figure M6

At high power To-Pro-3 and β-Gal do not appear to colocalise even though they are labelling the same cells.

A: Sequence of optical sections collected from barrel C2 0.8μM apart. Cells are labelled with ant-β-Galactosidase antibody and To-Pro-3. Blue To-Pro-3 cells are visible in optical sections prior to β-Gal cells while β-Gal cells are visible in optical sections after To-Pro-3 is no longer visible.

B: 'Top-Hat' effect where To-Pro-3 cells appear to be sitting on top of β-Gal cells. Large image is the image of a single optical section of a 0.8μM stack. Cross hairs in large image indicate position from which images in panels to right and below are taken through z-stack of image.

Figure M7

Movie available to view on enclosed disc.

Movie shows rotating 3D reconstruction of barrel C2 using at least 50 optical images captured 0.8μM apart. Volocity programme is used to reconstruct images into 3D and identify and count cells.

Figure M8

Figure to show Z-plane through stack of images collected of barrel C2 labelled with β–Gal and To-Pro-3.

A: Schematic to show position within a 3D reconstruction of the images given in b and c.

B: Images of barrel C2 in Z plane. A single cell is surrounded by a yellow box. Due to the parameters of the microscope, the two labels do not completely co-localise to the same cell body. Scale 25μm.

C: There is a 'top-hat' effect where cell labelled with To-Pro-3 appears above β-Gal labelled cell. Measurements of cell diameter through z-axis are taken to be: a 12.23μm (To-Pro-3), b 11.38μm (β-Gal). Scale 5μm.

Figure M9

Figure to show placement of counting grid in Layer 4 S1 cortex for counting of PNNs labelled with Cat-315 and Cat-315. The number of PNNs was counted in each rectangle and density 'per rectangle' calculated. This was then translated into number of PNNs per mm^2.

3 Data Chapter One:

Small G-protein and ERK-MAPK signalling in barrel formation

3.1 Introduction

During early postnatal development, the neurotransmitter glutamate plays an important role in the activity-dependent development of the somatosensory system. Glutamate is the most commonly found neurotransmitter at excitatory synapses and plays major roles in signalling at thalamocortical synapses. Glutamate acts on ionotropic NMDARs, kainate receptors, AMPARs and metabotropic receptors (mGluRs). Although all these receptors are multi-functional, in general, AMPARs are primarily involved in the transmission of action potentials, while NMDARs and mGluRs activate 'signal transduction' pathways that alter neuronal phenotype, including strengthening or weakening of the synapse by modifying the proteins in the post-synaptic density (PSD) and/or by initiating actin cytoskeleton rearrangements. The PSD complex is highly organised and disruptions can have wide ranging effects.

Identification of members of the NRC/MASC has been carried out over the last few years by various labs; Grant and the G2C team at the Sanger Institute (Grant, 2006), Sheng and colleagues at Howard Hughes MI (Sheng, 1996), Kennedy and colleagues at CIT, Pasedena (Kennedy, 1997), and Gundelfinger and colleagues at Magdeburg, Germany (Boeckers et al., 2002). These studies have identified several key signalling molecules and pathways within NRC/MASC that regulate development and plasticity. These include small G-proteins (i.e. Ras, Rap, Rho) and their regulatory enzymes (GTPase Activating Proteins (GAPs) and Guanine exchange factors (GEFs)) as well as their downstream targets (i.e. mitogen-activating protein kinase (MAPK)). The adenyl cyclase/cyclic AMP (AC/cAMP) signalling pathways also play a key role in translating signals from glutamate receptors into physiological and anatomical changes during development and both of these pathways have been implicated in learning and memory and plasticity deficits observed in several neurodevelopmental diseases (Wang et al., 2007, Davis and Laroche, 2006). One approach to study the role of individual NRC/MASC members is mice by genetically altering or deleting the protein in mice (Grant, 1996).

This investigation is part of an ongoing collaboration with G2C to identify NMDAR signalling pathways that regulate cortical development. Here investigation of one of the G-protein signalling pathways was carried out by examining mice with null mutation of a RhoGAP (RICS), two RasGAPs (SynGAP and NF1) and an ERK phosphatase (Dusp6).

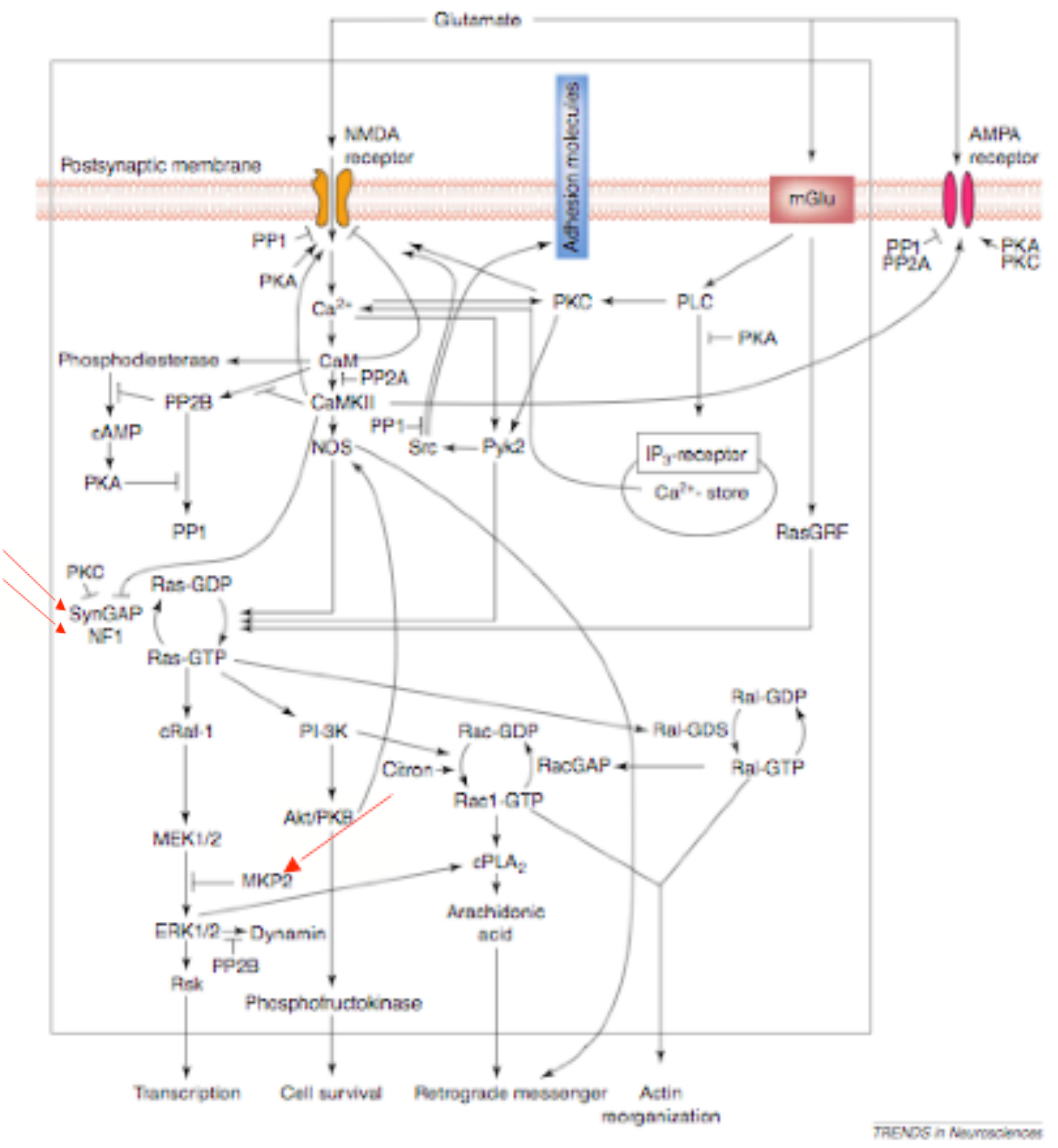

Diagram 5 **Overview of signalling pathways in the NRC/MASC**

Red arrows indicate molecules SynGAP, Nf1 & Dusp6 (here MKP2) (diagram taken from Husi and Grant, 2001).

The aim was to determine their contribution to the formation of barrels, a well-defined model of early development that requires the accurate translation of glutamate signalling into anatomical and physiological alterations. First, each molecule investigated will be introduced. All molecules are present in developing cortex and are downstream of NMDAR signalling (see diagram 5), and most have previously defined roles in modulating plasticity, or activity dependent processes in early development.

3.1.1 The RasGAP SynGAP

A 135/143 kDa **Syn**aptic **G**TPase **A**ctivating **P**rotein, SynGAP was identified in 1998 (Chen et al., 1998, Kim et al., 1998) and is an abundant member of the NRC/MASC. SynGAP is phosphorylated via NMDAR-dependent CaMKII (Oh et al., 2004) and its activation leads to inactivation of Ras and Rap GTPs (Ras; Kim et al., 1998, Chen et al., 1998, Rap; Krapivinsky et al., 2004). When activated by neurotrophins or intracellular calcium (such as that resulting from repeated NMDAR activation), Ras signalling is essential for activation of the cascade leading to MAPK phosphorylation (Finkbeiner and Greenberg, 1996) (see diagram 6). Rap signalling can act as an inhibitor to Ras signalling perhaps by competing for binding of downstream targets of Ras, and can be activated by AC/cAMP and PLC pathways (Reuther and Der, 2000).
There are 5 distinct splice variants of *Syngap* detected and published so far, each with unique C-terminal tails (see diagram 7). $\alpha 1$ has a PDZ-binding domain that binds CaMKII via MUPP1 (Krapivinsky et al., 2004). All variants have a C2 domain involved in calcium-dependent phospho-lipid binding, a plextrin-homology (PH) domain that also binds phospholipids and may play a role in membrane recruitment and a GAP domain responsible for activating Ras or Rap GTPases. The GAP domain is necessary for formation of normal synapses in culture, as is the ability of SynGAP to bind PSD-95 and other MAGUKs by its c-terminal t-T/SXV domain.
SynGAP is selectively expressed in brain (Kim et al., 2003, Vazquez et al., 2004). Two *Syngap* KOs have been generated, both homozygous mutants die shortly after birth, and heterozygotes are viable and have decreased activity-dependent LTP (Kim et al., 2003, Komiyama et al., 2002) and a reduced rate of spatial learning (Komiyama et al., 2002). SynGAP is essential for the formation of barrels in

Diagram 6 **Schematic to show function of RasGAP SynGAP**

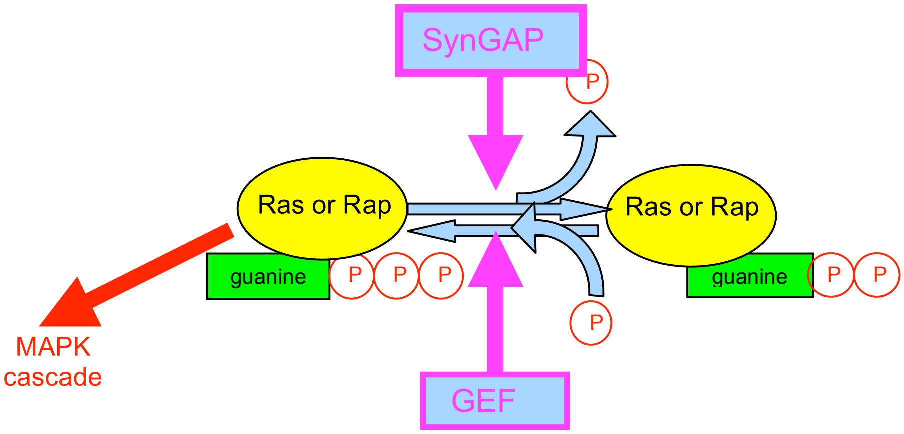

KEY	Name	Action
SynGAP	GTPase activating protein of Ras/Rap GTPases	Down regulates Ras/Rap signalling
guanine P P P	Guanine Tri-phosphate	Binds Ras/Rap GTPase is activated
guanine P P	Guanine Di-phosphate	Binds Ras/Rap GTPase is inactivated
Ras or Rap	Ras/Rap family of small GTPases	Activates MAPK cascade
GEF	Guanine exchange factor	Reverses GAP

This diagram was created using information from Chen et al., 1998, Kim et al., 1998.

somatosensory cortex. In homozygotes TCAs segregate into rows but not patches and layer 4 cells are uniformly distributed- they do not show any pattern. In heterozygotes TCAs segregate into barrel-related patches but layer 4 cells do not segregate completely, the cells partially form barrels but the ratio of density of cells wall: hollow is much less (+/- 1.2 vs +/+ 1.8) (Barnett et al., 2006). To investigate why *Syngap* KO mice die, conditional mutant mice were created using the cre/loxP system under the control of α-CaMKII promotor (Knuesel et al., 2005). This promotor drives expression in excitatory forebrain neurons beginning at about 1 week after birth. In the conditional KO, neurons gradually lose SynGAP protein from postnatal week 1 and loss is maximal by 3 weeks of age. Mice analysed fell into two groups; those that lose 75-80% of SynGAP protein and die by 3 weeks of age, and those that only lose 60% of SynGAP protein and survive, but with a high number of hippocampal neurons undergoing apoptosis (Knuesel et al., 2005). In these mice, expression of Cre recombinase is restricted to forebrain excitatory neurons, leaving interneurons with normal expression of SynGAP, hence the incomplete loss of

SynGAP protein. SynGAP is therefore essential for preventing cell death and for survival of the mouse.

KO embryonic neurons can be maintained in culture even though KO mice die by P7. KO hippocampal neurons show signs of developing prematurely (Vazquez et al., 2004); spines are larger and clusters of synaptic proteins PSD-95, AMPARs and NMDARs are seen in spines at 10DIV when in wild-type neurons they are mostly located to the dendritic shaft. KO neurons have increased synaptic strength due to an increased frequency of AMPAR-mediated mEPSCs (Rumbaugh et al., 2006). A decrease in AMPAR clusters is seen in *Syngap* over-expressing neurons, suggesting that SynGAP regulates glutamate signalling by the regulation of synaptic AMPARs (Rumbaugh et al., 2006). In *Syngap* KO hippocampal and cortical neurons ERK activation is up-regulated while p38MAPK function is depressed, while in *Syngap* over-expressing neurons ERK activation is decreased and p38MAPK activation is increased, indicating that SynGAP is essential for maintaining a balance of MAPK activity, probably via specificity of Ras/Rap activity. The ERK-MAPK cascade is involved in mediating synaptic plasticity; it is involved in initiating and maintaining LTP (Brambilla et al., 1997, Sweatt, 2001 a & b) and in cultured neurons regulates pathways leading to immune responses and cell death. CaMKII phosphorylates SynGAP and is critical for NMDAR-dependent LTP, making SynGAP an important target for research investigating mechanisms of plasticity and learning and memory. CaMKII, Ras and Rap GTPases, ERK, p38MAPK & PI3 Kinase all contribute to the regulation of AMPAR trafficking to synapses. Of these molecules, SynGAP has been shown to regulate or be regulated by all except PI3K (Zhu et al., 2002, Rumbaugh et al., 2006). It is likely that MAPK signalling is a mechanism through which SynGAP regulates AMPAR insertion and function, spine shape, ability to undergo LTP and behaviour, since ERK-MAPK has previously been implicated in these mechanisms and SynGAP regulates ERK-MAPK (Krapivinsky et al., 2004, Komiyama et al., 2002, Rumbaugh et al., 2006). MAPK signalling leads to a variety of outcomes due to the PSD having microdomains. This allows MAPK pathways to be compartmentalised to allow an appropriate response (Brown and Sacks, 2008). Other molecules in the NRC/MASC modulate the ERK-MAPK pathways that may lead to barrel formation.

Diagram 7 SynGAP C-terminal splice variants

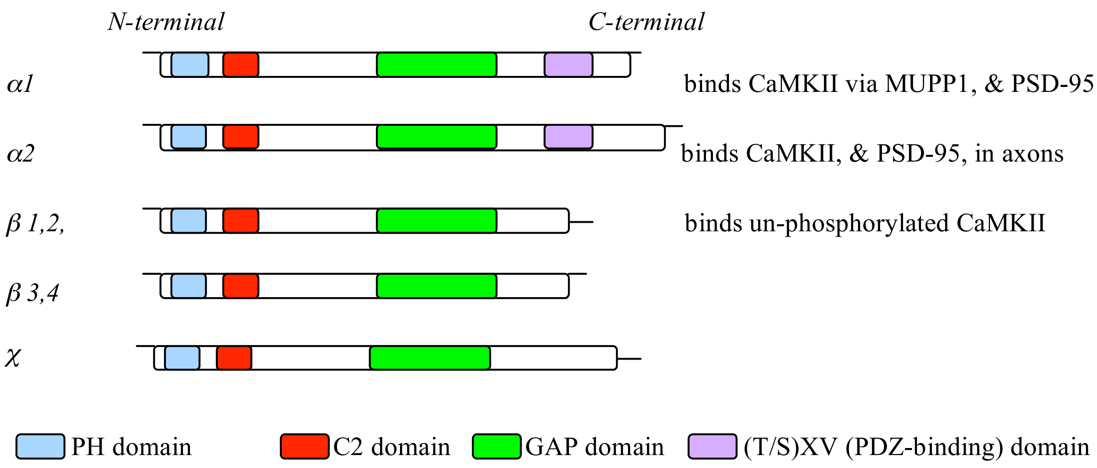

(Diagram constructed using information from Li et al., 2001)

Here investigation of the effects of NF1 and Dusp6 on barrel formation will be carried out. The aim is to determine whether the defect in formation of barrels in *Syngap* mutants is rescued or accentuated by additional mutations to either Dusp6 or NF1, two other molecules acting to negatively regulate ERK signalling.

3.1.2 The RasGAP NF1

Neurofibromatosis type 1 (NF1) is a RasGAP from the same family as SynGAP. It is a tumour suppressor protein that has a RasGTPase activation domain, and activates MAPK and PI3K pathways (see diagram 8). Genetic alterations inactivating the GAP domain result in the condition neurofibromatosis type 1 (Viskochil et al., 1990, Wallace et al., 1990), which affects 1 in 3500 individuals worldwide (Cichowski & Jacks, 2001, Zhu and Parada, 2001). Most individuals develop astrocytic tumours, but some have intellectual deficits (Costa and Silva, 2003) and autism spectrum disorders (Mbarek et al., 1999, Marui et al., 2004).

The GAP-related domain (GRD) of NF1 is located in the central region of the 220-250kDa protein (DeClue et al., 1991, Gutmann et al., 1991) (see diagram 9). NF1 is highly expressed in neurons, Schwann cells and oligodendrocytes (Daston et al., 1992) and is located

Diagram 8 **Schematic to show function of RasGAP NF1**

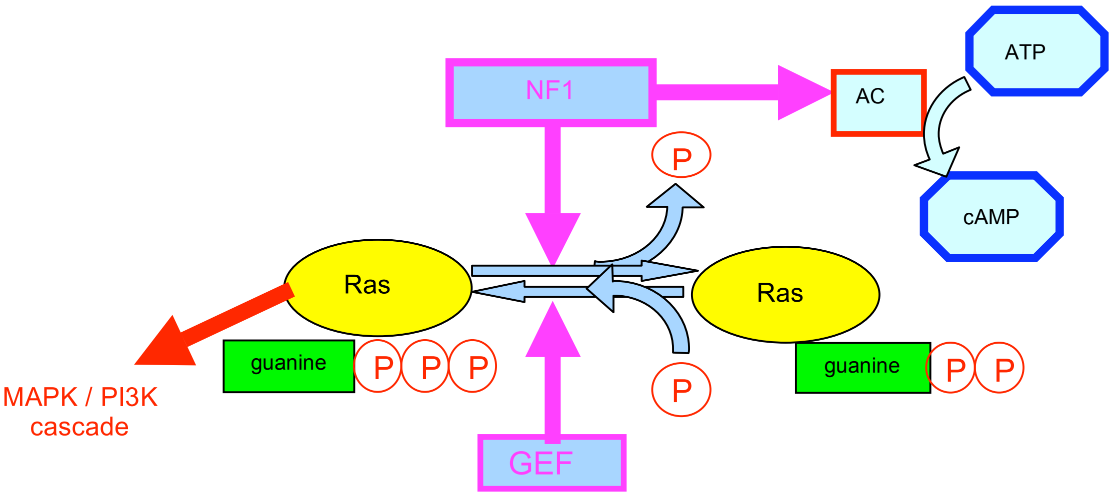

KEY	Name	Action
NF1	GTPase activating protein of Ras GTPases	Downregulates Ras signalling, activates AC
guanine P P P	Guanine Tri-phosphate	Binds Ras GTPase is activated
guanine P P	Guanine Di-phosphate	Binds Ras GTPase is inactivated
Ras	Ras family of small GTPs	Activates MAPK/PI3K cascade
ATP	Adenosine tri-phosphate	When dephosphorylated releases energy
cAMP	cyclic adenosine mono-phosphate	Active form, can activate Protein Kinase A
AC	Adenyl Cyclase	Converts ATP to cAMP
GEF	Guanine exchange factor	Reverses GAP

This diagram was created using information from Hsueh, 2007 (review)

Diagram 9 **NF1 protein domains**

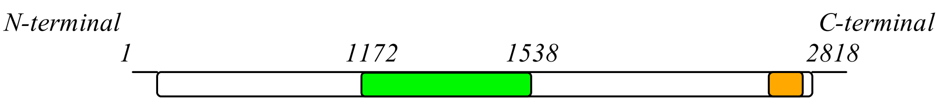

300-residue GAP-related domain (GRD) C-terminal domain

in the cytoplasm. NF1 was identified to be a member of the NRC/MASC (Husi et al., 2000), making it an ideal candidate for regulating plasticity and disease-related processes at the synapse. The major function of NF1 is via its GRD domain on Ras, but also acts on a Ras-independent pathway, via its GRD and the C-terminal domain (see diagram 9). The C-terminal domain regulates adenyl cyclase/cAMP signalling

(Ho et al., 2007), which can activate PKA. PKA is known to be involved in learning and memory, and its RIIβ subunit plays a key role in the formation of barrels in cortex (Inan et al., 2006, Watson et al., 2006).

Deletion of the *Nf1* gene in mouse results in embryonic lethality by E13.5 due to heart defects (Brannan et al., 1994, Jacks et al., 1994). Heterozygotes are prone to develop tumours but do not exhibit other symptoms of the human disease (Jacks et al., 1994). Although *Nf1* global KOs die embryonically, *Nf1* heterozygotes and or *Nf1* conditional KOs are useful tools to investigate the function of NF1 in the synapse as models of Neurofibromatosis 1. This study will utilise the *Nf1* heterozygotes to look for an interaction between NF1 and SynGAP and Dusp6. All 3 molecules negatively regulate the Ras-MAPK pathway at different levels, and SynGAP has already been found to be necessary for barrel formation. Analysing the barrel cortex of double-mutants will reveal whether any two of these molecules act on the same pathway necessary to barrel development, and will reveal whether there are additional defects by further disruption ERK-MAPK signalling.

3.1.3 The ERK phosphatase Dusp6

Dual-**sp**ecificity phosphatases (Dusps) are a subset of the protein tyrosine phosphatase (PTP) 106-member superfamily. They were first identified in 1993 by having dual phosphatase activity on the threonine *and* tyrosine residues on MAPK and are sometimes referred to as MKPs or MAPKPs (MAPK Phosphatases) or DSPs (see diagram 10). There are 48 members originating from different genes in the family and their specific expression patterns help to regulate the size and magnitude of a MAPK-mediated physiological response in different cells and tissues (Jeffrey et al., 2007). Dusps can be further subdivided into Class 1 (nuclear, 4 exons) Class II (cytoplasmic, 3 exons) and Class III (preferentially recognise JNK and/or p38MAK). Many of the Dusps have functions in modifying immune responses and are increasingly becoming targets for drug discovery to treat inflammation in cancers, HIV and infectious diseases. Of the 48 members, so far 15 Dusps (Dusps 1-10, 12, 14, 18, 22 & 26) have been found to regulate MAPK activity.
Dusp6 protein is 42 kDa, the gene has 3 exons and is categorized in Class II of the subclasses of Dusps, along with Dusp 7 & 9. It is also known as MAPK Phosphatase

Diagram 10 **Schematic to show function of phosphatase Dusp6**

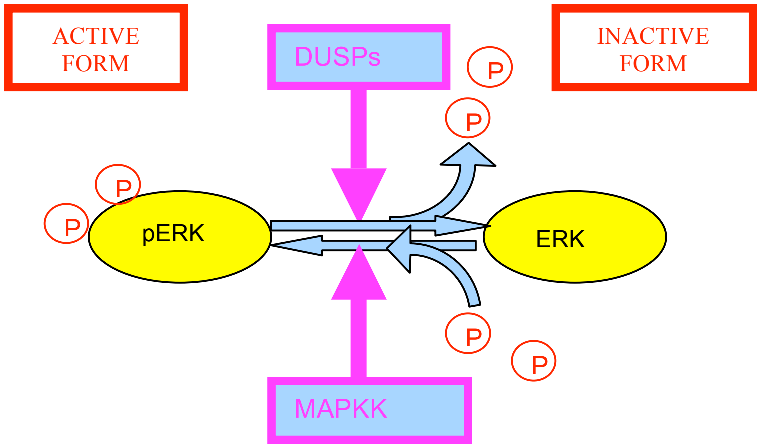

KEY	Name	Action
	Dual-specificity phosphatases	De-phosphorylates Thr and Tyr residues on MAPKs
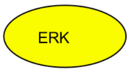	Mitogen-Activated Protein Kinase	Inactive form of MAPK
	MAPK Kinase	Phosphorylates MAPK - works in opposition to Dusps.
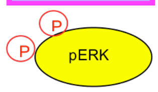	Phosphorylated MAPK	Activated form of MAPK, leads to gene transcription

This diagram was created using information from Jeffrey et al, 2007 (review)

3 (MKP3), Pyst1 and rVH6 (Mourey et al., 1996). Dusp6 is expressed highly in lungs, and at low levels in heart, brain, spleen, liver, kidney (Muda et al., 1998) and neuromuscular junction (NMJ) (Nazarian et al., 2004) and is implicated in neuronal and muscle cell differentiation. It is localised in the cytoplasm of cells and when expressed in cos7 cells has preferential specificity for inactivating extracellular signal-regulated kinase 1/2 (ERK1/2) (see diagram 10), and low specificity for the stress-activated kinases c-Jun NH_2-terminal kinase (JNK) and p38MAPK (Muda et al., 1996). In vivo Dusp6 is unable to inhibit responses that result from stress-mediated activation of JNK-1 or p38 MAPK, suggesting that ERK1/2 is the main target in vivo (Groom et al., 1996).

Dusp6 contains a nuclear export signal and causes ERK2 to be retained in the cytoplasm (see diagram 11). This function is dependent upon both its nuclear export signal and its KIM motif that binds MAPK (Karlsson et al., 2004). This is one of the first discoveries that Dusps play a role in the localisation as well as the dephosphorylation of MAPK.

Diagram 11 Dusp6 protein domains

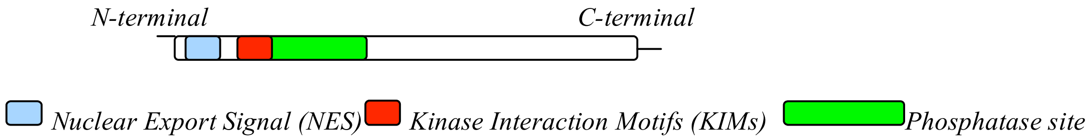

The first *Dusp6* mouse mutant was described in 2007 (Li et al., 2007), and was found to have a number of phenotypes. The *Dusp6* mutation can cause postnatal lethality. When offspring from a +/- x +/- cross were genotyped at weaning there was a slightly lower representation of 22% -/- offspring in F1 and 18% in F2 rather than the Mendelian-expected 25%. Approximately 40% -/- and 15% +/- mice were smaller than wildtypes (less than 75% body mass of wt) and when P5-15 mice were stained to reveal cartilage and bone, these mice were found to have premature fusions of the cranial sutures (coronal craniosynostosis). However, most -/- and +/- mice were normal in size and these mice did not exhibit coronal craniosynostosis. This is a condition in which the sutures of the skull close to early causing problems in brain and skull growth. In a similar pattern, small mutants but not normal sized ones have hearing loss (Li et al., 2007), probably also due to skull defects.

Dusp6 is in a unique position to directly mediate ERK responses that may result from NMDAR stimulation. In mouse visual cortex ERK has been shown to play a role in OD plasticity and in NMDAR-dependent LTP (Di Cristo et al., 2001). ERK is also involved in hippocampal LTP (Winder et al., 1999) and memory (for review, see Adams & Sweatt, 2002). SynGAP has been shown to regulate the ERK pathway through its role as a RasGAP (Komiyama et al., 2002). Since Dusp6 inactivates ERK, removal of Dusp6 is likely to cause an increase in activated ERK. Therefore removing Dusp6 from *Syngap* KOs or heterozygotes may enhance the defect of increased ERK activation, resulting in an accentuation of the phenotype seen in *Syngap* mutants. However it is possible that SynGAP mediates the formation of barrels through an ERK-independent pathway (Barnett et al., 2006), therefore loss or reduction of Dusp6 would not be expected to affect the *Syngap* mutant phenotype. Evidence for SynGAP acting on an alternative pathway comes from electrophysiological studies where *Syngap* heterozygotes show defects in LTP induction (Komiyama et al., 2002) when protocols are used that are ERK-independent in wildtype slices (Winder et al., 1999, Watabe et al., 2000). However, no evidence has been shown that Dusp6 acts on kinases other than ERK1/2 and so it is unlikely that Dusp6 is acting on this ERK-independent pathway that SynGAP regulates.

Dusp6 mutants were also made at the Sanger Institute as part of the investigation into the role of NRC/MASC complex molecules in learning and memory, plasticity and disease. *Dusp6* -/- mice have been previously investigated and have normal barrels (Kind et al., unpublished observations). However the analysis did not quantify the extent of segregation of cortical cells into barrels, nor did it take into account body size and so it is quite possible that those analysed were of normal body size and may not have exhibited abnormal phenotypes that may have been present in smaller mutants. Dusp6 negatively regulates ERK, one of the key activators of both SynGAP and NF1. Therefore it is possible that a *Dusp6* mutation will cause greater disruption to barrel formation than a *Syngap* or *Nf1* mutation alone. To investigate regulatory interactions between Dusp6 and SynGAP and NF1 and to see whether any pair act on the same pathway in barrel formation, double mutants were created and analysis carried out on somatosensory cortex.

3.1.4 The RhoGAP RICS

Following the discovery that spines change their shape in response to NMDAR activity there was a rush to identify the pathways and molecules involved (reviewed in Bonhoeffer and Yuste, 2002). The Rho family of GTPases regulate actin cytoskeleton modifications and are likely candidates for NMDAR dependent anatomical modifications (Newey et al., 2005, Tada & Sheng, 2006). Abnormal dendritic structure and spine morphology often coincides with mental retardation (MR) so understanding the molecules involved in regulating dendrites and spines is key to understanding diseases such as MR (Newey et al., 2005).

Diagram 12 **Schematic showing function of RhoGAP RICS**

This diagram was created using information from Lamarche and Hall, 1994, Hall, 1998,

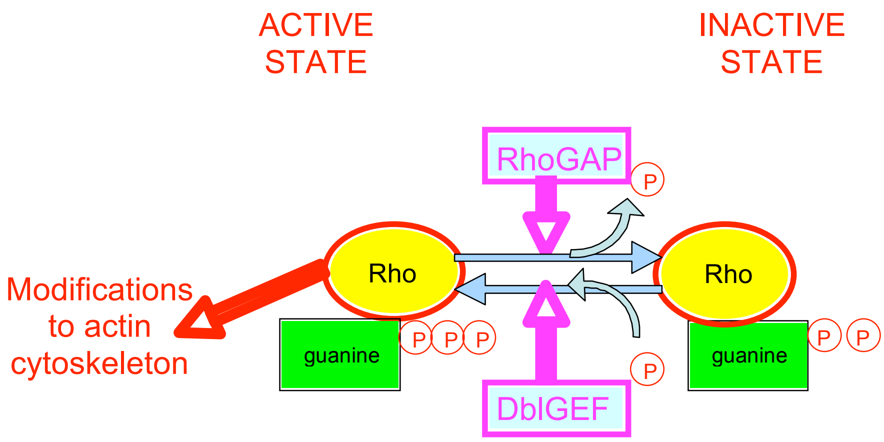

KEY	Name	Action
Dbl GEF	Guanine nucleotide exchange factors of Dbl family	Activates Rho GTPases
RhoGAP	GTPase activating protein of Rho family of GTPase	Inactivates Rho GTPases
guanine P P P	Guanine Tri-phosphate	Binds Rho GTPase becomes active
guanine P P	Guanine Di-phosphate	Binds Rho GTPase becomes inactive
Rho	Rho family of small GTPs (e.g. RhoA, Rac1, Cdc42)	Contols actin dynamics

RhoGTPases are small molecules that are active when bound to GTP, and inactive when bound to GDP. Rho **G**TPase **A**ctivating **P**roteins (RhoGAPs) inactivate small G-proteins by catalysing their endogenous GTPase activity resulting in a conversion to the inactive GDP-bound state (see diagram 12). GEFs carry out the reverse – they activate small G-proteins by causing the GDP-bound form to become GTP-bound. Activation of NMDARs therefore results in the inactivation of small G-proteins via the activation of GAPs (i.e. SynGAP). Enhancing the activation of RhoGTPs results in modifications to actin cytoskeleton, such as those needed to alter spine shape.

Identifying RhoGAPs became the focus to understanding the pathways leading to cytoskeletal modifications, and resulted in numerous groups identifying the same proteins and giving them names as they thought appropriate. RICS, an abbreviation for '**R**hoGAP **I**nvolved in the β-**C**atenin-N-Cadherin and NMDAR **S**ignalling' was identified in 2003 and defined by its role in NMDAR signalling (Okabe et al., 2003). RICS was previously named 'Grit' by the same Japanese group (Nakamura et al., 2002), when they identified a RhoGAP that regulates NGF-induced neurite extension through its interaction with TrkA. This regulation involved activating Rac1 and suppressing RhoA when NGF was applied to PC12 cells expressing RICS. As RhoA was the preferred target for RICS GAP activity, it suggests RhoA is the significant regulator of neurite extension in this assay.

A smaller-mass RICS was named p200RhoGAP by a second group at the same time (Moon et al., 2003). The RhoGAP domain of the p200 RICS stimulates RhoA and Rac1 activity in vitro and in vivo. Interaction studies found that RICS was capable of binding to the Src homology 3 domains of tyrosine kinases Src, Crk and PLCχ in vitro, raising the possibility that its activity may be regulated through these interactions.

Meanwhile a third group identified an NMDAR-associated larger-mass RICS and named it 'p250GAP' (Nakazawa et al., 2003). Nakazawa and colleagues continue to publish using 'p250GAP' as the name and have identified spine regulatory functions of RICS using knock-down of *Rics* in primary cultured neurons (Nakazawa et al., 2008). These neurons have increased spine width, a phenotype that was described in cultured *Syngap*$^{-/-}$ neurons (Vazquez et al., 2004). Over-expressing *Rics* in these neurons results in a decreased spine width and increased spine length (Nakazawa et al., 2008), suggesting that RICS has a role in keeping spines from maturing too rapidly. In response to NMDAR activation of primary cultured hippocampal neurons, GFP-tagged *Rics* redistributed from spine necks to spine heads, indicating that it plays an essential role in initiating a response to NMDAR activation. The NMDAR-mediated modulation of spine morphology was found to be a result of RICS acting via the RhoA pathway and not via Rac1 or Cdc42. GCGAP is another name given to RICS, and the antibody used by this group identifies a smaller protein of approximately 200kDa (Zhao et al., 2003). Until recently, it was not known that the two different sized proteins (200 and 250kDa) originate from the same gene. When mouse brain is lysed and immunoprecipitated with anti-RICS antibody, a doublet of

2 bands can be seen on a western blot (Okabe et al., 2003). They turn out to be 250 & 210 kDa and correspond to PX-RICS (250kDa) and RICS (210kDa), the protein product of two splice variants of the *Rics* gene (Hayashi et al., 2007) (see diagram 13).

Diagram 13 *Rics* Splice Variants

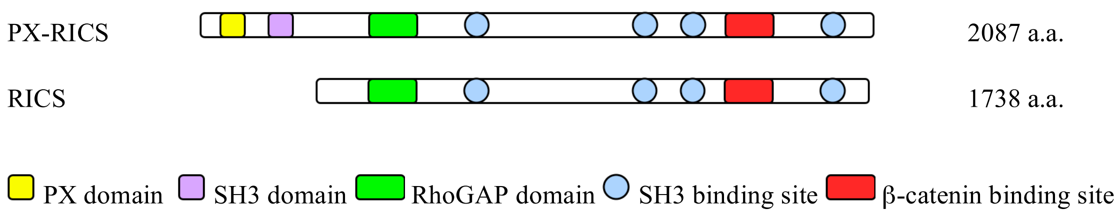

Adapted from Hayashi et al., 2007

Hayashi and colleagues carried out a number of expression and interaction studies on both RICS and PX-RICS. Both variants are expressed in brain, and PX-RICS is also present in lung, kidney and spleen at relatively low levels. Co-IP experiments indicate that both variants are associated with β-Catenin, PSD-95, N-Cadherin and NR2B in vivo (Hayashi et al., 2007). The PX-domain is specific to PX-RICS and is thought to interact with phosphatdylinositides to regulate its GAP activity. PX-RICS is present in brain from E13, while RICS is not detected until 2 weeks postnatal (Hayashi et al., 2007). Both are detected at the tips of axons, but the early expression of PX-RICS suggests that this form is important in early development. Primary neurons that lack both forms of RICS have longer neurites that wildtypes, and this function is attributed to both variants (Hayashi et al., 2007). When NIH3T3 cell lines are transfected with PX-*Rics* and *Rics*, both have an inhibitory effect on neurite outgrowth (Hayashi et al., 2007). This is likely to be due to their inactivation of RhoGTPases, inhibiting the processes leading to increases in actin cytoskeleton growth. β-Catenin links cadherins and the actin cytoskeleton and has functions modulating synaptic structure and cadherin adhesion. The interaction of RICS with this complex and also with NMDARs and PSD-95 suggest that it is through this interaction that modifications of the synapse occur (Okabe et al., 2003). NMDARs and PSD-95 are both important for the formation of normal barrels in layer 4 of cortex. The cortex-specific *Nr1* KO does not form normal barrels (Iwasato et al.,

2000) and MAGUKs PSD-95 and SAP102 bind SynGAP to NMDARs. SynGAP is also a GTPase activating protein and acts on Ras and Rap GTPases. In the context of this complex, RICS was found to act on Cdc42 & Rac1, rather than on Rho A as found in *Rics* knock-down cultured neurons. The *Rics* knock-down cultures were prepared from hippocampus primary neurons (Nakazawa et al., 2008), while the β-catenin – N-cadherin – NMDAR complex was identified by IP studies using adult brain homogenate (Hayashi et al., 2007) - a likely explanation for the spine differences.

The regulation by NMDAR activity and the fact that RICS is involved in neuronal development as part of the NRC/MASC complex raises the possibility that RICS is essential in NMDAR signalling pathways that results in normal barrel formation, perhaps in a similar way to the way SynGAP acts.

3.1.5 Summary of key findings leading to specific aims

The role of the RhoGAP 'RICS' in barrel formation has not been previously investigated, but RICS is regulated by NMDARs and interacts with PSD-95 and NMDARs at the synapse. In culture *Rics* knockdown neurons have a similar phenotype to *Syngap* KO neurons, suggesting that RICS may act on similar pathways to SynGAP. SynGAP is required for development of barrels in layer 4 and heterozygotes also have abnormal barrels (Barnett et al., 2006). NF1 is a RasGAP and in humans mutations inactivating the GAP domain are responsible for the neurofibromatosis 1 condition. *Nf1* KOs do not survive beyond birth, but cortex-specific KOs survive and have abnormal barrels (Lush et al., 2008). Dusp6 inactivates ERK and is part of a large family of Dusps. Preliminary experiments found that barrels form in *Dusp6* KOs (Kind et al., unpublished data). To further investigate the role these molecules play and their potential interactions with other molecules in the NRC/MASC, *Rics* knockouts and double mutants of each combination of *Syngap*, *Nf1*& *Dusp6* were created. The offspring include mice with a number of different genotypes that were analysed at P7, the time by which barrels have normally formed.

3.1.5.1 Specific aims of this chapter

This chapter uses new mutants of NRC/MASC components to try to understand which molecules and pathways are necessary for formation of barrels. In this chapter the mutants analysed are the RhoGAP *Rics*$^{-/-}$, and double-mutants *Syngap*/*Nf1*, *Syngap*/*Dusp6* and *Dusp6*/*Nf1*. It attempts to decipher whether these molecules show genetic interaction and hence whether they are part of a common pathway that regulates barrel formation.

3.2 Results

3.2.1 Lamination is normal in *Syngap/Nf1* double mutants

Measuring the thickness of different layers of the cortex gives an indication of whether there are defects in cortical development (e.g. division and/or migration of cortical neurons, or defects in cell death). Abnormal lamination could also reflect abnormal innervation of the cortex. Reduced thickness of upper layers of cortex could signify a delay in cortical development as the cells in the upper layers continue to migrate into their final position. Alternatively, reduced overall cortical thickness could be representative of a smaller brain, or could be indicative of gross cortical defects. Measurements of cortex in P7/8 wild type, *Syngap*$^{+/-}$, *Nf1*$^{+/-}$ and *Syngap*$^{+/-}$ *Nf1*$^{+/-}$ were made on images of coronal sections through PMBSF and AS stained with Nissl, calretinin and PKARIIβ. Nissl labels cell bodies enabling cortical layers to be identified due to the different cell densities in each layer. In PMBSF of all genotypes layer 4 is visible due to the increase in the cell density and the lack of large pyramidal-shaped cell bodies. Furthermore, cell-dense bands extending radially can be seen in layer 4 corresponding to barrel walls in some coronal Nissl-stained sections (see arrows, fig 1.1). The barrel walls are less clearly obvious in *Syngap*$^{+/-}$, and *Syngap*$^{+/-}$ *Nf1*$^{+/-}$ indicating that barrels may not be fully formed (arrow heads, fig 1.1). Measuring total cortical thickness from Nissl-stained sections shows no difference in thickness between any genotypes in PMBSF and AS regions (fig 1.1-1.3). Cortical thickness is higher in AS region compared to PMBSF region as the anterior cortex has thicker upper and lower layers, with layer 4 being the only layer which is reduced in the anterior brain (fig 1.3). Calretinin stained sections show an immuno-positive stripe corresponding to the layer 4 and 5 border, immediately ventral to barrels in PMBSF and AS of S1 (fig 1.1-1.12). Measuring the thickness of upper layers 1-4 and lower layers 5-6 shows no differences between any genotypes indicating that the cortex is maturing normally in each mutant (fig 1.3). PKARIIβ stained sections show a diffuse stain throughout most brain regions. There are darker patches of immunostain in layer 4 corresponding to barrels. Measurements of the thickness of layer 4 as delineated by the PKARIIβ immunostain reveals no difference in thickness between any genotype (Fig 1.1-1.2). This is consistent between measurements taken in AS region and PMBSF (fig 1.3).

3.2.2 Normal levels of NF1 are required for formation of normal barrels.

As previously described, *Nf1*$^{-/-}$ die before birth (Brannan et al., 1994, Jacks et al., 1994). I examined whether the effect of reducing levels of NF1 altered cortical development by examining mice with a null mutation of one copy of this gene. As described in the previous paragraph, layers 1-6, 1-4, 5-6 and layer 4 all have normal thicknesses (fig 1.3) indicating that there are no obvious defects in cell migration, cell density, cell cycling or innervation in the cortex. Nissl stain of flattened P7/8 cortices shows that, qualitatively, sell soma segregate normally into cell-dense walls and cell-sparse hollows with a pattern that corresponds to the whisker array on the facepad (fig 1.4). Barrels in both PMBSF and AS also appear qualitatively normal, as seen in serial sections from 3 separate brains (fig 1.4). However, quantification of density of cells in barrel C2 wall and hollow was carried out and revealed that cells in *Nf1*$^{+/-}$ mutants do *not* segregate properly into barrels (fig 1.5 a & b). Segregation of cells in layer 4 into barrels is reduced from that of 1.63±0.06 (*Nf1*$^{+/+}$, n=3) to 1.29±0.02 (*Nf1*$^{+/-}$, n=4). This result indicates that normal levels of NF1 are necessary for normal formation of barrels. Measuring the area taken up by TCA patches as labelled with αSERT antibody gives an indication as to whether TCAs are innervating the correct cortical area. Measurements of the area of patches corresponding to barrels B, C & D2-3 are taken to be representative of the area taken up by the whole of PMBSF. TCAs form discrete patches within cell dense walls and no differences are seen in the area taken up by B, C & D2-3 between WT (0.24 mm^2 ±0.01, n=4) and *Nf1*$^{+/-}$ (0.24 mm^2 ±0.01, n=4) (fig 1.5c).

3.2.3 The absence of one copy of *Syngap* does not accentuate or rescue the defect seen in *Nf1* heterozygotes

Reduction of SynGAP in mice on MF1 background results in poor segregation of cells into barrels (Barnett et al., 2006). SynGAP and NF1 are both members of the RasGAP family that regulate ERK. I hypothesised that SynGAP and NF1 regulate barrel formation via the same downstream signalling pathway (i.e. ERK). As a first step in testing this hypothesis I examined double mutants to determine whether there was an interaction (either additive or rescue effect) of reducing both SynGAP and NF1.

Barnett and colleagues reported a decrease in segregation of layer 4 cells in PMBSF in *Syngap*$^{+/-}$ mice on MF1 background (Barnett et al., 2006). The present experiments were carried out using mice on a Bl/6 129 mixed background, therefore I first re-examined the phenotype of the *Syngap*$^{+/-}$ mice on this background. Sections from P7/8 flattened cortices were labelled for SERT to reveal TCA patches and To-Pro-3, a fluorescent nuclear marker. Cell dense barrel walls are clearly visible surrounding a cell-sparse SERT-labelled hollow (fig 1.5). The SERT patches are discrete indicating that there are no major defects in TCA innervation and segregation into barrel-specific patches. To determine whether there is a quantifiable defect, density of cells in wall and hollow in barrel C2, and area of SERT patches were calculated. In this study, ratio of cells wall:hollow gave results of +/+ (1.63±0.13, n=2) and *Syngap*$^{+/-}$ (1.42±0.24, n=3) (fig 1.5 a & b). Analysis of the area taken up by the SERT patch shows that TCAs innervate the same area of layer 4 in *Syngap*$^{+/-}$ (0.24 mm^2 ± 0.02, n=2) as in WT (0.24 mm^2 ± 0.01, n=4) indicating that TCA innervation is not affected by the mutation. The small number of animals meant that t-tests cannot be performed, however there does appear to be reduced segregation in the *Syngap*$^{+/-}$ mice although the decrease is less severe than that published on the MF1 background (*Syngap*$^{+/+}$ 1.8; *Syngap*$^{+/-}$ 1.2; Barnett et al., 2006). However, more than two *Syngap*$^{+/-}$ mice were analysed in this study – the additional mice came from the breeding of *Dusp6* & *Syngap* double-mutants. If these *Syngap*$^{+/-}$ mice are included in the analysis, the n-numbers for *Syngap*$^{+/-}$ mice are increased from 2 to 4. *Syngap*$^{+/-}$ density ratio is 1.38±0.1 (n=4) and +/+ density ratio is 1.59±0.06 (n=8) and the difference is close to significance (p=0.1, student's t-test) (fig 1.14). It is possible that if more brains were analysed, this trend would show significance. Power analysis indicates that 13 samples of each genotype need to be analysed for a significant result, given the trend continues. Power analysis was carried out using the freely available software GPower. In performing this analysis assumptions are made about the data. First, that the data is normally distributed about the mean and second that the few samples collected are representative of the population. This analysis is not very reliable when only two samples are collected as the chances such a small number being representative are slim. Also, while it may be valid to assume that data on wildtype tissue is normally distributed about the mean, there is no basis for assuming that mutant data is normally distributed. Results from this analysis can be found in appendix III table 7. Therefore it is always preferable to collect as much data as possible before carrying out a power analysis.

I next examined the double mutants. *Nf1*$^{+/-}$*Syngap*$^{+/-}$ mice have barrels very similar to those seen in *Syngap*$^{+/-}$ or *Nf1*$^{+/-}$ alone (fig 1.5 a & b). Barrels were still visible and there is a ring of dense cells surrounding a SERT-labelled patch. The density ratio in *Nf1*$^{+/-}$*Syngap*$^{+/-}$ is 1.35±0.07 (n=6) compared to +/+ of 1.63±0.13 (n=3). This difference is approaching significance (p=0.08, student's t-test), indicating that there may be a difference if more animals had been analysed. When WT animals from other pairings were added into this analysis then the difference between +/+ (1.63±0.13 (n=8)) and *Nf1*$^{+/-}$*Syngap*$^{+/-}$ (1.35±0.07 (n=6)) is significant (p=0.03, student's t-test) (fig 1.17). In *Nf1*$^{+/-}$*Syngap*$^{+/-}$ mutants the area of patches B, C & D 2-3 taken to be representative of PMBSF area as labelled with SERT antibody is normal (*Nf1*$^{+/-}$*Syngap*$^{+/-}$ area=0.24 mm^2 ± 0.01, n=6; WT area =0.24 mm^2 ± 0.01, n=4)(fig 1.5 c) indicating that the double-mutation does not affect TCA innervation and segregation into barrel-specific patches.

3.2.4 Dusp6 and NF1 together are not necessary for normal development of barrels

Dusp6 negatively regulates ERK-MAPK signalling and could be involved in barrel formation through similar pathways that NF1 and SynGAP act on. Dusp6 inactivates ERK and further up stream, NF1 and SynGAP GAP activity results in inactivation of ERK. Therefore it is possible that removing Dusp6 results in a similar phenotype to removing NF1 or SynGAP. It is also possible that reducing Dusp6 accentuates the effect seen by reducing NF1 or SynGAP. While *Dusp6* mutants were previously examined, the defect was never quantified, and so first an analysis of this mutation was carried out.

3.2.4.1 Dusp6 KO

To examine whether cortical development occurs normally in *Dusp6* mutants, tissue was taken from P7/8 *Dusp6*$^{-/-}$ and *Dusp6*$^{+/-}$ mice and labelled with Nissl, calretinin and PKARIIβ. Measurements were taken of layer 1-4 and 5-6 thickness and layer 4 thickness from images of stained coronal sections in PMBSF and AS regions. Nissl labelling reveals cell bodies in all layers of the cortex and general anatomy of cortical layers appears normal. Dense radial bands of cells are seen in layer 4 labelled with Nissl corresponding to barrel walls.

Only one *Dusp6*$^{-/-}$ brain was analysed in this study due to the breeding arrangements, meaning that the KOs were rarely generated. The one *Dusp6*$^{-/-}$ brain was stained for Nissl, calretinin and PKARIIβ and measurements of cortical layers were taken. The mutant brain analysed had hydroencephaly (images not shown), resulting in thinner upper and lower layers in the cortex, most detectable in posterior regions of cortex (fig 1.8 a, c & g). It is not clear how common this condition is in *Dusp6*$^{-/-}$or at what stage the hydroencephaly occurs. Preliminary qualitative experiments carried out by Kind and colleagues before this study did not detect any abnormalities in barrel formation and did not report occurrences of hydroencephaly in *Dusp6*$^{-/-}$, indicating that this one brain is not representative of most *Dusp6*$^{-/-}$. Previous publications find that cranial abnormalities occur in 40% of mice analysed at P5-15 and this varies with background (Li et al., 2007). However, despite hydroencephaly layer 4 does not appear reduced in thickness (although no statistical analysis could be carried out on one brain) indicating the brain forms layer 4 normally at the expense of other layers. Layer 4 is more cell dense than other layers and may therefore not be compressed so easily when the brain is under pressure. TCAs innervate layer 4 and segregate normally into barrel-specific discrete patches (fig 1.9 c). Cells in layer 4 segregate into cell-dense walls surrounding the TCA patch and the cells co-localising with the SERT-labelled patch are at a much lower density (fig 1.9 a & b). Interestingly, *Dusp6*$^{-/-}$ mouse has normal layer 4 thickness and well-segregated barrels, despite other layers being thinner as a result of hydroencephaly (fig 1.8g, 1.9a & b).

3.2.4.2 Dusp6 heterozygote

Measurements of the thickness of cortices in PMBSF and AS regions show no differences between *Dusp6*$^{+/-}$ and wildtype. Calretinin stain labels a population of cells at the boundary of layer 4 and 5 in S1, allowing the thickness below and above this boundary to be measured. Analysis of both in *Dusp6*$^{+/-}$ and wildtype showed that layer 1-4 thickness in PMBSF is slightly but significantly reduced in *Dusp6*$^{+/-}$ (383.0±2.8μm) compared to WT (398.7±2.3μm) (p=0.03 t-test) (fig 1.8 g) indicating that the effect seen on lamination in *Dusp6*$^{-/-}$ may be in part independent of hydroencephaly, and may be also due to reduced Dusp6 protein levels. A reduced thickness of upper cortical layers can be an indication of an immature cortex since upper layers form later than lower layers. Cortical layers 5-6 are normal in thickness in AS and PMBSF in *Dusp6*$^{+/-}$. However, *Dusp6*$^{+/-}$ *Nf1*$^{+/-}$ mice have normal layer 1-4 thickness (fig 1.8g) indicating that reduction of NF1 corrects the defect seen in *Dusp6*$^{+/-}$. PKARIIβ labelling reveals a band of staining corresponding to barrels in layer 4 in both PMBSF and AS regions. This labelling appears normal in *Dusp6*$^{+/-}$ (fig 1.6 & 1.7) and measurements of the thickness of this band indicate layer 4 is not affected by reduction of Dusp6 (fig 1.8).

3.2.4.3 Dusp6/NF1 double mutants

Analysis of mice with two mutations; *Dusp6*$^{+/-}$ *Nf1*$^{+/-}$ may reveal whether the two proteins are acting on the same ERK-pathway involved in barrel formation, resulting in an additive effect on the phenotype. Flattened tangential sections at P7/8 were labelled with a TCA marker SERT and a fluorescent nuclear marker To-Pro-3. Analysis was carried out of segregation on cells in barrel C2, assumed to be representative of the segregation of all barrels in PMBSF. Mice with reduced Dusp6 and reduced NF1 (*Dusp6*$^{+/-}$ *Nf1*$^{+/-}$) still form normal barrels in PMBSF. To-Pro-3 labelled cells appear to be denser in cell walls and surround the TCA patch. Quantitative analysis reveals a slightly reduced segregation of layer 4 cells into wall and hollow in *Dusp6*$^{+/-}$ *Nf1*$^{+/-}$ compared to +/+ littermates but the difference is not significant (Fig 1.9 a & b). The reduced segregation is more likely to be due to NF1 reduction than Dusp6 reduction as *Dusp6*$^{-/-}$ mouse has barrels very similar to +/+ despite hydroencephaly. Unfortunately *Nf1*$^{+/-}$ from this mixed breeding were not analysed for barrels (see section 3.2.2 for *Nf1*$^{+/-}$ analysis). TCAs segregate normally and the area of PMBSF represented by area of patches B, C & D 2-3 is normal when both Dusp6 and NF1 are reduced (fig 1.9 c). This suggests that the reduced amount of both of these proteins is still sufficient for the segregation of TCA patches and the formation of barrels in layer 4, and indicates that these two proteins are not acting on the same molecular pathway.

3.2.5 The absence of one copy of *Dusp6* does not accentuate or rescue the trend towards a defect seen in *Syngap* heterozygotes.

To test whether Dusp6 acts on the same molecular pathway downstream of glutamate as SynGAP, the development of the cortex and formation of barrels in double mutants were analysed. Both proteins negatively regulate ERK-MAPK signalling and it is possible that this pathway could be involved in formation of barrels; therefore reducing both proteins might further disrupt barrel formation. As found with *Dusp6* mutants analysed previously when bred with *Nf1* mutants (fig 1.8 & 1.9), *Dusp6*$^{+/-}$ have no lamination defect or defect in barrel formation (fig 1.12 & 1.13). As described previously, *Syngap*$^{+/-}$ show a trend towards poorly segregated barrels (ratio 1.35±0.02) but this difference is not significant (p=0.26 t-test), due to a low number of *Syngap*$^{+/-}$ being analysed (n=2) (fig 1.13 a & b). When combined with data from *Syngap*/*Nf1* mutants, n=4 in *Syngap*$^{+/-}$ and the trend continues to a greater extent, with p=0.1 (fig 1.14), indicating that if more were analysed a significant difference would be detected. When Dusp6 is reduced or absent in *Syngap*$^{+/-}$, lamination still occurs as normal (fig 1.10-1.12), but the ratio of cell density is low similar to *Syngap*$^{+/-}$, (*Syngap*$^{+/-}$*Dusp6*$^{+/-}$ ratio =1.22±0.02 (n=2), *Syngap*$^{+/-}$ *Dusp6*$^{-/-}$ ratio =1.25 (n=1)) but numbers of animals are too low for statistical analysis (figure 1.13 a & b). In all mutants the area of patches B, C & D 2-3 labelled with SERT antibody is normal (figure 1.13 c), indicating that TCA innervation and segregation into patches is not affected by this mutation.

3.2.6 RICS does not influence lamination of the cortex

Measuring the thickness of different layers of the cortex give an indication of whether there are defects in division or migration of cortical neurons, or defects in cell death or cell cycling. Abnormal lamination could also reflect abnormal innervation of the cortex. Reduced thickness of upper layers of cortex signifies an immature cortex, as upper layers are formed after lower layers. The cortex of P7/8 *Rics*$^{-/-}$ looks very similar to *Rics*$^{+/+}$ (fig 1.15a&b), all layers appear to have formed normally. Measurements of the separate layers of the cortex reveal that there is a trend towards a thinner cortex labelled by Nissl in *Rics*$^{-/-}$ in AS (p=0.14) and PMBSF region (p=0.48), (fig 1.16), with both upper (AS p=0.85, PMBSF p=0.054) and lower layers (AS p=0.05, PMBSF p=0.15) being thinner in *Rics*$^{-/-}$ and layer 4 being thicker (AS p=0.25, PMBSF p=0.3) (fig 1.16). However, none of the differences seen between *Rics*$^{+/+}$ and *Rics*$^{-/-}$ give significant p- values when t-tests are performed (p-values given above, +/+ n=4, -/- n=3). If increasing the number of samples analysed confirmed that this mutation does result in altered lamination then further analysis could be carried out to determine whether cell density or cell body size is altered in different cortical layers.

3.2.7 RICS is expressed in layer 4 somatosensory cortex but is not necessary for the formation of normal barrels, or segregation of TCAs into normally sized patches.

When *Rics* mutants were generated the LacZ gene was inserted as a reporter. The protein product of the *LacZ* reporter, β-Galactosidase (β-Gal) is detected in layer 4 *Rics*$^{+/-}$ (fig 1.17c), indicating that RICS is expressed in barrels. β-Gal does not seem to be as highly expressed in barrel walls as hollows and further analysis needs to be performed to determine the precise intercellular location of β-Gal. Nissl stain of flattened cortex shows cells in *Rics*$^{-/-}$ segregate normally into cell-dense walls and cell-sparse hollows (fig 1.17a). Serial sections through flattened Nissl-stained cortex show that barrels that are not visible in one section appear in the next section in both +/+ and -/- (fig 1.17a). Sections from 3 separate mice of each genotype labelled with a fluorescent nuclear stain show that barrels have cell dense walls and hollows at higher magnification (fig 1.18), and quantification of cell density ratios of wall: hollow confirms that there is no significant difference between *Rics*$^{+/+}$ (1.55± 0.07) and *Rics*$^{-/-}$ (1.54± 0.06) in (fig 1.18 b & d). SERT immunohistochemistry shows that thalamic axons innervate and segregate normally into discrete patches within each barrel in layer 4 (fig 1.17b). Quantification of the area covered by 6 barrels, taken to be representative of the area of PMBSF shows no significant difference between *Rics*$^{+/+}$ and *Rics*$^{-/-}$ (fig 1.18 c & e).

3.3 Discussion

3.3.1 RasGAPs and dual specificity ERK phosphatases

3.3.1.1 Nf1

The RasGAP NF1regulates signalling at the synapse by acting as a GTPase Activating Protein on RasGTPs to negatively regulate ERK-MAPK and also via a Ras-independent pathway on AC/cAMP signalling. AC/cAMP and ERK-MAPK pathways are intertwined and may not always function independently. For example, PKA phosphorylates Rap1 (Lerosey et al., 1991), a small G-protein upstream of ERK. SynGAP also acts by negatively regulating the ERK-MAPK signalling pathway so it is possible reduction of both molecules together causes further disruption to barrel formation. *Nf1* KOs die, and data presented here shows that a reduction in NF1 (*Nf1*$^{+/-}$) results in a failure of cells to segregate normally into barrels; therefore NF1 is involved in barrel formation. While this thesis was being written, a paper confirming our hypothesis about the role of NF1 in barrel formation was published (Lush et al., 2008). Cortical conditional KOs of NF1 were created using the Cre/loxP system, under the control of hGFAP promoter. When NF1 is absent from the majority of cortical neurons and astrocytes, the cortex is thinner but with the same number of cells, and barrels do not form in layer 4 (Lush et al., 2008). Thalamic axons do not have *Nf1* deleted and patches do segregate but appear smaller (similar to those seen in *CxNr1* mutants), suggesting that the axons require appropriate signalling back from layer 4 cells to prune branches and elaborate to the correct extent. NF1 may regulate the formation of barrels through either its Ras activity (as demonstrated is possible with SynGAP) or through it's activation of cAMP (as demonstrated is possible with PKARIIβ). Together with results presented here, this paper by Lush and colleagues indicates that NF1 may have a dose-dependent effect on barrel formation.

To further understand the role NF1 plays specifically in neurons, conditional KOs were created where *Nf1* is deleted in neurons (*Nf1*$^{\mathrm{SynI}}$KO) using synapsin I as a Cre-driven promoter (Zhu et al., 2001). Like the cortex-specific mice, *Nf1*$^{\mathrm{SynI}}$KO mice have a reduced cortical thickness, an increase in cell density in cortex and reduced lamination. This suggests that *Nf1* deletion in neurons results in a migration defect. While *Nf1*$^{\mathrm{SynI}}$KO mice do not develop tumours, they exhibit an abnormal increase in the number of astrocytes at the expense of neurons (astrogliosis), even though *Nf1* is not deleted from astrocytes, suggesting cell-non-autonomous role by neurons lacking *Nf1* (Zhu et al., 2001). Heterozygote mice with deleted *Nf1* on one allele also have abnormalities (Rizvi et al., 1999, Gutmann et al., 2001).

Data here along with findings from Lush and colleagues indicates that NF1 may act in a dose-dependent manner on pathways required for barrel formation. The pathway is likely to be ERK-independent but not necessarily Ras-independent since RasGTPases may act ERK-independently via other MAPKs such as p38MAPK and PI3K or via AC/cAMP pathways.

It was interesting to see that *Nf1*$^{+/-}$*Syngap*$^{+/-}$ mice have abnormal barrels, but to no further extent than *Nf1*$^{+/-}$. This indicates that SynGAP and NF1 do not have an additive effect, that is that one allele of either (or both) is sufficient for barrels to partially form, but the ratio of cell density in wall:hollow is significantly different from controls. Loss of two alleles of one (or of both we presume, should they survive) results in complete loss of formation of barrels (Barnett et al., 2006, Lush et al., 2008). The defect created by having only one allele of *Nf1* is saturated and cannot be further accentuated by loss of quantity of other RasGAPs, only by loss of further NF1 *(Nf1*$^{-/-}$).

3.3.1.2 SynGAP

The RasGAP SynGAP regulates signalling downstream from NMDAR and plays a crucial role in the formation of barrels, as well as in hippocampal LTP, anatomy of spines and postnatal survival (Komiyama et al., 2002). The barrel mutation in *Syngap* mutants was described in transgenic mice on MF1 background (Barnett et al., 2006); in this study mice were largely C57 Bl/6 (with 25% or 12.5% 129). It has been reported extensively that mutant phenotypes are not always reproducible on different backgrounds (Owen et al., 1997, for example). In this study there is a trend for *Syngap*$^{+/-}$ mice having less well-segregated barrels but the difference from wildtype is not significant with n=4 *Syngap*$^{+/-}$. The lack of a significant result may well be due to the fact that the mutation is on a different background, likewise it may be due to there being too much variance in the group, which should be reduced if there were more samples analysed. Evidence for this comes from the combined mutation of *Syngap* with *Dusp6* - the trend towards a defect in *Syngap* mutants is not altered. It is still less than wildtype but not significantly so.

3.3.1.3 Dusp6

Dusp6 is further downstream in the MAPK cascade relative to the GTPase activating proteins SynGAP and NF1 that are being investigated. Dusp6 inactivates ERK1&2. By itself, Dusp6 does not regulate the development of barrels. Preliminary investigations indicated that *Dusp6*$^{-/-}$ have normal barrel development. Due to the nature of the cross being set up between *Dusp6* mutants and the other two mutants, the probability of generating *Dusp6*$^{-/-}$ was low and only one *Dusp6* KO was created. Despite the brain being swollen due to hydroencephaly, barrels still form normally, albeit with reduced thickness of cortex. This phenomenon has been demonstrated before in a preliminary study (not presented here) with MUPP1 mutant mice (a multi PDZ-domain scaffolding protein in the NRC/MASC). MUPP1 KO brains are large due to hydroencephaly but TCAs still reach layer 4 and barrels still form. Hydroencephaly in *Dusp6* mutants may be due to coronal craniosynostosis. Previous studies of *Dusp6* mutants found that some knockouts and heterozygotes are smaller and suffer from this condition (Li et al., 2007). The *Dusp6* mutation also can cause hearing loss. Mutations that result in inappropriate activation of fibroblast growth factor receptors (FGFRs) result in similar phenotypes. FGF signals can be amplified through ERK signalling pathways, and FGF activation of FGFRs results in di-phosphorylation of ERK1/2 on the Thr/Tyr residues upon which Dusp6 acts. FGF signalling also occurs in areas of the embryo that express Dusp6, indicating a link in regulation (Dickinson et al., 2002), in fact; FGFRs are required for transcription of Dusp6 (Li et al., 2007). Dusp6 was recently found to be present at the neuromuscular junction (NMJ) and its expression is enhanced during regeneration (Nazarian et al., 2005). At the NMJ ERK1 signalling is essential for normal structure and function; ERK1 transmits downstream signals through v-Crk and v-Crk mutants have abnormal NMJs. However, the function of Dusp6 in this mechanism is not yet fully understood.

In this study, body mass was not recorded and bone structure was not described when brains were removed. *Dusp6* heterozygotes were also created from breeding of

Dusp6 mutants with *Nf1* mutants and *Syngap* mutants, and have barrels with cells segregated to the same extent as wildtype. When combined with other mutations of *Nf1* and *Syngap*, reduction of Dusp6 does not accentuate or rescue any defects seen, emphasising the theory that ERK activation does not regulate the formation of barrels. An alternative explanation may be that Dusp6 is expressed in different cells or synapses to SynGAP and NF1. Further investigations would need to be carried out to determine the exact sub-cellular location of each molecule. The Dusp family of proteins is extensive and many act of ERK-MAPK. Therefore it is possible that other Dusps compensate when Dusp6 is reduced or absent.

Unfortunately, no *Dusp6*$^{-/-}$ *Nf1*$^{+/-}$ mice were generated in the breeding pairs arranged for generation of *Dusp6*/ *Nf1* double mutants. 17 mice were produced from 3 litters, so based on Mendelian genetics there should have been 2. The expected number of *Dusp6*$^{-/-}$ pups were generated from 3 litters, although other groups found a decreased representation of *Dusp6*$^{-/-}$ in +/- x +/- cross (Li et al., 2007). It is not possible to tell from 3 litters whether in this case lack of *Dusp6*$^{-/-}$ *Nf1*$^{+/-}$ is due to chance or not.

3.3.2 RhoGAPs

3.3.2.1 RICS

The RhoGAP RICS negatively regulates the actin cytoskeleton by inactivating RhoGTPases, reducing their modification function. Such modification functions may be important in translating glutamate signals into anatomical changes such as those occurring when cells relocate to form barrels. RICS is associated with and activated by NMDARs and *Rics* knock-down neurons have larger premature development of spines (Nakazawa et al., 2008) similar to that seen in *Syngap*$^{-/-}$ cultured neurons (Vazquez et al., 2004), so is a candidate for being part of the pathway that regulates formation of barrels. Mice with a deletion of *Rics* were studied at the age of P7/8, the stage by which barrels have normally formed. Despite RICS function being regulated by NMDAR activity, and despite RICS being expressed in barrel hollows, *Rics*$^{-/-}$ were found to have normal barrels, observed by examination of Nissl stain and quantified by counting the density of cells in wall and hollow of barrel C2. As might be expected, innervation by TCAs in mutants of layer 4 of cortex is normal; TCAs branch into patches and take up an area similar area to that measured in wildtype brains. *Rics*$^{-/-}$ brains have normal lamination of the cortex, indicating that RICS does not regulate the processes of cell division and migration leading to correct formation of layers in the cortex. RICS is different from SynGAP in that RICS mainly acts on Rho GTPases while SynGAP acts on Ras/Rap GTPases. While both Rho and Ras/Rap pathways regulate the anatomy of spines, their function is not identical. Other RhoGTPases such as Oligophrenin-1 (Kasri et al., 2008) and p190RhoGAP (Zhang et al., 2008) perform similar spine-regulating functions to RICS and may compensate when RICS is lost. The evidence for a premature development of spines in *Rics* knockdown neurons was from primary culture (Nakazawa et al., 2008), and has not yet been seen in vivo. Biochemistry could be carried out on *Rics* mutant tissue to measure levels of other RhoGAPs and molecules in the RhoGTPase pathway. Evidence for Rho or Ras/Rap pathways being directly involved in barrel development has not yet been found (unpublished evidence from examining ERK1/2 & H-Ras mutants). SynGAP regulates the Ras/Rap pathway that leads to ERK activation but may also regulate AC/cAMP activity (Barnett et al., 2006). Pathways associated with AC/cAMP are shown to be necessary for normal formation of barrels (Watson et al., 2006) and it is likely that this ERK-independent pathway is the key pathway necessary for normal barrel function.

3.3.3 Summary

This study aimed to further reveal the pathways downstream of glutamate leading to barrel formation. It has shown that two regulators of the ERK-MAPK pathway NF1 and SynGAP regulate the segregation of cells into barrels, also reported elsewhere (Barnett et al., 2006, Lush et al., 2007). However, *Rics* and *Dusp6* mutations do not affect barrel formation, indicating that either 1.) barrels form in an ERK-independent manner or 2.) other molecules compensate for the loss of RICS and Dusp6. Analysis of double mutants has shown that the role of SynGAP and NF1 is not simple. It seems that the two RasGAPs have overlapping but different roles, and the variety and specificity of small G-proteins activated by each is key to each function. Further investigations could reveal which G-proteins are involved in barrel formation, and biochemical analyses is necessary to identify any compensation mechanisms that are occurring.

In this study and other investigations into the analysis of mutants with abnormal barrels, there seems to be three classes of defects amongst those with mutations in NRC/MASC members (see table 1 for table of classes). In the first class are the mutants where barrels partially form but TCAs segregate normally, in the second class are the mutants where barrels partially form- cells start to form dense walls but not to the same extent as in a wildtype and TCAs do not segregate normally. The third class includes mutants where no barrel pattern is visible and TCAs show no segregation. If these mutants are classified according to the phenotype, then it is possible to see which pathways are necessary for complete loss of barrels, and which for partial defects.

Disruption to AC/cAMP signalling results in partially formed barrels, but in order to completely disrupt the formation of barrels there needs to be loss of a gene involved in ERK/MAPK signalling pathways in addition to disruption of AC/cAMP signalling. These findings suggest that the two pathways have overlapping but distinct roles in the signalling pathways leading to the formation of barrels which may explain why some molecules involved in only the ERK/MAPK pathway do not regulate barrel formation.

Table 1 Summary of Barrel Phenotypes

Summary of Barrel Phenotypes			
Normal barrel formation and normal TCA segregation	Class 1: Partial formation of barrels & complete TCA segregation	Class 2: Partial formation of barrels & incomplete TCA segregation	Class 3: No barrel pattern visible & no TCA segregation
Dusp6-/- *Rics-/-* *H-Ras-/-* *Psd-95-/-*	*Syngap+/-* *Nf1+/-* *Prkar2b-/-* Cortex AC1-/-	*Plcβ-1-/-* *Mglur5-/-* *CxNr1KO*	*Syngap-/-* *Nf1*$^{flox/flox}$;hGFAP-Cre

3.4 Figures Chapter One

Figure 1.1

Coronal sections from P7/8 *Syngap*/*Nf1* mutants. PMBSF region of cortex stained for Nissl, calretinin and PKARIIβ to show lamination of cortex. Scale bar 1000μm (hemisphere) 500μm (cortex). Arrows indicate barrels in Nissl coronal sections that appear normal in WT and Nf1+/-. Arrow heads indicate barrels that are less clearly visible in *SG*+/- and *SG+/-Nf1*+/-.

Figure 1.2

Coronal sections from P7/8 *SynGAP*/*Nf1* mutants. AS region of cortex stained for Nissl, calretinin and PKARIIβ to show lamination of cortex. Scale bar 1000μm (hemisphere) 500μm (cortex).

Figure 1.3

Measurements of lamination in PMBSF and AS region in P7/8 *Syngap*/ *Nf1* mutants. Error bars are standard error. Student's t-test * = $p<0.05$.

WT n=3, *Nf1*+/- n=4, *SG*+/- n=2, *Nf1*+/-*SG*+/- n=4, unless otherwise stated.

A; Layer 1-6 PMBSF region, measurements taken from Nissl stained sections.

B; Layer 1-6 AS region, measurements taken from Nissl stained sections. (*Nf1*+/- n=3)

C; Layer 5-6 PMBSF region, measurements taken from calretinin-stained sections.

D; Layer 5-6 AS region, measurements taken from calretinin-stained sections.

E; Thickness of layer 4 in PMBSF region, measurements taken from PKARIIβ stained sections. (WT n=2, *SG*+/- *Nf1*+/- n=2)

F; Thickness of layer 4 in AS region, measurements taken from PKARIIβ stained sections. (WT n=2, *SG*+/- *Nf1*+/- n=2)

G; Layer 1-4 PMBSF region, measurements taken from calretinin-stained sections.

H; Layer 1-4 AS region, measurements taken from calretinin-stained sections.

Figure 1.4

Nissl stained flattened cortices from three P7 wild-type and three P7 *Nf1*+/- mice. From each mouse two serial sections are shown so that all PMBSF is visible. It is difficult to tell whether there are differences between the two genotypes from Nissl, so quantification will be carried out. Scale bar 500μm.

Figure 1.5

Analysis of cell segregation in barrels of *Syngap/Nf1* mutants.

A; Images to show barrel C2 from *Syngap*/*Nf1* mutants immunostained for SERT and To-Pro-3, from which cells were counted to analyse ratio of cells in wall:hollow. Scale bar 100μm.

B; Wall:hollow cell ratio in *Syngap*/*Nf1* mutants. WT n=3, *Nf1*+/- n=2, SG+/- n=4. *Nf1*+/-SG+/- n=6.

C; Area covered by SERT- labelled patches from barrels B2&3, C3&3 and D2&3. WT n=4, *Nf1*+/- n=2, SG+/- n=4. *Nf1*+/-SG+/- n=6.

Figure 1.6

Coronal sections from P7/8 *Dusp6*/ *Nf1* mutants. PMBSF region of cortex stained for Nissl, calretinin and PKARIIβ to show lamination of cortex. Scale bar 1000μm (hemisphere) 500μm (cortex).

Figure 1.7

Coronal sections from P7/8 *Dusp6*/ *Nf1* mutants. AS region of cortex stained for Nissl, calretinin and PKARIIβ to show lamination of cortex. Scale bar 1000μm (hemisphere) 500μm (cortex).

Figure 1.8

Measurements of lamination in PMBSF and AS region in P7/8 *Dusp6*/ *Nf1* mutants. Error bars are standard error. Student's t-test * = $p<0.05$.

WT n=2, *D6*+/- n=4, *D6*+/- *Nf1*+/- n=4, *Nf1*+/- n=2 *D6*-/- n=1.

A; Layer 1-6 PMBSF region, measurements taken from Nissl stained sections.

B; Layer 1-6 AS region, measurements taken from Nissl stained sections.

C; Layer 5-6 PMBSF region, measurements taken from calretinin stained sections.

D; Layer 5-AS region, measurements taken from calretinin stained sections.

E; Thickness of layer 4 in PMBSF region, measurements taken from PKARIIβ stained sections. Thickness of layer 4 in WT is significantly greater than *D6*+/- *Nf1* +/-. Student's t-test * = $p<0.05$.

F; Thickness of layer 4 in AS region, measurements taken from PKARIIβ stained sections.

G; Layer 1-4 PMBSF region, measurements taken from calretinin stained sections. Thickness of layer 1-4 in WT is significantly greater than D6 +/-. Student's t-test *= $p<0.05$.

H; Layer 1-4 AS region, measurements taken from calretinin stained sections.

Figure 1.9

Analysis of cell segregation in barrels of *Dusp6*/ *Nf1* mutants.

A; Images to show barrel C2 from *Dusp6*/ *Nf1* mutants immuno-stained for SERT and To-Pro-3, from which cells were counted to analyse ratio of cells in wall:hollow. Scale bar 100μm.

B; Wall:hollow cell ratio in *Dusp6*/ *Nf1* mutants. *WT* n=2, *D6*+/- *Nf1*+/- n=3, *D6*-/- n=1.

C; Area covered by SERT- labelled patches from barrels B2&3, C3&3 and D2&3. *WT* n=2, *D6*+/- *Nf1*+/- n=3, *D6*-/- n=1.

Figure 1.10

Coronal sections from P7/8 *Dusp6*/*Syngap* mutants. PMBSF region of cortex stained for Nissl, calretinin and PKARIIβ to show lamination of cortex. Scale bar 1000μm (hemisphere) 500μm (cortex).

Figure 1.11

Coronal sections from P7/8 *Dusp6*/*Syngap* mutants. AS region of cortex stained for Nissl, calretinin and PKARIIβ to show lamination of cortex. Scale bar 1000μm (hemisphere) 500μm (cortex).

Figure 1.12

Measurements of lamination in PMBSF and AS region in P7/8 *Dusp6*/*Syngap* mutants. Error bars are standard error. Student's t-test * = $p<0.05$.

WT n=3, *D6*+/- n=2, *SG*+/- n=2. *D6*+/-*SG*+/- n=1.

A; Layer 1-6 PMBSF region, measurements taken from Nissl stained sections.

B; Layer 1-6 AS region, measurements taken from Nissl stained sections.

C; Layer 5-6 PMBSF region, measurements taken from calretinin stained sections.

D; Layer 5-6 AS region, measurements taken from calretinin stained sections.

E; Thickness of layer 4 in PMBSF region, measurements taken from PKARIIβ stained sections.

F; Thickness of layer 4 in AS region, measurements taken from PKARIIβ stained sections. (NB n=0 *D6*-/-*SG*+/-)

G; Layer 1-4 PMBSF region, measurements taken from calretinin stained sections.

H; Layer 1-4 AS region, measurements taken from calretinin stained sections.

Figure 1.13

Analysis of cell segregation in barrels of *Dusp6*/*Syngap* mutants.

A; Images to show barrel C2 from *Dusp6*/*Syngap* mutants immunostained for SERT and To-Pro-3, from which cells were counted to analyse ratio of cells in wall:hollow. Scale bar 100μm.

B; Wall:hollow cell ratio in *Dusp6*/*Syngap* mutants. *WT* n=3, *SG*+/- n=2, *D6*+/-*SG*+/- n=2, *D6*+/- n=1, *D6*-/-*SG*+/- n=1.

C; Area covered by SERT- labelled patches from barrels B2&3, C3&3 and D2&3. *WT* n=3, *SG*+/- n=2, *D6*+/-*SG*+/- n=2, *D6*+/- n=1, *D6*-/-*SG*+/- n=1.

Figure 1.14

Combination of density counts in double mutants of *Dusp6/Nf1/Syngap* to show extent of segregation of cells into barrels.

(*WT* n=8, *SG*+/- n=4, *D6*+/- n=1, *D6*-/- n=1, *Nf1*+/- n=4, *D6* +/-*SG*+/- n=2, *D6*-/-*SG*+/- n=1, *SG*+/-*Nf1*+/- n=6, *D6*+/- *Nf1*+/- n=3)

* =Density ratio is significantly different from WT. Student's t-test ($p<0.05$)

Figure 1.15

Coronal sections stained to label cortical layers for lamination analysis.

A; Coronal sections from P7/8 *Rics* mutants. PMBSF region of cortex stained for Nissl, calretinin and PKARIIβ to show lamination of cortex. Scale bar 1000μm (hemisphere) 500μm (cortex).

B; Coronal sections from P7/8 *Rics* mutants. AS region of cortex stained for Nissl, calretinin and PKARIIβ to show lamination of cortex. Scale bar 1000μm (hemisphere) 500μm (cortex).

Figure 1.16

Analysis of lamination of cortex in *Rics* mutants.

A; Layer 1-6 PMBSF region, measurements taken from Nissl stained sections. (+/+ n=4, -/- n=3)

B; Layer 1-6 AS region, measurements taken from Nissl stained sections. (+/+ n=4, -/- n=3)

C; Layer 5-6 PMBSF region, measurements taken from calretinin stained sections. (+/+ n=4, -/- n=3)

D; Layer 5-6 AS region, measurements taken from calretinin stained sections. (+/+ n=4, -/- n=3)

E; Thickness of layer 4 in PMBSF region, measurements taken from PKARIIβ stained sections. (+/+ n=4, -/- n=3)

F; Thickness of layer 4 in AS region, measurements taken from PKARIIβ stained sections. (+/+ n=4, -/- n=3)

G; Layer 1-4 PMBSF region, measurements taken from calretinin stained sections. (+/+ n=4, -/- n=3)

H; Layer 1-4 AS region, measurements taken from calretinin stained sections. (+/+ n=4, -/- n=3)

Figure 1.17

Staining of cortex in *Rics* mutants to reveal barrels and TCA patches.

A; Serial tangential sections of cortex from P7/8 *Rics* mutants. Nissl stain shows normal barrels in *Rics* -/-. Scale bar 1000μm.

B; Serial tangential sections of cortex from P7/8 *Rics* mutants. SERT stain shows normal patches in *Rics* -/-. Scale bar 1000μm

C; To-Pro-3 and β-Galactosidase immuno stain on coronal sections from *Rics*+/- P7 shows *LacZ* reporter is present in barrel region of cortex. Scale bars; upper row 400μm, lower row 100μm.

Figure 1.18

Analysis of segregation of TCAs into patches and cells into barrels in *Rics* mutants.

A; To-Pro-3 labelling of tangential sections from 3 separate WT and 3 separate *Rics*-/- P7 mice reveals normal distribution of cells into walls and hollows. Scale bar, 200μm.

B; Images to show barrel C2 from *WT* and *Rics* -/- immunostained for SERT and To-Pro-3, from which cells were counted to analyse ratio of cells in wall:hollow. Scale bar 100μm.

C; SERT-labelled patches in *WT* and *Rics* -/-, from which the area of patches from barrels B2&3, C2&3, D2&3 were measured.

D; Wall:hollow cell ratio in *Rics* mutants. *WT* n=3, *Rics*+/- n=4, *Rics*-/- n=5.

E; Area covered by SERT- labelled patches from barrels B2&3, C3&3 and D2&3. *WT* n=4, *Rics*+/- n=4, *Rics*-/- n=5. Scale bar, 200μm.

4 Data Chapter Two:

SAP102 and PSD-95 in barrel formation

4.1 Introduction

Modulators of G-protein signalling cascades have been discussed in the previous chapter, and the role they play in regulating mechanisms that lead to barrel development. Scaffolding molecules interact with and modulate receptors, linking them to signalling molecules such as G-proteins & their modulators, kinases and phosphatases (Migaud et al., 1998, Sprengel et al., 1998). PDZ (**P**ostsynaptic **D**ensity 95/Discs large/**Z**ona occludens 1) domains are ~90amimo acid protein-interaction domains that bind the C-terminal of proteins in a sequence-specific fashion (Ponting, 1997, Doyle et al., 1996, Songyang et al., 1997). It is through these domains that scaffolding molecules assemble the multi-protein complexes found at the PSD. There are many different families of scaffolding molecules, and within each family there are many very similar proteins that perform overlapping roles. For example, within the PSD-95 –like family there are 4 proteins (PSD-95, PSD-93, SAP102 & SAP97), all with three PDZ-domains, a GK domain and an SH3 domain. Recently the protein interactions of these four PSD-MAGUKS (membrane associated guanylate-kinase domain containing proteins) and their individual roles have been subject to investigation. Isolation of NMDAR-associated components by NR1-IP revealed 77 proteins that may modulate glutamate activity (NMDAR-complex (NRC); Husi et al., 2000). The complex has now been re-named due to the abundance and significance of MAGUKs (and the similarity between proteins isolated with NMDARs and MAGUKs in IP studies) to the 185-member NRC/MASC complex (NRC/MAGUK-associated signalling complex; Collins et al., 2006, Grant, 2006).

SAP102, PSD-95 and PSD-93 bind NMDAR subunits and their downstream signalling enzymes creating signalling microdomains that translate glutamate binding into intracellular signalling cascades (see diagram 14). The precise interactions between MAGUKs and other PSD molecules is confused by the ability of the proteins to upregulate when one is absent (Elias and Nicoll, 2007, Ehrlich et al., 2004 & 2007, McGee et al., 2001). Signalling enzymes such as PKA and SynGAP rely on MAGUKs to associate with NMDARs and AMPARs. PKA is recruited to the NRC/MASC via direct interaction with the PDZ-domain of MAGUKs PSD-95 and

SAP97 and AKAP79/150 (Colledge et al., 2000). It is through this interaction that PKA mediates NMDAR-induced AMPAR removal at the synapse, one of the key mechanisms involved in the weakening of synapses in LTD (Snyder et al 2005). SynGAP associates with NMDARs via direct interactions with the PDZ-domains of SAP102 and PSD-95 and regulates downstream pathways such as the ERK-MAPK pathway (Chen et al., 1998, Kim et al., 1998, Komiyama et al., 2002).

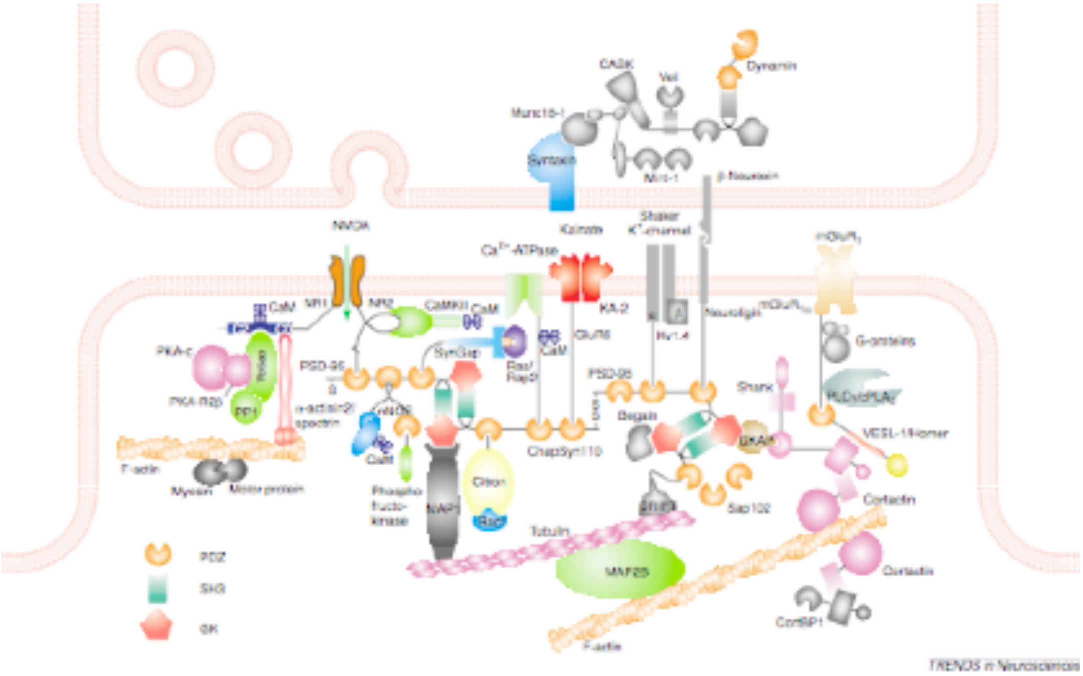

Diagram 14 **Schematic of NRC/MASC components in the PSD**

SAP102 and PSD-95 are localised near the post-synaptic membrane and interact with NMDARs, and Neuroligin linking them to downstream signalling molecules (diagram from Husi and Grant, 2001)

Genetic deletion of *Nr1, Syngap* or *Prkar2b* (the genes encoding NMDAR subunit1, SynGAP and the RIIβ subunit of PKA respectively) results in the disruption of barrel formation. It is proposed that this close interaction between receptors and their enzymes is crucial to mediate normal barrel formation, therefore loss of the MAGUKs we predict, would affect barrel formation. This chapter aims to investigate this possibility and bring clarity to the interactions between SAP102 and PSD-95 in the role they play in maintaining intact signalling pathways necessary for barrel formation. First a review will be presented describing key findings that led to SAP102 and PSD-95 being implicated in activity-dependent development and plasticity.

4.1.1 MAGUK Family

In adult PSD, PSD-95 (post-synaptic density protein 95kDa) (DLG4; Cho et al., 1992) is the most abundant of PDZ-domain containing proteins at glutamatergic synapses (Dosemeci et al., 2007) and interacts with many other NRC/MASC members. SAP102 (synapse-associated protein 120kDa) (DLG3, dlgh3, NE-DLG; Makino et al., 1997) is very similar to PSD-95 in structure and has overlapping but distinct interactions and functions (Cuthbert et al., 2007) (see diagram 15 for comparison of structure). Together with Chapsyn110/PSD-93 (dlg2; Mazoyer et al., 1995, Brenman et al., 1996) and SAP97 (Muller et al., 1995) these four are collectively referred to as the PSD-95 family (Kim and Sheng, 2004) or the PSD-MAGUKs due to their abundance at the PSD. The four MAGUKs are in the MAGUKs/Scaffolders/Adaptors group of the NRC/MASC (Funke et al., 2005). They were identified first in Drosophila as being Discs Large Genes (dlg) 1-4 (see Appendix I table 3 for identification).

Diagram 15 **Structure of PSD-95, SAP102, PSD-93 & SAP97**

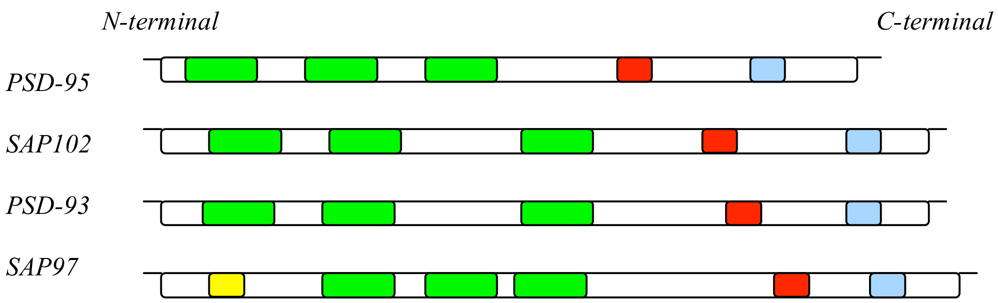

KEY

GK (guanylate kinase –like) Domain *SH3 (Src homology) Domain* *PDZ-binding Domain*

MRE/L27 domain (initially found in LIN2&7)

4.1.2 Structure and domain function of MAGUKs

4.1.2.1 Structure

Electron microscope (EM) images of monomers and nuclear magnetic resonance (NMR) studies of PDZ 2&3 show that PSD-95 monomers fold into c-shaped particles and the C terminal may interact with the N-terminal (Sheng Lab, unpublished observations described in Kim & Sheng, 2004, Long et al., 2003). The same is often assumed for other members of the PSD-95 family, although not confirmed. PSD-95 can forms multimers, either with PSD-95 or other MAGUKs. PSD-93 has been found to associate with PSD-95 and forms a multimeric scaffold that may aid clustering of receptors, ion channels and other signalling proteins at the synapse (Kim et al., 1996).

4.1.2.2 Domain Function

MAGUKs are defined by having a SH3 domain, a GK domain and 3 PDZ domains. The different domains allow each MAGUK to mediate different functions in different subcellular localizations.

PDZ Domains

PDZ-domains 1 & 2 of PSD-95 interact with the long cytoplasmic tails of NR2 subunits of NMDARs containing a conserved –ESDV or –ESEV sequence at the C-terminus (Cho et al., 1992, Kistner et al., 1993, Kornau et al., 1995, Niethammer et al., 1996, Sheng, 1996, Kornau et al., 1997, O'Brien et al., 1998), coupling it to downstream signalling molecules. The first and second PDZ domains of PSD-95 were found to bind Shaker K+ channels as well as NR2 subunits (Kim et al., 1995, Kornau et al., 1995). The third PDZ domain of PSD-95 mediates the interaction of PSD-95 with the neuronal signalling molecule nitric oxide synthase (nNOS) (Brenman et al., 1996), causing the $\alpha2\beta1$ isoform of NO-sensitive guanylyl cyclase receptor to be recruited to the membrane, and the $\alpha1\beta1$ isoform to remain in the cytosol (Russwurm et al., 2001). PSD-95 therefore regulates the cellular location of a receptor for NO, through which the freely diffusible transmitter NO carries out most of its functions.

SH3 domains

SH3 domains have been found in a wide variety of signal-transduction and membrane –associated cytoskeletal proteins. They mediate protein-protein interactions by binding a specific target sequence (Koch et al., 1991, Mayer and Eck, 1995). Recent evidence suggests that the SH3 domain binds ubiquitin, which can lead to gene regulation, endosomal sorting and protein degradation (He et al., 2007).

GK Domains

MAGUKs are defined by having a ~300 amino acid region (GK domain) with 40% homology to yeast guanylate kinase (Guk1) (Berger et al., 1989), an enzyme that makes GDP by adding phosphate to GMP. It is not known whether the GK–homology domain of MAGUKs has GK activity, they do not bind nucleotides (Kuhlendahl et al., 1998, Olsen & Bredt, 2003) but some studies indicate there may be a role for GK activity in MAGUKs (Kistner et al., 1995, Li et al., 2002). It is thought that the GK domain has evolved from an enzyme to a protein-protein interaction motif binding a variety of ligands. For example, the GK domain of PSD-95 binds microtubule-associated-protein-1a (Reese et al., 2007)

N-terminal

The N-termini of MAGUKs play a role in targeting of MAGUKs to the correct location. The N-terminal motifs of PSD-95 and PSD-93 are palmitoylated (has the post-translational addition of palmitate, a 16-carbon fatty acid) but the N-terminal of SAP-97 and SAP102 are not, instead the N-terminal cysteines tightly bind zinc (El-Husseini et al., 2000). It is thought that the lipid modifications and association with metals allow the mediation of different functions in different subcellular locations. In PSD-95, dual-palmitoylation is required for proper postsynaptic targeting, but PSD-93 targets to the PSD independent of palmitoylation (Craven and Bredt, 2000, Craven et al., 1999, Firestein et al., 1999). When the N-terminus of PSD-95 is replaced with the palmitoylated PSD-93 N terminus, it does not localise correctly. However, when the N-terminus of PSD-95 is replaced with the non-palmitoylated N-terminus of SAP102, postsynaptic targeting is maintained, suggesting that SAP102, PSD-93 and PSD-95 use different N-termini sequences and mechanisms to target them to the PSD (Firestein et al., 2000). Findings such as this indicate how MAGUKs may be able to compensate by localising to the correct place when one MAGUK is reduced or absent. However, due to the differences in specificity of each domain on each MAGUK, compensation at the level of protein expression may not be able to restore function to 100% (Vickers et al., 2006).

4.1.3 Localisation and expression of MAGUKs

4.1.3.1 MAGUKs at the synapse

The position of MAGUKs is shown in a schematic of the synapse (diagram 16) MAGUKs SAP102 and PSD-95 are linked to NMDARs and bind SynGAP, which regulates the Ras/MAPK pathway. This pathway regulates transcription and adhesion and regulates plasticity via modulating AMPARs.

4.1.3.2 Localisation of MAGUKs

EM immunocytochemical detection of PSD-95 family members shows that in rat visual cortex they are not strictly localised to PSDs, but are also found diffusely in pre-synaptic membranes and in axons and dendritic shafts throughout postnatal development (Aoki et al., 2001). Direct comparisons between each MAGUK in a single preparation revealed that SAP97, SAP102, PSD-95 and PSD-93 are all found both pre- and post-synaptically in postnatal and adult cortical tissue (Aoki et al., 2001). There is a population of PSDs that do not contain PSD-95; likewise there are

Diagram 16 Schematic to show position of MAGUKs in synapse

MAGUKs PSD-95, SAP102 and SAP97 bind NMDARs, AMPARs and Neuroligin and mediate the interaction with downstream pathways such as the MAPK pathway (adapted from Laumonnier et al., 2007).

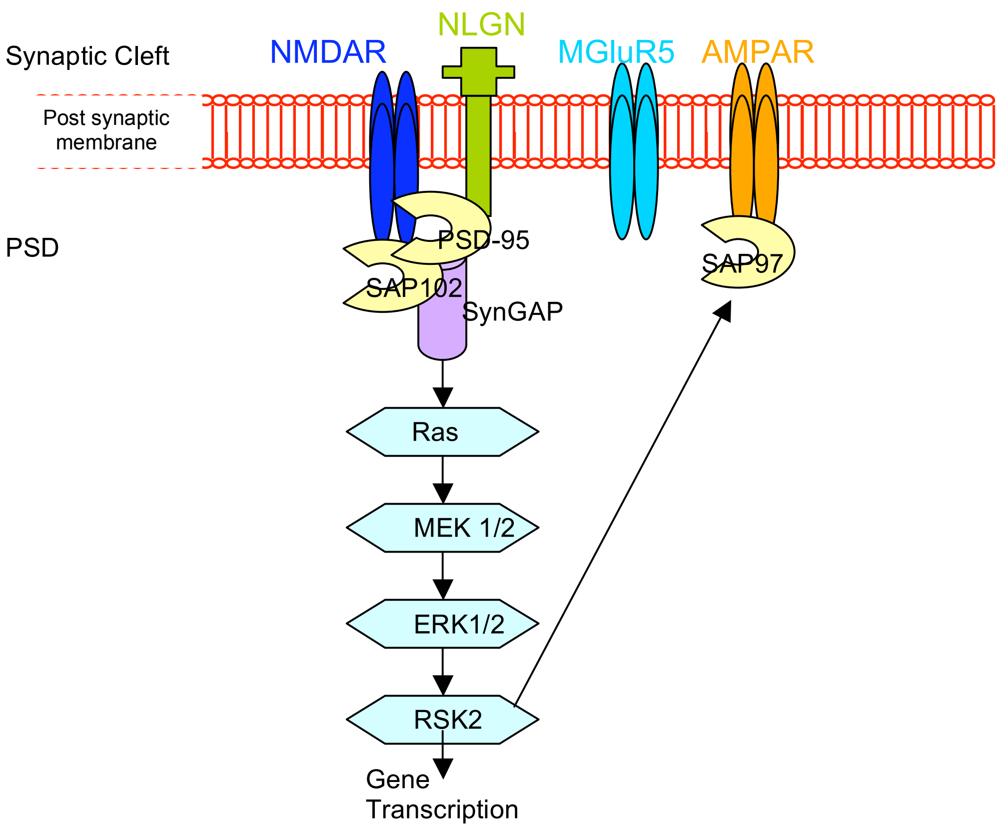

populations that do not contain PSD-93 or SAP102. It is possible that in these synapses, other MAGUKs that are still present are used to anchor NMDARs (Aoki et al 2001). The non-synaptic localisation of MAGUKs suggests that MAGUKs may have an important role in shuttling receptors between synapses and non-synaptic sites as well as regulating signal transduction in the PSD. SAP-97 tends to be predominantly pre-synaptic in hippocampus (Muller at al., 1995) and is enriched in axons of cerebral cortex as well (Aoki et al., 2001). SAP-97 is unique in that it interacts directly with AMPAR subunit GluR1 (Leonard et al., 1998), while the other three interact with NMDAR subunits. PSD-95, PSD-93 and SAP102 are prominent at the PSD where their function is best understood (Ehlers et al., 1996, Sheng et al., 1996 a & b, O'Brien et al., 1998, Craven & Bredt, 1998) but a more recent study has found that they also localise to cortical axons and non-synaptic dendritic shafts in rat visual cortex from 2-3 weeks to adulthood (Aoki et al., 2001). EM immunolocalisation indicated that PSD-95 is situated about 12nm from the postsynaptic membrane and it can be isolated from particular fractions of biochemical PSD preparations (Valtschanoff and Weinberg, 2001), putting it in a prime position for regulating clustering of receptors and channels at the synapse.

MAGUKs have distinct but overlapping expression patterns. PSD-95 and PSD-93 have N-terminal similarities and are both densely located to the PSD, but SAP102 has different N-terminal features which target it to the PSD, explained in detail in the previous section (El-Husseini et al., 2000). PSD-93 has functions in regulating acetyl cholinergic synapses as well as glutamatergic while PSD-95 regulates predominantly glutamatergic (Conroy et al., 2003, Parker et al., 2004). SAP102 and SAP97 are abundant in the cytoplasm, axons and dendrites as well as being found in the synapse (Valtschanoff et al., 2000, Sans et al., 2001, Rumbaugh et al., 2003). SAP102 interacts with Sec8, a member of the exocyst complex responsible for sorting and trafficking of molecules. This interaction via PDZ domains is involved in delivery of NMDARs from the cytoplasm to membranes (Sans et al., 2003).

4.1.3.3 Expression throughout development

SAP102 is expressed more highly than the other 3 early on in development whereas PSD-93 and PSD-95 dominate later (Sans et al., 2000). PSD-95 increases dramatically in expression throughout the first two postnatal weeks (Watson et al., 2006). NR2A follows a similar expression profile throughout development to PSD-95, and NR2A immunoprecipitates with PSD-95 (Townsend et al., 2003). In *Nr2A* KOs, PSD-95-NMDAR binding is significantly decreased, suggesting NR2A is necessary for normal PSD-95 localisation within the synapse. If PSD-95 is over-expressed in neurons, an increase is seen in NR2A-containing NMDARs and not NR2B. SynGAP expression peaks at times of synaptogenesis and developmental plasticity (Porter et al., 2005). Conversely, SAP102 is heavily expressed from birth and is associated more with NR2B, especially in immature synapses. As synapses mature there seems to be a replacement with NR2A-PSD-95/PSD-93 complexes. (Sans et al., 2000, Townsend et al., 2003).

4.1.4 PSD-95 in synaptic plasticity

Initiating the appropriate response to NMDAR activation requires the correct architecture of molecules in the PSD, and PSD-95 is in a prime situation for regulating signal transduction. Studies that have found roles for PSD-95 used null mutant mice made by Grant and colleagues (Migaud et al., 1998), or in vitro studies using knock-down or over-expression in cultured neurons (Beique and Andrade 2003, Ehrlich et al., 2007, for example). Generation of KO mice involved insertion of a stop codon into the third PDZ domain and replacement of the downstream sequence with an IRES entry site driving a β-Galactosidase reporter gene. The first two PDZ domains remain intact and a 40kDa truncated non-functional peptide is expressed but doesn't reach synapses (Migaud et al., 1998). The peptide is not thought to be functional as other *Psd-95* mutants (such as *Psd-95 GK*, also made by Grant and colleagues (Yao et al., 2004)) have a similar phenotype to the truncated one.

Plasticity is often measured by the ability of a cell or a system to make long-term changes in synaptic strength in response to a given stimuli (LTP; long term potentiation or LTD; long term depression (Bliss & Lomo, 1970 & 1973, Levy & Steward, 1979, Barrionuevo et al., 1980). The ability to undergo LTP and LTD is thought to underlie learning and memory (Xu et al., 1998, Manahan-Vaughan & Braunewell, 1999, Kemp & Manahan-Vaughan et al., 2004) and may coincide with alterations in dendritic complexity, spine density and spine shape. *Psd-95* null mutant mice have an altered threshold for LTP induction (Migaud et al., 1998), a 15% decrease in density of spines in the striatum and a 40% increase in the hippocampus (Vickers et al., 2006). The spine density alterations coincide with altered SAP102 expression in the *Psd-95* mutant, but dendritic complexity is unaffected. In the absence of PSD-95 quantitative analysis of SAP102 in Western Blots shows a 100% increase in striatum and a 50% increase in the hippocampus, while PSD-93 and SAP97 remain unaltered (Vickers et al., 2006). In cultured hippocampal neurons over-expression of PSD-95 results in an increase in spine density with enhanced post-synaptic clustering of AMPARs but not NMDARs and increased GluR1 levels by 250%, mimicking a more mature synapse (El-Husseini et al., 2000). Over expression of PSD-95 in cultured cells increases the magnitude of LTD induction (Stein et al., 2003, Beique et al., 2003) and in hippocampus of *Psd-95* mutant mice, LTD was not induced by 1Hz stimuli (Migaud et al., 1998). The mechanism for regulating LTD may be through the ability of PSD-95 to cluster itself with AMPARs in response to calcium-dependent palmitoylation (El Husseini et al., 2000). These results showing different effects of PSD-95 on spine density indicating that there is not a straightforward one-way correlation between PSD-95 and spine density. In vitro and in vivo compensation by other MAGUKs (SAP102) and regulation of AMPARs may be occurring in different tissues to contribute to synapse stabilization and plasticity, so that effects of PSD-95 loss are minimal.

In developing sensory systems PSD-95 also has been shown to regulate synaptic plasticity. PSD-95 regulates the development of the visual system. Cells in the visual cortex of mice carrying a null mutation of *Psd-95* show alterations in orientation preference but OD plasticity is normal (Fagiolini et al., 2003). Since PSD-95 expression rapidly increases during post-natal development it is possible that other MAGUKs (such as SAP102) perform key roles in regulating plasticity mechanisms that occur early postnatal development (such as OD plasticity). In the Morris water maze mice without PSD-95 spend longer looking for a hidden platform in spatial learning tasks, but show no difference from wild types when a visible cue is given (Migaud et al., 1998). This result is similar to that seen in mice where NMDARs are blocked (Morris et al., 1986, Tsien et al., 1996). Therefore PSD-95 has multiple roles in mechanisms that require synapses to be plastic.

4.1.5 SAP102 in synaptic plasticity

The first *Sap102* null mutant mouse was made in 2004 and published in 2007 (Cuthbert et al., 2007), and similar experiments were performed to those carried out on *Psd-95* mutants (Migaud et al., 1998). *Sap102*$^{-/y}$ mutant slices show no differences from wild type in LTP-inducing protocol of 2 pulses of 100Hz stimuli, whereas the same LTP induction protocol showed a severe defect in *Psd-95*$^{-/-}$ slices (see Appendix 1 table 4 for summary). *Psd-95*$^{-/-}$ mice undergo LTP with levels 49% above that achieved in wild type slices. LTP also saturated at much greater potentiated level in *Psd-95*$^{-/-}$ mice (123% greater than wild type). Low frequency stimulation at 5Hz results in *Sap102*$^{-/y}$ mice undergoing 51% more LTP than wt, while in *Psd-95*$^{-/-}$ there is 152 % more LTP than wild type. In single pyramidal cells paired pulses fail to induce LTP in wt, but *Sap102* mutants undergo 50% LTP.

MAGUKs PSD-95 and SAP102 have been implicated in regulating LTP, but the molecular pathways of this function are not fully known. SAP102 plays a role in ERK-dependent (Winder et al., 1999) low-frequency induced forms of LTP and regulates modifications to synaptic strength during coincident firing of pre and post-synaptic cells. PSD-95 however alters the threshold for induction of LTP, allowing potentiation of responses to a signal that usually results in depression. Slices from *Sap102* mutant mice have significantly more pERK than wildtype, after stimulation relative to basal levels, while unphosphorylated ERK remains unchanged (Cuthbert et al., 2007). The MEK inhibitor U0126 blocks the enhancement of LTP seen in *Sap102* mutants, indicating that this form of LTP is ERK- dependent. This indicates that absence of SAP102 either activates or removes inhibition of ERK. A similar outcome is seen when SynGAP, a negative regulator of ERK, is reduced (Komiyama et al., 2002). Application of NMDA to a water bath containing a hippocampal slice stimulates NMDARs, and causes phosphorylation of ERK (Komiyama et al., 2002). This indicates that SAP102 regulates NMDAR-dependent MAPK signalling, and this mechanism is responsible for the physiological defects in hippocampal synapses.

4.1.6 MAGUKs and Disease

It is important to understand the roles of MAGUKs in development and plasticity because there is a strong correlation between defects in synaptic proteins and cognitive disorders in humans. Studying mice with plasticity and developmental defects due to mutations to synaptic proteins helps us to better understand the function of that gene, and as a result better understand the mechanisms affected in disease. Of the 1180 genes coding for post-synaptic proteins (PSPs), more than 1100 are autosomal, and a recent literature review (Grant et al., 2005) found that almost 50 NRC/MASC genes were involved in various brain disorders. 19 out of 39 (49%) of the PSP genes found on the X-chromosome, and 6 out of 7 (86%) of the X-linked NRC/MASC genes are implicated in human psychiatric disorders (Laumonnier et al., 2007). These 7 genes are DLG3 (*Sap102*), RPS6KA3, PLP1, M1CAM, SLC25a5, NLGN3, and NLGN4. The high correlation between NRC/MASC components and cognition disorders is also seen in mouse mutants and indicates that the NRC/MASC complex is forming an essential structure that must be intact for cognition to be normal. Many more 'cognition genes' are found on the X-chromosome than any other comparable segment of the autosomes, and comparisons of the frequency of autism spectrum disorders and mental retardation between males and females showed that in nearly all disorders males outnumbered females (Skuse et al., 2005). X-linked mental retardation (XLMR) has a prevalence of 2.6 per 1000 in the general population, and accounts for more than 10% of MR cases (Stevenson et al., 2002, Ropers et al., 2005)

4.1.6.1 SAP102 in mental retardation

DLG3, the human gene encoding SAP102 is mutated in a subset of families with XLMR (Tarpey et al., 2004). For the study, 329 unrelated families with undefined moderate to severe X-linked mental retardation in at least 2 males of that family were selected (Tarpey et al., 2004). Of the 329 families investigated, 4 families were found to have mutations that mapped to the X-chromosome human *Sap102 (DLG3)*. In each case a premature stop codon is inserted within or before the third PDZ domain in exons 6,7,8 or 9, therefore disrupting interactions with NR2 and other signalling proteins. In one family, this resulted in loss of 54% of the translated protein, in other families, mutations occurred around the same region. It is likely that the mutated protein causes a disruption to interactions with NMDARs, one of the key receptors involved in learning and memory. Female carriers in the affected families show variable but milder phenotypes with lower than average IQ. In the two families where carrier females were available for investigation, the clinical manifestation was not related to the extent of X-chromosome inactivation that occurs in lymphocytes. However skewed X-inactivation in *brain cells* during development could explain the variable female phenotype. The low prevalence of this *Sap102* –related condition is representative of the other 7 X-linked genes that have been associated with nonsyndromic (where cognitive impairment is the only definable feature) mental retardation to date. In many families with XLMR, the causative mutation is not yet identified. It has been estimated that up to 75 additional genes may eventually be assigned to a mental retardation phenotype (Ropers et al., 2003). Linkage studies and automated high throughput mutation detection such as that used in the Tarpey study are a useful approach to identifying new conditions due to inherited mutations.

4.1.6.2 PSD-95 in disease

So far, mutations in *Psd-95* resulting in human disorders have not been detected. If a spontaneous mutation of *Psd-95* gene occurs on one allele, it is likely that the remaining intact allele is sufficient for normal function. To date, no abnormalities have been reported in *Psd-95*$^{+/-}$ mice, indicating that protein produced from one allele is sufficient for normal development. Humans with a null mutation to *Psd-95* may die in utero, and so the disorder has not been detected. A form of mental retardation detected in 6 patients was associated with autosomomal microdeletion of a 1.5Mb fragment on 3q29 (Willatt et al., 2005). The deletion includes 22 genes, one of which codes for SAP97. SAP97 is an autosomal gene and has only recently been implicated in mental retardation, raising the possibility that PSD-95 and many other NRC/MASC proteins may eventually be associated with a human disease.

4.1.7 Other functions of SAP102

SAP102 is regulated in other diseases, often when NMDAR subunits remain unchanged, indicating that glutamatergic transmission defects are often modulated by changes in intracellular signalling molecules. Similarly, in patients with bipolar disorder, there was a decrease in SAP102 and PSD-95 transcripts, and in major depression a decrease in SAP102 levels but NMDAR subunits were unchanged (Clinton & Meador-Woodruff, 2004). However, in these cases the decrease in SAP102 may be secondary rather than causal to the development of the disorder. For example, in-situ hybridisation of post-mortem thalamus of patients with schizophrenia found increased levels of PSD-95 and SAP102, along with decreased NR1 (Meador-Woodruff et al., 2003). Whether the loss of SAP102 occurs early and contributes to the development of the disease, or whether earlier causal events lead to the later loss of SAP102 is unknown.

4.1.8 Summary of key findings leading to specific aims

SAP102 is the major MAGUK that is expressed in neurons during early brain development, and localised to the PSD of excitatory synapses. In hippocampus, SAP102 expression is very high at P2, increases through the first postnatal week, and then remains high until 6 months, before tailing off (Sans et al., 2000). PSD-95 on the other hand, is expressed relatively less in early development and is up regulated between P2 and 6 months, coinciding with an increase in synapse number. In tissue taken from S1 cortex PSD-95 is present from birth and increased dramatically with age until adulthood (Barnett et al., 2006). One reason for this may be due to the preferential binding of SAP102 to NR2B and PSD-95 to NR2A, as found by Co-IP studies (Sans et al., 2000). During postnatal development there is a switch in hippocampus in the relative ratios of NR2 subunits, which coincides with SAP102 and PSD-95 expression. NR2B is more highly expressed early on with SAP102, then they both decrease. NR2A appears later with PSD-95 when NR2A is reduced (Sans et al., 2000).

Since SAP102 is highly expressed during early postnatal development, it may play a more important role than PSD-95 in cortical development of S1 cortex, although PSD-95 is expressed at developing synapses (Barnett et al., 2006). Preliminary data from Kind and colleagues found no defects in segregation of cells into barrels at P7 when either *Sap102* or *Psd-95* (Barnett et al., 2006) was deleted. However, since these proteins can alter their expression to compensate for each other during development, it is possible that a role for either during development may be masked (Vickers et al., 2006, Cuthbert et al., 2007). One way to examine the relationship between the two proteins and the role they play together in development is to examine double mutants.

4.1.8.1 Specific aims of this chapter

To determine whether loss of one or two copies of both *Sap102* and *Psd-95* results in defects in barrel formation.

4.2 Results

4.2.1 Double KO mice do not survive beyond P3

Experimental animals were perfused at P7-9 or P14 for analysis of cortical development defects. No pups were found to be double KO at this age, so breeding pairs were monitored for post-natal mortality. Pups were found daily over the first 4 days after birth, and genotyping of tissue revealed that double KOs died between P0 and P3. Analysis of offspring from one particular breeding pair (pair 211; *Sap102*$^{-/y}$ *Psd-95*$^{+/-}$ x *Sap102*$^{+/-}$*Psd-95*$^{+/-}$) arranged to produce all 12 combinations of genotypes showed that homozygous KOs for both *Psd-95* and *Sap102* were generated at near predicted Mendelian ratios (10% actual, compared to 12.5% predicted) (fig 2.1). Unfortunately sex was not recorded when post-natal mortalities were monitored so *Sap102* KO or WT pups could be either sex. In other breeding pairs, double KOs were never found beyond P3 (data not shown).

4.2.2 *Sap102*$^{+/-}$*Psd-95*$^{-/-}$ mutants are not under-represented in all litters

Cuthbert and colleagues reported an under-representation of *Sap102*$^{+/-}$*Psd-95*$^{-/-}$ mice at weaning (Cuthbert et al., 2007). In order to see whether this was occurring in mice for this study, pair 211 was monitored for postnatal mortalities and all pups whether they died or survived were genotyped. The observed number of *Sap102*$^{+/-}$*Psd-95*$^{-/-}$ mice (5%) is very close to the expected number (6.25%), however all these mutants from this pair were found dead before P3. Another breeding pair of exactly the same genotype as that presented in Cuthbert et al., 2007 (pair, 202; *Sap102*$^{+/y}$*Psd-95*$^{+/-}$ x *Sap102*$^{+/-}$*Psd-95*$^{+/-}$) was analysed in the same way. In this pair a total of 6 *Sap102*$^{+/-}$ *Psd-95*$^{-/-}$ mice reached P7 or above out of 51 offspring genotyped, giving an observed frequency of *Sap102*$^{+/-}$*Psd-95*$^{-/-}$ (aged P15 & above) of 11.7%, while expected frequency is 12.5%. This result is contrary to that found by Cuthbert, where *Sap102*$^{+/-}$*Psd-95*$^{-/-}$ mice were under-represented (Cuthbert et al., 2007).

4.2.3 Lamination of cortex is normal in *Sap102*/*Psd-95* mutants

To gain insight into whether these MAGUKs were regulating the early development of the cortex, I analysed the lamination of the cortex. Abnormalities in thickness of a particular layer could be due to defects in cell migration, differentiation, cell density, cell body size (indicating defects in neurite extension), cell cycling or innervation of the cortex. Thinner upper layers may indicate maturation of the cortex is delayed as upper layers form after lower layers. In order to assess lamination, coronal sections were taken at P7/8 and labelled with Nissl, and immunohistochemistry performed to label calretinin and PKARIIβ. Nissl stains all cell bodies and allows thickness of whole cortex to be measured. Changes in density of staining indicate different layers and no differences are seen between mutants and wild type (images not shown). Measuring layer 1-6 thickness in AS and PMBSF shows no significant differences between any double mutants produced from breeding *Sap102* mutants with *Psd-95* mutants (fig 2.2) (*Sap102*$^{+/-}$*Psd-95*$^{-/-}$ were not analysed due to shortage of tissue available at this age. Few breeding pairs were arranged to produce this genotype and most were kept until weaning for breeding purposes). Calretinin stain labels the border between layer 5 and layer 4 in S1 ventral to barrels. Measuring the thickness below and above the stained band gives measurements of upper layers 1-4 and lower layers 5-6. Images of the sections indicate that the stained band is appearing as normal between layer 4 and 5 in S1 (images not shown). Quantification of total cortical thickness, upper layers 1-4, lower layers 5-4 & layer 4 thickness are unchanged in *Sap102*/*Psd-95* mutants (fig 2.2). PKARIIβ labels patches corresponding to barrels in layer 4. Measuring the thickness of this band of patches gives an indication as to whether layer 4 is developing properly. If TCA innervation was abnormal, this may be reflected in layer 4 thickness. Analysis of *Sap102*/*Psd-95* double mutants shows that there are no differences between the thickness of layer 4 in any mutants (fig 2.2) (tissue not available for *Sap102*$^{+/-}$*Psd-95*$^{+/-}$). This data suggests that that cell division, differentiation and migration are not greatly affected by the mutation, and maturation of the cortex is occurring relatively normally.

4.2.4 Sap102$^{-/-}$ & $^{-/y}$ have reduced body mass

Stanford and colleagues reported that the *Sap102* mutation affects body mass during early postnatal development (Stanford et al., 2005). *Sap102*/*Psd*-95 mutants were all weighed prior to perfusion on both backgrounds to check whether this defect was occurring in these mice. On the original MF1/129 background, mice at all different ages were weighed, and the weight plotted against age for each genotype. At certain ages the number of samples is low (fig 2.3 a) resulting in a large variation. When data is analysed at 2 specific ages (P7/8 & P14/15), and compared to wild-type no significant differences between any genotypes are detected by ANOVA (fig 2.3 b). Brain mass was also measured and ANOVA detected no significant differences between any mutants (fig 2.3c).

On the new Bl/6 129/DBA background a significantly lower body mass was detected in *Sap102*$^{-/y}$ males (78% of WT male litter mates) and *Sap102*$^{-/-}$ females (83% of heterozygote female littermates). Also there is a difference between male and female KOs; male mutants have a 12% lower mass than female mutants at P7 (fig 2.4). No defect was seen in any double mutants. This time data was strictly from mice aged P7 and so less variation in mass is seen.

4.2.5 Cells do not segregate fully into barrels in Sap102$^{-/y}$Psd-95$^{+/-}$ mutants

In order to evaluate the formation of barrels in postnatal mouse layer 4 of cortex, brains were perfused at various ages from P7-P14 and sections taken tangential to pia. Using mice on the original 50%129/50%MF1 background, Nissl staining reveals cell bodies and gives a qualitative indication of whether cells form dense barrel walls and sparse barrel hollows. Of the mutants studied, the only genotype in which altered segregation was visible is *Sap102*$^{-}$*Psd-95*$^{+/-}$. Barrel walls of this mutant do not seem as dense and well defined as litter-mates of other genotypes. At P7 in wild type litter-mates all PMBSF barrels are visible, (fig 2.5) but in *Sap102*$^{-}$*Psd-95*$^{+/-}$ only a few barrels are visible in the region close to AS whisker barrels. By P9, segregation is more visible but nowhere near complete as only rows C & D barrels are visible. No improvement is seen in segregation between P10 and P14 at which age only two rows of barrels are visible. The sections in this figure represent the best-segregated section from each brain (fig 2.5). Only one brain from *Sap102*$^{+/-}$*Psd-95*$^{-/-}$ was examined at P9 due to their short supply at this age and surprisingly it has well segregated barrels similar to that in wild type. Cell segregation in each of the mutants was quantified at P7/8 & P14/15 and the density in *Sap102*$^{-/y}$*Psd-95*$^{+/-}$ (seen also in Nissl) was found to be statistically different from wild type litter-mates at P7/8 (*Sap102*$^{-/y}$*Psd-95*$^{+/-}$ ratio 1.06±0.05 n=4; WT littermates ratio 1.60±0.1 n=6) (p=0.003) (fig 2.6a&b). The defect is also significant at P14/15 (fig 2.6c), although the defect is less severe at P14 (p=0.03).

When this study was repeated using the mice on the Bl/6 129 /DBA mixed background after re-derivation into a clean mouse facility following a MHV outbreak, the same extent of defect was not seen (fig 2.8). *Sap102*$^{-/y}$*Psd-95*$^{+/-}$ mice have the lowest ratio of cell density wall:hollow (ratio =1.28±0.04 n=7) and in a t-test when compared to *Sap102*$^{-/y}$*Psd-95*$^{+/+}$ mice (ratio =1.54±0.08 n=4) there is a significant difference (p=0.006) (fig 2.9). When an ANOVA was carried out comparing quantitative analysis of barrels in all genotypes there is no significant defect in any genotype (*Sap102*$^{-/y}$*Psd-95*$^{+/-}$ ratio=1.28±0.04 n=7, *Sap102*$^{+/-}$*Psd-95*$^{+/-}$ ratio=1.39±0.08 n=5, *Sap102*$^{-/y}$*Psd-95*$^{+/+}$ ratio= 1.54±0.08 n=4, *Sap102*$^{+/+}$*Psd-95*$^{+/-}$ ratio 1.37±0.06 n=7, WT ratio=1.48 n=1, *Sap102*$^{+/+}$*Psd-95*$^{-/-}$ ratio=1.42 n=1, *Sap102*$^{+/-}$*Psd-95*$^{+/+}$ ratio=1.33 n=1) (ANOVA f=1.437, df=3.19, p=0.252). It is likely that the difference is not detected by ANOVA as some genotypes have a very small number of samples (n=1) and so the variance is high. When those genotypes with small n-numbers are excluded (WT, *Sap102*$^{+/+}$*Psd-95*$^{-/-}$, *Sap102*$^{+/-}$*Psd-95*$^{+/+}$) ANOVA shows significance is reached at 7% level (p=0.07), indicating that the defect may still be there in mice on this mixed background if more mice were analysed.

4.2.6 TCA patches labelled with α-SERT are smaller in Sap102$^{-/y}$Psd-95$^{+/-}$ mutants

To determine whether the defect in barrels seen in *Sap102*$^{-/y}$*Psd-95*$^{+/-}$ mice may be a result of the inability of TCAs to segregate, the area represented by patches was measured in tangential sections on MF1/129 background. Sections taken from flattened cortices of mutants at P7 were immunolabelled with α-SERT to reveal TCA patches. All mutants form discrete TCA patches, indicating that axons segregate into bundles matching the pattern of the main mystacial whiskers on the snout (fig 2.6). However, qualitatively TCA patches in *Sap102*$^{-/y}$*Psd-95*$^{+/-}$ in PMBSF look smaller than wild-type (fig 2.5b & white arrow, fig 2.6). Even when consecutive sections are labelled, the TCA patches do not appear better in another section (fig 2.5b) To determine whether the appearance of smaller patches are the result of a shrunken area of PMBSF or whether it was due to a selective decrease in patch size, the area of patches was quantified. The area occupied by 6 patches (B,C&D2-3) taken to be representative of the area of PMBSF was measured (for details, see methods). Also, the area of each individual patch within the region occupied by the 6 patches was measured. There are no differences between the total areas occupied by 6 individual patches (fig 2.7a) indicating that PMBSF area is not smaller. However, individual patches occupy a smaller % area within the region occupied by B,C&D 2-3 in *Sap102*$^{-}$*Psd-95*$^{+/-}$ (63±4.2% n=3) compared to WT (76±1.4% n=6) (fig 2.7b) ($p=0.009$, t-test). To determine whether the decrease in patch area coincided with an increase in barrel wall thickness, barrel wall thickness was measured using a 'Pixel density across the width of a barrel' described in methods (methods figure M3.2a). Smaller patches were found to coincide with thicker barrel walls.

4.2.7 SAP102 is expressed when PSD-95 is reduced or absent in males and females

To determine whether SAP102 was present in double-mutants when PSD-95 is reduced or absent, SAP102 was immunolabelled in coronal sections of P7 males and females of mixed genotypes. This technique is not quantitative, but gives an idea as to the localisation of SAP102 and lack of stain may indicate if SAP102 were absent altogether. Coronal sections show that in all double-mutants of *Sap102* and *Psd-95* SAP102 is localised to cytoplasm of cells in pyramidal cell layers of cortex and hippocampus (fig 2.10). In layer 4, SAP102 stain is localised to neuropil and cell bodies are not clearly visible. There are dense patches of stain corresponding to barrels in layer 4. In *Sap102*$^{+/y}$*Psd-95*$^{-/-}$ males the staining pattern of SAP102 looks very similar to *Sap102*$^{+/y}$*Psd-95*$^{+/-}$, except perhaps in the former there is a lower level of staining in regions corresponding to barrels (fig 2.10). In *Sap102*$^{+/-}$ females there are dense regions corresponding to barrels when *Psd-95* is not deleted (fig 2.10 c) and also when *Psd-95* is reduced (fig 2.10 d) or absent (fig .10 c). Due to X-chromosome inactivation SAP102 is only expressed in a population of cells in mice that are *Sap102*$^{+/-}$. Therefore there should be a reduction in density of SAP102-labelled cells in females that are *Sap102*$^{+/-}$ (Fig 2.10 c, d & e). In *Sap102*$^{+/-}$ females (fig 2.10 c, d & e) the density of cells in pyramidal layers looks slightly lower than in males (fig 2.10, a & b), but the reduction is not obvious. This data highlights the need to count the two populations of cells, if the contribution of both populations to barrels is to be assessed. This is investigated fully in the next chapter.

4.3 Discussion

4.3.1 SAP102 and PSD-95 regulation

The four MAGUKs have similar structures with 3 PDZ domains, a SH3 domain and a GK domain. Previous investigations have presented evidence to show that when one is reduced or removed in mice, other MAGUKs up-regulate (Vickers et al., 2006, Cuthbert et al., 2007). This does not necessarily mean that the function of the missing protein is carried out by another up-regulated MAGUK. In fact, in many cases loss of the particular MAGUK results in dramatic phenotypes (Migaud et al., 1998, Cuthbert et al., 1997). MAGUKs SAP102 and PSD-95 play a key role in activity-dependent plasticity mechanisms downstream of glutamate, as demonstrated by electrophysiological approaches to synaptic plasticity (Migaud et al., 1998, Cuthbert et al., 2007). They have many overlapping functions associated with their roles in signal transduction downstream of NMDARs, as might be expected due to their high structural homology (for example, both SAP102 and PSD-95 couple NMDARs to the ERK/MAPK pathway (Komiyama et al., 2002, Cuthbert et al., 2007)). However they have distinct functions (for example, *Psd-95* mutants showed abnormal responses to LTP (100Hz) but *Sap102* mutants did not (Migaud et al., 1998, Cuthbert et al., 1007)) which may be due in part to the preferential binding of SAP102 to NR2B and PSD-95 to NR2A, coinciding with SAP102 & NR2B being the more dominant couplet of the two in early development (Sans et al., 2000). As synapses mature and PSD-95/NR2A expression increases, SAP102/NR2B couplets tend to be located at extra-synaptic membrane sites, while PSD-95/NR2A couplets are inserted and become more predominant at the PSD (Clark and Cull-Candy, 2002, Townsend et al., 2003). The timing of expression and the specific synaptic localisation raises the likelihood that each couplet may be linked to different cytoplasmic signalling cascades (van Zundert et al., 2004). Another reason for their distinct functions may be a result of the different N-termini sequences which mean PSD-95 requires palmitoylation to locate to the PSD (Craven and Bredt, 2000), while SAP102 forms a zinc finger (El-Husseini et al., 2000). Their similarities are sufficient for one protein to compensate for the other in its absence by up-regulating, but there are defects in each of the mutants so any compensation is only partial. For example, in *Psd-95* mutant protein extracts, hippocampal SAP102 is increased by nearly 50%, and striatal SAP102 by almost 100% relative to wild-type levels (Vickers et al., 2006, Cuthbert et al., 2007). Other MAGUKs SAP97 and Chapsyn110/PSD-93 were not altered in striatum and hippocampus of *Psd-95* mutants (Vickers et al., 2006). This indicates that the *Psd-95* mutation results in an increase in production of *Sap102* in many brain regions. In *Sap102* mutant hippocampal protein extracts, PSD-95, PSD-93 and SAP97 levels are unchanged, however NR1-IP with forebrain tissue shows that more PSD-95 is bound to NR1 in *Sap102* mutant compared to wild-type (Cuthbert et al., 207). It is possible that the *Sap102* mutation causes changes in the way that PSD-95 is trafficked to the synapse, rather than affecting transcription of new *Psd*-95. These different patterns of up-regulation point to SAP102 having a broader and perhaps more significant role than PSD-95 in early development, since it is the more prominent of the two in early development (Sans et al., 2000, van Zundert et al., 2004), and is more readily up-regulated (Vickers et al., 2006). Studies from double mutants examined here fit in with this finding, and suggest that SAP102 also plays a more important role than PSD-95 in the anatomical responses to glutamate signalling in early cortical development.

The presence of at least one copy of either *Sap102* or *Psd-95* is necessary for survival beyond P3, since double KOs were never found alive after P3. This may be a result of the inability to feed but further analysis of newborns is necessary to determine the cause of death. Upon examination of the formation of barrels by P7, mice with no *Sap102* and one copy of *Psd-95* on the 129/MF1 background do not form normal barrels. This indicates that in the absence of *Sap102,* one copy of *Psd*-95 is sufficient to prevent death but is not sufficient to mediate the correct signalling downstream of NMDARs necessary for normal formation of barrels. All other mutants have normal barrels and survive to adulthood. It is possible that PSD-95 is not involved in barrel formation at all, but can partially compensate for the loss of SAP102, perhaps by being up-regulated when SAP102 is reduced or absent. Therefore when SAP102 is absent and PSD-95 is reduced, there is not sufficient PSD-95 to fully compensate as it could in *Sap102*$^{-/y}$ *Psd-95*$^{+/+}$. The two MAGUKs are not completely redundant since both single mutations results in behavioural and physiological phenotypes (Migaud et al., 1998, Cuthbert et al., 2007). However, it is clear from the biochemical analyses described above that there is some up-regulation of one when the other is lost, indicating that there is partial compensation.

Mice with one copy of *Sap102* when *Psd-95* is deleted (*Sap102*$^{+/-}$*Psd-95*$^{-/-}$) are generated at normal ratios in some breeding pairs (pair, 202), but appeared to be weaker and more prone to early death in other breeding pairs (pair 211 & Cuthbert et al., 2007). When monitoring litters after birth I noticed that there was a tendency for whole litters to die during early postnatal life when there was a high % of double-KOs born, making detection of survival of specific genotypes complicated. This was seen by a tendency for parents to neglect and eat the whole litter once weaker pups started to die, perhaps as a reaction to an insecure environment. This could explain why Cuthbert and colleagues saw an under-representation of *Sap102*$^{+/-}$*Psd-95*$^{-/-}$ mice and I did not (Cuthbert et al., 2007). It is possible that by monitoring young litters and removing dead pups before they were eaten I was increasing the chances that weaker pups (such as *Sap102*$^{+/-}$*Psd-95*$^{-/-}$ perhaps) survived and were not cannibalised. Some studies have been carried out to investigate behavioural differences between strains. C57Bl/6J have an increased tendency over DBA/2J to exhibit infanticidal behaviour (pup-killing) and differences in nest-building behaviour, suggesting that inherent biological differences can affect these behaviours (Svare and Broida, 1982, Bond et al., 2002). This may be a result of differences in pre-natal hormone levels or sensitivity to these hormones (Svare et al., 1984). The effect of genetic strain on phenotype will be discussed in more detail later.

In order to understand the role that SAP102 and PSD-95 are playing in development, it is first necessary to understand the genetics of their gene expression. SAP102 is X-linked and therefore undergoes X-inactivation. In females almost all genes on one X-chromosome in every cell are inactivated. This has the effect of equalling the gene dosage of X-linked genes between males (XY) and females (XX) (Lyon et al., 1961). In wild-type females, cells in the whole body need to be able to function normally with one copy of *Sap102* inactivated. In female mice heterozygote for *Sap102*, barrels develop normally, even though a population of the cells do not have SAP102 expressed at all. In fact, to date no abnormalities have been reported in *Sap102*$^{+/-}$ mice although these mice are in early stages of investigation. Even though *Sap102*$^{+/-}$*Psd-95*$^{-/-}$ mice and *Sap102*$^{-/y}$*Psd-95*$^{+/-}$ mice both have only one copy of either *Sap102* or *Psd-95*, the former form normal barrels while the latter do not. Therefore formation of barrels is not related to the 'quantity' of total SAP102 & PSD-95 but is related to the specific ability of only one copy of *Sap102* to perform the function required for normal barrel formation in the absence of *Psd-95*. The ability of *Sap102* to maintain its function in barrel formation when only one copy is present in *Sap102*$^{+/-}$*Psd-95*$^{-/-}$ may be linked to the fact that *Sap102* is on the X-chromosome. In males there is only one copy of *Sap102* and cells need to be adapted to function normally with this amount.

4.3.2 Mechanism of barrel formation in Sap102$^{-/y}$Psd-95$^{+/-}$

Measurements of lamination of the cortex indicate that the cortex forms layers normally in double heterozygotes and *Sap102*$^{-/y}$*Psd-95*$^{+/-}$. This indicates that the defects in barrel development are unlikely to arise from a general delay in the development of the cortex. Furthermore, even at P14 barrels in *Sap102*$^{-/y}$*Psd-95*$^{+/-}$ are not fully formed indicating that the altered barrel formation does not reflect a delay in barrel formation. The mice that showed the most dramatic defect in barrel segregation (*Sap102*$^{-/y}$*Psd-95*$^{+/-}$ on MF1/129 background) also did not show differences in body size at P7 indicating that the defect was due to specific deletion of the genes in S1 and not due to poor health of these mice. Investigations into the formation of TCA patches showed that while the area taken up by patches in PMBSF is not altered, individual patches are smaller in size. This correlates with an increase in the width of barrel walls and suggests there may be a pre-synaptic role for MAGUKs in the formation of barrels. It is known that the formation of barrels requires the normal segregation of TCA into barrel-specific patches since if TCAs do not segregate, layer 4 cells do not segregate (Gaspar et al., 2003). Therefore a valid explanation for the inability of cells in *Sap102*$^{-/y}$*Psd-95*$^{+/-}$ to form barrels may be attributed to the incomplete arborisation of innervating axons. DiI injection into the thalamus and tracing of axons such as that carried out in *CxNr1* mutants (Lee et al., 2005) would be a good approach to analyse arborisation of axons in these mutants. EM studies on neonatal and adult rat visual cortex slices found that SAP102 and

PSD-95 are present presynaptically in axons as well as the PSD (Aoki et al., 2001) although other studies using a different procedure (immuno-gold EM of synaptosomes) for labelling found PSD-95 to be only post-synaptic in rat forebrain synapses (Hunt et al., 1996). If MAGUKs are present in the pre-synaptic cytoplasm they would not be detected in synaptosomes, which only include the pre-synaptic membrane. EM studies on these two MAGUKs specifically in barrel cortex would be necessary to identify the precise cellular location of each protein.

An alternative explanation for the defect in barrel formation comes from comparing the *CxNr1* mutation to the mutation described here of *Sap102*$^{-/y}$*Psd-95*$^{+/-}$. Even when NR1 is present in innervating thalamus, TCAs form smaller patches, elaboration of TCAs within the barrel hollow is reduced and TCA pruning outwith the hollow is reduced (Iwasato et al., 2000). This indicates that an NR1-dependent retrograde post-synaptic signal exists in layer 4 cortical neurons to regulate the refinement of TCAs into complete patterns (Iwasato et al., 2000, Lee et al., 2005). Therefore there may not necessarily be a pre-synaptic role for MAGUKs in TCA segregation. SAP102 may be acting post-synaptically to translate this NR1-dependent retrograde signal to refine TCA arborisation. Evidence for this mechanism may also be found in mice lacking SynGAP. TCAs do not segregate normally even though EM studies show SynGAP is postsynaptic in barrels. However, SynGAP is expressed in thalamus so SynGAP may alter thalamic neuron function such that segregation is impeded (Barnett et al., 2006). SynGAP associates with NMDARs via direct interactions with the PDZ-domains of SAP102 and PSD-95 and regulates downstream pathways such as the ERK-MAPK pathway (Chen et al., 1998, Kim et al., 1998, Komiyama et al., 2002).

4.3.3 MAGUKs and molecular signalling pathways

SAP102 and PSD-95 bind SynGAP to the NMDAR enabling SynGAP to negatively regulate the ERK-MAPK signalling pathway (Chen et al., 1998, Kim et al., 1998, Komiyama et al., 2002). PSD-95 enables the PKA-AKAP complex to associate with the PSD and regulate AMPAR removal at the synapse (Colledge et al., 2000). PKA activates AC/cAMP signalling pathways. Both SynGAP and PKA are necessary for the formation of segregated barrels (Barnett et al., 2006, Watson et al., 2006, Inan et al., 2006). There is evidence to suggest that SynGAP acts via an ERK-independent pathway to signal for barrels to form, possibly the AC/cAMP pathway (Barnett et al., 2006). It is possible that there is a threshold amount of activity required to drive one or more of the signalling pathways resulting in translation of the glutamate signal into layer 4 cell segregation. If the threshold of activity is not reached then cell segregation is poor. This could explain why different mutations result in various extents to the barrel defect. For example, if PSD-95 is only partially compensating for the loss of SAP102 in *Sap102*$^{-/y}$/*Psd-95*$^{+/-}$ mutants then the threshold may be not quite reached. In *Sap102*$^{+/-}$*Psd-95*$^{-/-}$ mutants however, one copy of *Sap102* is sufficient for the threshold to be reached. Together, data presented here and elsewhere indicate that complete molecular architecture of a specific PSD micro-complex is required for the threshold to be reached so that barrels can segregate completely. This complex contains molecules that act on a number of pathways such at the RasGAP/ERK-MAPK, PKA/AC/cAMP, PLC/IP3, and it unknown whether these pathways perform overlapping functions, or whether there is convergence on one particular pathway that is key to barrel formation.

4.3.4 Variation due to background

Results here and elsewhere indicate that there is large variability in phenotypes between backgrounds. My results show that wild type mice have better segregated barrels on MF1/129 background compared to Bl/6/129/DBA. In *Sap102*$^{-/y}$*Psd-95*$^{+/-}$ there is a greater defect on the MF1/129 background than on the Bl/6/129/DBA background. I also show that body weight at P7 is more severely affected by a *Sap102* mutation on Bl/6/129/DBA background than on MF1/129 background. Unfortunately body mass was not recorded at other ages on the Bl/6/129/DBA background but it has been reported that body mass returns to normal by weaning (Stanford et al., 2005, and Cuthbert et al., 2007). The early delay in weight gain may be due to a slight advantage of wild types when competing for food. The fact that weight loss is not sustained beyond weaning indicates that there are not metabolic problems as a result of loss of SAP102, (in fact SAP102 is largely neuronal) but that it may be a result of feeding behaviour. Behavioural studies of adult *Sap102* mutants found a small defect in spatial learning (Cuthbert et al., 2007), but it is unknown whether this phenotype correlates with feeding behaviour in young mice.

Phenotype is a product of the interaction between DNA and the environment. The extent to which a phenotype is a result of genetic variation is unclear. In inbred strains of lab mice unique variation patterns can arise through a result of natural evolution and selective breeding. The mouse ‘phenome’ project compares many phenotypic traits from coat colour to body size and growth to reproduction and various behaviours between 50 commonly used strains of mice (http://phenome.jax.org). This information provided in this interactive database highlights the extent to which phenotypes vary between strains at different ages. With such variation between strains it is possible to see how genetic deletion can have different effects on different background strains. This is more obvious when the phenotype of interest is complex and involves interactions between many proteins (such as the glutamate-dependent formation of barrels). There is wide scope among the proteins involved in barrel formation for strains to develop variations in genetic sequence of the molecules in pathways downstream of glutamate (or in molecules that regulate them), leading to changes in specificity, regulation, localisation and expression. The result of which can be a different response to the effect of a genetic mutation such as *Sap102* or *Psd-95*. Screening for SNPs is one way to detect changes in genes between strains but this method has faced some criticism as there is not a direct correlation between strain phenotype and inter-strain SNP variation (Wade and Daly, 2005).

4.3.5 Other functions of PSD-95

As well playing a role in physiological and synaptic plasticity, development and learning and memory, PSD-95 has other regulatory functions in sensitization, phosphorylation and organization of other membrane components.

PSD-95 is down-regulated in the striatum in 3 lines of mice carrying mutations for monoamine transporters when chronically cocaine-treated indicating that PSD-95 may be involved in sensitization to this drug. In *Psd-95* mutant mice the locomotor-stimulating effects of cocaine are enhanced, indicating PSD-95 plays a role in dopamine-mediated sensitisation to cocaine (Yao et al., 2004). Sensitization to neuropathic pain is poor in *Psd-95* mutant mice, possibly as a result of failure of CaMKII to dock to NMDARs (Garry et al., 2003).

CaMKII modulates synaptic structure and composition by phosphorylation of the Ser48 residue of Drosophila DLG (Koh et al., 1999). Cdk5 phosphorylates the N-terminal domain of PSD-95, and Cdk5 is critical for brain development. *Cdk5*$^{-/-}$ die perinatally (Ko et al., 2001) but embryos have enlarged clusters of PSD-95 at synapses indicating a role for PSD-95 phosphorylation in organization of the synapse (Koh et al., 1999).

PSD-95 also organizes other membrane proteins. It negatively regulates the tyrosine kinase Src, which in turn regulates activity of NMDARs by phosphorylation. The regulation depends on the SH2 domain of Src interacting with a 12-amino acid sequence at the N-terminal region of PSD-95 not previously known to have protein interaction properties (Kalia et al., 2006). In mouse forebrain PDZ domain 3 of PSD-95 binds the C-terminus of neuroligins, neuronal cell adhesion molecules that form intercellular junctions (Irie et al., 1997). PSD-95 regulates the clustering of kainate receptors through its interaction with PDZ1. Kainate receptor expression is involved in drug addiction and epilepsy and inhibiting the interaction may provide a novel route for treatment (Piserchio et al., 2004).

4.3.6 Summary

Examination of formation of barrels is an indication of how well glutamate signals can be translated into anatomical responses. NMDARs are necessary in this signalling pathway, along with intracellular molecules in the PSD that transduce NMDAR signals. Until now, MAGUKs have been known to play a role in synaptic plasticity, cell adhesion and regulation of receptor insertion and activity, but a role in the formation of barrels has not been described. Here data has been presented that shows that double knockouts of *Sap102* and *Psd-95* die shortly after birth but all other double mutants survive and are viable. All mutants surviving to P7 were examined for formation of barrels and a defect was found in *Sap102*$^{-/y}$*Psd-95*$^{+/-}$ mice. Cells do not segregate fully into cell dense walls and cell sparse hollows, TCA patches are smaller and walls are thicker, suggesting there may be a presynaptic role for SAP102 & PSD-95 in formation of barrels. Surprisingly *Sap102*$^{+/-}$*Psd-95*$^{-/-}$ have normal barrels, adding to the evidence that SAP102 plays a more critical role in early development and that either PSD-95 is less capable of compensating for loss of SAP102 than SAP102 is of PSD-95, or PSD-95 is not involved in barrel formation at all but can partially compensate for the loss of SAP102. The reason for SAP102 being more important in early development is not clear. SAP102 is the more predominantly expressed of the two in early development. Both have small differences in the binding partners and mechanisms of interactions, which may enhance or inhibit the ability of one to compensate in the absence of another. The answer may be in part due to the fact that *Sap102* is X-linked and so the brain is better used to coping with a reduced quantity of SAP102 protein being available. In female *Sap102*$^{+/-}$ mice, a population of the cells are not expressing SAP102 due to X-inactivation. This raises the possibility that the two populations of cells may not contribute equally to barrel formation as one population may be at a disadvantage by not expressing SAP102. It is unknown whether SAP102 acts cell autonomously or non-autonomously in barrel formation. The study of these two populations of cells in barrels will allow the role of *Sap102* in barrel formation to be examined. This approach is used in the next chapter.

4.4 Figures Chapter Two

Figure 2.1

Analysis of genotypes of 88 mice born from a pair generating *Sap102*/*Psd-95* double mutants. Statistical tests cannot be performed as mice were taken and genotyped at different ages, and in many cases sex was not recorded. Nine double KO mice were generated by this pair and were found dead at P0 (2), P1 (2), P2 (3) & P3 (2).

Squares: Males

Circles: Females

Shaded area: gene deleted

Unshaded area: gene unaffected

Figure 2.2

Measurements of lamination in PMBSF and AS region in P7 *Sap102/Psd-95* mutants. Error bars are standard error. WT n=6, S+/-P+/- n=1, S- P+/- n=2 unless otherwise stated.

A; Layer 1-6 PMBSF region, measurements taken from Nissl stained sections.

B; Layer 1-6 AS region, measurements taken from Nissl stained sections.

C; Layer 5-6 PMBSF region, measurements taken from calretinin stained sections.

D; Layer 5-6 AS region, measurements taken from calretinin stained sections.

E; Thickness of layer 4 in PMBSF region, measurements taken from PKARIIβ stained sections. (NB S+/- P+/- n=0)

F; Thickness of layer 4 in AS region, measurements taken from PKARIIβ stained sections. (NB S+/- P+/- n=0)

G; Layer 1-4 PMBSF region, measurements taken from calretinin stained sections.

H; Layer 1-4 AS region, measurements taken from calretinin stained sections.

Figure 2.3

Figure to show growth of *Sap102/Psd-95* mutants and body and brain mass at P7/8 and P14/15.

A: Growth of *Sap102*/*Psd-95* mutants prior to weaning. *Sap102* abbreviated to S. *Psd-95* abbreviated to P.

B: Body mass of *Sap102*/*Psd-95* mutants aged P7/8 (grey bars) & P14/15 (black bars). N-numbers under bars. ANOVA shows no significant differences between any genotype at both ages. (P 7/8 f=1.958, df=5, p=0.101; P14/15 f=0.945, df=4, p=0.460). Levene's test at 5% indicates all genotypes have equal variance at both ages.

C: Brain mass of *Sap102*/*Psd-95* mutants aged P7/8 (grey bars) & P14/15 (black bars). N-numbers under bars. ANOVA shows no significant differences between any genotype at both ages. (P7/8 f=1.142, df=5, p=0.373, P14/15 f=0.831, df=5, p=0.542) Levene's test at 5% indicates all genotypes have equal variance at both ages.

Figure 2.4

Body Mass of P7 *Sap102* mutants, *Psd-95* mutants and double mutants. *=p<0.05 student's t-test, **=p<0.01 student's t-test.

Sap102 male KOs (S-/Y) have significantly lower body mass at P7 than wild-type litter-mates (p=0.002). *Sap102* male KOs have significantly lower body mass than *Sap102* KO females (p=0.04)

(S+/Y n=5, S-/Y n=14, S+/- n=16, S-/- n=5, P+/+ n=3, P+/- n=11, S+/-P+/- n=3)

Figure 2.5

Analysis of barrels and TCA patches in *Sap102/Psd-95* mutants.

A: Nissl stain of tangential flattened cortices shows barrels are poorly segregated at P7 in *Sap102* KO/*Psd-95* heterozygotes as cell dense walls are barely visible and. Barrels appear normal in *Sap102* heterozygote/*Psd-95* KO. There is only slight improvement in *Sap102* KO *Psd-95* heterozygote at P9 and P14, where one or two rows of barrels are visible. Scale 500μm.

B: Anti-serotonin transporter antibody (SERT) labels TCA patches in P7 double-mutants of *Sap102* & *Psd-95*. Barrel patches look normal in all mutants, although patches appear small in *Sap102- Psd-95+/-*. Scale: 500μm.

C: Anti-mGluR5 antibody labels metabotropic glutamate receptor (5) in synapses within barrels in layer 4 in P9 double-mutants of *Sap102* & *Psd-95*. *Sap102- Psd-95+/-* mutant only shows faint regions corresponding to barrels, while all other mutants are normal. Scale: 500μm.

Figure 2.6

Quantification of segregation of cells into barrels at P7/8 and P14/14 on MF1/129 background.

A: Examples of barrel C2 in *Sap102*/*Psd-95* double-mutants on MF1/129 background, labelled with nuclear stain To-Pro-3 and SERT antibody from which cells were counted to determine ratio of cells wall:hollow. White arrow: TCA patches appear smaller in S-/-P+/-. Scale bar 100μm.

B: Analysis of ratio of cells in wall:hollow of mutants at P7 on MF1/129 background. *Sap102 ko Psd-95 het* is significantly different from wt. p=0.003 Student's t-test. S+/+ P+/+ n=6, S+/+ P+/- n=2, S+/- P+/+ n=2, S+/- P+/-n=2, S-/- P+/- n=4.

C: Analysis of ratio of cells in wall:hollow of mutants at P14 on MF1/129 background. (N.B. wild-type litter-mates not available.) S- P+/- is significantly different from S+/- P-/- & S+P-/- at p<0.01 and p<0.05 respectively. ANOVA & post-hoc tukey's test.

S+/+ P+/- n=7, S+/+ P-/- n=4, S+/- P-/- n=3, S- P+/- n=6,

Figure 2.7

Quantification of TCA patch size in *Sap102/Psd-95* mutants at P7/8.

A: Total area covered by SERT-labelled barrels B2&3, C2&3, D2&3 on MF1/129 background.

B: Percentage area covered by SERT-labelled barrels B2&3, C2&3, D2&3 on MF1/129 background. S- P+/- is significantly different from WT, student's t-test p=0.009.

Figure 2.8

Quantification of segregation of cells into barrels at P7/8 and P14/14 on Bl6/129/DBA background.

A: Examples of barrel C2 in *Sap102*/*Psd-95* double-mutants on Bl/6/129/DBA mixed background, labelled with nuclear stain To-Pro-3 and SERT antibody from which cells were counted to determine ratio of cells wall:hollow. Scale bar 100μm.

Figure 2.9

Analysis of segregation of cells into barrels in *Sap102/Psd-95* double mutants on Bl/6/129/DBA mixed background. No statistical differences are seen between any mutants in density ratio.

WT (1.48 n=1), S+/+ P+/- (1.38±0.06 n=7), S+/+ P-/- (1.42 n=1), S+/- P+/+ (1.33 n=1), S-/y P+/+ (1.54±0.08 n=4), S+/- P+/- (1.38±0.08 n=5), S-/y P+/- (1.28±0.03 n=7). (P=0.2, t-test on ratios S+/+ P+/- (n=7) vs S-/y P+/- (n=7))

Figure 2.10

SAP102 immuno stain on P7 *Sap102*/*Psd-95* double mutants. Low power coronal section showing cortex and hippocampus (left column) and high power coronal section of PMBSF (right column). SAP102 is highly expressed throughout cortex, in particular layer 4. It is not possible to identify immuno-positive cell bodies in layer 4 of cortex due to the dendritic location of SAP102. Therefore it is not possible to identify *Sap102*-ve and *Sap102*+ve cells in female *Sap102*+/- that are mosaic. In layers 5/6 cortex it is possible to see immuno-positive cell bodies and it appears that density is lower in female *Sap102*+/- (lower 3 rows) than in male *Sap102*+/y (upper two rows), consistent with a mosaic expression of SAP102 in female *Sap102+/-* mice.

Scale bars: left column 500μm, right column 500μm.

5 Data Chapter Three:

SAP102 mosaicism in barrels

5.1 Introduction

During early embryonic development in female mammals one of the two X-chromosomes in every somatic cell becomes transcriptionally inactive. This process begins at E6.5 and is thought to be complete by E10.5 (Monk & Harper, 1979, Tan et al., 1993). Almost all genes encoded by the X-chromosome undergo this phenomenon that has the effect of equalizing the gene dosage between males (XY) and females (XX) (Lyon et al., 1961). In each cell, one X-chromosome becomes inactivated (Xi), and the other remains active (Xa), and each descendent cell retains the same X-inactivation status of the parent cell. The result is two populations of cells, one that expresses the X-linked genes of the paternally inherited X-chromosome (Xp), and the other that expresses the maternally inherited X-linked (Xm) genes (Nance, 1964). Females are therefore mosaics for X-linked genes. Studies in mouse and human have revealed many X-linked genetic diseases that coincide with an imbalance in X-chromosome inactivation (XCI). The study of these disorders along with transgenic mice carrying alterations to the genes responsible for XCI have enabled mechanisms of XCI to become further understood (see appendix II for further information).

5.1.1 Skewed X-inactivation

A cell autonomous effect of SAP102 resulting in fewer mutant cells contributing to a barrel would be detected as a skew in XCI. In most tissues of the female mammal there is a normal distribution of XCI around a mean of 50% such that 50% cells express Xp genes, and 50% express Xm genes. However, sometimes there is a deviation from 50:50 in either a particular tissue or in the whole organism. A deviation from 50:50 results from one of two things.

1.) The under-represented cells are selected against, due to being at a disadvantage in survival, or due to carrying a mutation slowing their replication.
2.) The tissue is derived from a single cell and so all cells in that tissue have the same chromosome inactivated. In the case of a whole organism, by chance at early embryonic stages more cells had the same X-chromosome inactivated.

In the female population there is a normal distribution of X-inactivation around 50%. It is estimated that approximately 10% of all females have a skewed distribution of 80:20 or more Xi (Nance et al., 1964, Gale et al., 1994 a & b, Naumova et al., 1996, Plenge et al., 1997, 1999) (see diagram 17). Often a skewing of X-inactivation can be a result of mutations to X-linked genes effecting viability or proliferation.

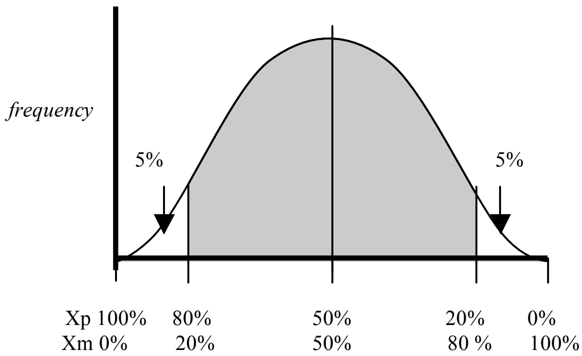

Diagram 17 **Distribution of XCI in normal female population**

Approximately 10% of the population have, 20%:80% or more Xp:Xm or vice versa. 90% of the population it situated between 20% and 80% (grey shaded region). Those falling into the unshaded region have skewed XCI. (Nance et al., 1964, Gale et al., 1994, Naumova et al., 1996, Plenge et al., 1997, 1999)

5.1.2 Detecting and measuring XCI

The techniques used to analyse whether there is skewed XCI in a mouse model of a X-linked genetic disease require the ability to label an entire population of cells (either Xa or Xi). For female mice carrying a *Sap102* null mutation on one chromosome, the two populations are those cells that express SAP102 (*Sap102*$^{+}$) and those that do not express SAP102 (*Sap102*$^{-}$). Labelling is much more straightforward if the mutated protein has nuclear localisation or is expressed embryonically, but even this procedure does not label a complete population since some tissues/cells may not normally express SAP102. Generation of transgenic mice with an easily detectable nuclear protein sequence (such as *LacZ, GFP or YFP*) inserted onto the X-chromosome has provided a solution to labelling one population of cells. The X-linked *HMG CoA LacZ* mouse was generated for the purposes of studying XCI throughout all stages of development (Tan et al., 1993, Tan and Breen, 1993). The *E.Coli LacZ* transgene is under the control of a ubiquitously active promoter for the mouse housekeeping gene *3-hydroxy-3-mehtylglutaryl coenzyme A reductase (HMG*

CoA), producing a nuclear-localised β-Galactosidase protein. If either Xm or Xp cells carry the *LacZ* transgene, female heterozygote offspring will be mosaic with one population of cells having the X-chromosome carrying the LacZ transgene (*Xb*) activated, and the other population inactivated (*X*). Cells Xa for *LacZ* (*Xb*) can be labelled with X-Gal, the substrate for β-Galactosidase enzyme that turns blue or an antibody against β-Gal, the protein product of *LacZ*. This tool will be utilised here to study of the role of XCI in *Sap102/Psd-95* transgenic mice. By breeding the *Sap102/Psd-95* mutants with the HMG CoA *LacZ* mice, it is possible to label populations of cells that may carry the wild type *Sap102 (Sap102^{+})* or have *Sap102* deleted (*Sap102^{-}*). This is particularly useful since SAP102 is localised to synapses, axons and dendrites and is found within the cytoplasm so labelling and counting nuclei expressing SAP102 is impossible. The other advantage of using *HMG CoA LacZ* mice is that β-Gal should be expressed in every cell that has *Xb* activated after XCI regardless of whether the cell would normally have SAP102 expressed (i.e. β-Gal expression is not subject to SAP102 regulation due to age/tissue type/cell type).

5.1.3 X-linked diseases

X-linked diseases are identified due to their occurrence within families with affected males in alternate generations. They are caused by a mutation of a gene on the X-chromosome therefore they have a higher frequency in males and are inherited from the mother. In female carriers, XCI causes mosaicism, with one population of cells expressing from the mutated X-chromosome, and the other population expressing genes from the unaffected X-chromosome. Therefore females often exhibit a milder form of the disease, although there may be a range of phenotypes depending on the relative contribution of each cell population. One cell population may be at a selective disadvantage in growth, resulting in a clonal outgrowth of Xp or Xm cells (Belmont, 1996, Puck and Willard, 1998, Willard, 2000).

Around 10% of all Mendelian-inherited genetic diseases are due to mutated X-linked genes (Ross et al., 2005). This may be because these diseases are more easily identified due to their inheritance pattern. Approximately 1100 genes have been identified on the X-chromosome, of which 80% are protein-coding (Ross et al., 2005, Harsha et al., 2005, Vallender et al., 2005). Over 500 of these genes are expressed in the human brain (Ropers, 2006), making them candidates for X-linked brain diseases. Many genes affecting cognition are found on the X-chromosome (Skuse, 2005), and epidemiological studies show that there is an excess of males with mental retardation and autism spectrum disorders. X-linked Mental Retardation (XLMR) is a common cause of moderate to severe forms of mental retardation affecting 1/1000 males. Many of the genes responsible have not yet been identified. 215 XLMR conditions have been identified, and of these 82 of the XLMR genes have been cloned and 97 of these conditions have been positioned by linkage analysis and cytogenetic break points. These are useful mapping tools that hopefully along with high-throughput genomic DNA re-sequencing of the X-chromosome (such as that carried out at the Sanger Institute), in time will be used to identify further XLMR conditions (Chiurazzi et al, 2008). One such disorder that as already been identified by the project based at Sanger Institute, along with international collaborators is the human XLMR condition resulting from mutations to *DLG3* (Tarpey et al., 2004). Recent generation of *Sap102* mutant mice has provided a mouse model for the *DLG3* condition (Cuthbert et al., 2007).

5.1.4 Summary of key findings leading to specific aims

In the previous chapter the role of SAP102 along with another scaffolding molecule of similar structure, PSD-95 was investigated in the formation of barrels in the mouse somatosensory cortex. Both proteins are bound to NMDARs and are responsible for maintaining stability and signalling in the PSD complex. The function of each is redundant, that is removal of one protein does not disrupt barrel formation, probably due to compensation by the other. Examination of double mutants revealed that double KOs die by P3 and loss of SAP102 and reduction of PSD-95 ($Sap102^{-/y}Psd\text{-}95^{+/-}$) results in the incomplete segregation of cells into barrels. Interestingly, barrel segregation is normal in $Sap102^{+/-}Psd\text{-}95^{-/-}$ despite the fact that XCI, if it occurred normally, would result in 50% of the cells being double KO for *Sap102* and *Psd-95*. Normal barrels are also seen in $Sap102^{+/-}Psd\text{-}95^{+/-}$ females, despite the fact that a population of the cells are of the genotype not able to segregate into normal barrels (the $Sap102^{-}$ population). These results could be explained by either of two mechanisms relating to XCI and SAP102 function, and will be investigated in this chapter.

5.1.4.1 Specific aims of this chapter

1. To determine whether X-linked *Sap102* has a cell-autonomous or non-autonomous role in the formation of normal barrels in *Sap102*$^{+/-}$ and *Sap102*$^{+/-}$*Psd-95*$^{+/-}$ females.

    a) A cell autonomous effect would be if *Sap102*$^{-}$ cells are selected against. This would be seen as a skewed XCI in a population of cells.

    b.) A cell non-autonomous effect would be if *Sap102*$^{-}$ cells are normally expressed but their inability to segregate into normal barrels is rescued by neighbouring *Sap102*$^{+}$ cells enabling both populations of cells in that mouse to respond appropriately to glutamatergic signals and form well-segregated barrels.

2. To determine whether XCI is skewed when *LacZ* transgene is maternally or paternally inherited.

3. To determine the proportion of *Sap102*$^{+}$ cells that are required for a barrel to form normally when PSD-95 is reduced (in *Sap102*$^{+/-}$ *Psd-95*$^{+/-}$).

5.2 Methods

5.2.1 Generation of *Sap102/Psd-95/β-Gal* mice

The breeding of *Sap102/Psd-95* mutants with mutants carrying the *LacZ* transgene is complicated and requires a number of generations of breeding. Mice need to be generated so that analysis of the effect of the *LacZ* transgene on barrel segregation in mice with other mutations not known to affect barrels can be carried out. The method for labelling $Sap102^+$ cells using the X-linked *LacZ* transgenic line of mice is described in the earlier methods chapter of this thesis.

The first aim is to determine whether insertion of the *LacZ* transgene disrupts barrel formation or causes skewed XCI. The formation of barrels in mice with one and two copies of *LacZ* will be analysed, and the contribution of each cell population calculated. The genotype of these female mice is abbreviated to *XbX* and *XbXb* respectively. Previous studies using the *HMG CoA LacZ* mice found that the presence of the additional autosomal (*HMG CoA*) and prokaryotic (*E.Coli LacZ*) sequences did not produce an obstacle for inactivation of the transgene (Tan et al., 1993). However, this study was carried out on the C57Bl/6 x DBA/2 background and without specific analysis of XCI in the barrel cortex, and so analysis of barrel segregation on the mixed background of the *Sap102/Psd-95* mutants (Bl/6 129 DBA) needed to be performed.

The second aim is to investigate whether there is genetic interaction between *LacZ* and *Sap102,* resulting in abnormal barrel formation or skewed XCI in barrels. The mice used for this are female mice carrying mutations to *Sap102* on a separate X-chromosome to β-Gal (genotype abbreviated to XbX^- where '-' refers to the *Sap102* mutation).

The third aim is to investigate whether there is genetic interaction between *LacZ* and *Psd-95,* resulting in abnormal barrel formation or skewed XCI in barrels. The mice used for this are females carrying a *LacZ* transgene on one chromosome with a *Psd-*

95 mutation to one allele (*XbX Psd*$^{+/-}$). These mice enable any effect of incorporating *LacZ* with a *Psd-95* mutation to be analysed.

The final aim is to investigate the role of SAP102 in barrel formation when PSD-95 is reduced. This will involve two analyses 1) To determine whether a population of *Sap102*$^{-}$ *Psd-95*$^{+/-}$ cells are selected against (resulting in skewed XCI) in barrel formation when surrounded by a population that are *Sap102*$^{+}$ *Psd-95*$^{+/-}$, or whether they contribute equally to barrels. 2) To determine whether one population or the other segregates to a greater extent into cell dense walls and cell dense hollows. The genotype of the mice used in this investigation is *XbX*$^{-}$*Psd*$^{+/-}$. In order to investigate the role of SAP102 in barrel formation when PSD-95 is *absent, XbX*$^{-}$*Psd*$^{-/-}$ mice are required. These mice are particularly useful since one population of cells are double KO and so may be selected against or may not segregate into barrels. Both the genotypes of mice in this investigation have normal barrels in the absence of the *LacZ* transgene (see previous chapter).

5.3 Results

5.3.1 *LacZ* transgene does not disrupt barrel formation

To determine whether the *LacZ* transgene disrupts barrel formation, segregation of cells into barrels in mice with one or two copies of *LacZ* is quantified. If the transgene interfered with barrel formation then interpretation of results in *Sap102/Psd-95/β-Gal* mutants would be very difficult. Initially, coronal and tangentially flattened sections from mice with one copy of the *LacZ* transgene were stained for the X-Gal reaction. β-Gal is expressed in cell bodies and β-Gal staining alone showed labelled cells segregating into barrels in *XbX* and *XbXb* females (fig 3.1 a). This indicates that qualitatively, barrels form normally in mice expressing the *LacZ* transgene. There are fewer cells expressing β-Gal in *XbX* (fig 3.1 a left panel) mice than in *XbXb* (fig 3.1a right panel) as expected due to one population of cells not expressing β-Gal in *XbX* mice. Very few *XbX* mice showed coronal sections where stripes were visible as might be expected due to clonal radial migration of cortical cells, and this was most obviously seen in coronal sections showing visual cortex (images not shown). In fact it was more common to see a uniform distribution of cells throughout the cortex as expected due to lateral migration after birth (fig 3.1a & b). Coronal sections show that β-Gal antibody labelling of cell bodies in layer 4 is not as clear as other cortical layers (fig 3.1 c), making the job of counting populations of cells difficult. Cell density is highest in layer 4 (fig 3.1c) and the staining of neuropil may be obscuring the labelled cell bodies. In tangential sections is is possible to identify and count cell bodies labelled with the β-Gal antibody, although there is background labelling not localised to cell bodies. Initially a green fluorescent antibody was used to label β-Gal-expressing cells in tangential sections but after optimisation and due to reasons described in methods chapter, a red fluorescent antibody was favoured (see section 2.4). Quantification of barrel C2 in female P7 mice with one or two copies (*XbX or XbXb*) using β-Gal antibody labelled with a red fluorophore (λ568) shows that the barrels segregate normally with ratios of 1.4 in both populations of cells (fig 3.4a).

5.3.2 Addition of *LacZ* transgene reveals sub-100% labelling

In female mice homozygous for *LacZ*, or in hemizygous male mice expressing *LacZ* it is expected that every cell will express *LacZ* due to *HMG CoA* being a ubiquitously expressed house-keeping gene. Female heterozygotes would be expected to show a normal distribution of XCI around 50%. After optimising the α-β-Gal antibody, the number of β-Gal and To-Pro-3 (nuclear stain) labelled cells were counted in barrel C2 in P7 female mice with one copy (*XbX* n=4) and mice with two copies (*XbXb* n=5) of the *LacZ* transgene (fig 3.2). On average *XbX* mice have 36.5% (±4.6) of their cells labelled with β-Gal antibody, made up of 36.8% (±5.3) in wall and 35.3% (±3.2) in hollow (fig 3.3 a). *XbXb* mice have approximately double that seen in *XbX* mice, with 76.7% (±3.9) of cells in C2 labelled with β-Gal antibody, made up of 77.9% (±3.5) in barrel wall and 74.3% (±5.9) in barrel hollow (fig 3.3 a). This sub-50% expression of *LacZ* in heterozygous mice is also found in mice with mutations to *Sap102* and *Psd-95*. If all mice hemizygous for LacZ are grouped together, there is a normal distribution around the mean of 40.63 (fig 3.6 a). As mentioned in the methods, the optical slice thickness may vary depending on the wavelength of light emmitted by a given fluorophore. If adjustments are made to the data based on optical slice thickness for the two fluorophores for To-Pro-3 (λ647) and β-Gal (λ568) the data is normally distributed around the mean of 48.75 (fig 3.6 b) (see Methods for in-depth discussion about this). The Shapiro-Wilk is a good test of skewness in a population where $n<50$. For this data ($n=29$) the significance level is 0.156, which is greater than the significance level of 0.05, therefore the null hypothesis is accepted, and the population *is* normally distributed around the mean.

5.3.3 There is no difference in XCI when *LacZ* is on Xp (paternal X-chromosome) or Xm (maternal X-chromosome)

In some tissue types there is a tendency towards XCI occurring to a greater extent in either favour of Xm or Xp. This has been shown to occur in extra-embryonic tissue where cells show preferential paternal XCI (West et al., 1977 & 1978). Therefore I decided to analyse whether there is a different in the extent of XCI when *LacZ* is paternally or maternally inherited. Of all the 28 female mice analysed of different genotypes, some inherited the X-chromosome carrying *LacZ* from the maternal side, and some from the paternal side. In order to rule out a contributory role of the source of the X-chromosome in the amount of XCI in barrel C2 the data was split into two groups according to the parent from which *LacZ* was inherited (fig 3.7). There were 19 females that have an Xm locus of *LacZ*, and 9 that have Xp. The mean XCI for the Xm group was 42.9% β-Gal labelled cells and for the Xp group was 35.0% β-Gal labelled cells, but there is no significant difference (p=0.21). Standard deviations are 17.5 and 7.7 respectively. Kurtosis test was carried out to see if the two populations of those with *LacZ* on Xm and Xp are normally distributed. Kurtosis for Xp and Xm produced values close to zero, indicating a normal distribution about the mean XCI in both. Levene's test was carried out to check on the significance of the difference between the two variances, as there is a large difference between the two variances. Levene's test takes into account the differences in size of the two populations, and produces a number of p=0.027, which is less than p=0.05. This shows the variances are significantly different, suggesting that inheriting *LacZ* from the maternal side results in a greater tendency for barrel C2 to have skewed XCI, but Kurtosis test indicates there is no tendency towards XCI occurring in a particular direction in either those inheriting *LacZ* from Xp or Xm.

5.3.4 *Sap102$^-$* cells in *Sap102$^{+/-}$* segregate normally and are not selected against

Prior to analysing mice with both *Sap102* and *Psd-95* mutations, it was important to determine whether *Sap102$^-$* cells in a female *Sap102$^{+/-}$* are selected against or do not localise properly to barrel walls (i.e. if there is an interaction between the *LacZ* transgene and the mutant *Sap102* locus that would reduce a cells ability to segregate). Barrel C2 was analysed in mice that had a *Sap102* mutation as well as carrying the *LacZ* transgene. In the mice analysed, *Sap102* mutation was on the separate X-chromosome from *LacZ*, therefore β-Gal antibody is labelling *Sap102$^+$* (wt) cells *(XbX$^-$)*. These mice were compared to females carrying only the *LacZ* transgene (*XbX*). No differences were found between these genotypes; barrels look well segregated with a ring of dense cells surrounding an area of sparse cells. Both *XbX$^-$* and *XbX* mice have a population of β-Gal labelled cells (fig 3.2) that are localised to both wall and hollow of barrel C2. *XbX* mice have 36.5% (±4.6) of their cells labelled with β-Gal antibody, made up of 36.8% (±5.3) in wall and 35.3% (±3.2) in hollow (fig 3.3b). *XbX⁻* mice have 43.9% (±5.1) of cells labelled with β-Gal, with 42.5% (±5.3) in wall and 48% (±5.5) in hollow. There is no significant difference between the % β-Gal labelled cells in either genotype (p=0.43, *XbX* n=4, *XbX*- n=10), although there is a trend towards fewer *Sap102*$^{-}$ than *Sap102*$^{+}$ cells being present in *XbX*$^{-}$ mice. Density of cells in barrel C2 wall and hollow was calculated and the ratio wall:hollow gives a measure of the extent of segregation. Both genotypes (*XbX* and *XbX-)* have very similar ratios of density wall:hollow of 1.39±0.11 and 1.46±0.44 respectively, and there is no significant difference (p=0.68, *XbX* n=4, *XbX*- n=10) in the extent of segregation between the two populations of cells (fig 3.4 b).

5.3.5 *Sap102*$^{-}$ *Psd*$^{+/-}$ cells segregate normally in *XbX*$^{-}$*Psd*$^{+/-}$ mice and are not selected against

Examination of double-heterozygote mice carrying the *LacZ* transgene will indicate whether SAP102 has a cell autonomous or non-autonomous role in the formation of barrels. In double heterozygote mice (*XbX*$^{-}$*Psd*$^{+/-}$), due to XCI a population of the cells will be *Sap102*$^{-}$*Psd95*$^{+/-}$ (the genotype with poorly segregated barrels- see chapter 2) and the other population will be *Sap102*$^{+}$*Psd95*$^{+/-}$ and will be labelled with β-Gal. Qualitatively, barrels appear to be formed normally; cells dense walls are seen surrounding cell sparse hollows. Counting cells in wall and hollow and calculating density shows that *XbX*$^{-}$*Psd*$^{+/-}$ mice have normally segregated barrels (ratio=1.48±0.05, n=7) (fig 3.2, 3.4 c). β-Gal labelled cells (*Sap102*$^{+}$; black bars) segregate (ratio=1.53±0.06, n=7) to the same extent as To-Pro-3 labelled cells (ratio=1.53±0.05, n=7) (*Sap102*$^{-}$;grey bars) (fig 3.4 c). Therefore a population of *Sap102*$^{-}$ cells which are also *Psd95*$^{+/-}$ that would not alone be able to form normal barrels, appear to be rescued by the presence of *Sap102*$^{+}$ cells which are also *Psd95*$^{+/-}$. Litter-mates of other genotypes were processed together and compared to these mice. The two other genotypes produced as litter-mates are *XbX*$^{-}$*Psd*$^{+/+}$ and *XbX Psd*$^{+/-}$. Interestingly *XbX Psd*$^{+/-}$ have reduced segregation of cells into barrels, with a ratio of cells wall: hollow of around 1.2 (fig 3.4 c) compared to 1.4- 1.5 in *XbX*$^{-}$*Psd*$^{+/+}$ and *XbX*$^{-}$ *Psd*$^{+/-}$. Only 3 mice of this genotype (*XbX Psd*$^{+/-}$) were analysed compared to n=4 and n=7 of the other two genotypes. However, males that are *Psd95* $^{+/-}$ (n=3) also have low segregation of cells wall:hollow of around 1.2, indicating that there may be a genuine phenotoype in *Psd95*$^{+/-}$ mice (fig 3.4 d). In the previous chapter there was no significant defect in barrel segregation in *Psd95*$^{+/-}$ mice, although ratios were lower than wildtype on this background (see fig 2.9, *Psd95*$^{+/-}$ n=7) and on MF1/129 background (see fig 2.6 b, *Psd95*$^{+/-}$ n=2). It is possible that PSD-95 *is* required for the normal formation of barrels but in *Psd95*$^{-/-}$ mice SAP102 compensates for the loss of PSD-95. If this is the case, then it is possible that this compensation does not occur when PSD-95 is reduced, and only when PSD-95 is lost. Then there may be a defect in cell segregation in *Psd95*$^{+/-}$ but not in *Psd95*$^{-/-}$. While this explains the appearance of a defect in *Psd-95* it is not a realistic explanation.

5.3.6 There is no correlation between the extent of segregation in C2 and XCI in any mutants

It is possible that a mouse that has skewed XCI may be less likely to form normal barrels, especially if the outnumbered population of cells have the intact *Sap102* gene inactivated, and the mouse is also *Psd95*$^{+/-}$. For each mouse analysed, the amount of XCI (β-Gal stained cells÷To-Pro-3 labelled cells) was plotted against the extent to which cells segregate into barrels (wall:hollow density). The data was plotted on graphs with linear regression lines and correlation coefficients for each genotype (fig 3.5 a-c). A r^2 value of 1 indicated perfect correlation, and deviation from 1 indicated the extent of de-correlation. Tables can be used to determine the r^2 value that is considered significant based on how many mice were plotted for a particular genotype. None of the coefficients were considered significant based on the current number of samples. Therefore for any particular genotype there is no correlation between the number of cells that undergo XCI and the extent to which cells segregate into barrels. This also shows that a mouse with as few as 15% *Sap102*$^{+}$ cells in a *XbX*$^{-}$ *Psd*$^{+/-}$ mouse still has barrels that segregate as well as controls (see black arrow in fig 3.5 c, for example), so a low % of *Sap102* wildtype cells is enough to form normal barrels. The slope of a linear regression line also provides information about the relationship between the two variances. Most of the lines are straight, indicating that there is no relationship between % β-Gal cells and extent to which barrels segregate. This result indicates that Sap102 wldtype cells may rescue the inability of surrouding cells to segregate properly into barrels by cell non-autonomous mechanisms.

5.4 Discussion

Data here and previous investigations have shown the importance of SAP102 in development of the postnatal brain. Two populations of cells within female mice were analysed for segregation of cells into barrels. The *lacZ* transgene may have affected the ability of cells to form normal barrels since the ratios of cell segregation wall:hollow are lower in these mice than those previously analysed. This issue will be discussed here in more depth. It appears that cell non-autonomous mechanisms may enable Xb^{+} $Psd^{+/-}$ cells to rescue the inability of X^{-} $Psd^{+/-}$ cells to segregate into normal barrels in the XbX^{-} $Psd^{+/-}$ mouse. It will be very interesting to see whether double null mutant cells for *Sap102* and *Psd-95* are able to contribute to barrel formation in XbX^{-} $Psd^{-/-}$ mosaic mice.

This study has emphasised that even a small amount of SAP102 is sufficient when PSD-95 is reduced (or absent) for cells to interpret NMDAR signalling and segregate into barrels. In the activity-dependent developmental mechanisms of barrel formation, SAP102 plays an important role in compensating for the loss of PSD-95 but PSD-95 is not as efficient at compensating for the loss of SAP102. A similar one-way up-regulation was demonstrated by protein quantification of hippocampus in *Sap102* mutants and *Psd-95* mutants (Vickers et al., 2006, Cuthbert et al., 2007). However, PSD-95 has functions in plasticity mechanisms in adult, especially induction of LTD that SAP102 cannot undertake in its absence. This indicates that the two MAGUKs have very distinct but overlapping roles in numerous activity-dependent plasticity mechanisms that occur throughout development in numerous brain regions. It emphasises the importance of MAGUKs and their role in signal transduction that can result in conditions such as mental retardation. SAP102 may have influence over the formation of barrels by its regulation of NMDAR subunits at the synapse, as well as by modulating downstream signalling events. The signal transduction mechanisms can be well studied in the somatosensory system of mice where the formation of barrels is sensitive to quantities of interacting molecules and complex compensation mechanisms that occur between them during the first postnatal week. In the first postnatal week the appropriate transmission of activity from the periphery to the cortex is key for normal formation of barrels, and genetic disruption to the molecular pathways that mediate this transmission can have dramatic effects. Later plasticity mechanisms such as LTD and LTP and the physiological response of cells to whisker trimming, involve different molecular mechanisms to weaken and strengthen synapses and many of the molecules in these mechanisms are not necessary for barrel formation. As SAP102 is more prominent than PSD-95 in the first postnatal week, loss of SAP102 (with reduced PSD-95) has a more dramatic effect on barrel formation than loss of PSD-95 (with reduced SAP102).

5.4.1 SAP102 and mosaicism

In *Sap102*$^{+/-}$ females I have shown that there is no selection bias against *Sap102*$^{-}$ cells and both *Sap102*$^{+}$ and *Sap102*$^{-}$ cells are equally expressed and equally contribute to barrel formation. This result is not surprising since *Sap102*$^{-/y}$ mice have normal barrels. Therefore, any defect in transducing signals from NMDAR necessary for formation of barrels either does not require SAP102, or PSD-95 is compensating for the loss of SAP102. As described in the previous chapter, the latter is more the likely correct interpretation since one copy of *Psd-95* is not sufficient to form normal barrels in the absence of SAP102.

In *Sap102/Psd-95* double heterozygote mice where *Sap102* wildtype cells are labelled with β-Gal, both populations of cells (*Sap102*$^{-}$ and *Sap102*$^{+}$) contribute to walls and hollows to the same extent indicating that no one population has a disadvantage in responding to NMDAR signalling. Data in the previous chapter showed that when all cells in mouse are *Sap102*$^{-}$*Psd-95*$^{+/-}$ then barrels do not form properly. This, along with data from this chapter provides evidence, albeit limited, indicating that in mosaic female double heterozygotes, *Sap102*$^{+}$*Psd-95*$^{+/-}$ cells may be rescuing the segregation defect of *Sap102*$^{-}$*Psd-95*$^{+/-}$ cells. The role is described to be cell-non-autonomous since the ability to rescue appears to be the result of a neighbouring cell. This indicates that interpreting the signal from NMDARs requires cell:cell interactions and does not depend wholly on an individual cell's ability to transduce the signal and respond appropriately. The mechanisms involved in cell:cell interactions may involve the extracellular matrix which is known to be regulated by

NMDARs (Kalb & Hockfield, 1990), adhesion molecules, neurotrophins, or purely excitiatory/inhibitory signalling signalling between neighbouring layer 4 cells.

5.4.2 Skewed XCI

No particular genotype shows a skew in XCI as a population. However, there were a few brains analysed where barrel C2 did have an unusually high or low number of β-Gal labelled cells. In these mice, no difference was detected in the ability to form normal barrels, indicating that cells that do not express SAP102 are at no disadvantage from those expresing SAP102 whether the *Psd-95* genotype is wildtype or heterozygote. This is based on the assumption that relatively small sample of barrel C2 is representative of the extent of XCI in the whole brain. This assumption is made because I did not see evidence of stripes or patches in layer 4 S1 as might be expected due to clonal migration of cortical cells. Further analysis of XCI in whole brain is required to determine accurately the extent to which XCI in C2 is representative. Whatever the outcome, my results do show that the segregation of cells into a dense wall and sparse hollow in a particular barrel is not affected by the extent of XCI within that barrel.

It will be interesting to investigate more brains to try to include analysis of those with a greater extent of skewed XCI. It may then be possible to determine the % *Sap102* wildtype cells necessary to rescue the defect. Data here showed that as few as 15% *Sap102* wildtpe cells are sufficient for normal barrel formation, but no mice were analysed with fewer than 15%. In human patients with mutations to DLG3 resulting in non-syndromic mental retardation, 4 families out of 329 were found to have DLG3 mutations resulting in no SAP102 protein being produced (Tarpey et al., 2004). In one of these families, there were three carrier females and one mildly mentally retarted female. Investigation of lymphocytes to determine the extent of XCI showed no correlation between the extent of XCI and the carrier status or clinical manifestation. However, this does not mean that there is skewed XCI in the brain cells of the affected female. Similarly, in mice carrying mutations to MECP2, the gene responsible for Rett syndrome in humans, XCI is measured by lymphocyte XCI and is claimed not to be conclusive for XCI in brain cells (Kleefstra et al., 2003). This evidence from the human DLG3 condition combined with data from mosaic mice indicates that skewed XCI in *Sap102*$^{+/-}$ *or DLG3*$^{+/-}$ is not linked to either the ability to form barrels or the clinical presentation of mental retardation respectively.

5.4.3 Role of LacZ transgene in barrel formation

Barrels look normal in mice with one and two copies of the *LacZ* transgene, and quantification shows that wall:hollow density ratio is 1.4:1. This number is smaller than numbers for wild type barrels (1.6) quantified in other chapters of this thesis. There are several reasons as to why this may be.

Firstly, a different approach was used to count cells in sections double-labelled with To-Pro-3 and β-Gal antibody. In double-labelled sections from *XbXb* mice all cells should be labelled with both To-Pro-3 and β-Gal. However, when looking at high power confocal images taken through a barrel, some cells appear to be labelled with only one or the other fluorophore. This could be due to a number of reasons associated with the parameters of microscopy, as described in the Methods chapter. Another reason for the discrepancy may be due to the fact that labelling for either or both fluorophores may not be 100% efficient. Upon counting cells in sections containing barrel C2, it became clear that some faintly labelled To-Pro-3 cells appeared to also be labelled quite strongly with β-Gal antibody, indicating that perhaps some cells simply do not express β-Gal at detectable levels. Therefore in order to include faintly-labelled β-Gal cells the counting criteria described in the Methods were altered so that cells that were faintly labelled with To-Pro-3 that previously were not counted, now were counted. Extending the criteria for what is considered a 'cell' means that a faint To-Pro-3 positive cell is now more likely to be counted if it lies in the hollow than the wall, because cell density is higher in the wall, and here faint cells are more likely to be shielded by other cells. As a consequence wild-type ratios for a well-segregated barrel become lower (i.e. 1.4 rather than 1.6). It should still be possible to detect a defect in barrel formation if the new criteria are applied consistently in all barrels analysed. However, the effect of shielding in barrel wall should be reduced in β-Gal cells than To-Pro-3 cells since only a population of cells are labelled with β-Gal, and both β-Gal and To-Pro-3 cells segregate to the same extent indicating that perhaps the density ratio is affect by another factor. One way to minimalise the effect of shielding would be to analyse thinner sections however it is more difficult to identify barrel wall and hollow in thinner sections.

A second reason could be that the reduction in cell density ratio is a direct result of the *LacZ* transgene, and further studies are currently being carried out by Dr P. Kind's lab to investigate this. If it were found to be the case that the addition of *LacZ* is directly linked to a reduction in segregation of barrels it could be due to disruption of other genes necessary for barrel formation when the *HMG CoA LacZ* gene is incorporated into the X-Chromosome. If this occurred, then it is not possible to tell whether in mosaics, *Sap102*$^{+}$ cells are rescuing *Sap102*$^{-}$ cells, as the *Sap102*$^{+}$ cells may also be affected by the disrupted gene causing the reduced density ratio. A comparison of barrels in male mice carrying the transgene may help in this investigation, as there are no complicated effects of XCI. Again, further investigation in the lab is being planned to reveal the exact site of *LacZ* incorporation.

A third reason for the reduced density ratio may be related to the genetic background of these mice. This issue is discussed in more depth in the conclusions of this thesis. The barrels of mice on this background (Bl/6/129/DBA) were studied in chapter 2 (fig 2.9) and density ratio of wildtype is 1.48 (n=1) but other genotypes have density ratios of 1.54 (n=4) indicating that background does not cause the reduced segregation.

5.4.4 Inheritance of *LacZ* and XCI

In some tissue types there is a tendency towards XCI occurring to a greater extent in either Xm or Xp. This has been shown to occur in extra-embryonic tissue where cells show preferential paternal XCI (West et al., 1977 & 1978).

After the X-linked *LacZ* mice were generated, studies were carried out to ensure that random patchy expression occurs in somatic tissues. While it was found that different tissues undergo XCI at different stages between E6 and E9 no differences were found in the source of the X-chromosome that undergoes XCI, or the extent to which XCI occurs (Tan et al., 1993). This was attributed to the fact that all mice used were on strains (C57Cl/6 and DBA/2) with the same *Xce* type (West et al., 1978) and so a 50:50 balance of XCI was expected. The locus of *Sap102* in mice appears to be very close to *Xist,* however there is 2Mb between these genes (www.ensembl.org) (see appendix II for explanation of the role of *Xist* and *Xce*). The *Xce* gene maps to within the region containing *Xist* and so does not impinge on the *Sap102* locus, therefore it is unlikely that *Sap102* is interfering with the randomness of XCI. Data here shows that while mice inheriting LacZ from Xm have a greater tendency towards skewed XCI, it is not in particular direction, and the population falls around the mean of 50:50. This indicates the importance of recording in each animal studied the source of LacZ (maternal or paternal).

5.4.5 Cross-over in meiosis

The generation of mice used for this study involved labelling a population of cells with β-Gal so that XCI could be detected in that population. The aim was that mice would be generated where either *Sap102+* or *Sap102-* chromosomes were labelled with β-Gal. To label the *Sap102-* population, the lacZ transgene needed to be inserted onto the X-chromosome carrying the *Sap102* mutation, and required cross over during meiosis. The probability of occurrence of a cross-over event during meiosis is related to the distance between the two X-linked genes on the X-chromosome. If genes are far apart there is a higher chance of a cross over event

Diagram 18 Schematic of *DLG3/Sap102* gene

Human *DLG3* is located at Xq13.1 in the region 69.58-69.64 Mb.
Mouse *Sap102* is located at C3 in the region 97.97-98.01 Mb.
HMG CoA LacZ is estimated to be inserted in or near A6.
Human *XIST* is located at Xq13.2, in the region 72.96-72.99 Mb.
Mouse *Xist* is located at C3, in region 100.65-100.68 Mb.

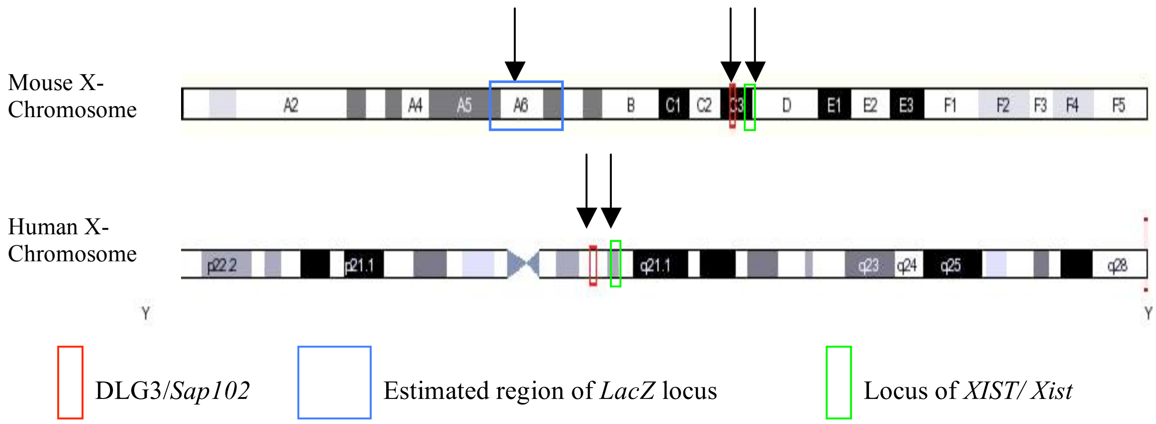

(figure taken from Ensembl and annotated (www.ensembl.org)) occurring between them, but different regions of the chromosome have different tendencies towards crossover. 1 centimorgan (cM) means there is a 1% chance of two genetic markers being separated by crossing over in a single generation. Chromosomal mapping permits an estimated probability of the event to be calculated but the exact location of incorporation of the *LacZ* transgene is not known (see diagram 18). It is estimated to be in the region of A6 on the mouse chromosome. The mouse genome is 2.7million kb, and is an estimated 1600-2000 cM in length (Laird et al., 1971). Therefore it has an average of 1350-1700kb of DNA per cM. There is an estimated 32-39Mb between mouse *Sap102* (98Mb) and the A6 region (59-66Mb) thought to be occupied by *LacZ,* translating to somewhere between 18.8 and 28.8cM, which is 19-29%. In reality, the occurrence of cross-over was found to be much less. For example, in one pair (pair 14) expected to produce *Xb-Y* males only one was generated from over 40 males weaned. Generation of $Xb^{-}Y\ Psd^{+/-}$ proved to be even more difficult. After 12 months of breeding, 4 males of this genotype were generated, and 3 did not survive to successfully breed. Therefore in this thesis I am not able to present analysis of the female mosaic of the genotype $Xb^{-}X\ Psd^{-/-}$.

5.4.6 Further study

All the mice used in experiments described here involve the *Sap102* mutation to be on the separate X-chromosome to the *LacZ* transgene. For a thorough analysis to be carried out mice would ideally be generated where the *LacZ* transgene is also expressed from the same chromosome as the *Sap102* mutation ($Xb^{-}X$, $Xb^{-}X\ Psd^{+/-}$, $Xb^{-}X\ Psd^{-/-}$). This additional investigation will confirm whether or not the *LacZ* transgene or the mutations to *Sap102* and *Psd-95* are affecting the ability of a population of cells to not segregate within barrels. To generate these mice there needs to be a cross over event whereby during meiosis the female mother which is XbX^{-} passes on both the *LacZ* transgene and the $Sap102^{-}$ to one of her offspring, resulting in a female which is $Xb^{-}X$ or a male which is $Xb^{-}Y$. The former type of offspring are difficult to identify since they genotype the same as XbX^{-}, but significant progress was made with the generation of the latter, resulting in two $Xb^{-}Y$ males. Unfortunately there was insufficient time to generate and analyse the experimental animals ($Xb^{-}X$, $Xb^{-}X\ Psd^{+/-}$, $Xb^{-}X\ Psd^{-/-}$), the latter of which are produced a number of generations later for this thesis. Therefore data is presented only from analysis of *XbX, XbXb,* XbX^- and $XbX^-Psd^{+/-}$, where *LacZ* is on a separate X-chromosome to the *Sap102* mutation.

5.5 Figures Chapter Three

Figure 3.1

Analysis of cortex in mice with *LacZ* transgene.

A: X-Gal stain of P7 flattened cortices labels β-Gal expressing cells. Barrels look normal in mice with one (XbX) and two (XbXb) copies of *LacZ. LacZ* expressing cells contribute to barrel wall and hollow. Scale bar, 200μm.

B: X-Gal stain of XbX adult females shows barrels form normally when *LacZ* transgene is present. A population of cells are labelled and an absence of stripes in most regions of the cortex shows clonally derived cortical cells mix with other cortical cells (due to lateral migration).

C: Labelling of β-Gal with a fluorescently-labelled antibody has the advantage of enabling all cells to be labelled with a nuclear stain such as To-Pro-3. Cells in layer 4 undergo more lateral migration than other layers, as no stripes of cells were seen. Cells in layer 4 are less well defined, probably due to a higher density of cells and neuropil in this layer resulting in cell bodies being masked by neuropil. Scale bars: upper left 1000μm, upper right 250μm, lower images, 200μm.

Figure 3.2

Analysis of mice carrying *Sap102/Psd-95* mutations and the LacZ transgene. Barrel C2 in *Sap102/Psd-95/β-Ga*l mutant females where *Sap102*$^{+}$ve cells contain *LacZ* DNA and therefore can be labelled with α-β-Galactosidase antibody. To-Pro-3 labels all nuclei regardless of genotype. *Sap102*$^{-}$ cells are To-Pro-3 positive and β-Gal negative. See methods for justification of using red fluorescent labelling rather than green. Scale bar 100μM.

Figure 3.3

Percentage contribution of β-Gal positive cells to different regions of barrel C2. Black bars: wall cells, dark grey bars: hollow cells, pale grey bars: wall and hollow cells combined. **$p<0.01$ student's t-test. (*XbX* n=4, *XbXb* n=5, *XbX-* n=10, *XbX-PSD*+/+ n=4, *XbX PSD*+/- n=4, *XbX-PSD*+/- n=7,)

A: β-Gal females containing LacZ on both X-chromosomes (*XbXb*) have significantly more β-Gal positive cells than females containing LacZ on only one X-chromosome (*XbX*) in all regions of barrel.

B: There is no significant difference in % contribution of β-Gal cells to barrel C2 between female *Sap102* heterozygotes (*XbX-*) and wild-types (*XbX*).

C: Females that are heterozygote for both *Sap102* & *Psd-95* (*XbX- PSD*+/-) have no significant difference in % contribution to barrel C2 than females that are heterozygote for only *Sap102* (*XbX- PSD*+/+) and for only *Psd-95* (*XbX PSD* +/-)

Figure 3.4

Cell ratio in wall: hollow of barrel C2 in *Sap102/Psd-95/β-Gal* mutants. Black bars, β-Gal positive cells (wild-type for *Sap102*); grey bars, To-Pro-3 positive cells (all cells regardless of genotype) (*XbX* n=4, *XbXb* n=5, *XbX*- n=10, *XbX-PSD*+/+ n=4, *XbX PSD*+/- n=4, *XbX-PSD*+/- n=7, *XbY PSD* +/- n=3, *XbY PSD*+/+ n=2,)

A: Cells in barrel C2 segregate normally into cell-dense walls and cell sparse hollows regardless of whether LacZ is present on one (*XbX*) or two (*XbXb*) X-chromosomes.

B: There is no statistical difference in segregation of cells in barrel C2 between females that are *Sap102* heterozygote (*XbX*-) or wild type (XbX). Cells containing LacZ in these females segregate to the same extent as all cells.

C: SAP102- cells in barrel C2 in female heterozygote for both *Sap102* & *Psd-95* (*XbX- PSD*+/-) segregate normally to barrel wall and hollow. However, there is a statistical difference between the double-het female and littermates that are only heterozygote for *Psd-95*.

D: In males where all cells are labelled with β-Gal, *Psd-95*+/- males have the same extent of barrel segregation as *Psd-95* +/+.

Figure 3.5

Correlation between cell density ratio (wall:hollow) in barrel C2 and % cells labelled with β-Gal in *Sap102/Psd-95/β-Gal* mutants. None of the genotypes shows correlation of density ratio to extent of XCI. A product moment correlation coefficient indicates that none of the r^2 values are significant based on existing sample numbers. (*XbX* n=4, *XbXb* n=5, *XbX*- n=10, *XbX*-*PSD*+/+ n=4, *XbX PSD*+/- n=4, *XbX*-*PSD*+/- n=7,)

A: There is no correlation between cell ratio and % β-Gal cells in females with *LacZ* on one (*XbX*; blue line, r^2=0.73) and two (*XbXb*; red line, r^2= 0.002) X-chromosomes.

B: There is no correlation between cell ratio and % β-Gal cells in *Sap102* wild-type (*XbX*; blue line, r^2=0.73) and heterozygote (*XbX*-; red line, r^2=0.10) females where one wild-type chromosome has LacZ.

C: There is no correlation between cell ratio and % β-Gal cells in females heterozygote for both *Sap102 & Psd-95* (*XbX- PSD*+/-; red line, r^2= 0.01). Comparisons are made on this graph to single heterozygotes of *Sap102* (*XbX*-*PSD*+/+; blue line, r^2=0.84) and *Psd-95* (*XbX PSD*+/-; green line, r^2=0.61) litter-mates.

Figure 3.6

Plot of % X-inactivation (no of β-Gal labelled cells / no of To-Pro-3 labelled cells) histogram for barrel C2 in each mouse analysed. NB all genotypes are grouped together, since no specific genotype showed a skew in X-inactivation (means are all around 40% see figure 3.2).

A: Plot of X-inactivation prior to normalisation. Mean = 40.63, standard deviation = 15.18, n=29.

B: Plots of X-inactivation after normalisation for estimated difference in optical section thickness due to use of red (β-Gal secondary excited at λ568) & blue (To-Pro-3 excited at λ647) fluorophores. Mean= 48.75, standard deviation = 18.21, n=29.

C: Data is not skewed around the mean and is normally distributed indicated by statistical normality test. The Shapiro-Wilk is a good test of skewness in a population where n<50. For this data (n=29) the significance level is 0.156, which is greater than 0.05, therefore the null hypothesis is accepted, and the population is normally distributed around the mean.

* This is a lower bound of the true significance.

Figure 3.7

Figure to show distribution of XCI in barrel C2 in females inheriting LacZ from either Xp or Xm.

In those with *LacZ* on Xp, mean = 35.0%, n=9, SD=7.7

In those with *LacZ* on Xm, mean = 42.9%, n=19, SD=17.5

There is no significant difference between the means (p=0.21, Student's t-test).

Kurtosis for Xp and Xm produced values close to zero, indicating a normal distribution about the mean XCI in both.

Levene's test determines whether the variances are significantly different from each other. This test produces a number of p=0.027, which is less than p=0.05 and shows the variances *are* significantly different, suggesting that inheriting *LacZ* from the maternal side results in a *greater tendency* for barrel C2 to have skewed XCI, but in no particular direction (as the means are not significantly different).

6 Data Chapter Four:

Signalling pathways involved in CSPG expression

6.1 Introduction

6.1.1 The Extracellular Matrix

The extracellular matrix (ECM) is the non-cellular part of the tissue filled with an intricate network of macromolecules consisting of proteins and carbohydrates. The ECM is important in aiding development of the CNS and maintaining normal function. The ECM is highly organised and accounts for approximately 20% of brain volume in adults, and up to perhaps 40% in newborns (Nicholson & Sykova, 1998). The ECM of the CNS has very small amounts of the common fibrous ECM proteins (for e.g. elastins and collagens), instead brain tissues express other types of ECM molecules such as proteoglycans, hyaluronan, link proteins and tenascins (Novak and Kaye, 2000, Galtrey and Fawcett, 2007). The role of the ECM was formerly considered to be mainly structural but more and more functions are being discovered as new techniques in immunohistochemistry and biochemistry enable its components to be studied in detail.

6.1.2 Components of ECM

Components of the ECM aggregate with the existing matrix after being secreted into the ECM by exocytosis. ECM components consist of the secreted proteins and carbohydrate polymers ‘glycosaminoglycans’ (GAGs- polysaccharides containing amino acids) that are added post-translationally in response to the environment. The addition of GAGs to the secreted proteins forms glycoproteins or proteoglycans, which then perform functions that may be specific to that cell, tissue or organ. A glycoprotein is a compound containing a carbohydrate covalently linked to a protein. Proteoglycans are a subset of glycoproteins where the carbohydrate units are GAGs. See Appendix III table 5 for summary of some ECM components. Chondroitin sulphate proteoglycans (CSPGs) are components of the ECM that have key roles in regulating processes in the CNS related to development, plasticity, and repair. This introduction will review evidence showing that CSPGs have a role in determining the timing of the end of the critical period for OD plasticity, and how their expression may be modulated by NMDAR activity.

6.1.3 Structure of CSPGs

The CSPG molecule consists of a core protein with Chondroitin-Sulphate glycosaminoglycan (CS-GAG) chains attached. There is variation in the identity of the core protein and in the position, number and length of attached GAG chains resulting in the diverse family of CSPGs (see Appendix III table 6). The core protein has multiple domains that determine its interactions with the ECM and its signalling functions. The CS-GAGs are linear chains of repeating disaccharide units (Silbert and Sugumaran, 2002) linked to the serine residue in core proteins. Xylosetransferase performs the linkage using Xylose to link to serine residues of the core protein. Glucuronic acid (GlcA) forms the basic disaccharide unit of CSPGs and after xylose addition is linked via a β-glyosolic bond to N-acetyl galactosamine (GalNAc) (Prydz & Dalen, 2000). The disaccharides are then polymerized into long chains by chondroitin synthase and chondroitin polymerizing factor (Kitagawa et al., 2001, 2003). CS disaccharides can be either mono-sulphated or di-sulphated by chondroitin sulphotransferases at various positions on the GlcA or the GalNAc. Sulphation modifications further enhance the diversity of CSPGs and define the type of CSPG.

6.1.4 Identification of CSPGs

There are four main groups of CSPGs, leticans; phosphacan/receptor-type protein-tyrosine phosphataseβ (RPTPβ); small leucine-rich proteoglycans; others including part-time proteoglycans and NG2 (Yamaguchi, 2000, Maurel et al., 1994, Garwood et al., 2003, Hocking et al., 1998, Stallcup, 2002). Part-time proteoglycans are in this category because the core protein does not always carry GAGs.

Monoclonal antibodies Cat-301, Cat-315 & Cat-316 were created as part of an immunisation strategy for the purpose of identifying cell-surface CSPGs and investigating their role in neuronal plasticity (Hockfield group; Cat-301 – McKay & Hockfield, 1982, Cat-315 & 316 – Lander et al., 1997). Antibodies were raised against the GAG chain of a CSPG and do not show reactivity in tissue from aggrecan KO mice (*cmd*), confirming that the antibodies recognise CSPGs containing the aggrecan core (Matthews et al., 2002). Each antibody identifies a distinct yet overlapping subset of cells that express aggrecan CSPGs (Lander et al., 1997, Matthews et al., 2002). Different staining patterns arise from these antibodies because they each recognise different glycosylations of aggrecan. Cat-301 recognised epitopes on the aggrecan protein core, while Cat-315 & Cat-316 recognise carbohydrate epitopes. Immunodepletion experiments show that CSPGs can carry one, two or three of the epitopes recognised by Cat-301, Cat-315 & Cat-316 (Lander et al., 1997). In total this identifies seven immunologically distinct CSPGs. Aggrecan mRNA is expressed rather late in development; it is low at E17 and rises steadily with a peak at P21. At this time CSPGs are seen to colocalise with a subset of maturing cortical GABA-containing interneurons and pyramidal neurons (Pizzorusso et al., 2002, Hausen et al., 1996), and there is a change from a general period of synaptogenesis to the period during which synapses become stabilized, the first indicator that CSPGs may inhibit plasticity (Guimaraes et al., 1990; Hockfield et al., 1990).

6.1.5 Role of CSPGs in axon guidance and synaptogenesis

During early mammalian development axonal tracts containing signalling molecules define the pathway to be taken by axons that grow into the cortex from thalamus. ECM components are candidates for this role, and CSPGs are heavily present in the subplate, part of the route taken by TCAs (Pearlman and Sheppard, 1996). However, the efferent connections that cross the subplate earlier follow a region containing much fewer CSPGs, suggesting that CSPGs may act as guidance cues to distinguish afferent from efferent pathways. Most publications acknowledge that CSPGs both promote and inhibit axon growth as a result of their wide variety of structural identity and through regulation of other guidance cues. For example, CSPGs have been found to regulate Semaphorin 5A a well-known axon guidance cue resulting in axon growth (Kantor et al., 2004) but NG2, a CSPG expressed on glial progenitor cells inhibits neural growth (Dou and Levine, 1994).

In vivo the antigens recognised by Cat-antibodies are expressed postnatally in the form of peri-neuronal nets (PNNs), but some components of PNNs are expressed earlier in rodent CNS development, even before synaptogenesis (Milev et al., 1998, Popp et al., 2003). In primary culture of neurons ECM components detected by monoclonal antibody Cat-315 are detected as soon as 24 hours after plating, suggesting a key role for them in synaptogenesis (Dino et al., 2006). The precise location of the immuno-positive stain is revealed to be in extrasynaptic sites prior to synapse formation, indicating a role similar to that in the NMJ where ECM components pre-pattern the synaptic sites on the muscle (basal lamina) prior to innervation by the motor neuron (reviewed in Arber et al., 2002, Kummer et al., 2006). This basal lamina exists following nerve injury and is thought to aid regeneration of the synapse (reviewed in Sanes & Lichtman, 1999, 2001). While there is no basal lamina in the CNS, other significant components of the ECM perform similar roles, such as CSPGs. In culture, Dino and colleagues found that Cat-315 labels RPTPβ isoforms (listed in column 2, table 6, Appendix III) (Dino et al., 2006) while in adult Cat-315 labels aggrecan (Matthews et al., 2002). The difference in the type of CSPG labelled indicates that it may be the carbohydrate motif that has significant functions in synaptogenesis, as well as the type of protein core it associates with.

6.1.6 The source of CSPGs

The cellular source of CSPGs has been subject to some debate over the past two decades. Recent data suggests that PNNs form between glial processes and the neurons that they outline (Celio & Blumcke, 1994) and in culture both cell types can produce CSPGs (Maleski and Hockfield, 1997, Deyst and Toole, 1995). Neurons can even produce PNNs in dissociated cortical cell culture in the absence of glia (Miyata et al., 2005). Protein core molecules aggrecan, brevican and phosphacan are all produced by cultured neurons (Hayashi et al., 2005, Lander et al., 1998, Seidenbecher et al., 2002). Labelling PNNs for the presence of GalNAc and CSPG identified by Cat-301 also reveals stain in the golgi apparatus and endoplasmic reticulum/perinuclear region respectively of the cell ensheathed by the PNN indicating that perineuronal net components (namely CSPGs) are produced by the cell they surround in vivo too (Streit et al., 1986, Hockfield & MacKay, 1983, Hendry et al., 1988). In 1998 the group that created monoclonal antibody Cat-315 also found that Cat-315 colocalizes with golgi markers in cells that are surrounded by PNNs (Lander et al., 1998). In this study synthesis and transport of CSPGs was inhibited in primary cultures using β-xyloside or monensin, resulting in retention of intracellular Cat-315 immunoreactivity within cells that have Cat-315 positive PNNs. The above evidence all contributes to the belief that CSPGs are generated and secreted by the cell around which the PNN will form. No evidence to date has been found to suggest that PNNs may be produced by synaptic contacts of neighbouring cells, the only other possible source.

6.1.7 Expression of perineuronal nets

The PNN is a well-described specialised form of the ECM. It is a lattice-like matrix sheath that surrounds synapses and a subset of mature neuronal cell bodies and their proximal dendrites. PNNs were first identified in cat spinal cord by Camillo Golgi in 1893 and in cerebral cortex by Ramon & Cajal 1897. They were subsequently named 'Golginetze' by a Polish CNS pathologist (Adamkiewicz, 1919). PNNs can be labelled with a variety of techniques, using the original method of golgi stain but more recently using lectins to label GalNAc (Nakagawa et al., 1986, Bruckner et al., 1993) and using immunohistochemistry to label the GAG chains (Rambourg et al., 1966, Bondareff et al., 1967, Castejon et al., 1970a & b) or CSPGs (Hockfield and McKay, 1983, Fujita et al., 1989, Watanabe et al., 1989, Bertolotto et al., 1990, Guimaraes et al., 1990, Asher et al., 1995, Wintergerst et al., 1996). In postnatal mammals PNNs are first seen at 2-3 weeks of age (Bruckner et al., 2000) but are seen much earlier in culture as already described. Immunohistochemistry has revealed that PNNs consist of glycoproteins, proteoglycans and hyaluronan and contain neurocan, aggrecan, brevican, phosphacan and all members of the letican family (Bandtlow & Zimmermann, 2000, Yamaguchi, 2000). They most often form around interneurons but sometimes also on pyramidal cells of cortex, hippocampus, dentate nucleus of cerebellum, olivary nuclei and dentate horn of spinal cord in many species, including human (see review, Celio & Blumcke, 1994).

6.1.8 Role of CSPGs in injury, repair and disease

CSPGs have an inhibitory role in axon growth, as demonstrated by experiments that use Chondroitinase ABC (ChABC), an enzyme that degrades GAG chains from CSPGs. After nerve injury an injection of ChABC can be administered to the region of interest and its effectiveness analysed using a 2B6 antibody that reacts with the four-sugar stub left behind after degradation. At various points after the injection the extent of axon re-growth is analysed. These experiments have been carried out in adult rat cerebellum (Corvetti & Rossi, 2005) where terminal branches extend from the Purkinje infraganglionic plexus 4 – 7 days after ChABC application. Myelinated axon segments do not extend, indicating they are not affected by the removal of growth-inhibitory CSPGs. These alterations are not permanent as the tendency is for the newly sprouted terminals to regress as CSPGs re-appear, complete 42 days after original ChABC application. In rat nigrostriatal tract, a similar reaction to ChABC occurs (Moon et al., 2001). In this case, rats were given unilateral nigrostriatal axotomy lesions, and an increase in appearance of CSPGs is seen at 1-2 weeks. If ChABC is delivered after axotomy, CSPGs do not appear and nigrostriatal axons regrow along the original nigrostriatal tract. Axons often grow ectopically, and branch extremely frequently rather than growing directly to their target in the ipsilateral striatum. Recovery from spinal cord injury has also been a key target for investigating the use of ChABC. This is perhaps the most advanced region of research in terms of prospects of a therapeutic application. Following the injury a glial scar develops containing CSPGs and other ECM components (Fawcett & Asher, 1999). Removing GAG chains following lesions to dorsal column of adult rats leads to a promotion in regeneration of both ascending sensory projections and descending corticospinal tract axons (Bradbury et al., 2002). Function is also improved in the use of limbs in rats treated with ChABC after injury. ChABC removes CS-GAGs whether or not they are forming part of a PNN. This is important when interpreting data that attribute the function after use of ChABC to the PNN when other mechanisms of CSPGs may be in use. For example, only last year new CSPG matrix structures named DACS (DAndelion Clock-like Structure) were discovered in cortex (Hayashi et al., 2007a). They are unique from PNNs as they surround a number of non-GABAergic cells rather than a single cell body and its proximal dendrites. DACS are identified by CSPG (CS56) antibody, are expressed at similar stages to PNNs and are also susceptible to digestion by ChABC.

The expression of CSPGs has been associated with protection against disease processes. The brains of Alzheimers patients have a build up of amyloid β protein - rich neurofibrillary plaques. Some cortical fields that are less susceptible to the build up of plaques are also high in PNNs, and so a possibility that PNNs may protect against neurotoxicity arises (Bruckner et al., 1999). This was investigated using primary cortical cultures, to test the resistance of cells with CS-GAGs to amyloid β1-42, an agent that mimics amyloid β in cultured neurons by aggregating and causing neurotoxicity. A significant number of neurons with no PNNs are killed after 48hours of amyloid β 1-42 treatment, while those with PNNs escape the toxicity. After the removal of CS-GAGs with ChABC the neuro-protection is removed and these neurons also die (Miyata et al., 2007).

6.1.9 Role of PNNs in plasticity

The unique position of PNNs on a subset of neuronal cell bodies, proximal dendrites and synapses, and their developmental expression profiles makes them ideal candidates for influencing synaptic development and stabilization (Hockfield et al., 1990, Celio & Blumcke, 1994) and therefore regulating synaptic plasticity. Experiments to investigate this have been carried out in the visual and somatosensory systems.

6.1.9.1 CSPGs in visual system plasticity

The correlation between CSPG expression and plasticity can be investigated by analysing the presence of PNNs in visually deprived rats and cats during and after the deprived period. Monoclonal antibody Cat-301 detects PNNs in cat visual system at the close of the critical period (Sur et al., 1988). Following dark rearing of cats there is a reduction in Cat-301 positive PNNs in LGN and visual cortex (Sur et al., 1990, Guimaraes et al., 1990). Following dark rearing of cats from birth to 1 year of age there is also a reduction in the density of Cat-315 & Cat-316 positive PNNs, most noticeably in layers 2/3 & 5/6 of visual cortex (Lander et al., 1997). At the end of a 70-day light deprivation period in rats there is a reduction in the number of WFA and neurocan-positive PNNs and the critical period for OD plasticity is prolonged beyond the normal 70 days. Reintroducing these animals into light for one week is sufficient to restore neruocan reactivity and terminate the critical period (Pizzorusso et al., 2002). These studies show a correlation between PNN expression and activity, indicating a role for PNNs in plasticity. They do not however, provide causal evidence that PNNs restrict plasticity. That evidence came from further studies carried out by Pizzorusso and colleagues that adjust the critical period and monitor PNN expression. It is possible to extend the critical period in mice and cats by digestion of PNNs with the enzyme Chondroitinase ABC (Galtrey and Fawcett, 2007). Pizzorusso and colleagues found that OD plasticity in adult rats can be restored after the critical period has passed if ChABC is injected into the visual cortex (Pizzorusso et al., 2002). In this study CSPGs were degraded in adult rats after the termination of the critical period (P>100). At the same time as the first injection one eye was closed. After 7 or 15 days MD the OD distribution was assessed by extracellular recordings in the cortex contralateral to the deprived eye. After 7 days, there was pronounced shift in OD that was not further enhanced after 15 days. In control cortex there was no OD shift. This evidence suggests that the plasticity of critical period in cats and rodents is regulated by CSPGs in development. It also suggests that CSPG-PNNs play a key role in determining the closure of the critical period, and that the expression of some subtypes of CSPGs are sensitive to the specific pattern or level of activity in that system.

6.1.9.2 CSPGs in barrel map plasticity

The barrel cortex also undergoes activity-dependent development and in this system it is possible to examine the effects of whisker trimming in circuits in the barrel cortex. CSPG subsets identified with Cat-301, Cat-315 & Cat-316 monoclonal antibodies are also expressed in mouse cortex and so further studies into the role of these CSPGs in developmental cortical plasticity have been carried out. Cat-315 has been shown to label CSPGs containing the aggrecan protein core in adult (Dino et al., 2006), and when McRae and colleagues found a decrease in the expression of Cat-315 expression following 30 days whisker trimming, there was a corresponding decrease in aggrecan mRNA in layer 4 of the cortex (McRae et al., 2007). This study also found that there is no overall change in number of PNNs labelled with WFA (a lectin that labels GalNAc, the sugar component of CSPGs) following whisker trimming. This indicates that it is only a specific subset of PNNs (Cat-315-positive PNNs) that are altered in barrels after whisker trimming, as WFA-PNNs are not affected. WFA has broad reactivity for PNNs and only occasionally colocalises with Cat-315-PNNs.

6.1.10 NMDARs and CSPG function

Selecting the appropriate synaptic connections in early development is key to the development of the visual and somatosensory systems. Activation of NMDARs has been shown to play an important role in this process. In mouse many of the proteins that interact with NMDARs have been identified and those important in the signalling pathways leading to selection of appropriate synaptic connections are being investigated. The activation of NMDARs results in altered anatomy and physiology and may be regulated by the ECM. In hamster spinal cord blockade of NMDARs with MK-801 or APV results in inhibition of the expression of Cat-301 in a dose-dependent manner. This effect is not seen in adults (Kalb & Hockfield, 1988), but only in hamsters that had the drug administered between the ages of 7 and 21 days of age (Kalb & Hockfield, 1990). Since CSPG expression can be regulated by NMDARs, we sought to identify the intracellular signalling pathways downstream of NMDAR activation that are responsible for this regulation. We examined mutant mice with genetic deletion of NRC/MASC components known to regulate early barrel development. These included:

1 & 2.) Metabotropic glutamate receptor 5 (mGluR5) is a group-1 glutamate receptor, it activates PLCβ-1 and both molecules are essential for formation of normal barrels. Homozygous null mutation of either molecule results in failure of layer 4 cells to form normal barrels despite normal TCA innervation and segregation (Hannan et al., 2001).

3.) Synaptic Ras-GTP activating protein (SynGAP) is bound to post-synaptic NMDARs via PSD-95 and following activation of NMDARs, it inhibits the MAPK pathway, which results in many plasticity –related defects. Homozygous null mutants of SynGAP fail to form normal barrels and heterozygotes also have defects (Barnett et al., 2006).

4.) Protein Kinase A (PKA) is an activator of the adenyl cyclase-cAMP pathway and is situated downstream of NMDARs in the post -synaptic membrane of layer 4 cortical cells. Null mutants of the second regulatory subunit of PKA (PKARIIβ) do not form normal barrels (Inan et al., 2006, Watson et al., 2006).

These 4 transgenic mice may have increased, reduced or delayed expression of CSPGs due to their inability to translate activity via the NMDAR into appropriate organization of cells and reorganization of dendritic structure. This possibility will be investigated in this chapter.

6.1.11 Summary of findings leading to specific aims

Determining the latency of the critical period during which barrels are formed may involve the extra-cellular matrix (ECM). NMDARs have been shown to regulate the expression of a subset of chondroitin-sulphate proteoglycans (CSPGs), identified with monoclonal antibody Cat-301 (Kalb and Hockfield, 1988). Cat 301, Cat-315 and Cat-315 antibodies all label overlapping but distinct subsets of CSPGs (Lander et al., 1997, Matthews et al., 2002), which appear as a diffuse neuropilar stain in early development but by P21 Cat-315 and Cat-316 label perineuronal nets (PNNs). PNNs have been shown to coincide with the close of the critical period, and removing them extends the period (Galtrey and Fawcett, 2007). Injecting an enzyme that digests CSPGs into the cat visual cortex after the normal period of OD plasticity reopens the period (Pizzorusso et al., 2002). Similarly in mice, 30 days of whisker trimming causes a reduction in Cat-315 PNNs in barrels (McRae et al., 2007). If disrupting mechanisms downstream of NMDARs causes a reduced or delayed expression of CSPGs, then this molecular pathway may be responsible for regulating physiological plasticity. CSPGs form a matrix that has been shown in cerebellum, nigro-striatal tract and spinal cord to inhibit dendritogenesis and synaptogenesis (Corvetti & Rossi, 2005, Moon, 2001, Bradbury et al., 2002), two mechanisms that occur during the period of barrel formation. The role of CSPGs in visual cortex makes CSPGs valid candidates for a function in somatosensory development such as determining the close of the sensitive period. One way to examine this would be to analyse the expression of CSPGs in mice that do not form barrels. This would indicate if any of the molecules in the pathways leading to barrel formation also regulate expression of CSPGs.

6.1.11.1 Specific aims

1. To describe the normal expression pattern of CSPGs identified with Cat-301, 315, & 316 antibodies in brains (specifically cortex) throughout development in mice.
2. To establish a method of quantifying the density of PNNs in barrel cortex.

3. To determine the intercellular mechanism downstream of glutamate neurotransmission that regulate CSPG expression.

6.2 Results

6.2.1 Cat-301 is expressed in mouse brain but does not localise to PNNs

In order to determine the normal expression pattern of CSPGs labelled with Cat-301, a developmental expression staining profile was established in mouse wild-type brains at P7, P14, P21 and adult. In coronal sections through S1 at P7 Cat-301 immunoreactivity appears in two discrete bands in the supragranular and infragranular layers (fig 4.1c). Staining appears dense and evenly distributed, reminiscent of neuropil staining in almost all regions of the brain (fig 4.1a) Staining is absent from layer 4 but present in other cortical layers (fig 4.1c), and absent from pyramidal cell body layers of hippocampus (fig 4.1b) but present in dendritic layers. White matter tracts are immuno-labelled the most strongly, defining the boundaries of different brain regions. At this age, no Cat-301 positive PNNs around cell bodies are visible (as seen in figure 4.13). At P14 Cat-301 is expressed much less in all brain regions (fig 4.2a). Staining is still visible in dendritic layers of hippocampus (fig 4.2b) but less than at P7, and absent from pyramidal cell body layers. In cortex there is no staining visible in any layers, although the pia is strongly labelled (fig 4.2c). This down-regulation of Cat-301 in cortex is temporary as by adulthood cortical stain has returned. The images in these figures are representative of other Cat-301 immuno stain at this age. At P21 again, pyramidal cell layers of hippocampus have no stain (fig 4.3b), but elsewhere there is uniform expression (fig 4.3a). By adulthood, Cat-301 is absent from white matter tracts, and still absent from pyramidal cell body layers of hippocampus. The most densely stained region in the whole of adult brain is the dendritic layers of dentate gyrus (DG) and CA1 (fig 4.4a&b) of hippocampus. There is uniform staining throughout different layers of the cortex (fig 4.4c) although the most medial region of the cortex appears to be more darkly labelled than other regions. There is some punctate staining in adult cortex that may be localised to glia. These regions of stain are not localised to PNNs (see table 2 for summary of PNN expression), contrary to what this antibody labels in cat brain (Lander at al., 1997).

6.2.2 Cat-315 is highly expressed in dendrites of hippocampus CA3 and forms PNNs in cortex

I carried out similar experiments to determine the expression profile of Cat-315 in wild-type tissue at various ages. At P7 Cat-315 is expressed in neuropil in most brain regions (fig 4.5 a & b), in a similar pattern to Cat-301. The cortex has uniform stain, apart from a slightly reduced expression in layer 4 (fig 4.5 c & fig 4.13 a). At P14 there is no expression at all of Cat-315 in cortex or midbrain (fig 4.6 a & c), but an unusual expression pattern of Cat-315 in hippocampus is apparent (fig 4.6 b). As with Cat-301, there is no stain visible in pyramidal cell layers, however, there is dense stain in the hilar region (CA4) of dentate gyrus (DG), where mossy cells are found, and also in dendritic layers of CA1. The expression in dendritic layers of CA1 terminates sharply at the boundary of CA2. This pattern in the hippocampus is evident much more strongly at P21, where again the expression in CA1 dendritic layer terminates in a sharp expression boundary at CA2 (fig 4.7 a & b). Lamination of the hippocampus can be identified by the different intensities of immunoreactivity. Stratum radiatum (St.R) is the most densely stained, followed by stratum oriens (St.O) and stratum lacunosum (St.L). Stratum pyramidale (pyramidal cell layer) has no stain. The strata expressing Cat-315 are where interneurons are found, consistent with the evidence that Cat-315 labels PNNs surrounding a sub-population of inhibitory interneurons (McRae et al., 2007). Mossy fibres in the hilar region (CA4) and the molecular layers of dentate gyrus both express Cat-315 while the granular layer does not. Mossy fibres project axons that terminate in the inner molecular layer of dentate gyrus, indicating that this cell type expresses the CSPG identified by Cat-315. In cortex at P21 the first PNNs are visible (fig 4.7 c), they are seen in S1 lower layer 4/layer 5 and surround very few cells (see table 2 for summary of PNN expression). In adult the PNNs are much more widely expressed and surround a population of cells in layer 4 and layer 5/6 (fig 4.8 a & c). In adult groups of PNNs can be seen to clump in regions corresponding to barrels in layer 4 (fig 4.13 c), and there is a much lower abundance of PNNs in surrounding cortical areas. High power images of PNNs in cortex reveal a matrix surrounding cell bodies and proximal dendrites (fig 4.13 e & g), as previously described in cat cortex (Lander et al., 1997) and mouse cortex (McRae et al., 2007). The hippocampus maintains dense staining as described at P21 but in adult the sharp expression boundary between CA1 and CA2 is no longer there (fig 4.8 b). Instead Cat-315 is seen in all dendritic layers of hippocampus, regardless of which group of cells they associate with.

6.2.3 Cat-316 localises to barrels from P7 and PNNs appear sooner and cover a greater cortical area than Cat-315

To establish a normal expression profile for Cat-316 CSPGs, mouse brains were stained at P7, P14, P21 and Adult and images were taken. At P7 a coronal section indicates that Cat-316 uniformly labels neuropil in all brain regions (fig 4.9 a), except for pyramidal cell layers of hippocampus (fig 4.9 b). There is no difference in density of Cat-316 stain throughout the layers of the cortex (fig 4.9 c), contrary to Cat-301 & Cat-315 which are absent from layer 4. Tangential flattened cortices at P7 even show an intensity of Cat-316 in barrels of layer 4 S1, this is not seen by any other Cat-3XX (fig 4.13 b). At P14 there is a reduction in the expression of the Cat-316 epitope (fig 4.10 a), although labelling is still seen in dendrites of hippocampus, especially ventral to CA3 and DG (fig 4.10 b). In P14 cortex few very faint PNNs are visible surrounding layer 4 cell soma (fig 4.10 c) and these become much more evident at P21 (fig 4.11 c) when there is very little labelling elsewhere in the brain (fig 4.11 a & b) (see table 2 for summary of PNN expression). Amongst the strongly labelled S1 region of layer 4, there is some labelling not associated with PNNs indicating that PNNs are just beginning to develop and are not complete. In adult, dendritic layers of hippocampus show strong expression (fig 4.12 b), and many more PNNs are seen in cortex (fig 4.12 c). There is less neuropilar background in adult layer 4 compared to P21, and in adult the neuropilar background is more uniform in its expression. The PNNs in cortex are seen in layer 4 and 5 and extend along S1 and V1 (fig 4.12 a & fig 4.13 d). This extension of the area of labelling laterally beyond S1 is greater than that seen with Cat-315 that is restricted to S1 (fig 4.13 c), indicating that the PNNs are surrounding a different but perhaps overlapping population of cells. High power images of PNNs in cortex show them to be a matrix with holes surrounding cell bodies, (often pyramidal cells) and proximal dendrites (fig 4.13 f & h) as previously described (Lander et al., 1997 & McRae et al., 2007).

	P7	P14	P21	Adult
Cat-301				
Cat-315			*	**
Cat-316		**	***	***

Table 2 Table to show expression of PNNs through development

Stars represent the density of PNNs. * Very few PNNs. ** Moderate amount of PNNs. *** Many PNNs.

6.2.4 Cat-315-positive neurons are in barrel hollows and some are labelled with parvalbumin

McRae and colleagues found that in adult layer 4 barrel cortex almost all Cat-315 –positive neurons also express parvalbumin, but less co-localisation was seen in other cortical layers (McRae et al., 2007). In this study very few neurons in adult layer 4 barrel cortex are labelled with both (lightening bolts, fig 4.14 e). Instead most Cat-315 –positive cells do not appear to express parvalbumin (yellow arrows, fig 4.14 a & e) and most parvalbumin positive cells do not express Cat-315-positive PNNs (white arrow heads, fig 4.14 d). There is a tendency for Cat-315 PNNs to localise to barrel hollows and walls and avoid regions of barrel cortex between barrels named 'septae' (fig 4.13 c & white arrows, fig 4.14 a & b).

6.2.5 MGluR5 and PLCβ-1 do not regulate expression of Cat-301, Cat-315 or Cat-316

To determine the pathways downstream of glutamate that regulate expression of CSPGs I examined staining patterns in tissue taken from *Mglur5* and *Plcβ-1* mutants. Nissl stain was used to label consecutive sections to those labelled with Cat-antibodies to enable different brain regions to be identified. Qualitatively, no differences can be seen between sections taken from P14 & P21 brains of *Mglur5* and *Plcβ-1*$^{-/-}$ and $^{+/+}$ (fig 4.15, 4.16, 4.18, & 4.19). In adult labelling of Cat-315 appears to be more uniform across layer 4 barrel cortex in *Mglur5*$^{-/-}$ & *Plcβ-1*$^{-/-}$ due to poor barrel formation in these mutants (Hannan et al., 2001), compared to the discrete clumps of PNNs in *Mglur5*$^{+/+}$ & *Plcβ-1*$^{+/+}$ corresponding to normal barrels as seen in Nissl (fig 4.17 & 4.20). Since Cat-315 and Cat-316 label PNNs in S1, the density of PNNs can be quantified and compared between mutants and wildtypes.

Quantitative analysis of Cat-315 & Cat-316 PNN density in layer 4 shows no statistical difference between *Mglur5* $^{+/+}$ & *Mglur5* $^{-/-}$ (Cat-315: WT 331±24 cells/mm^2 (n=6), KO 269±23 cells/mm^2 (n=4), p=0.11) (Cat-316: WT 298±14 cells/mm^2 (n=6), KO 269±13 cells/mm^2 (n=4), p=0.19) and *Plcβ-1* $^{+/+}$ & *Plcβ-1* $^{-/-}$ (Cat-315 WT 257±23 cells/mm^2 (n=4), KO 212±20 cells/mm^2 (n=5), p=0.18) (Cat-316 WT 308±8 cells/mm^2 (n=2), KO 332±28 cells/mm^2 (n=2), p=0.43) (fig 4.27, 4.28 & 4.31). Power analysis on data collected shows that if the current trends continue, a statistical difference between mean densities of PNNs in these mice will be obtained if the number of samples analysed is increased as shown in column 3 of table 7 (Appendix III). Power analysis indicates that the number of samples required to reach significance is unreasonable. Therefore the expression of PNNs labelled with Cat-315 and Cat-316 is not regulated by either PLCβ-1 or MGluR5.

6.2.6 Cat-301, Cat-315 and Cat-316 expression is normal in Syngap$^{+/-}$ mice

Syngap$^{+/-}$ and wild-type litter mates were labelled at various ages to determine whether SynGAP regulates Cat 301, Cat-315 or Cat-316 expression. *Syngap* null mutants die by P7 and show no cellular segregation and only partial TCA patch formation. *Syngap* heterozygotes have normal TCA patch segregation but reduced cellular segregation (Barnett et al., 2006). At ages P14 & P21 there are no obvious differences between *Syngap*$^{+/+}$ and $^{+/-}$ sections labelled with Cat-301, Cat-315 & Cat-316 (fig 4.21 & 4.22). Both show similar staining patterns and PNNs start to appear at P21 in Cat-316 labelled sections as per normal. In adult where PNN-positive cells can be counted there is no statistical difference between PNN-positive cell density in *Syngap*$^{+/+}$ and *Syngap*$^{+/-}$ (Cat-315 WT 269±6 cells/mm^2 (n=2), HET 224±29 cells/mm^2 (n=4), p=0.35) (Cat-316 WT 253±35 cells/mm^2 (n=2), HET 224±18 cells/mm^2 (n=4), p=0.56) (fig 4.23, 4.29 & 4.31). A trend is beginning to emerge indicating that in *Syngap*$^{+/-}$ there may be fewer PNNs. Power analysis on data collected shows that if the current trend continues then a significant difference between density of Cat-315 PNNs will be reached when 'n' reaches 21 *Syngap*$^{+/+}$ and 21 *Syngap*$^{+/-}$ as shown in table 7, appendix III. For Cat-316 PNNs, a significant difference between *Syngap*$^{+/+}$ and $^{+/-}$ will be reached when there are 39 of each genotype. This is an unreasonable number to analyse and so I conclude that SynGAP does not regulate PNNs labelled with Cat-315 or Cat-316. Power analyses are carried out assuming that the data collected has certain characteristics. This is discussed in more depth in appendix III.

6.2.7 PKARIIβ regulates expression of CSPGs identified in adult by Cat-315 but not those identified by Cat-316

Prkar2b mutants were also stained at various ages to determine whether the expression of Cat 301, Cat-315 or Cat-316 is regulated by PKA. CSPGs identified by Cat-301 show no difference between *Prkar2b*$^{+/+}$ and *Prkar2b*$^{-/-}$ at any age (fig 4.24, 4.25, & 4.26). Expression remains in neuropil and does not identify PNNs. Cat-315 and Cat-316 identify PNNs and there are no obvious differences at early ages. In adult the density of Cat-315 and Cat-316-positive PNNs in layer 4 of cortex was quantified. There is a significant decrease in Cat-315-positive PNN density in *Prkar2b*$^{-/-}$ compared to *Prkar2b*$^{+/+}$ of more than 30% (WT 274±25 cells/mm^2 (n=4), KO 188±13 cells/mm^2 (n=4); student's t-test p=0.02) (fig 4.26, 4.30 & 4.31), indicating that in S1 layer cortex, PKA regulates the expression of Cat-315-positive PNNs. There is no difference between *Prkar2b*$^{+/+}$ and *Prkar2b*$^{-/-}$ in Cat-316-positive PNNs (WT 171±11cells/mm^2 (n=2), KO 189±23 cells/mm^2 (n=4), p=0.624) and power analysis indicated that a total number of samples to be collected before student's t-test shows significance is 71 (table 7, appendix III). This is an unrealistic number to analyse and therefore I conclude that there is no difference in Cat-316-PNNs in barrels of *Prkar2b* KO and WT adult mice.

6.3 Discussion

6.3.1.1 Aim and key background studies

The aim of this study was to identify signalling pathways that regulate the expression of CSPGs in mouse barrel cortex. Previous research had identified specific subsets of CSPGs identified by monoclonal antibodies Cat-301, Cat-315 and Cat-316 that are expressed in visual cortex at the end of the critical period in OD plasticity in cats and are delayed by dark rearing (Guimaraes et al., 1990, Hockfield et al., 1990, Lander et al., 1997). This indicated a potential role for CSPGs in inhibiting plasticity and determining the close of the critical period. Removal of CSPGs using a chondroitinase enzyme extends the critical period (Pizzorusso et al., 2002), providing evidence that CSPGs do indeed determine the close of the critical period for plasticity in this system. The expression of CSPGs is regulated by NMDAR activation (Kalb and Hockfield, 1990), and activation of this receptor and downstream signalling pathways are known to play a key role in formation of barrels in mouse cortex (Iwasato et al., 2000). As well as the formation of barrels, many other functional and anatomical plasticity periods in mouse barrel cortex are well described. Other studies investigating the effect of whisker trimming on CSPG expression in mouse found that Cat-315-but not Cat-316 positive PNNs are reduced in barrels after 30 days whisker trimming (McRae et al., 2007), suggesting that in mouse barrel cortex the expression of Cat-315 is experience-dependent. Taken together these findings make the mouse barrel cortex an ideal model for investigating the glutamate-dependent pathways that may regulate CSPGs expression in barrels.

6.3.1.2 Approach used

I began by establishing the wild-type staining patterns in mice throughout development of three subsets of CSPGs identified by monoclonal antibodies Cat-301, Cat-315 and Cat-316. Cat-315 and Cat-316 identify epitopes that contribute to PNNs very clearly in adult so quantification of the epitopes was carried out in adult cortex. I quantified the expression of PNNs identified with these antibodies in mice with genetic mutations resulting in defects in barrel formation (*Syngap, Plcβ-1, Mglur5* and *Prkar2b*). The mutations affect molecules involved in glutamate signalling and NMDARs, which are known to regulate CSPGs in spinal cord (Kalb and Hockfield, 1990), therefore I hypothesised that these molecules may also be part of the pathways that regulating the expression of CSPGs.

6.3.1.3 Overview of findings

In the literature, Cat-301, Cat-315 and Cat-316 antibodies have been reported to identify epitopes that are differentially expressed in various regions of the CNS of different species (McKay and Hockfield, 1982, Hockfield et al., 1983 & 1990, DeYoe et al., 1990, Hendry et al., 1988, Matthews et al., 2002, Bruckner et al., 2003, Lander et al., 1997). I found that each antibody also identifies antigens in mouse brain that are expressed in different regions throughout development. Most notably, I found an absence of PNNs immuno-labelled with Cat-301 in mouse brain at all ages, despite previous descriptions of them in adult hippocampus (Bruckner et al., 2003). In agreement with other findings, Cat-315 and Cat-316 antibodies identify PNNs in barrel cortex from P21-adult and P14-adult respectively. Some PNNs identified with Cat-315 colocalise with parvalbumin, but others do not indicating that Cat-315 epitopes may localise to PNNs surrounding multiple cell-types in layer 4 of cortex. I quantified expression of PNNs in barrels in mice that have genetic alterations disrupting pathways necessary for barrel formation. In *Syngap*, *Plcβ-1* and *Mglur5* mutants there are no differences from wild-type in density of PNNs identified with Cat-315 and Cat-316 antibodies. In *Prkar2b* mutants however, there is a significant decrease in the density of PNNs identified with Cat-315, and no change in those labelled with Cat-316. This finding indicates that PKA is involved in the pathways that regulate expression of Cat-315-positive PNNs in mouse barrel cortex. Next I will explain the significance of my findings with respect to other studies investigating the role of CSPGs, and why some of my findings appear to be unusual and do not correlate with other work.

6.3.2 PKARIIβ & Cat-315

Mice with mutations to genes with known functions in translating glutamate signals into the cellular segregation of barrels were used to determine the intercellular pathways that may be regulating the expression of PNNs identified with Cat-315 and Cat-316. My findings indicate the expression of Cat-315 and not Cat-316 -positive PNNs are affected by a genetic disruption to PKARIIβ, a protein necessary for barrel formation (Inan et al., 2006, Watson et al., 2006). My findings are in good agreement with previous findings that Cat-315 (but not Cat-316) expression is regulated by whisker trimming (McRae et al., 2007), and that therefore the expression of Cat-315-positive PNNs is more sensitive to activity than Cat-316-positive PNNs. Two other findings have indicated key differences between the expression of epitopes identified by Cat-315 and Cat-301/316. Firstly, Cat-301/316 epitopes but not Cat-315 epitopes are expressed on pyramidal neurons in cat cortex (Lander et al., 1997). Secondly, Cat-315 but not Cat-301/316 immunoreactivity is increased in layer 4 of cat visual cortex after dark rearing (Lander et al., 1997). This indicates that CSPG epitopes have different mechanisms of regulation in response to experience. Since both antibodies are known to recognise different carbohydrate epitopes of aggrecan, these findings may reflect activity dependent regulation of GAG side chains, alternatively they may reflect a down-regulation of aggrecan.

I demonstrated that genetic deletion of *Prkar2b* results in a decrease in expression of Cat-315-positive PNNs in adult barrels. Expression of PKARIIβ is post-synaptic in layer 4 S1 synapses (Watson et al., 2006). This indicates that PKARIIβ, as well as being necessary for the normal segregation of layer 4 cells into barrels also regulates the pathways that result in CSPG expression. Cat-315 epitope expression is not affected in any other mutants examined and so the altered expression in *Prkar2b* $^{-/-}$ must be a result of the altered intercellular signalling rather than being the result of the cytoarchitectural defects in layer 4. In order to understand the mechanism by which PKARIIβ functions, it would be helpful to first identify which cell-type most Cat-315 –positive PNNs are associated with in adult layer 4 of cortex.
As previously published, most PNNs seem to surround GABAergic interneurons (Celio and Chiquet-Ehrismann, 1993), a subset of which can be labelled with parvalbumin antibodies. McRae and colleagues found that almost all Cat-315-positive PNNs in layer 4 (but not layer 6) S1 were also labelled with parvalbumin. In my experiments a substantial number of Cat-315-positive PNNs did not colocalise with parvalbumin –positive neurons in layer 4 (the extent of colocalisation was not quantified). The difference could be due to a difference in penetration of the antibodies. The sections I used were 48μm thick and the results could be repeated on

thinner sections. Alternatively, the age or background of the mice used may be different, McRae and colleagues used CD-1 mice aged 1-4 months. The adult mice used in my studies were all over 2 months and of Bl/6 and Bl/6 129 mixed backgrounds. It is possible that these Cat-315-positive parvalbumin-negative cells are glia or excitatory neurons. PNNs have been shown to localise to glia (Luth et al., 1992) and excitatory neurons (Lander et al 1997). Further investigations need to be carried out using high-power microscopy with double-immunolabelling to identify these cells. It should then be possible to analyse the contribution of this cell type to barrels in *Prkar2b* mutants to see if there is a regulation of the cell type, which results in fewer Cat-315 PNNs. While this would not prove a causal relationship between expression of Cat-315 PNNs and interneurons/glia/excitatory neurons, it would indicate a link that could be further investigated.

PKARIIβ regulates GluRA insertion into the synapse and there are fewer GluRA receptors associated with the synapse in *Prkar2b*$^{-/-}$ (Watson et al., 2006). PKARIIβ has also been shown to play a role in LTP in layer 4 barrel cortex synapses during development (Inan et al., 2006). AMPA receptors influence the excitability of neurons and the expression of Cat-315-positive PNNs is regulated by neuronal activity (Lander et al., 1998, McRae et al., 2007), indicating that a change in neuronal excitability as a result of deletion of *Prkar2b* may result in decreased Cat-315-positive PNNs.

6.3.3 Regulation of Cat-315 expression

Data presented here indicates that it is not the inability to form normal barrels that causes the reduction in expression of Cat-315-positive PNNs but the actual PKA-associated intercellular mechanisms in the layer 4 cells. There are two possibilities that may result in altered expression of Cat-315-positive PNNs. Either 1.) there is an alteration in the total amount of secreted aggrecan that results in less Cat-315-positive PNNs being detected, or 2.) there is an alteration in the post-translational modifications to aggrecan that result in fewer Cat-315-specific epitopes being expressed. My experiments provide evidence to indicate that the latter is true since Cat-316 also recognises an epitope of aggrecan and no changes in expression of Cat-316 epitopes were detected in *Prkar2b* mutants. One way to investigate the first possibility is to label aggrecan in *Prkar2b* mutants, but there is not a reliable pan-aggrecan antibody available. However, aggrecan mRNA can be detected by in situ-hybridization, and aggrecan mRNA is highly expressed in barrel cortex, particularly layers 4 & 6. Aggrecan mRNA is decreased in layer 4 after 30 days of whisker trimming (McRae et al., 2007), suggesting that aggrecan expression is activity-dependent, and providing some evidence to suggest the former reason for decreased Cat-315-positive PNNs may be true. To bring clarity, further experiments are required to quantify aggrecan mRNA in *Prkar2b*$^{+/+}$ and *Prkar2b*$^{-/-}$. Both Cat-315 and Cat-316 antibodies label distinct but overlapping subsets of neurons (Lander et al., 1997), and so identifying and quantifying the neuron type that is being labelled by Cat-315 in *Prkar2b*$^{+/+}$ and *Prkar2b*$^{-/-}$ barrels would indicate whether PKA is regulating the number of neurons.

6.3.4 CSPG expression and function

CSPGs expressed in early development have roles in synapse formation and stabilisation, and axon outgrowth (Dino et al., 2006, Corvetti and Rossi, 2005). In contrast, the expression of some CSPG epitopes correlates with the termination of critical periods in cats and dark rearing delays this expression (Guimaraes et al., 1990, Sur et al., 1988, Lander et al., 2007). Removing CSPGs after the termination of the critical period for OD plasticity in cats reintroduces a period of OD plasticity indicating that CSPG expression not only correlates with, but also causes the termination of critical periods (Pizzorusso et al., 2002). Here I will review the known critical periods in mouse barrel cortex, and discuss how my findings fit in with established expression patterns and functions of CSPGs.

6.3.4.1 Expression and localisation of the Cat-301 epitope

Cat-301 was first of the three antibodies to be generated, and was initially reported to be labelling the surface of dendrites and cell bodies of neurons in cat spinal cord that resemble long-distance projection neurons (McKay and Hockfield, 1982). The surface antigens were later discovered to be contributing to PNNs, specialisations of the ECM surrounding cell bodies and proximal dendrites (Celio and Blumcke, 1994). In cats and primates Cat-301 is localised to PNNs and is expressed in visual cortex at the end of the period of synaptic plasticity (Hockfield et al., 1983, 1990, DeYoe et al., 1990). In cats the expression of Cat-301 CSPG is activity dependent. Dark rearing from birth extends the critical period in the visual cortex and inhibits the cortical expression of Cat-301 epitope, indicating a potential role in determining the close of the critical period of synaptic plasticity (Guimaraes et al., 1990, Hockfield et al., 1990). In rodents Cat-301 is expressed less extensively than in cats and primates. In adult rat Cat-301 labels neurons in spinal cord and brainstem and very few neurons in hippocampus (Hendry et al., 1988, Matthews et al., 2002). In adult mouse Cat-301 has been reported to label a very small population of Cat-301–positive PNNs in hippocampus, dentate gyrus and subculiculum (Bruckner et al., 2003). To date, Cat-301-positive PNNs have not been described in mouse brain in regions other than hippocampus. My experiments show that expression of the Cat-301 epitope is distinct from Cat-315 & Cat-316 epitopes, and it does not localise to PNNs in mouse brain. The Cat-301 epitope is expressed at P7 in dendritic layers of hippocampus and cortex but is absent from layer 4. Expression is reduced at P14 and P21 and then increased in adulthood, where it is most strongly expressed in dendritic layers of hippocampus. In adult the Cat-301 epitope is expressed in all layers of cortex but is still not associated with PNNs in cortex or hippocampus. One possible reason for the difference between my results and the findings of Bruckner and colleagues detecting Cat-301 epitopes localising to PNNs (Bruckner et al., 2003) may be due to two reasons. Either the background strain may be different between their experiments and mine, or the age of mice may be different. It is unlikely that the difference is due to age as the adult mice used in my experiments investigating PNNs in mutants ranged from 2 months to over 13 months, and Cat-301-positive PNNs weren't detected at any age. The background strain of mice used by Bruckner and colleagues is C57Bl/6J x129Ola, and the mice used in my experiments are C57Bl/6J Ola or C57Bl/6J Ola/129 - very similar but similar backgrounds have been shown in the past to have different phenotypes (the mGluR5 phenotype, for example; Hannan et al., 2001, Wijetunge et al., submitted). This will be discussed in more depth in the conclusions section of this thesis.

6.3.4.2 Expression and localisation of Cat-315 and Cat-316 epitopes

In adult cats visual deprivation has no effect on PNN expression (Sur et al., 1988) but dark rearing during the early postnatal period reduces the number of Cat-315 and

Cat-316 -positive neurons in layers2/3 and 5/6 in visual cortex to as similar extent as the reduction of Cat-301 positive neurons (Lander et al., 1997). In layer 4, dark rearing during the early postnatal period causes an increase in the number of Cat-315 positive neurons and a decrease in the number of Cat-301 and Cat-316 positive neurons (Lander et al., 1997). This suggests that PNN expression is dependent upon sensory activity during a specific critical period. In my experiments examining the expression of CSPGs in mice, the Cat-316 antigen is first located to barrels at P7 and Cat-316 –positive PNNs are first expressed at cortex at P14. In adult PNNs are expressed in cortex layer 4 & 6 and cover an area greater than S1. The Cat-315 antigen appears later in barrels and Cat-315-positive PNNs are first seen at P21. In adult Cat-315-positive PNNs are restricted to the region occupied by S1. This indicates that Cat-315 & Cat-316-positive PNNs may play a role in regulating plasticity in the barrel cortex of mice, and it is possible that their expression is activity-dependent. Pizzorusso and colleagues used a chondroitinase enzyme to demonstrate that in cats CSPGs cause the termination of the period of OD plasticity (Pizzorusso et al., 2002). To date there are no known techniques for selectively removing one particular antigen of CSPGs so a function in plasticity cannot be attributed to a particular antigen. McRae and colleagues investigated whether their expression is activity dependent and found that PNNs identified with Cat-315 (but not those labelled with Cat-316 or other many other PNN markers - personal communication, RT Matthews) are reduced in layer 4 mouse barrel cortex after 30 days whisker trimming (McRae et al., 2007).

6.3.4.3 Critical periods in mouse barrel cortex

Genetic disruption to pathways necessary for barrel formation indicates that there is a critical period for barrels to form in mice during the first postnatal week. During this period glutamate is released from innervating TCAs and induces the rearrangement of cortical cells from a uniform distribution to a pattern of barrels mimicking the whisker pattern on the facepad (Erzurumlu and Kind, 2001). Neural activity plays a key role in accurately transmitting the signals from segregated TCAs to layer 4 cortical cells that are necessary for forming the barrel pattern.

The original deprivation experiments by Van der Loos where barrels were found to merge to form a megabarrel were carried out using row C whisker follicle lesioning

rather than whisker trimming. Even though both techniques disrupt sensory activity, the two procedures have very different effects. Lesioning the follicle is similar to infraorbitol nerve (ION) transection, which when performed at birth, causes a decrease in volume of the contralateral VB as a result of cell death (Hamori et al., 1986, Waite et al., 1992, Baldi et al., 2000). For the anatomical shrinkage of deprived cortical barrels the lesioning must take place by P3/P4 in mice (Van der Loos and Woolsey, 1973). Therefore the anatomical plasticity in deprived barrels may not result from altered activity per se, but instead may result from cell death, nerve degeneration and primary afferent regeneration (Waite and Cragg, 1982).
In support of this notion, whisker trimming induces alterations in functional connectivity between neurons in rat barrel cortex (Hand, 1982, Simon and Land, 1987) but does not alter the segregation of TCAs or layer 4 cells (i.e. barrel formation is unaffected). This indicates that barrels do not require experience to form, but only require an intact physiological pathway and intact molecular pathways from the follicle to the cortex. However, an interesting rescue of cell death in VB is seen when nerve growth factor (NGF) or brain derived growth factor (BDNF) is applied to the ION stump (Baldi et al., 2000), indicating that growth factors can mimic follicle stimulation to induce pattern formation in this pathway.

It is important to note that patterned spontaneous activity (which is absent from lesioned follicles/ION) may be necessary for formation of barrels, in the same way as retinal waves are necessary for the segregation of inputs in the dLGN (Wong, 1999). After a period of whisker deprivation, the percentage of cells that respond physiologically to the deprived whisker is reduced most dramatically in layer 2/3 but also in layer 4 (Fox, 1992). These alterations are NMDAR sensitive (Fox et al., 1996) and take place during a critical period in early postnatal development. Initial studies found that for deprivation to have an effect trimming must begin before P4 (for the effect to be detected in layer 4) or P7 (for the effect to be detected in layer 2/3) (Fox, 1992). However, later investigations found that the plasticity seen in cells in layer 2/3 extends beyond P28 when trimming takes place over longer periods of 20 or more days (Glazewski and Fox 1996). This physiological plasticity induced by whisker trimming occurs at a time when there is a massive increase in the number of synapses being formed in cortex (White et al., 1997). The formation of connections at this stage is dependent upon normal sensory experience, which is disrupted by whisker deprivation. When one whisker is left untrimmed then a greater number of cells over a greater cortical area respond to the intact whisker (Fox, 1992), indicating that the connectivity between cells responding to this whisker is enhanced as a result of increased activity relative to neighbouring deprived whiskers.

Whisker trimming does not cause a major disruption to the formation of barrels, the only alterations seen when one whisker was left intact was a small increase in barrel size corresponding to the intact whisker when trimming began at P0 (Fox, 1992). No changes in barrels were seen when trimming began at P2 or later (Fox, 1992). The antigens recognised by all three Cat-antibodies are present in barrels at the end of the first postnatal week, correlating with the decline in physiological plasticity to whisker trimming (Glazewski and Fox, 1996). As I did not analyse expression earlier than P7 it is not possible to know at exactly what stage the epitopes are first expressed, although PNNs are first identified with Cat-315 at P21 and Cat-316 at P14. Therefore expression of PNNs does not correlate with the end of the critical period (although expression of the first antigens does seem to correlate). This is important since it is the perisynaptic location of CSPGs (i.e. in PNNs) that is hypothesized to act as “biological glue” and end the critical period. More recently, the plasticity induced by whisker trimming in more mature rodents has been investigated. Whisker trimming beginning at P40 after barrels have formed in young adult hamsters causes a decrease in metabolic labelling in deprived cortex and an increase in the remaining whiskers, with the activated regions becoming enlarged after longer periods of trimming. This suggests that there is a widespread synaptic reorganisation in deprived cortex in adult as well as during early postnatal development (Maier et al., 2003). In adult rats whisker pairing (where two neighbouring whiskers are left untrimmed) for 3 days causes the receptive fields to be enhanced in response to the stimulation of the remaining whiskers, and decreased in response to stimulation of the trimmed whisker. This indicates that a brief change in sensory activity can cause remodelling in cortical receptive fields (Diamond et al., 1993). Two of the mechanisms taking place during brief alterations to sensory activity are the insertion of new inhibitory synapses and a depression of neuronal responses as a result of uncorrelated activity between stimulated and nonstimulated whiskers (Quairiaux et al., 2007). The presence of adult periods of deprivation-induced plasticity indicates that the critical periods previously described may be extended if the duration of deprivation is long enough. Therefore the appearance of PNNs at P14 (Cat-316) and P21 (Cat-315) in my experiments may be carrying out these roles in inhibiting later plasticity periods through modulation of inhibitory circuits. The mechanism by which CSPGs inhibit plasticity is not known. It is presumed that they glue synapses together, preventing changes from occurring. In adult plasticity, in order for synapse modifications to occur the CSPGs at that synapse must be broken down. A candidate for this digestion is a tissue plasminogen activator (tPa), a protease that is secreted at active synapses and digests CSPGs. (Wu et al., 2000, Berardi et al., 2004)

6.3.4.4 Expression of Cat-315 in hippocampus

Investigation into the highly specific staining of Cat-315 in the hippocampus is intriguing albeit beyond the aims of this study. In order to gain a better understanding of what the function may be of the highly specific staining I decided to search for other molecules that have a similar staining pattern. In hippocampus Cat-315 labels epitopes expressed only in dendrites and only in CA3 region. It suggests that there is a specific mechanism occurring to restrict the expression in a specific manner during development. Previous work investigating Cat-315 epitope expression in lamination of mouse hippocampus only looked in adult and therefore described expression of PNNs (Bruckner et al., 2003). They found similar results to that seen in this present study - an absence of Cat-315 epitopes from pyramidal layers in CA3, and the presence in molecular layers of dentate gyrus (Bruckner et al., 2003). To investigate what may be regulating the expression in hippocampus resulting in such a specific pattern, I looked for other molecules with similar lamination expression profiles. Using expression data that has been entered into the MGI website (Jackson Labs), there are a few other molecules that have been found to be expressed in regions similar to the Cat-315 epitope. Table 8 in appendix III shows lists of molecules expressed in each layer of hippocampus, alongside a summary of hippocampal expression of the Cat-315-epitope. CA stratum oriens and stratum radiatum contain mostly interneurons and it is in these hippocampal layers that the Cat-315 epitope is expressed. Of all the proteins found to be expressed in hippocampus according to MGI, the only ones that occur in dendritic layers and not pyramidal layers are Odz 1, 3 & 4. As there is an overlap in the expression of the Cat-315 epitope and some of the Odz proteins it would be interesting to see if there is a link in the regulation of these two molecules. Odz proteins are type II transmembrane proteins and their function is unknown. They are expressed away from cell bodies along axons in adults and may be shed into the extracellular space to diffuse. In man and chicken this protein family is called teneurin, and in rat neurestin. The drosophila orthologue, also called *tenm* functions as a patterning gene, and is a large extracellular protein related to tenascin (Baumgartner et al., 1994). In rats neurestin has been implicated in synapse regulation throughout adulthood, it is found in olfactory bulbs, and hippocampal granule cells (Otaki & Firestein, 1999). Its expression is broadly consistent with the period of synapse formation. In olfactory bulb the expression of neurestin is consistent with the division of the glomerular and nerve layer by the presence of lectins (Jia and Halpern, 1996, 1997) and cell adhesion molecule OCAM (Yoshihara et al., 1997). This suggests that neurestin is involved in some of the same functions as the Cat-315 epitope such as synapse regulation and its transmembrane location permits it to be a potential interacting partner. The association could be investigated by looking at co-expression of Cat-315 and Odz and by investigating expression of Odz proteins in hippocampus after ChABC treatment.

6.3.5 Summary

During mouse brain development there is a changing pattern in the expression of the epitopes identified by monoclonal antibodies Cat-301, Cat-315 & Cat-316. All three antibodies identify aggrecan-containing CSPGs (Matthews et al., 2002), which form part of the extracellular matrix and their expression in mouse barrel cortex correlates with a decline in plasticity. The Cat-301 antigen is expressed early in development when barrels are first formed but its absence from PNNs means that it is not possible to quantify differences in expression in mutants without carrying out biochemical analyses. The epitopes identified by Cat-315 & Cat-316 are expressed as early as P7 and localise to PNNs from as early as P14 in layer 4 barrel cortex. Data presented here indicates that PKA, an important molecule in layer 4 NRC/MASC, is involved in regulating the expression of Cat-315-positive PNNs. This reduction in Cat-315 epitope expression is only quantified in adult due to its contribution to PNNs, and so it is possible that there are alterations in expression earlier, which are not quantifiable without biochemistry. PKA acts downstream of NMDARs and regulates the AC-cAMP pathway, and it's genetic deletion results in poor barrel formation and a decrease in AMPA receptor subunit insertion into the PSD (Watson et al., 2007). To date, no other molecules within the synapse other than NMDARs and PKARIIβ have been identified to be involved in regulating CSPG expression. Expression of CSPGs terminates the critical period, therefore down regulating CSPGs could be a potential treatment to allow re-growth and plasticity following brain trauma. PKA is a potential target for regulating CSPG expression in such conditions.

6.4 Figures Chapter Four

Figure 4.1

Wild type expression of Cat-301 in P7 coronal sections. Cat-301 is uniformly expressed in most regions, but is absent from layer 4 of cortex and cell bodies of hippocampus.

A: Coronal section through PMBSF cortex. Scale bar: 1000µm.

B: Coronal section through hippocampus. Scale bar: 500µm.

C: Coronal section through PMBSF cortex. Scale bar: 200µm.

Figure 4.2

Wild type expression of Cat-301 in P14 coronal sections. Cat-301 is barely expressed in all regions, a small amount of stain can be seen in dendritic layers of hippocampus.

A: Coronal section through PMBSF cortex. Scale bar: 1000µm.

B: Coronal section through hippocampus. Scale bar: 500µm.

C: Coronal section through PMBSF cortex. Scale bar: 200µm.

Figure 4.3

Wild type expression of Cat-301 in P21 coronal sections. Cat-301 is expressed at low levels in all regions, a small amount of stain can be seen in dendritic layers of hippocampus, while stain is absent from cell bodies of hippocampus.

A: Coronal section through PMBSF cortex. Scale bar: 1000μm.

B: Coronal section through hippocampus. Scale bar: 500μm.

C: Coronal section through PMBSF cortex. Scale bar: 200μm.

Figure 4.4

Wild type expression of Cat-301 in Adult coronal sections. Cat-301 is expressed at low levels in all regions except hippocampus. Labelling is absent from cell bodies of hippocampus but dense in dendritic layers.

A: Coronal section through PMBSF cortex. Scale bar: 1000μm.

B: Coronal section through hippocampus. Scale bar: 500μm.

C: Coronal section through PMBSF cortex. Scale bar: 200μm.

Figure 4.5

Wild type expression of Cat-315 in P7 coronal sections. Cat-315 is expressed at low levels throughout the brain but is absent from cell bodies of hippocampus and layer 4 of cortex.

A: Coronal section through PMBSF cortex. Scale bar: 1000μm.

B: Coronal section through hippocampus. Scale bar: 500μm.

C: Coronal section through PMBSF cortex. Scale bar: 200μm.

Figure 4.6

Wild type expression of Cat-315 in P14 coronal sections. Cat-315 is expressed only in dendritic layers of hippocampus, more densely in stratum radiatum and stratum oriens of CA1 and ventral region of dentate gyrus, and less in dendritic layers of CA3 and CA2.

A: Coronal section through PMBSF cortex. Scale bar: 1000μm.

B: Coronal section through hippocampus. Scale bar: 500μm.

C: Coronal section through PMBSF cortex. Scale bar: 200μm.

Figure 4.7

Wild type expression of Cat-315 in P21 coronal sections. Cat-315 is expressed in dendritic layers of hippocampus, in stratum radiatum and stratum oriens of CA1. In layer 4 of cortex a small number of cells have perineuronal nets surrounding cell body and proximal dendrites.

A: Coronal section through PMBSF cortex. Scale bar: 1000μm.

B: Coronal section through hippocampus. Scale bar: 500μm.

C: Coronal section through PMBSF cortex. Scale bar: 200μm.

Figure 4.8

Wild type expression of Cat-315 in Adult coronal sections. Cat-315 is expressed in dendritic layers of hippocampus. Perineuronal nets surround cells in layer 4 & 5 cortex, and can be seen localising to regions of layer 4 where barrels appear.

A: Coronal section through PMBSF cortex. Scale bar: 1000μm.

B: Coronal section through hippocampus. Scale bar: 500μm.

C: Coronal section through PMBSF cortex. Scale bar: 200μm.

Figure 4.9

Wild type expression of Cat-316 in P7 coronal sections. Cat-316 is sparsely expressed in most brain regions but is absent from cell bodies of hippocampus.

A: Coronal section through PMBSF cortex. Scale bar: 1000μm.

B: Coronal section through hippocampus. Scale bar: 500μm.

C: Coronal section through PMBSF cortex. Scale bar: 200μm.

Figure 4.10

Wild type expression of Cat-316 in P14 coronal sections. Cat-316 is sparsely expressed in the brain at this age.

A: Coronal section through PMBSF cortex. Scale bar: 1000μm.

B: Coronal section through hippocampus. Scale bar: 500μm.

C: Coronal section through PMBSF cortex. Scale bar: 200μm.

Figure 4.11

Wild type expression of Cat-316 in P21 coronal sections. Cat-316 is expressed sparsely in cortex layer 4 & 5 where perineuronal nets can be seen surrounding cells bodies and proximal dendrites.

A: Coronal section through PMBSF cortex. Scale bar: 1000μm.

B: Coronal section through hippocampus. Scale bar: 500μm.

C: Coronal section through PMBSF cortex. Scale bar: 200μm.

Figure 4.12

Wild type expression of Cat-316 in Adult coronal sections. Cat-316 is expressed in dendritic layers of hippocampus in and also in layer 4 & 5 where perineuronal nets surround cell bodies.

A: Coronal section through PMBSF cortex. Scale bar: 1000μm.

B: Coronal section through hippocampus. Scale bar: 500μm.

C: Coronal section through PMBSF cortex. Scale bar: 200μm.

Figure 4.13

Wild type expression of Cat -316 and Cat-316 in tangential sections of layer 4 of cortex.

A: At P7/8 Cat-315 is not specifically localised to the barrel field. Scale bar 500μm.

B: Cat-316 can be seen in PMBSF. Scale bar 500μm.

C: In Adult Cat-315 is visible in whole barrel fields where perineuronal nets surround cell bodies. Barrel septae have very few labelled cells, most seem to localise to within barrels. Scale bar 500μm.

D: Perineuronal nets are visible in PMBSF. Scale bar 500μm.

E-H: Coronal sections of both Cat-315 and Cat-316 reveal perineuronal nets in layer 4 of cortex of adult. Scale bar 20μm.

Figure 4.14

Cat-315 labels a subset of parvalbumin-positive cells in layer 4 of tangential flattened cortex.

A: Cat-315 label on tangential section reveals perineuronal nets in barrels. Yellow arrow: perineuronal net. White arrows: perineuronal nets are absent from septae. Scale bar 100μm.

B: To-Pro-3 label on tangential section to show orientation of barrel. White arrows: perineuronal nets are absent from septae. Scale bar 100μm.

C: Merge of Cat-315 and To-Pro-3 from B & C. Scale bar 100μm.

D: Parvalbumin labels gabaergic cells uniformly distributed across barrels. White arrow head: parvalbumin-positive cell not labelled with Cat-315. Scale bar 100μm.

E: Cat-315 and parvalbumin double-label shows very few cells are double-labelled with both. White lightening bolts: Double labelled cells. Scale bar 100μm.

F: Schematic to show position of barrel in tangential section of flattened cortex labelled with To-Pro-3, Cat-315 and Parvalbumin in A-E.

Figure 4.15

Nissl, Cat-301, Cat-315 & Cat-316 label of coronal sections in *Mglur5* mutants at P14. Scale bar 1000μm. Arrow heads indicate barrels.

Figure 4.16

Nissl, Cat-301, Cat-315 & Cat-316 label of coronal sections in *Mglur5* mutants at P21. Scale bar 1000μm.

Figure 4.17

Nissl, Cat-301, Cat-315 & Cat-316 label of coronal sections in *Mglur5* mutants in Adult. Scale bar 1000μm.

Figure 4.18

Nissl, Cat-301, Cat-315 & Cat-316 label of coronal sections in *Plcβ-1* mutants at P14. Scale bar 1000μm.

Figure 4.19

Nissl, Cat-301, Cat-315 & Cat-316 label of coronal sections in *Plcβ-1* mutants at P21. Scale bar 1000μm.

Figure 4.20

Nissl, Cat-301, Cat-315 & Cat-316 label of coronal sections in *Plcβ-1* mutants in Adult. Scale bar 1000μm.

Figure 4.21

Nissl, Cat-301, Cat-315 & Cat-316 label of coronal sections in S*yngap* mutants at P14. Scale bar 1000μm.

Figure 4.22

Nissl, Cat-301, Cat-315 & Cat-316 label of coronal sections in *Syngap* mutants at P21. Scale bar 1000μm.

Figure 4.23

Nissl, Cat-301, Cat-315 & Cat-316 label of coronal sections in *Syngap* mutants in Adult. Scale bar 1000μm.

Figure 4.25

Nissl, Cat-301, Cat-315 & Cat-316 label of coronal sections in *Prkar2b* mutants at P21. Scale bar 1000μm.

Figure 4.26

Nissl, Cat-301, Cat-315 & Cat-316 label of coronal sections in *Prkar2b* mutants in Adult. Scale bar 1000µm.

Figure 4.27

Nissl, Cat-315 & Cat-316 label of *Mglur5* mutant adult cortex. Cat 315 & Cat 316 perineuronal nets in layer 4 are counted to give a density of cells that can be compared between wild-type and mutant. Scale bar, 200μm.

Figure 4.28

Nissl, Cat-315 & Cat-316 label of *Plcβ-1* mutant adult cortex. Cat 315 & Cat 316 perineuronal nets in layer 4 are counted to give a density of cells that can be compared between wild-type and mutant. Scale bar, 200μm.

Figure 4.29

Nissl, Cat-315 & Cat-316 label of *Syngap* mutant adult cortex. Cat 315 & Cat 316 perineuronal nets in layer 4 are counted to give a density of cells that can be compared between wild-type and mutant. Scale bar, 200μm.

Figure 4.30

Nissl, Cat-315 & Cat-316 label of *Prkar2b* mutant adult cortex. Cat 315 & Cat 316 perineuronal nets in layer 4 are counted to give a density of cells that can be compared between wild-type and mutant. Scale bar, 200μm.

Figure 4.31

Analysis of cell density of Cat-315 & Cat-316 positive neurons in Layer 4 of cortex. Student's t-test ** $p<0.05$

A: Cat-315 –positive PNN density in layer 4 *Mglur5* mutants. WT 331±24 cells/mm^2 (n=6), KO 269±23 cells/mm^2 (n=4)

B: Cat-316 –positive PNN density in layer 4 *Mglur5* mutants. WT 298±14 cells/mm^2 (n=6), KO 269±13 cells/mm^2 (n=4)

C: Cat-315 –positive PNN density in layer 4 *Plc*β1 mutants. WT 255±57 cells/mm^2 (n=2), KO 248±40 cells/mm^2 (n=2)

D: Cat-316 –positive PNN density in layer 4 *Plc*β1 mutants. WT 304±16 cells/mm^2 (n=2), KO 377±18 cells/mm^2 (n=2)

E: Cat-315 –positive PNN density in layer 4 *Prkar2b* mutants. WT 274±25 cells/mm^2 (n=4), KO 188±13 cells/mm^2 (n=4), WT has significantly higher density than KO, student's t-test p=0.02.

F: Cat-316 –positive PNN density in layer 4 *Prkar2b* mutants. WT 171±11cells/mm^2 (n=2), KO 189±23 cells/mm^2 (n=4)

G: Cat-315 –positive PNN density in layer 4 *Syngap* mutants. WT 269±6 cells/mm^2 (n=2), HET 224±29 cells/mm^2 (n=4)

H: Cat-316 –positive PNN density in layer 4 *Syngap* mutants. WT 253±35 cells/mm^2 (n=2), HET 224±18 cells/mm^2 (n=4)

7 Conclusions

In this section I will discuss the significance and value of my investigations in the light of other research. There will be discussion of some important issues that were raised with respect to experimental limitations and suggestions made as to the future direction of this work.

7.1 Significance of my research for treatment of disease

Understanding the mechanisms of biological processes in health and disease is key to targeting therapies. My experiments have taken advantage of numerous advances in mouse molecular biology and in identifying molecules in the PSD to investigate molecular pathways involved in activity dependent development of the mouse somatosensory cortex. Many of these pathways are also implicated in human cognition and dissecting these pathways will aid understanding of diseases such as mental retardation, schizophrenia, bipolar, autism spectrum and depressive disorders, many of which result from or coincide with defects in signalling.

If a mutation to a signalling molecule causes a medical condition, the molecules that regulate that signalling process may provide a target for reversing the defect.

7.1.1 Cloning the mouse and human genome

Cloning of the mouse genome has enabled individual genes to be targeted and the role of that gene examined in vivo. The Mouse Genome Sequencing Consortium (MGSC) is a public-private consortium of institutes (NIH, Wellcome Trust, GlaxoSmithKline, Merck Genome Research Institute and Affymetrix Inc) involved in sequencing and genomics, and aims to coordinate global mouse genomic sequencing. Sequencing the mouse genome was completed and published in 2002. The C57BL/6J strain sequence is publicly available at www.ensembl.org. The mouse X-chromosome is amongst the first of the chromosomes to be fully sequenced, along with chromosomes 2, 4 & 11. Sequencing of the X-chromosome in mice and humans has aided identification of many X-linked disorders since they are easily identified by their pattern of occurrence in families. Usually approximately twice as many males than females are affected, with females being less severely affected. An annual publication monitors and summarises data identifying and describing the discovery of X-linked disorders in humans, and whether the gene is cloned and a mouse model generated (Chiurazzi et al., 2008). Identification of genes in the mouse genome is not yet complete, and the total number is approaching 30000. The identification of genes and targeted deletions/modifications has rapidly advanced the understanding of the function of the gene product. Due to 85% sequence similarity (and 99% of genes shared) with the human genome, mice are a valuable tool in the understanding of human disease. The cloning of the mouse genome has aided my research immensely as many of the NRC/MASC component- mutants have been generated as a result of the MGSC (Laumonnier et al., 2007).

Cloning the human genome has directly affected my research. As a result of the human genome project (HGP) the XLMR condition resulting from mutations to *DLG3* was discovered, showing a direct link between MAGUKs and human disease (Tarpey et al., 2004). Through similar linkage studies, many other human genetic disorders are being identified, aided by the HGP. The HGP began in 1990 and was completed in 2003. It was coordinated by the U.S. Department of Energy and the National Institutes of Health with collaborations from the Wellcome Trust and other partners in Japan, France, Germany and China. The goals were to identify all the genes in human DNA, determine the chemical sequence of human DNA, improve tools for data analysis and transfer related techniques to the private sector. Analysis of the data is still taking place and has many medical applications. For example, new techniques of pharmacogenetics aim to enable drugs to be tailored for an individual's specific genetic makeup. The drugs should then be safer and have greater efficacy and dosages should be more appropriate, leading to reduced cost of treatment. Another example of a medical application of the HGP is in identifying genetic disorders. Without the HGP, the XLMR condition resulting from mutations to human *DLG3* (*Sap102*) would not have been identified.

7.1.2 The G2C project

Taken together, my results indicate the significance of the HGP and how generation of mice with deletions of synaptic proteins leads to a greater understanding of cognition in health and disease. The Genes to Cognition (G2C) project is a collaboration between the Wellcome Trust and other partners to put into practise some of the aims of the HGP.

The G2C project website (www.genes2cognition.org) states the following aims to provide a foundation of knowledge to aid therapeutic research into treating cognitive disorders

1.) To use genetic methods to identify and investigate NRC/MASC and PSD genes involved in brain disorders.

2.) To generate large-scale data sets (with bioinformatics) to enable a systems-based approach to understanding the synapse.

The G2C project has made substantial advancements in understanding human conditions and this thesis has taken advantage of the high throughput production of mouse mutants to contribute to understanding the role of individual proteins (Migaud et al., 1998, Cuthbert et al., 2007). As a result of the proteomic dissection of the PSD (Husi et al., 2000, Collins et al., 2006), this thesis set out to discover new mutants that have defects in glutamate signalling leading to barrel defects. Molecules that are necessary for the formation of barrels are often found to be regulators of the ERK-MAPK pathway, but it seems that an intact AC/cAMP pathway is more important for the formation of barrels than the ERK-MAPK pathway (Barnett et al., 2006). Following the findings that humans with null mutations of the *Sap102* gene have MR (Tarpey et al., 2004), the focus of the thesis was adjusted to analyse mosaicism in double mutants of *Sap102 & Psd-95*. My finding that SAP102 acts cell-autonomously in signalling for cells to segregate into barrels indicates that the ability of a cell to respond to signals is regulated by SAP102-dependent secreted or cell-surface-expressed molecules. While this extracellular-signalling pathway is not fully understood, it indicates that potential accessible therapeutic targets for reversing the effects of loss of SAP102 may be cell surface or secreted molecules. SAP102 is known to regulate neuroligin, a transynaptic adhesion molecule (Meyer et al., 2004) indicating that synapse adhesion may be a mechanism of SAP102 function. At the same time as the experiments in this thesis were carried out, Dr Kind's lab is switching its focus to understanding mosaicism in mice with other forms of X-linked mental retardation. The discovery of a valuable link between mental retardation and defects in barrel development indicate how useful the barrel cortex is as a tool in understanding brain development. I have identified barrel abnormalities linked to SAP102, and colleagues in Dr. Kind's lab have identified barrel abnormalities in *Fmr1* mutant mice (unpublished findings). These abnormalities in synapse development and pattern formation occur very early in postnatal development, indicating that MR is not just a synaptic plasticity disorder. The study of mosaicism in formation of a barrel opens many doors to investigate the role of X-linked diseases in cognition. Recent reviews from the Grant lab (for example, Laumonnier et al., 2007). have drawn particular attention to X-linked members of the NRC/MASC complex as potential candidates for genetic diseases known to affect men more than women. There are a surprisingly high number of X-linked genes encoding NRC/MASC and PSD members and many of them are already known to be involved in human psychiatric disorders. 28% of the genes causing XLMR encode post-synaptic proteins. NRC/MASC genes are strongly associated with mental retardation and autism spectrum disorders. This bias towards cognition disorders indicates that the PSD is a highly organised complex with roles in many cognitive functions, and systematic studies of the NRC/MASC complex will provide insights into many novel genes involved in human disease (Laumonnier et al., 2007) The synapse is a fundamental structure that forms the basis of all cognitive activity. Therefore mutations to proteins in the synapse (especially glutamate synapses since glutamate is the major excitatory neurotransmitter) are likely to have wide-ranging and extensive effects on cognition. Therefore understanding the role and regulation of each of the NRC/MASC genes may well provide useful information when diseases and therapies for MR and Autism are developed. For example, Retts Syndrome and Fragile X Syndrome (FXS) are two conditions resulting from mutations to X-linked genes (MECP2 and FMR1 respectively) (Kleefstra et al., 2003, Penagarikano et al., 2007). As a result of studying mouse models of these disorders, new theories of gene function have emerged leading to suggestions of therapeutic interventions. In Retts Syndrome affected males rarely survive to term and so the disease is much more common in females. The severity in females can vary widely due to the extent of XCI. An attempt to reverse the phenotype by restoring the gene in adult female mice with *Mecp2* mutations has provided exciting results (Guy et al., 2007). While the treatment does not offer an immediate therapeutic approach for humans, it establishes the fact that neurological function can be restored sufficiently to reverse symptoms at late developmental stages. Loss of FMRP, the protein product of FMR1 increases LTD in mouse hippocampus. Many of the protein-synthesis-dependent functions of mGluRs are exaggerated in mice with FXS and therefore mGluRs are considered to be pharmacological targets for therapeutic intervention (Bear et al., 2004). Over the next few years it is likely that numerous advances will be made in identifying new genes involved in mental retardation as the anatomical and molecular defects are described and high-throughput screening methods take off.

7.1.3 Terminating developmental plasticity

My data showed that PKA is involved in regulating the expression of PNNs identified with Cat-315 antibody in mouse barrel cortex. This provides a target for regulating a specific subset of CSPGs that have specific functions. In spinal cord, digestion of CSPGs with chondroitinase promotes axonal re-growth after injury (Bradbury et al., 2002), although using this approach in brain may be considered to be a sledge-hammer approach since all CSPGs are degraded by chondroitinase. This approach may have some use in permitting plasticity to allow re-growth after brain damage if it is temporally controlled. In brain, specific CSPG epitopes have been associated with specific role in plasticity, and therefore patients suffering brain damage may require a specifically targeted regulation (such as via PKA) of a subset of CSPGs (such as those identified by Cat-315) to restore plasticity in order for the brain to make a recovery. Other targets for modulating CSPG epitopes are the enzymes that modify the carbohydrate side-chains. For example, HSPG (heparan sulphate proteoglycan) is modified by two enzymes HS6ST and HS2ST that are necessary for correct axon guidance (Pratt et al., 2006). These two enzymes post-translationally modify HSPGs giving them extensive structural diversity. Mice lacking either HS6ST or HS2ST display disorganised axon navigation indicating that normal sulfation by the two enzymes is necessary for correct axon navigation.

7.2 Limitations of my research

7.2.1 Strain of mice

A thesis such as this cannot be discussed without some description of the effects of different background strains on different transgenic lines. An increasing number of reports are being published describing how a specific phenotype alters in severity when presented in a mouse with a different background. The differences are due to ‘modifier genes’, which act in combination with the causative gene (Montagutelli, 2000). In some cases the effect of the modifier can be major, for example in the mouse models of polycystic kidney disease. Similarly, in naturally occurring human and mouse diseases the defect is rarely due to a single gene. For example, insulin-dependent diabetes is under the control of a number of genes (Vyse and Todd, 1996). Often modulatory genes at different loci influence the phenotype. In some cases the phenotype can vary between genetically identical (or very similar) individuals (such as that described in *Dusp6* mutants in chapter 1), known as ‘variable expressivity’. This is when there is variety in phenotype of individuals of the same genotype. It can be caused by modifier genes as described above, or by the effects of aging or environmental factors.

In the analysis of my experiments I came across a number of differences in outcomes when mice were on different genetic strains. The original analysis of *Sap102*/*Psd-95* mutants performed for this thesis were carried out on an MF1/129 background, and following the MHV outbreak, MF1/129 mice were culled and the new colony was maintained on Bl/6 129 and then bred with *LacZ* transgenics on DBA mixed background. This may explain why the defect in *Sap102*$^{-/y}$ *Psd-95*$^{+/-}$ was less severe in mice on Bl/6 129 /DBA than MF1/129.

The existence of inbred strains of mice allows the effect of different background strains to be analysed, and so data is not necessarily invalid because it cannot be repeated in experiments in a different mouse strain. To some extent, there are advantages of the varying phenotype. If the mutation is designed to mimic a human disorder then the background strain can be used where the characteristics of the disorder are best modelled. However, for studies such as those described in this thesis, varying backgrounds means comparisons should be made hesitantly between different mutants if the mice are on a different background and data from a single colony on a mixed background needs to be carefully controlled. Examples of this are the *Prkar2b* mutants, *Syngap* mutants and *Mglur5* mutants. When first investigated the *Prkar2b* mutant mice appeared to have more severe abnormalities in formation of barrels than those investigated for the recent publication (Watson et al., 2006) which were on a slightly different strain of Bl/6 (C57 Bl/6J Ola Hsd) than the original Bl/6. The original description of poor barrels in S*yngap*$^{-/-}$ and $^{+/-}$ was relating to animals on MF1 background. Mice described in this thesis are bred on a Bl/6 129 background and the defect is not as severe in the S*yngap*$^{+/-}$ (S*yngap*$^{-/-}$ were not examined) Similarly, *Mglur5*$^{-/-}$ C57Bl/6J 129 mice described in Hannan et al., 2001 had no barrels and TCAs formed rows not patches. However, recently C57Bl/6J 129 *Mglur5*$^{-/-}$ mice, which have been inbred for a number of years since the Hannan study, are found to have TCAs that appear to segregate into patches in a whisker-related pattern although cellular segregation is still largely absent (Wijetunge et al., submitted). This suggests that the phenotype may change over time, perhaps due to an inadvertent bias towards one of the two strains during breeding, or perhaps due to a mutation in a modifier gene becoming passed down from generation to generation. There are ways to avoid inadvertent bias when breeding over a number of generations.

A powerful approach is to develop a ‘congenic strain’ also known as ‘back-crossing’. This involves crossing F1 generation of homozygous or heterozygous mice with a mouse from say, ‘strain A’, then selecting offspring that carry the mutation, and crossing them to a mouse from strain A. If this procedure is continued over 10 generations, taking care to select both males and females over the generations, the result is a strain of mice that are very similar to strain A, but which carry the mutation that was originally on a different background. After 10 generations the only similarity between the new mutants on strain A and the original donor strain is the single chromosomal segment containing the locus selected for. This segment is estimated to be 20cM in length and contains 300-1000 genes (Montagutelli, 2000).

Quicker congenics over fewer generations is often used and 6 generations is often deemed acceptable. This technique is specifically useful if comparing different mutants or generating double or triple mutants, as both originate from the same background. For example, an application of congenics is being carried out already. Further experiments are going to be carried out using the *Sap102*/*Psd-95* double mutants after they are backcrossed onto a Bl/6 (Jackson Ola Hsd) background along with the *LacZ* mutants. This should reduce variability seen within the results. The fact that there are such variations in the barrel phenotype in mice with the same mutations on different backgrounds indicates that barrel formation is a multi-factorial process involving many molecules and mechanisms.

Many of the pathways investigated in this thesis are intercellular mechanisms but it is clear that intracellular mechanisms also pay a key role in translating the glutamate signal into cellular responses. The regulatory effects of glutamate are wide ranging. In barrels and elsewhere, this extends to the regulation of the ECM. From the data presented in this thesis, my most interesting finding is that PKA may be a target for regulating expression of specific subsets of CSPGs. Pharmacological agents specific for PKA are readily available and so the function of this pathway can be examined in experimental models previously described (such as those in McRae et al., 2007 and Pizzorusso et al., 2002).

Bibliography

Abdel-Majid RM, Leong WL, Schalkwyk LC, Smallman DS, Wong ST, Storm DR, Fine A, Dobson MJ, Guernsey DL, Neumann PE (1998) Loss of adenylyl cyclase I activity disrupts patterning of mouse somatosensory cortex. Nat Genet 19:289-291.

Abdel-Mannan O, Cheung AF, Molnar Z (2008) Evolution of cortical neurogenesis. Brain Res Bull 75:398-404.

Adamkiewicz A (1919) Uber die pericellularen Golginetze im Zentralnervensystem. Z Ges Neurol Psych 51:279-309.

Adams JP, Sweatt JD (2002) Molecular psychology: roles for the ERK MAP kinase cascade in memory. Annu Rev Pharmacol Toxicol 42:135-163.

Agmon A, Yang LT, O'Dowd DK, Jones EG (1993) Organized growth of thalamocortical axons from the deep tier of terminations into layer IV of developing mouse barrel cortex. J Neurosci 13:5365-5382.

Agmon A, Yang LT, Jones EG, O'Dowd DK (1995) Topological precision in the thalamic projection to neonatal mouse barrel cortex. J Neurosci 15:549-561.

Al-Ghoul WM, Miller MW (1989) Transient expression of Alz-50 immunoreactivity in developing rat neocortex: a marker for naturally occurring neuronal death? Brain Res 481:361-367.

Alvarez C, Vitalis T, Fon EA, Hanoun N, Hamon M, Seif I, Edwards R, Gaspar P, Cases O (2002) Effects of genetic depletion of monoamines on somatosensory cortical development. Neuroscience 115:753-764.

Angevine JB, Jr., Sidman RL (1961) Autoradiographic study of cell migration during histogenesis of cerebral cortex in the mouse. Nature 192:766-768.

Antonini A, Stryker MP (1993) Rapid remodeling of axonal arbors in the visual cortex. Science 260:1819-1821.

Antonini A, Stryker MP (1996) Plasticity of geniculocortical afferents following brief or prolonged monocular occlusion in the cat. J Comp Neurol 369:64-82.

Anttonen AK, Mahjneh I, Hamalainen RH, Lagier-Tourenne C, Kopra O, Waris L, Anttonen M, Joensuu T, Kalimo H, Paetau A, Tranebjaerg L, Chaigne D, Koenig M, Eeg-Olofsson O, Udd B, Somer M, Somer H, Lehesjoki AE (2005) The gene disrupted in Marinesco-Sjogren syndrome encodes SIL1, an HSPA5 cochaperone. Nat Genet 37:1309-1311.

Aoki C, Miko I, Oviedo H, Mikeladze-Dvali T, Alexandre L, Sweeney N, Bredt DS (2001) Electron microscopic immunocytochemical detection of PSD-95, PSD-93, SAP-102, and SAP-97 at postsynaptic, presynaptic, and nonsynaptic sites of adult and neonatal rat visual cortex. Synapse 40:239-257.

Arber S, Burden SJ, Harris AJ (2002) Patterning of skeletal muscle. Curr Opin Neurobiol 12:100-103.

Ariel M, Robinson E, McCarrey JR, Cedar H (1995) Gamete-specific methylation correlates with imprinting of the murine Xist gene. Nat Genet 9:312-315.

Armstrong-James M, Fox K, Das-Gupta A (1992) Flow of excitation within rat barrel cortex on striking a single vibrissa. J Neurophysiol 68:1345-1358.

Asher RA, Scheibe RJ, Keiser HD, Bignami A (1995) On the existence of a cartilage-like proteoglycan and link proteins in the central nervous system. Glia 13:294-308.

Baldi A, Calia E, Ciampini A, Riccio M, Vetuschi A, Persico AM, Keller F (2000) Deafferentation-induced apoptosis of neurons in thalamic somatosensory nuclei of the newborn rat: critical period and rescue from cell death by peripherally applied neurotrophins. Eur J Neurosci 12:2281-2290.
Bandtlow CE, Zimmermann DR (2000) Proteoglycans in the developing brain: new conceptual insights for old proteins. Physiol Rev 80:1267-1290.
Bansal A, Singer JH, Hwang BJ, Xu W, Beaudet A, Feller MB (2000) Mice lacking specific nicotinic acetylcholine receptor subunits exhibit dramatically altered spontaneous activity patterns and reveal a limited role for retinal waves in forming ON and OFF circuits in the inner retina. J Neurosci 20:7672-7681.
Barnett MW, Watson RF, Vitalis T, Porter K, Komiyama NH, Stoney PN, Gillingwater TH, Grant SG, Kind PC (2006) Synaptic Ras GTPase activating protein regulates pattern formation in the trigeminal system of mice. J Neurosci 26:1355-1365.
Barr ML, Bertram EG (1949) A morphological distinction between neurones of the male and female, and the behaviour of the nucleolar satellite during accelerated nucleoprotein synthesis. Nature 163:676.
Barrionuevo G, Schottler F, Lynch G (1980) The effects of repetitive low frequency stimulation on control and "potentiated" synaptic responses in the hippocampus. Life Sci 27:2385-2391.
Barth AL, Malenka RC (2001) NMDAR EPSC kinetics do not regulate the critical period for LTP at thalamocortical synapses. Nat Neurosci 4:235-236.
Bates CA, Killackey HP (1985) The organization of the neonatal rat's brainstem trigeminal complex and its role in the formation of central trigeminal patterns. J Comp Neurol 240:265-287.
Baumgartner S, Martin D, Hagios C, Chiquet-Ehrismann R (1994) Tenm, a Drosophila gene related to tenascin, is a new pair-rule gene. EMBO J 13:3728-3740.
Bayer SA, Altman J, Russo RJ, Dai XF, Simmons JA (1991) Cell migration in the rat embryonic neocortex. J Comp Neurol 307:499-516.
Bear MF, Abraham WC (1996) Long-term depression in hippocampus. Annu Rev Neurosci 19:437-462.
Bear MF, Kleinschmidt A, Gu QA, Singer W (1990) Disruption of experience-dependent synaptic modifications in striate cortex by infusion of an NMDA receptor antagonist. J Neurosci 10:909-925.
Bear MF, Huber KM, Warren ST (2004) The mGluR Theory of Fragile X Mental Retardation. TINS 27:370-377)
Beique JC, Andrade R (2003) PSD-95 regulates synaptic transmission and plasticity in rat cerebral cortex. J Physiol 546:859-867.
Belmont JW (1996) Genetic control of X inactivation and processes leading to X-inactivation skewing. Am J Hum Genet 58:1101-1108.
Berardi N, Pizzorusso T, Ratto GM, Maffei L (2003) Molecular basis of plasticity in the visual cortex. Trends Neurosci 26:369-378.
Berardi N, Pizzorusso T, Maffei L (2004) Extracellular matrix and visual cortex plasticity freeing the synapse. Neuron 44:905-608.
Berger A, Schiltz E, Schulz GE (1989) Guanylate kinase from Saccharomyces cerevisiae. Isolation and characterization, crystallization and preliminary X-

ray analysis, amino acid sequence and comparison with adenylate kinases. Eur J Biochem 184:433-443.
Berry M, Rogers AW (1965) The migration of neuroblasts in the developing cerebral cortex. J Anat 99:691-709.
Bertolotto A, Rocca G, Schiffer D (1990) Chondroitin 4-sulfate proteoglycan forms an extracellular network in human and rat central nervous system. J Neurol Sci 100:113-123.
Bishop KM, Goudreau G, O'Leary DD (2000) Regulation of area identity in the mammalian neocortex by Emx2 and Pax6. Science 288:344-349.
Bishop KM, Rubenstein JL, O'Leary DD (2002) Distinct actions of Emx1, Emx2, and Pax6 in regulating the specification of areas in the developing neocortex. J Neurosci 22:7627-7638.
Blakemore C, Cooper GF (1970) Development of the brain depends on the visual environment. Nature 228:477-478.
Bliss TV, Lomo T (1970) Plasticity in a monosynaptic cortical pathway. J Physiol 207:61P.
Bliss TV, Lomo T (1973) Long-lasting potentiation of synaptic transmission in the dentate area of the anaesthetized rabbit following stimulation of the perforant path. J Physiol 232:331-356.
Boeckers TM, Bockmann J, Kreutz MR, Gundelfinger ED (2002) ProSAP/Shank proteins - a family of higher order organizing molecules of the postsynaptic density with an emerging role in human neurological disease. J Neurochem 81:903-910.
Bond TL, Neumann PE, Mathieson WB, Brown RE (2002) Nest building in nulligravid, primigravid and primiparous C57BL/6J and DBA/2J mice (Mus musculus). Physiol Behav 75:551-555.
Bondareff W (1967) Demonstration of an intercellular substance in mouse cerebral cortex. Z Zellforsch Mikrosk Anat 81:366-373.
Bradbury EJ, Moon LD, Popat RJ, King VR, Bennett GS, Patel PN, Fawcett JW, McMahon SB (2002) Chondroitinase ABC promotes functional recovery after spinal cord injury. Nature 416:636-640.
Brambilla R, Gnesutta N, Minichiello L, White G, Roylance AJ, Herron CE, Ramsey M, Wolfer DP, Cestari V, Rossi-Arnaud C, Grant SG, Chapman PF, Lipp HP, Sturani E, Klein R (1997) A role for the Ras signalling pathway in synaptic transmission and long-term memory. Nature 390:281-286.
Brannan CI, Perkins AS, Vogel KS, Ratner N, Nordlund ML, Reid SW, Buchberg AM, Jenkins NA, Parada LF, Copeland NG (1994) Targeted disruption of the neurofibromatosis type-1 gene leads to developmental abnormalities in heart and various neural crest-derived tissues. Genes Dev 8:1019-1029.
Brenman JE, Christopherson KS, Craven SE, McGee AW, Bredt DS (1996) Cloning and characterization of postsynaptic density 93, a nitric oxide synthase interacting protein. J Neurosci 16:7407-7415.
Brockdorff N, Ashworth A, Kay GF, McCabe VM, Norris DP, Cooper PJ, Swift S, Rastan S (1992) The product of the mouse Xist gene is a 15 kb inactive X-specific transcript containing no conserved ORF and located in the nucleus. Cell 71:515-526.
Brockdorff N, Ashworth A, Kay GF, Cooper P, Smith S, McCabe VM, Norris DP, Penny GD, Patel D, Rastan S (1991) Conservation of position and exclusive

expression of mouse Xist from the inactive X chromosome. Nature 351:329-331.
Brown CJ, Ballabio A, Rupert JL, Lafreniere RG, Grompe M, Tonlorenzi R, Willard HF (1991a) A gene from the region of the human X inactivation centre is expressed exclusively from the inactive X chromosome. Nature 349:38-44.
Brown CJ, Lafreniere RG, Powers VE, Sebastio G, Ballabio A, Pettigrew AL, Ledbetter DH, Levy E, Craig IW, Willard HF (1991b) Localization of the X inactivation centre on the human X chromosome in Xq13. Nature 349:82-84.
Brown MD, Sacks DB (2008) Compartmentalised MAPK pathways. Handb Exp Pharmacol:205-235.
Brown SD (1991) XIST and the mapping of the X chromosome inactivation centre. Bioessays 13:607-612.
Bruckner G, Hausen D, Hartig W, Drlicek M, Arendt T, Brauer K (1999) Cortical areas abundant in extracellular matrix chondroitin sulphate proteoglycans are less affected by cytoskeletal changes in Alzheimer's disease. Neuroscience 92:791-805.
Bruckner G, Grosche J, Schmidt S, Hartig W, Margolis RU, Delpech B, Seidenbecher CI, Czaniera R, Schachner M (2000) Postnatal development of perineuronal nets in wild-type mice and in a mutant deficient in tenascin-R. J Comp Neurol 428:616-629.
Bruckner G, Brauer K, Hartig W, Wolff JR, Rickmann MJ, Derouiche A, Delpech B, Girard N, Oertel WH, Reichenbach A (1993) Perineuronal nets provide a polyanionic, glia-associated form of microenvironment around certain neurons in many parts of the rat brain. Glia 8:183-200.
Caleo M, Maffei L (2002) Neurotrophins and plasticity in the visual cortex. Neuroscientist 8:52-61.
Cang J, Renteria RC, Kaneko M, Liu X, Copenhagen DR, Stryker MP (2005) Development of precise maps in visual cortex requires patterned spontaneous activity in the retina. Neuron 48:797-809.
Carmignoto G, Vicini S (1992) Activity-dependent decrease in NMDA receptor responses during development of the visual cortex. Science 258:1007-1011.
Carrasco MM, Razak KA, Pallas SL (2005) Visual experience is necessary for maintenance but not development of receptive fields in superior colliculus. J Neurophysiol 94:1962-1970.
Cases O, Vitalis T, Seif I, De Maeyer E, Sotelo C, Gaspar P (1996) Lack of barrels in the somatosensory cortex of monoamine oxidase A-deficient mice: role of a serotonin excess during the critical period. Neuron 16:297-307.
Castejon HV (1970a) Histochemical demonstration of sulphated polysaccharides at the surface coat of nerve cells in the mouse central nervous system. Acta Histochem 38:55-64.
Castejon HV (1970b) Histochemical demonstration of acid glycosaminoglycans in the nerve cell cytoplasm of mouse central nervous system. Acta Histochem 35:161-172.
Catalano SM, Robertson RT, Killackey HP (1996) Individual axon morphology and thalamocortical topography in developing rat somatosensory cortex. J Comp Neurol 367:36-53.
Cattanach BM, Williams CE (1972) Evidence of non-random X chromosome activity in the mouse. Genet Res 19:229-240.

Cattanach BM, Rasberry C (1991) Identification of the Mus spretus Xce allele Mouse Genome 89:565-566.
Celio MR, Chiquet-Ehrismann R (1993) 'Perineuronal nets' around cortical interneurons expressing parvalbumin are rich in tenascin. Neurosci Lett 162:137-140.
Celio MR, Blumcke I (1994) Perineuronal nets--a specialized form of extracellular matrix in the adult nervous system. Brain Res Brain Res Rev 19:128-145.
Chalupa LM (2007) A reassessment of the role of activity in the formation of eye-specific retinogeniculate projections. Brain Res Rev 55:228-236.
Chechlacz M, Gleeson JG (2003) Is mental retardation a defect of synapse structure and function? Pediatr Neurol 29:11-17.
Chen C, Regehr WG (2000) Developmental remodeling of the retinogeniculate synapse. Neuron 28:955-966.
Chen HJ, Rojas-Soto M, Oguni A, Kennedy MB (1998) A synaptic Ras-GTPase activating protein (p135 SynGAP) inhibited by CaM kinase II. Neuron 20:895-904.
Chen L, Yang C, Mower GD (2001) Developmental changes in the expression of GABA(A) receptor subunits (alpha(1), alpha(2), alpha(3)) in the cat visual cortex and the effects of dark rearing. Brain Res Mol Brain Res 88:135-143.
Chiaia NL, Fish SE, Bauer WR, Bennett-Clarke CA, Rhoades RW (1992) Postnatal blockade of cortical activity by tetrodotoxin does not disrupt the formation of vibrissa-related patterns in the rat's somatosensory cortex. Brain Res Dev Brain Res 66:244-250.
Chiaia NL, Fish SE, Bauer WR, Figley BA, Eck M, Bennett-Clarke CA, Rhoades RW (1994) Effects of postnatal blockage of cortical activity with tetrodotoxin upon lesion-induced reorganization of vibrissae-related patterns in the somatosensory cortex of rat. Brain Res Dev Brain Res 79:301-306.
Chiurazzi P, Schwartz CE, Gecz J, Neri G (2008) XLMR genes: update 2007. Eur J Hum Genet 16:422-434.
Cho KO, Hunt CA, Kennedy MB (1992) The rat brain postsynaptic density fraction contains a homolog of the Drosophila discs-large tumor suppressor protein. Neuron 9:929-942.
Cichowski K, Jacks T (2001) NF1 tumor suppressor gene function: narrowing the GAP. Cell 104:593-604.
Clark BA, Cull-Candy SG (2002) Activity-dependent recruitment of extrasynaptic NMDA receptor activation at an AMPA receptor-only synapse. J Neurosci 22:4428-4436.
Clerc P, Avner P (1998) Role of the region 3' to Xist exon 6 in the counting process of X-chromosome inactivation. Nat Genet 19:249-253.
Cline HT (1991) Activity-dependent plasticity in the visual systems of frogs and fish. Trends Neurosci 14:104-111.
Cline HT, Debski EA, Constantine-Paton M (1987) N-methyl-D-aspartate receptor antagonist desegregates eye-specific stripes. Proc Natl Acad Sci U S A 84:4342-4345.
Clinton SM, Meador-Woodruff JH (2004) Abnormalities of the NMDA Receptor and Associated Intracellular Molecules in the Thalamus in Schizophrenia and Bipolar Disorder. Neuropsychopharmacology 29:1353-1362.

Colledge M, Dean RA, Scott GK, Langeberg LK, Huganir RL, Scott JD (2000) Targeting of PKA to glutamate receptors through a MAGUK-AKAP complex. Neuron 27:107-119.

Collins MO, Husi H, Yu L, Brandon JM, Anderson CN, Blackstock WP, Choudhary JS, Grant SG (2006) Molecular characterization and comparison of the components and multiprotein complexes in the postsynaptic proteome. J Neurochem 97 Suppl 1:16-23.

Conroy WG, Liu Z, Nai Q, Coggan JS, Berg DK (2003) PDZ-containing proteins provide a functional postsynaptic scaffold for nicotinic receptors in neurons. Neuron 38:759-771.

Cook PM, Prusky G, Ramoa AS (1999) The role of spontaneous retinal activity before eye opening in the maturation of form and function in the retinogeniculate pathway of the ferret. Vis Neurosci 16:491-501.

Corvetti L, Rossi F (2005) Degradation of chondroitin sulfate proteoglycans induces sprouting of intact purkinje axons in the cerebellum of the adult rat. J Neurosci 25:7150-7158.

Costa RM, Silva AJ (2003) Mouse models of neurofibromatosis type I: bridging the GAP. Trends Mol Med 9:19-23.

Costanzi C, Pehrson JR (1998) Histone macroH2A1 is concentrated in the inactive X chromosome of female mammals. Nature 393:599-601.

Crair MC, Malenka RC (1995) A critical period for long-term potentiation at thalamocortical synapses. Nature 375:325-328.

Craven SE, Bredt DS (1998) PDZ proteins organize synaptic signaling pathways. Cell 93:495-498.

Craven SE, Bredt DS (2000) Synaptic targeting of the postsynaptic density protein PSD-95 mediated by a tyrosine-based trafficking signal. J Biol Chem 275:20045-20051.

Craven SE, El-Husseini AE, Bredt DS (1999) Synaptic targeting of the postsynaptic density protein PSD-95 mediated by lipid and protein motifs. Neuron 22:497-509.

Cuthbert PC, Stanford LE, Coba MP, Ainge JA, Fink AE, Opazo P, Delgado JY, Komiyama NH, O'Dell TJ, Grant SG (2007) Synapse-associated protein 102/dlgh3 couples the NMDA receptor to specific plasticity pathways and learning strategies. J Neurosci 27:2673-2682.

Cynader M, Berman N, Hein A (1976) Recovery of function in cat visual cortex following prolonged deprivation. Exp Brain Res 25:139-156.

Daston MM, Scrable H, Nordlund M, Sturbaum AK, Nissen LM, Ratner N (1992) The protein product of the neurofibromatosis type 1 gene is expressed at highest abundance in neurons, Schwann cells, and oligodendrocytes. Neuron 8:415-428.

Datwani A, Iwasato T, Itohara S, Erzurumlu RS (2002) NMDA receptor-dependent pattern transfer from afferents to postsynaptic cells and dendritic differentiation in the barrel cortex. Mol Cell Neurosci 21:477-492.

Davis AA, Temple S (1994) A self-renewing multipotential stem cell in embryonic rat cerebral cortex. Nature 372:263-266.

Davis S, Laroche S (2006) Mitogen-activated protein kinase/extracellular regulated kinase signalling and memory stabilization: a review. Genes Brain Behav 5 Suppl 2:61-72.

Daw N, Rao Y, Wang XF, Fischer Q, Yang Y (2004) LTP and LTD vary with layer in rodent visual cortex. Vision Res 44:3377-3380.
De Felipe J, Marco P, Fairen A, Jones EG (1997) Inhibitory synaptogenesis in mouse somatosensory cortex. Cereb Cortex 7:619-634.
DeClue JE, Cohen BD, Lowy DR (1991) Identification and characterization of the neurofibromatosis type 1 protein product. Proc Natl Acad Sci U S A 88:9914-9918.
Deyst KA, Toole BP (1995) Production of hyaluronan-dependent pericellular matrix by embryonic rat glial cells. Brain Res Dev Brain Res 88:122-125.
Diamond ME, Armstrong-James M, Ebner FF (1993) Experience-dependent plasticity in adult rat barrel cortex. Proc Natl Acad Sci U S A 90:2082-2086.Di Cristo G, Berardi N, Cancedda L, Pizzorusso T, Putignano E, Ratto GM, Maffei L (2001) Requirement of ERK activation for visual cortical plasticity. Science 292:2337-2340.
Dickinson RJ, Eblaghie MC, Keyse SM, Morriss-Kay GM (2002) Expression of the ERK-specific MAP kinase phosphatase PYST1/MKP3 in mouse embryos during morphogenesis and early organogenesis. Mech Dev 113:193-196.
Dino MR, Harroch S, Hockfield S, Matthews RT (2006) Monoclonal antibody Cat-315 detects a glycoform of receptor protein tyrosine phosphatase beta/phosphacan early in CNS development that localizes to extrasynaptic sites prior to synapse formation. Neuroscience 142:1055-1069.
Dityatev A, Schachner M (2003) Extracellular matrix molecules and synaptic plasticity. Nat Rev Neurosci 4:456-468.
Dosemeci A, Makusky AJ, Jankowska-Stephens E, Yang X, Slotta DJ, Markey SP (2007) Composition of the synaptic PSD-95 complex. Mol Cell Proteomics 6:1749-1760.
Dou CL, Levine JM (1994) Inhibition of neurite growth by the NG2 chondroitin sulfate proteoglycan. J Neurosci 14:7616-7628.
Doyle DA, Lee A, Lewis J, Kim E, Sheng M, MacKinnon R (1996) Crystal structures of a complexed and peptide-free membrane protein-binding domain: molecular basis of peptide recognition by PDZ. Cell 85:1067-1076.
Deyoe EA, Hockfield S, Garren H, Van Essen DC (1990) Antibody labeling of functional subdivisions in visual cortex: Cat-301 immunoreactivity in striate and extrastriate cortex of the macaque monkey. Vis Neurosci 5:67-81.
Drager UC (1978) Observations on monocular deprivation in mice. J Neurophysiol 41:28-42.
Duffy KR, Murphy KM, Jones DG (1998) Analysis of the postnatal growth of visual cortex. Vis Neurosci 15:831-839.
Ehlers MD, Mammen AL, Lau LF, Huganir RL (1996) Synaptic targeting of glutamate receptors. Curr Opin Cell Biol 8:484-489.
Ehrlich I, Malinow R (2004) Postsynaptic density 95 controls AMPA receptor incorporation during long-term potentiation and experience-driven synaptic plasticity. J Neurosci 24:916-927.
Ehrlich I, Klein M, Rumpel S, Malinow R (2007) PSD-95 is required for activity-driven synapse stabilization. Proc Natl Acad Sci U S A 104:4176-4181.
El-Husseini AE, Craven SE, Chetkovich DM, Firestein BL, Schnell E, Aoki C, Bredt DS (2000) Dual palmitoylation of PSD-95 mediates its vesiculotubular

sorting, postsynaptic targeting, and ion channel clustering. J Cell Biol 148:159-172.
Elias GM, Nicoll RA (2007) Synaptic trafficking of glutamate receptors by MAGUK scaffolding proteins. Trends Cell Biol 17:343-352.
Emerson VF, Chalupa LM, Thompson ID, Talbot RJ (1982) Behavioural, physiological, and anatomical consequences of monocular deprivation in the golden hamster (Mesocricetus auratus). Exp Brain Res 45:168-178.
Erskine L, Herrera E (2007) The retinal ganglion cell axon's journey: insights into molecular mechanisms of axon guidance. Dev Biol 308:1-14.
Erzurumlu RS, Kind PC (2001) Neural activity: sculptor of 'barrels' in the neocortex. Trends Neurosci 24:589-595.
Erzurumlu RS, Guido W, Molnar Z, eds (2006) Development and Plasticity in Sensory Thalamus and Cortex
1 edition Edition. New York: Springer-Verlag New York Inc.
Fagiolini M, Hensch TK (2000) Inhibitory threshold for critical-period activation in primary visual cortex. Nature 404:183-186.
Fagiolini M, Pizzorusso T, Berardi N, Domenici L, Maffei L (1994) Functional postnatal development of the rat primary visual cortex and the role of visual experience: dark rearing and monocular deprivation. Vision Res 34:709-720.
Fagiolini M, Fritschy JM, Low K, Mohler H, Rudolph U, Hensch TK (2004) Specific GABAA circuits for visual cortical plasticity. Science 303:1681-1683.
Fagiolini M, Katagiri H, Miyamoto H, Mori H, Grant SG, Mishina M, Hensch TK (2003) Separable features of visual cortical plasticity revealed by N-methyl-D-aspartate receptor 2A signaling. Proc Natl Acad Sci U S A 100:2854-2859.
Fawcett JW, Asher RA (1999) The glial scar and central nervous system repair. Brain Res Bull 49:377-391.
Feller MB, Wellis DP, Stellwagen D, Werblin FS, Shatz CJ (1996) Requirement for cholinergic synaptic transmission in the propagation of spontaneous retinal waves. Science 272:1182-1187.
Finkbeiner S, Greenberg ME (1996) Ca(2+)-dependent routes to Ras: mechanisms for neuronal survival, differentiation, and plasticity? Neuron 16:233-236.
Firestein BL, Craven SE, Bredt DS (2000) Postsynaptic targeting of MAGUKs mediated by distinct N-terminal domains. Neuroreport 11:3479-3484.
Firestein BL, Brenman JE, Aoki C, Sanchez-Perez AM, El-Husseini AE, Bredt DS (1999) Cypin: a cytosolic regulator of PSD-95 postsynaptic targeting. Neuron 24:659-672.
Fischer QS, Beaver CJ, Yang Y, Rao Y, Jakobsdottir KB, Storm DR, McKnight GS, Daw NW (2004) Requirement for the RIIbeta isoform of PKA, but not calcium-stimulated adenylyl cyclase, in visual cortical plasticity. J Neurosci 24:9049-9058.
Fletcher EL, Hack I, Brandstatter JH, Wassle H (2000) Synaptic localization of NMDA receptor subunits in the rat retina. J Comp Neurol 420:98-112.
Fon EA, Pothos EN, Sun BC, Killeen N, Sulzer D, Edwards RH (1997) Vesicular transport regulates monoamine storage and release but is not essential for amphetamine action. Neuron 19:1271-1283.
Forrest D, Yuzaki M, Soares HD, Ng L, Luk DC, Sheng M, Stewart CL, Morgan JI, Connor JA, Curran T (1994) Targeted disruption of NMDA receptor 1 gene abolishes NMDA response and results in neonatal death. Neuron 13:325-338.

Fox K (1992) A critical period for experience-dependent synaptic plasticity in rat barrel cortex. J Neurosci 12:1826-1838.
Fox K (1994) The cortical component of experience-dependent synaptic plasticity in the rat barrel cortex. J Neurosci 14:7665-7679.
Fox K (2002) Anatomical pathways and molecular mechanisms for plasticity in the barrel cortex. Neuroscience 111:799-814.
Fox K, Wong RO (2005) A comparison of experience-dependent plasticity in the visual and somatosensory systems. Neuron 48:465-477.
Fox K, Schlaggar BL, Glazewski S, O'Leary DD (1996) Glutamate receptor blockade at cortical synapses disrupts development of thalamocortical and columnar organization in somatosensory cortex. Proc Natl Acad Sci U S A 93:5584-5589.
Freeman RD, Olson C (1982) Brief periods of monocular deprivation in kittens: effects of delay prior to physiological study. J Neurophysiol 47:139-150.
Fujita SC, Tada Y, Murakami F, Hayashi M, Matsumura M (1989) Glycosaminoglycan-related epitopes surrounding different subsets of mammalian central neurons. Neurosci Res 7:117-130.
Fukuchi-Shimogori T, Grove EA (2001) Neocortex patterning by the secreted signaling molecule FGF8. Science 294:1071-1074.
Fukuchi-Shimogori T, Grove EA (2003) Emx2 patterns the neocortex by regulating FGF positional signaling. Nat Neurosci 6:825-831.
Funke L, Dakoji S, Bredt DS (2005) Membrane-associated guanylate kinases regulate adhesion and plasticity at cell junctions. Annu Rev Biochem 74:219-245.
Galarreta M, Hestrin S (2001a) Spike transmission and synchrony detection in networks of GABAergic interneurons. Science 292:2295-2299.
Galarreta M, Hestrin S (2001b) Electrical synapses between GABA-releasing interneurons. Nat Rev Neurosci 2:425-433.
Gale RE, Linch DC (1994) Interpretation of X-chromosome inactivation patterns. Blood 84:2376-2378.
Gale RE, Wheadon H, Boulos P, Linch DC (1994) Tissue specificity of X-chromosome inactivation patterns. Blood 83:2899-2905.
Galli L, Maffei L (1988) Spontaneous impulse activity of rat retinal ganglion cells in prenatal life. Science 242:90-91.
Galtrey CM, Fawcett JW (2007) The role of chondroitin sulfate proteoglycans in regeneration and plasticity in the central nervous system. Brain Res Rev 54:1-18.
Garber K (2007) Neuroscience. Autism's cause may reside in abnormalities at the synapse. Science 317:190-191.
Garry EM, Moss A, Delaney A, O'Neill F, Blakemore J, Bowen J, Husi H, Mitchell R, Grant SG, Fleetwood-Walker SM (2003) Neuropathic sensitization of behavioral reflexes and spinal NMDA receptor/CaM kinase II interactions are disrupted in PSD-95 mutant mice. Curr Biol 13:321-328.
Garwood J, Heck N, Reichardt F, Faissner A (2003) Phosphacan short isoform, a novel non-proteoglycan variant of phosphacan/receptor protein tyrosine phosphatase-beta, interacts with neuronal receptors and promotes neurite outgrowth. J Biol Chem 278:24164-24173.

Gaspar P, Cases O, Maroteaux L (2003) The developmental role of serotonin: news from mouse molecular genetics. Nat Rev Neurosci 4:1002-1012.
Glazewski S, Fox K (1996) Time course of experience-dependent synaptic potentiation and depression in barrel cortex of adolescent rats. J Neurophysiol 75:1714-1729.
Glazewski S, Herman C, McKenna M, Chapman PF, Fox K (1998) Long-term potentiation in vivo in layers II/III of rat barrel cortex. Neuropharmacology 37:581-592.
Goodman CS, Shatz CJ (1993) Developmental mechanisms that generate precise patterns of neuronal connectivity. Cell 72 Suppl:77-98.
Gordon JA, Stryker MP (1996) Experience-dependent plasticity of binocular responses in the primary visual cortex of the mouse. J Neurosci 16:3274-3286.
Gordon JA, Cioffi D, Silva AJ, Stryker MP (1996) Deficient plasticity in the primary visual cortex of alpha-calcium/calmodulin-dependent protein kinase II mutant mice. Neuron 17:491-499.
Gorski JA, Talley T, Qiu M, Puelles L, Rubenstein JL, Jones KR (2002) Cortical excitatory neurons and glia, but not GABAergic neurons, are produced in the Emx1-expressing lineage. J Neurosci 22:6309-6314.
Grant SG (2006) The synapse proteome and phosphoproteome: a new paradigm for synapse biology. Biochem Soc Trans 34:59-63.
Grant SG, O'Dell TJ (2001) Multiprotein complex signaling and the plasticity problem. Curr Opin Neurobiol 11:363-368.
Grant SG, Marshall MC, Page KL, Cumiskey MA, Armstrong JD (2005) Synapse proteomics of multiprotein complexes: en route from genes to nervous system diseases. Hum Mol Genet 14 Spec No. 2:R225-234.
Grant SGN (1996) Targeted Gene Disruption in the CNS to Study Learning and Behavior. Methods 10:406-416.
Groc L, Choquet D, Stephenson FA, Verrier D, Manzoni OJ, Chavis P (2007) NMDA receptor surface trafficking and synaptic subunit composition are developmentally regulated by the extracellular matrix protein Reelin. J Neurosci 27:10165-10175.
Groom LA, Sneddon AA, Alessi DR, Dowd S, Keyse SM (1996) Differential regulation of the MAP, SAP and RK/p38 kinases by Pyst1, a novel cytosolic dual-specificity phosphatase. EMBO J 15:3621-3632.
Grubb MS, Rossi FM, Changeux JP, Thompson ID (2003) Abnormal functional organization in the dorsal lateral geniculate nucleus of mice lacking the beta 2 subunit of the nicotinic acetylcholine receptor. Neuron 40:1161-1172.
Gu Q (2002) Neuromodulatory transmitter systems in the cortex and their role in cortical plasticity. Neuroscience 111:815-835.
Guimaraes A, Zaremba S, Hockfield S (1990) Molecular and morphological changes in the cat lateral geniculate nucleus and visual cortex induced by visual deprivation are revealed by monoclonal antibodies Cat-304 and Cat-301. J Neurosci 10:3014-3024.
Gupta DS, McCullumsmith RE, Beneyto M, Haroutunian V, Davis KL, Meador-Woodruff JH (2005) Metabotropic glutamate receptor protein expression in the prefrontal cortex and striatum in schizophrenia. Synapse 57:123-131.

Gutmann DH, Wood DL, Collins FS (1991) Identification of the neurofibromatosis type 1 gene product. Proc Natl Acad Sci U S A 88:9658-9662.
Gutmann DH, Wu YL, Hedrick NM, Zhu Y, Guha A, Parada LF (2001) Heterozygosity for the neurofibromatosis 1 (NF1) tumor suppressor results in abnormalities in cell attachment, spreading and motility in astrocytes. Hum Mol Genet 10:3009-3016.
Gutowski NJ, Newcombe J, Cuzner ML (1999) Tenascin-R and C in multiple sclerosis lesions: relevance to extracellular matrix remodelling. Neuropathol Appl Neurobiol 25:207-214.
Guy J, Gan J, Selfridge J, Cobb S, Bird A (2007) Reversal of Neuroloical Defects in a Mouse Model of Rett Syndrome. Science 315:1143-1147.
Hahm JO, Langdon RB, Sur M (1991) Disruption of retinogeniculate afferent segregation by antagonists to NMDA receptors. Nature 351:568-570.
Hall A (1998) Rho GTPases and the actin cytoskeleton. Science 279:509-514.
Hamasaki T, Leingartner A, Ringstedt T, O'Leary DD (2004) EMX2 regulates sizes and positioning of the primary sensory and motor areas in neocortex by direct specification of cortical progenitors. Neuron 43:359-372.
Hamori J, Savy C, Madarasz M, Somogyi J, Takacs J, Verley R, Farkas-Bargeton E (1986) Morphological alterations in subcortical vibrissal relays following vibrissal follicle destruction at birth in the mouse. J Comp Neurol 254:166-183.
Hand PJ, ed (1982) Plasticity of the rat cortical barrel system: New York: Academic.
Hannan AJ, Kind PC, Blakemore C (1998) Phospholipase C-beta1 expression correlates with neuronal differentiation and synaptic plasticity in rat somatosensory cortex. Neuropharmacology 37:593-605.
Hannan AJ, Blakemore C, Katsnelson A, Vitalis T, Huber KM, Bear M, Roder J, Kim D, Shin HS, Kind PC (2001) PLC-beta1, activated via mGluRs, mediates activity-dependent differentiation in cerebral cortex. Nat Neurosci 4:282-288.
Hanover JL, Huang ZJ, Tonegawa S, Stryker MP (1999) Brain-derived neurotrophic factor overexpression induces precocious critical period in mouse visual cortex. J Neurosci 19:RC40.
Harsha HC et al. (2005) A manually curated functional annotation of the human X chromosome. Nat Genet 37:331-332.
Hausen D, Bruckner G, Drlicek M, Hartig W, Brauer K, Bigl V (1996) Pyramidal cells ensheathed by perineuronal nets in human motor and somatosensory cortex. Neuroreport 7:1725-1729.
Hayashi H (1980) Distributions of vibrissae afferent fiber collaterals in the trigeminal nuclei as revealed by intra-axonal injection of horseradish peroxidase. Brain Res 183:442-446.
Hayashi N, Miyata S, Yamada M, Kamei K, Oohira A (2005) Neuronal expression of the chondroitin sulfate proteoglycans receptor-type protein-tyrosine phosphatase beta and phosphacan. Neuroscience 131:331-348.
Hayashi N, Tatsumi K, Okuda H, Yoshikawa M, Ishizaka S, Miyata S, Manabe T, Wanaka A (2007a) DACS, novel matrix structure composed of chondroitin sulfate proteoglycan in the brain. Biochem Biophys Res Commun 364:410-415.

Hayashi T, Okabe T, Nasu-Nishimura Y, Sakaue F, Ohwada S, Matsuura K, Akiyama T, Nakamura T (2007b) PX-RICS, a novel splicing variant of RICS, is a main isoform expressed during neural development. Genes Cells 12:929-939.

He W, Ingraham C, Rising L, Goderie S, Temple S (2001) Multipotent stem cells from the mouse basal forebrain contribute GABAergic neurons and oligodendrocytes to the cerebral cortex during embryogenesis. J Neurosci 21:8854-8862.

He Y, Hicke L, Radhakrishnan I (2007) Structural basis for ubiquitin recognition by SH3 domains. J Mol Biol 373:190-196.

Heard E, Clerc P, Avner P (1997) X-chromosome inactivation in mammals. Annu Rev Genet 31:571-610.

Hebb DO, ed (1949) The organisation of behaviour; A neuropsychological theory. New York: Wiley.

Henderson TA, Woolsey TA, Jacquin MF (1992) Infraorbital nerve blockade from birth does not disrupt central trigeminal pattern formation in the rat. Brain Res Dev Brain Res 66:146-152.

Hendry SH, Jones EG, Hockfield S, McKay RD (1988) Neuronal populations stained with the monoclonal antibody Cat-301 in the mammalian cerebral cortex and thalamus. J Neurosci 8:518-542.

Hensch TK (2004) Critical period regulation. Annu Rev Neurosci 27:549-579.

Hensch TK (2005a) Critical period plasticity in local cortical circuits. Nat Rev Neurosci 6:877-888.

Hensch TK (2005b) Critical period mechanisms in developing visual cortex. Curr Top Dev Biol 69:215-237.

Hensch TK, Stryker MP (2004) Columnar architecture sculpted by GABA circuits in developing cat visual cortex. Science 303:1678-1681.

Hensch TK, Fagiolini M, Mataga N, Stryker MP, Baekkeskov S, Kash SF (1998) Local GABA circuit control of experience-dependent plasticity in developing visual cortex. Science 282:1504-1508.

Heumann D, Leuba G (1983) Neuronal death in the development and aging of the cerebral cortex of the mouse. Neuropathol Appl Neurobiol 9:297-311.

Heumann D, Leuba G, Rabinowicz T (1978) Postnatal development of the mouse cerebral neocortex. IV. Evolution of the total cortical volume, of the population of neurons and glial cells. J Hirnforsch 19:385-393.

Heynen AJ, Yoon BJ, Liu CH, Chung HJ, Huganir RL, Bear MF (2003) Molecular mechanism for loss of visual cortical responsiveness following brief monocular deprivation. Nat Neurosci 6:854-862.

Ho IS, Hannan F, Guo HF, Hakker I, Zhong Y (2007) Distinct functional domains of neurofibromatosis type 1 regulate immediate versus long-term memory formation. J Neurosci 27:6852-6857.

Hockfield S, McKay RD (1983) A surface antigen expressed by a subset of neurons in the vertebrate central nervous system. Proc Natl Acad Sci U S A 80:5758-5761.

Hockfield S, McKay RD, Hendry SH, Jones EG (1983) A surface antigen that identifies ocular dominance columns in the visual cortex and laminar features of the lateral geniculate nucleus. Cold Spring Harb Symp Quant Biol 48 Pt 2:877-889.

Hockfield S, Kalb RG, Zaremba S, Fryer H (1990) Expression of neural proteoglycans correlates with the acquisition of mature neuronal properties in the mammalian brain. Cold Spring Harb Symp Quant Biol 55:505-514.
Hocking AM, Shinomura T, McQuillan DJ (1998) Leucine-rich repeat glycoproteins of the extracellular matrix. Matrix Biol 17:1-19.
Hollmann M, Heinemann S (1994) Cloned glutamate receptors. Annu Rev Neurosci 17:31-108.
Holmberg V, Jalanko A, Isosomppi J, Fabritius AL, Peltonen L, Kopra O (2004) The mouse ortholog of the neuronal ceroid lipofuscinosis CLN5 gene encodes a soluble lysosomal glycoprotein expressed in the developing brain. Neurobiol Dis 16:29-40.
Hooks BM, Chen C (2006) Distinct roles for spontaneous and visual activity in remodeling of the retinogeniculate synapse. Neuron 52:281-291.
Hooks BM, Chen C (2007) Critical periods in the visual system: changing views for a model of experience-dependent plasticity. Neuron 56:312-326.
Hooks BM, Chen C (2008) Vision triggers an experience-dependent sensitive period at the retinogeniculate synapse. J Neurosci 28:4807-4817.
Hsueh YP (2007) Neurofibromin signaling and synapses. J Biomed Sci 14:461-466.
Hubel DH, Wiesel TN (1963a) Receptive Fields of Cells in Striate Cortex of Very Young, Visually Inexperienced Kittens. J Neurophysiol 26:994-1002.
Hubel DH, Wiesel TN (1963b) Shape and arrangement of columns in cat's striate cortex. J Physiol 165:559-568.
Hubel DH, Wiesel TN (1970) The period of susceptibility to the physiological effects of unilateral eye closure in kittens. J Physiol 206:419-436.
Huberman AD, Wang GY, Liets LC, Collins OA, Chapman B, Chalupa LM (2003) Eye-specific retinogeniculate segregation independent of normal neuronal activity. Science 300:994-998.
Huffman KJ, Molnar Z, Van Dellen A, Kahn DM, Blakemore C, Krubitzer L (1999) Formation of cortical fields on a reduced cortical sheet. J Neurosci 19:9939-9952.
Husi H, Ward MA, Choudhary JS, Blackstock WP, Grant SG (2000) Proteomic analysis of NMDA receptor-adhesion protein signaling complexes. Nat Neurosci 3:661-669.
Husi H, Grant SG (2001) Proteomics of the nervous system. TINS 24:259-266.
Ichijo H (2004) Proteoglycans as cues for axonal guidance in formation of retinotectal or retinocollicular projections. Mol Neurobiol 30:23-33.
Ikeda K, Araki K, Takayama C, Inoue Y, Yagi T, Aizawa S, Mishina M (1995) Reduced spontaneous activity of mice defective in the epsilon 4 subunit of the NMDA receptor channel. Brain Res Mol Brain Res 33:61-71.
Inan M, Lu HC, Albright MJ, She WC, Crair MC (2006) Barrel map development relies on protein kinase A regulatory subunit II beta-mediated cAMP signaling. J Neurosci 26:4338-4349.
Irie M, Hata Y, Takeuchi M, Ichtchenko K, Toyoda A, Hirao K, Takai Y, Rosahl TW, Sudhof TC (1997) Binding of neuroligins to PSD-95. Science 277:1511-1515.
Ivanova A, Nakahira E, Kagawa T, Oba A, Wada T, Takebayashi H, Spassky N, Levine J, Zalc B, Ikenaka K (2003) Evidence for a second wave of

oligodendrogenesis in the postnatal cerebral cortex of the mouse. J Neurosci Res 73:581-592.
Iwai Y, Fagiolini M, Obata K, Hensch TK (2003) Rapid critical period induction by tonic inhibition in visual cortex. J Neurosci 23:6695-6702.
Iwasato T, Inan M, Kanki H, Erzurumlu RS, Itohara S, Crair MC (2008) Cortical adenylyl cyclase 1 is required for thalamocortical synapse maturation and aspects of layer IV barrel development. J Neurosci 28:5931-5943.
Iwasato T, Datwani A, Wolf AM, Nishiyama H, Taguchi Y, Tonegawa S, Knopfel T, Erzurumlu RS, Itohara S (2000) Cortex-restricted disruption of NMDAR1 impairs neuronal patterns in the barrel cortex. Nature 406:726-731.
Jacks T, Shih TS, Schmitt EM, Bronson RT, Bernards A, Weinberg RA (1994) Tumour predisposition in mice heterozygous for a targeted mutation in Nf1. Nat Genet 7:353-361.
Jacquin MF, Arends JJ, Xiang C, Shapiro LA, Ribak CE, Chen ZF (2008) In DRG11 knock-out mice, trigeminal cell death is extensive and does not account for failed brainstem patterning. J Neurosci 28:3577-3585.
Jaubert-Miazza L, Green E, Lo FS, Bui K, Mills J, Guido W (2005) Structural and functional composition of the developing retinogeniculate pathway in the mouse. Vis Neurosci 22:661-676.
Jeffrey KL, Camps M, Rommel C, Mackay CR (2007) Targeting dual-specificity phosphatases: manipulating MAP kinase signalling and immune responses. Nat Rev Drug Discov 6:391-403.
Jeppesen P, Turner BM (1993) The inactive X chromosome in female mammals is distinguished by a lack of histone H4 acetylation, a cytogenetic marker for gene expression. Cell 74:281-289.
Jia C, Halpern M (1996) Subclasses of vomeronasal receptor neurons: differential expression of G proteins (Gi alpha 2 and G(o alpha)) and segregated projections to the accessory olfactory bulb. Brain Res 719:117-128.
Jia C, Halpern M (1997) Segregated populations of mitral/tufted cells in the accessory olfactory bulb. Neuroreport 8:1887-1890.
Johnston PG, Cattanach BM (1981) Controlling elements in the mouse. IV. Evidence of non-random X-inactivation. Genet Res 37:151-160.
Jones EG, Hendry SH (1980) Distribution of callosal fibers around the hand representations in monkey somatic sensory cortex. Neurosci Lett 19:167-172.
Jones EG, Manger PR, Woods TM (1997) Maintenance of a somatotopic cortical map in the face of diminishing thalamocortical inputs. Proc Natl Acad Sci U S A 94:11003-11007.
Kalb RG, Hockfield S (1988) Molecular evidence for early activity-dependent development of hamster motor neurons. J Neurosci 8:2350-2360.
Kalb RG, Hockfield S (1990) Induction of a neuronal proteoglycan by the NMDA receptor in the developing spinal cord. Science 250:294-296.
Kalia LV, Pitcher GM, Pelkey KA, Salter MW (2006) PSD-95 is a negative regulator of the tyrosine kinase Src in the NMDA receptor complex. EMBO J 25:4971-4982.
Kantor DB, Chivatakarn O, Peer KL, Oster SF, Inatani M, Hansen MJ, Flanagan JG, Yamaguchi Y, Sretavan DW, Giger RJ, Kolodkin AL (2004) Semaphorin 5A is a bifunctional axon guidance cue regulated by heparan and chondroitin sulfate proteoglycans. Neuron 44:961-975.

Karlsson M, Mathers J, Dickinson RJ, Mandl M, Keyse SM (2004) Both nuclear-cytoplasmic shuttling of the dual specificity phosphatase MKP-3 and its ability to anchor MAP kinase in the cytoplasm are mediated by a conserved nuclear export signal. J Biol Chem 279:41882-41891.
Karnak D, Lee S, Margolis B (2002) Identification of multiple binding partners for the amino-terminal domain of synapse-associated protein 97. J Biol Chem 277:46730-46735.
Kasri NN, Govek EE, Van Aelst L (2008) Characterization of oligophrenin-1, a RhoGAP lost in patients affected with mental retardation: lentiviral injection in organotypic brain slice cultures. Methods Enzymol 439:255-266.
Katz LC, Crowley JC (2002) Development of cortical circuits: lessons from ocular dominance columns. Nat Rev Neurosci 3:34-42.
Kemp A, Manahan-Vaughan D (2004) Hippocampal long-term depression and long-term potentiation encode different aspects of novelty acquisition. Proc Natl Acad Sci U S A 101:8192-8197.
Kennedy H, Flandrin JM, Amblard B (1980) Afferent visual pathways and receptive field properties of superior colliculus neurons in stroboscopically reared cats. Neurosci Lett 19:283-288.
Kennedy MB (1997) The postsynaptic density at glutamatergic synapses. Trends Neurosci 20:264-268.
Killackey HP (1973) Anatomical evidence for cortical subdivisions based on vertically discrete thalamic projections from the ventral posterior nucleus to cortical barrels in the rat. Brain Res 51:326-331.
Kim E, Sheng M (2004) PDZ domain proteins of synapses. Nat Rev Neurosci 5:771-781.
Kim E, Cho KO, Rothschild A, Sheng M (1996) Heteromultimerization and NMDA receptor-clustering activity of Chapsyn-110, a member of the PSD-95 family of proteins. Neuron 17:103-113.
Kim E, Niethammer M, Rothschild A, Jan YN, Sheng M (1995) Clustering of Shaker-type K+ channels by interaction with a family of membrane-associated guanylate kinases. Nature 378:85-88.
Kim JH, Liao D, Lau LF, Huganir RL (1998) SynGAP: a synaptic RasGAP that associates with the PSD-95/SAP90 protein family. Neuron 20:683-691.
Kim JH, Lee HK, Takamiya K, Huganir RL (2003) The role of synaptic GTPase-activating protein in neuronal development and synaptic plasticity. J Neurosci 23:1119-1124.
Kind PC, Neumann PE (2001) Plasticity: downstream of glutamate. Trends Neurosci 24:553-555.
Kistner U, Garner CC, Linial M (1995) Nucleotide binding by the synapse associated protein SAP90. FEBS Lett 359:159-163.
Kistner U, Wenzel BM, Veh RW, Cases-Langhoff C, Garner AM, Appeltauer U, Voss B, Gundelfinger ED, Garner CC (1993) SAP90, a rat presynaptic protein related to the product of the Drosophila tumor suppressor gene dlg-A. J Biol Chem 268:4580-4583.
Kitagawa H, Uyama T, Sugahara K (2001) Molecular cloning and expression of a human chondroitin synthase. J Biol Chem 276:38721-38726.

Kitagawa H, Izumikawa T, Uyama T, Sugahara K (2003) Molecular cloning of a chondroitin polymerizing factor that cooperates with chondroitin synthase for chondroitin polymerization. J Biol Chem 278:23666-23671.
Kleefstra T, Yntema HG, Nillesen WM, Oudakker AR, Mullaart RA, Geerdink N, van Bokhoven H, de Vries BB, Sistermans EA, Hamel BC (2004) MECP2 analysis in mentally retarded patients: implications for routine DNA dianostics. Eur J Hum Genet 12:24-28.
Kleinschmidt A, Bear MF, Singer W (1987) Blockade of "NMDA" receptors disrupts experience-dependent plasticity of kitten striate cortex. Science 238:355-358.
Knott JC, Mahesparan R, Garcia-Cabrera I, Bolge Tysnes B, Edvardsen K, Ness GO, Mork S, Lund-Johansen M, Bjerkvig R (1998) Stimulation of extracellular matrix components in the normal brain by invading glioma cells. Int J Cancer 75:864-872.
Knudsen EI (2004) Sensitive periods in the development of the brain and behavior. J Cogn Neurosci 16:1412-1425.
Knuesel I, Elliott A, Chen HJ, Mansuy IM, Kennedy MB (2005) A role for synGAP in regulating neuronal apoptosis. Eur J Neurosci 21:611-621.
Ko J, Humbert S, Bronson RT, Takahashi S, Kulkarni AB, Li E, Tsai LH (2001) p35 and p39 are essential for cyclin-dependent kinase 5 function during neurodevelopment. J Neurosci 21:6758-6771.
Koch CA, Anderson D, Moran MF, Ellis C, Pawson T (1991) SH2 and SH3 domains: elements that control interactions of cytoplasmic signaling proteins. Science 252:668-674.
Koh YH, Popova E, Thomas U, Griffith LC, Budnik V (1999) Regulation of DLG localization at synapses by CaMKII-dependent phosphorylation. Cell 98:353-363.
Komiyama NH, Watabe AM, Carlisle HJ, Porter K, Charlesworth P, Monti J, Strathdee DJ, O'Carroll CM, Martin SJ, Morris RG, O'Dell TJ, Grant SG (2002) SynGAP regulates ERK/MAPK signaling, synaptic plasticity, and learning in the complex with postsynaptic density 95 and NMDA receptor. J Neurosci 22:9721-9732.
Konur S, Ghosh A (2005) Calcium signaling and the control of dendritic development. Neuron 46:401-405.
Kornau HC, Seeburg PH, Kennedy MB (1997) Interaction of ion channels and receptors with PDZ domain proteins. Curr Opin Neurobiol 7:368-373.
Kornau HC, Schenker LT, Kennedy MB, Seeburg PH (1995) Domain interaction between NMDA receptor subunits and the postsynaptic density protein PSD-95. Science 269:1737-1740.
Krapivinsky G, Medina I, Krapivinsky L, Gapon S, Clapham DE (2004) SynGAP-MUPP1-CaMKII synaptic complexes regulate p38 MAP kinase activity and NMDA receptor-dependent synaptic AMPA receptor potentiation. Neuron 43:563-574.
Kristiansen LV, Meador-Woodruff JH (2005) Abnormal striatal expression of transcripts encoding NMDA interacting PSD proteins in schizophrenia, bipolar disorder and major depression. Schizophr Res 78:87-93.
Krubitzer L (1995) The organization of neocortex in mammals: are species differences really so different? Trends Neurosci 18:408-417.

Kuhlendahl S, Spangenberg O, Konrad M, Kim E, Garner CC (1998) Functional analysis of the guanylate kinase-like domain in the synapse-associated protein SAP97. Eur J Biochem 252:305-313.
Kummer TT, Misgeld T, Sanes JR (2006) Assembly of the postsynaptic membrane at the neuromuscular junction: paradigm lost. Curr Opin Neurobiol 16:74-82.
Kutsuwada T, Sakimura K, Manabe T, Takayama C, Katakura N, Kushiya E, Natsume R, Watanabe M, Inoue Y, Yagi T, Aizawa S, Arakawa M, Takahashi T, Nakamura Y, Mori H, Mishina M (1996) Impairment of suckling response, trigeminal neuronal pattern formation, and hippocampal LTD in NMDA receptor epsilon 2 subunit mutant mice. Neuron 16:333-344.
Laird CD (1971) Chromatid structure: relationship between DNA content and nucleotide sequence diversity. Chromosoma 32:378-406.
Lamarche N, Hall A (1994) GAPs for rho-related GTPases. Trends Genet 10:436-440.
Lander C, Zhang H, Hockfield S (1998) Neurons produce a neuronal cell surface-associated chondroitin sulfate proteoglycan. J Neurosci 18:174-183.
Lander C, Kind P, Maleski M, Hockfield S (1997) A family of activity-dependent neuronal cell-surface chondroitin sulfate proteoglycans in cat visual cortex. J Neurosci 17:1928-1939.
Laumonnier F, Cuthbert PC, Grant SG (2007) The role of neuronal complexes in human X-linked brain diseases. Am J Hum Genet 80:205-220.
Laurent A, Goaillard JM, Cases O, Lebrand C, Gaspar P, Ropert N (2002) Activity-dependent presynaptic effect of serotonin 1B receptors on the somatosensory thalamocortical transmission in neonatal mice. J Neurosci 22:886-900.
Lee AW, Emsley JG, Brown RE, Hagg T (2003) Marked differences in olfactory sensitivity and apparent speed of forebrain neuroblast migration in three inbred strains of mice. Neuroscience 118:263-270.
Lee HK, Kameyama K, Huganir RL, Bear MF (1998) NMDA induces long-term synaptic depression and dephosphorylation of the GluR1 subunit of AMPA receptors in hippocampus. Neuron 21:1151-1162.
Lee JT, Jaenisch R (1997) Long-range cis effects of ectopic X-inactivation centres on a mouse autosome. Nature 386:275-279.
Lee LJ, Iwasato T, Itohara S, Erzurumlu RS (2005) Exuberant thalamocortical axon arborization in cortex-specific NMDAR1 knockout mice. J Comp Neurol 485:280-292.
Lein ES, Finney EM, McQuillen PS, Shatz CJ (1999) Subplate neuron ablation alters neurotrophin expression and ocular dominance column formation. Proc Natl Acad Sci U S A 96:13491-13495.
Leonard AS, Davare MA, Horne MC, Garner CC, Hell JW (1998) SAP97 is associated with the alpha-amino-3-hydroxy-5-methylisoxazole-4-propionic acid receptor GluR1 subunit. J Biol Chem 273:19518-19524.
Lerosey I, Pizon V, Tavitian A, de Gunzburg J (1991) The cAMP-dependent protein kinase phosphorylates the rap1 protein in vitro as well as in intact fibroblasts, but not the closely related rap2 protein. Biochem Biophys Res Commun 175:430-436.
Letinic K, Zoncu R, Rakic P (2002) Origin of GABAergic neurons in the human neocortex. Nature 417:645-649.

LeVay S, Stryker MP, Shatz CJ (1978) Ocular dominance columns and their development in layer IV of the cat's visual cortex: a quantitative study. J Comp Neurol 179:223-244.
LeVay S, Wiesel TN, Hubel DH (1980) The development of ocular dominance columns in normal and visually deprived monkeys. J Comp Neurol 191:1-51.
Levy WB, Steward O (1979) Synapses as associative memory elements in the hippocampal formation. Brain Res 175:233-245.
Li C, Scott DA, Hatch E, Tian X, Mansour SL (2007) Dusp6 (Mkp3) is a negative feedback regulator of FGF-stimulated ERK signaling during mouse development. Development 134:167-176.
Li W, Okano A, Tian QB, Nakayama K, Furihata T, Nawa H, Suzuki T (2001) Characterization of a novel synGAP isoform, synGAP-beta. J Biol Chem 276:21417-21424.
Li Y, Erzurumlu RS, Chen C, Jhaveri S, Tonegawa S (1994) Whisker-related neuronal patterns fail to develop in the trigeminal brainstem nuclei of NMDAR1 knockout mice. Cell 76:427-437.
Li Y, Spangenberg O, Paarmann I, Konrad M, Lavie A (2002) Structural basis for nucleotide-dependent regulation of membrane-associated guanylate kinase-like domains. J Biol Chem 277:4159-4165.
Lipton SA, Kater SB (1989) Neurotransmitter regulation of neuronal outgrowth, plasticity and survival. Trends Neurosci 12:265-270.
Lomo T (2003) The discovery of long-term potentiation. Philos Trans R Soc Lond B Biol Sci 358:617-620.
Long JF, Tochio H, Wang P, Fan JS, Sala C, Niethammer M, Sheng M, Zhang M (2003) Supramodular structure and synergistic target binding of the N-terminal tandem PDZ domains of PSD-95. J Mol Biol 327:203-214.
Lopez-Bendito G, Molnar Z (2003) Thalamocortical development: how are we going to get there? Nat Rev Neurosci 4:276-289.
Lu HC, Gonzalez E, Crair MC (2001) Barrel cortex critical period plasticity is independent of changes in NMDA receptor subunit composition. Neuron 32:619-634.
Lush ME, Li Y, Kwon CH, Chen J, Parada LF (2008) Neurofibromin is required for barrel formation in the mouse somatosensory cortex. J Neurosci 28:1580-1587.
Luskin MB (1998) Neuroblasts of the postnatal mammalian forebrain: their phenotype and fate. J Neurobiol 36:221-233.
Luskin MB, Shatz CJ (1985) Studies of the earliest generated cells of the cat's visual cortex: cogeneration of subplate and marginal zones. J Neurosci 5:1062-1075.
Luth HJ, Fischer J, Celio MR (1992) Soybean lectin binding neurons in the visual cortex of the rat contain parvalbumin and are covered by glial nets. J Neurocytol 21:211-221.
Lyon MF (1961) Gene action in the X-chromosome of the mouse (Mus musculus L.). Nature 190:372-373.
Ma PM (1993) Barrelettes--architectonic vibrissal representations in the brainstem trigeminal complex of the mouse. II. Normal post-natal development. J Comp Neurol 327:376-397.
Ma PM, Woolsey TA (1984) Cytoarchitectonic correlates of the vibrissae in the medullary trigeminal complex of the mouse. Brain Res 306:374-379.

Maffei L, Berardi N, Domenici L, Parisi V, Pizzorusso T (1992) Nerve growth factor (NGF) prevents the shift in ocular dominance distribution of visual cortical neurons in monocularly deprived rats. J Neurosci 12:4651-4662.
Maier DL, McCasland JS (1997) Calcium-binding protein phenotype defines metabolically distinct groups of neurons in barrel cortex of behaving hamsters. Exp Neurol 145:71-80.
Maier DL, Grieb GM, Stelzner DJ, McCasland JS (2003) Large-scale plasticity in barrel cortex following repeated whisker trimming in young adult hamsters. Exp Neurol 184:737-745.
Makino K, Kuwahara H, Masuko N, Nishiyama Y, Morisaki T, Sasaki J, Nakao M, Kuwano A, Nakata M, Ushio Y, Saya H (1997) Cloning and characterization of NE-dlg: a novel human homolog of the Drosophila discs large (dlg) tumor suppressor protein interacts with the APC protein. Oncogene 14:2425-2433.
Maleski M, Hockfield S (1997) Glial cells assemble hyaluronan-based pericellular matrices in vitro. Glia 20:193-202.
Malinow R, Schulman H, Tsien RW (1989) Inhibition of postsynaptic PKC or CaMKII blocks induction but not expression of LTP. Science 245:862-866.
Manahan-Vaughan D, Braunewell KH (1999) Novelty acquisition is associated with induction of hippocampal long-term depression. Proc Natl Acad Sci U S A 96:8739-8744.
Manuel M, Price DJ (2005) Role of Pax6 in forebrain regionalization. Brain Res Bull 66:387-393.
Manuel M, Georgala PA, Carr CB, Chanas S, Kleinjan DA, Martynoga B, Mason JO, Molinek M, Pinson J, Pratt T, Quinn JC, Simpson TI, Tyas DA, van Heyningen V, West JD, Price DJ (2007) Controlled overexpression of Pax6 in vivo negatively autoregulates the Pax6 locus, causing cell-autonomous defects of late cortical progenitor proliferation with little effect on cortical arealization. Development 134:545-555.
Marin O, Rubenstein JL (2001) A long, remarkable journey: tangential migration in the telencephalon. Nat Rev Neurosci 2:780-790.
Marshall CA, Suzuki SO, Goldman JE (2003) Gliogenic and neurogenic progenitors of the subventricular zone: who are they, where did they come from, and where are they going? Glia 43:52-61.
Marui T, Hashimoto O, Nanba E, Kato C, Tochigi M, Umekage T, Ishijima M, Kohda K, Kato N, Sasaki T (2004) Association between the neurofibromatosis-1 (NF1) locus and autism in the Japanese population. Am J Med Genet B Neuropsychiatr Genet 131B:43-47.
Mattei MG, Mattei JF, Vidal I, Giraud F (1981) Structural anomalies of the X chromosome and inactivation center. Hum Genet 56:401-408.
Matthews RT, Kelly GM, Zerillo CA, Gray G, Tiemeyer M, Hockfield S (2002) Aggrecan glycoforms contribute to the molecular heterogeneity of perineuronal nets. J Neurosci 22:7536-7547.
Maurel P, Rauch U, Flad M, Margolis RK, Margolis RU (1994) Phosphacan, a chondroitin sulfate proteoglycan of brain that interacts with neurons and neural cell-adhesion molecules, is an extracellular variant of a receptor-type protein tyrosine phosphatase. Proc Natl Acad Sci U S A 91:2512-2516.
Mayer BJ, Eck MJ (1995) SH3 domains. Minding your p's and q's. Curr Biol 5:364-367.

Mazoyer S, Gayther SA, Nagai MA, Smith SA, Dunning A, van Rensburg EJ, Albertsen H, White R, Ponder BA (1995) A gene (DLG2) located at 17q12-q21 encodes a new homologue of the Drosophila tumor suppressor dIg-A. Genomics 28:25-31.
Mbarek O, Marouillat S, Martineau J, Barthelemy C, Muh JP, Andres C (1999) Association study of the NF1 gene and autistic disorder. Am J Med Genet 88:729-732.
McAllister AK (1999) Subplate neurons: a missing link among neurotrophins, activity, and ocular dominance plasticity? Proc Natl Acad Sci U S A 96:13600-13602.
McCall MA, Gregg RG, Behringer RR, Brenner M, Delaney CL, Galbreath EJ, Zhang CL, Pearce RA, Chiu SY, Messing A (1996) Targeted deletion in astrocyte intermediate filament (Gfap) alters neuronal physiology. Proc Natl Acad Sci U S A 93:6361-6366.
McCullumsmith RE, Kristiansen LV, Beneyto M, Scarr E, Dean B, Meador-Woodruff JH (2007) Decreased NR1, NR2A, and SAP102 transcript expression in the hippocampus in bipolar disorder. Brain Res 1127:108-118.
McGee AW, Topinka JR, Hashimoto K, Petralia RS, Kakizawa S, Kauer FW, Aguilera-Moreno A, Wenthold RJ, Kano M, Bredt DS (2001) PSD-93 knock-out mice reveal that neuronal MAGUKs are not required for development or function of parallel fiber synapses in cerebellum. J Neurosci 21:3085-3091.
McKay RD, Hockfield SJ (1982) Monoclonal antibodies distinguish antigenically discrete neuronal types in the vertebrate central nervous system. Proc Natl Acad Sci U S A 79:6747-6751.
McLaughlin T, O'Leary DD (2005) Molecular gradients and development of retinotopic maps. Annu Rev Neurosci 28:327-355.
McLaughlin T, Torborg CL, Feller MB, O'Leary DD (2003) Retinotopic map refinement requires spontaneous retinal waves during a brief critical period of development. Neuron 40:1147-1160.
McRae PA, Rocco MM, Kelly G, Brumberg JC, Matthews RT (2007) Sensory deprivation alters aggrecan and perineuronal net expression in the mouse barrel cortex. J Neurosci 27:5405-5413.
Meador-Woodruff JH, Clinton SM, Beneyto M, McCullumsmith RE (2003) Molecular abnormalities of the glutamate synapse in the thalamus in schizophrenia. Ann N Y Acad Sci 1003:75-93.
Meister M, Wong RO, Baylor DA, Shatz CJ (1991) Synchronous bursts of action potentials in ganglion cells of the developing mammalian retina. Science 252:939-943.
Meyer G, Soria JM, Martinez-Galan JR, Martin-Clemente B, Fairen A (1998) Different origins and developmental histories of transient neurons in the marginal zone of the fetal and neonatal rat cortex. J Comp Neurol 397:493-518.
Meyer G, Varoqueaux F, Neeb A, Oschiles M, Brose N (2004) The complexity of PDZ-domain-mediated interactions at glutamateric synapses: a case study on neuroligin. Neurophrmacoloy 47:724-733.
Migaud M, Charlesworth P, Dempster M, Webster LC, Watabe AM, Makhinson M, He Y, Ramsay MF, Morris RG, Morrison JH, O'Dell TJ, Grant SG (1998)

Enhanced long-term potentiation and impaired learning in mice with mutant postsynaptic density-95 protein. Nature 396:433-439.
Milev P, Maurel P, Chiba A, Mevissen M, Popp S, Yamaguchi Y, Margolis RK, Margolis RU (1998) Differential regulation of expression of hyaluronan-binding proteoglycans in developing brain: aggrecan, versican, neurocan, and brevican. Biochem Biophys Res Commun 247:207-212.
Miller B, Blake NM, Erinjeri JP, Reistad CE, Sexton T, Admire P, Woolsey TA (2001) Postnatal growth of intrinsic connections in mouse barrel cortex. J Comp Neurol 436:17-31.
Miller KD, Keller JB, Stryker MP (1989) Ocular dominance column development: analysis and simulation. Science 245:605-615.
Miller MW (1995) Relationship of the time of origin and death of neurons in rat somatosensory cortex: barrel versus septal cortex and projection versus local circuit neurons. J Comp Neurol 355:6-14.
Mitrovic N, Mohajeri H, Schachner M (1996) Effects of NMDA receptor blockade in the developing rat somatosensory cortex on the expression of the glia-derived extracellular matrix glycoprotein tenascin-C. Eur J Neurosci 8:1793-1802.
Miyata S, Nishimura Y, Hayashi N, Oohira A (2005) Construction of perineuronal net-like structure by cortical neurons in culture. Neuroscience 136:95-104.
Molnar Z, Blakemore C (1991) Lack of regional specificity for connections formed between thalamus and cortex in coculture. Nature 351:475-477.
Molnar Z, Higashi S, Lopez-Bendito G (2003) Choreography of early thalamocortical development. Cereb Cortex 13:661-669.
Molnar Z, Lopez-Bendito G, Small J, Partridge LD, Blakemore C, Wilson MC (2002) Normal development of embryonic thalamocortical connectivity in the absence of evoked synaptic activity. J Neurosci 22:10313-10323.
Monk M, Harper MI (1979) Sequential X chromosome inactivation coupled with cellular differentiation in early mouse embryos. Nature 281:311-313.
Moon LD, Asher RA, Rhodes KE, Fawcett JW (2001) Regeneration of CNS axons back to their target following treatment of adult rat brain with chondroitinase ABC. Nat Neurosci 4:465-466.
Moon SY, Zang H, Zheng Y (2003) Characterization of a brain-specific Rho GTPase-activating protein, p200RhoGAP. J Biol Chem 278:4151-4159.
Morales B, Choi SY, Kirkwood A (2002) Dark rearing alters the development of GABAergic transmission in visual cortex. J Neurosci 22:8084-8090.
Morris RG, Anderson E, Lynch GS, Baudry M (1986) Selective impairment of learning and blockade of long-term potentiation by an N-methyl-D-aspartate receptor antagonist, AP5. Nature 319:774-776.
Mourey RJ, Vega QC, Campbell JS, Wenderoth MP, Hauschka SD, Krebs EG, Dixon JE (1996) A novel cytoplasmic dual specificity protein tyrosine phosphatase implicated in muscle and neuronal differentiation. J Biol Chem 271:3795-3802.
Mower GD (1991) The effect of dark rearing on the time course of the critical period in cat visual cortex. Brain Res Dev Brain Res 58:151-158.
Muda M, Theodosiou A, Rodrigues N, Boschert U, Camps M, Gillieron C, Davies K, Ashworth A, Arkinstall S (1996) The dual specificity phosphatases M3/6 and MKP-3 are highly selective for inactivation of distinct mitogen-activated protein kinases. J Biol Chem 271:27205-27208.

Muda M, Theodosiou A, Gillieron C, Smith A, Chabert C, Camps M, Boschert U, Rodrigues N, Davies K, Ashworth A, Arkinstall S (1998) The mitogen-activated protein kinase phosphatase-3 N-terminal noncatalytic region is responsible for tight substrate binding and enzymatic specificity. J Biol Chem 273:9323-9329.
Muller BM, Kistner U, Veh RW, Cases-Langhoff C, Becker B, Gundelfinger ED, Garner CC (1995) Molecular characterization and spatial distribution of SAP97, a novel presynaptic protein homologous to SAP90 and the Drosophila discs-large tumor suppressor protein. J Neurosci 15:2354-2366.
Munger BL, Ide C (1988) The structure and function of cutaneous sensory receptors. Arch Histol Cytol 51:1-34.
Muzio L, DiBenedetto B, Stoykova A, Boncinelli E, Gruss P, Mallamaci A (2002) Emx2 and Pax6 control regionalization of the pre-neuronogenic cortical primordium. Cereb Cortex 12:129-139.
Nakagawa F, Schulte BA, Spicer SS (1986) Selective cytochemical demonstration of glycoconjugate-containing terminal N-acetylgalactosamine on some brain neurons. J Comp Neurol 243:280-290.
Nakamura T, Komiya M, Sone K, Hirose E, Gotoh N, Morii H, Ohta Y, Mori N (2002) Grit, a GTPase-activating protein for the Rho family, regulates neurite extension through association with the TrkA receptor and N-Shc and CrkL/Crk adapter molecules. Mol Cell Biol 22:8721-8734.
Nakazawa T, Kuriu T, Tezuka T, Umemori H, Okabe S, Yamamoto T (2008) Regulation of dendritic spine morphology by an NMDA receptor-associated Rho GTPase-activating protein, p250GAP. J Neurochem 105:1384-1393.
Nakazawa T, Watabe AM, Tezuka T, Yoshida Y, Yokoyama K, Umemori H, Inoue A, Okabe S, Manabe T, Yamamoto T (2003) p250GAP, a novel brain-enriched GTPase-activating protein for Rho family GTPases, is involved in the N-methyl-d-aspartate receptor signaling. Mol Biol Cell 14:2921-2934.
Nance WE (1964) Genetic Tests with a Sex-Linked Marker: Glucose-6-Phosphate Dehydrogenase. Cold Spring Harb Symp Quant Biol 29:415-425.
Naumova AK, Plenge RM, Bird LM, Leppert M, Morgan K, Willard HF, Sapienza C (1996) Heritability of X chromosome--inactivation phenotype in a large family. Am J Hum Genet 58:1111-1119.
Nazarian J, Bouri K, Hoffman EP (2005) Intracellular expression profiling by laser capture microdissection: three novel components of the neuromuscular junction. Physiol Genomics 21:70-80.
Newey SE, Velamoor V, Govek EE, Van Aelst L (2005) Rho GTPases, dendritic structure, and mental retardation. J Neurobiol 64:58-74.
Nicholson C, Sykova E (1998) Extracellular space structure revealed by diffusion analysis. Trends Neurosci 21:207-215.
Niethammer M, Kim E, Sheng M (1996) Interaction between the C terminus of NMDA receptor subunits and multiple members of the PSD-95 family of membrane-associated guanylate kinases. J Neurosci 16:2157-2163.
Nieto M, Schuurmans C, Britz O, Guillemot F (2001) Neural bHLH genes control the neuronal versus glial fate decision in cortical progenitors. Neuron 29:401-413.

Norris DP, Patel D, Kay GF, Penny GD, Brockdorff N, Sheardown SA, Rastan S (1994) Evidence that random and imprinted Xist expression is controlled by preemptive methylation. Cell 77:41-51.
Novak U, Kaye AH (2000) Extracellular matrix and the brain: components and function. J Clin Neurosci 7:280-290.
O'Brien RJ, Lau LF, Huganir RL (1998) Molecular mechanisms of glutamate receptor clustering at excitatory synapses. Curr Opin Neurobiol 8:364-369.
O'Donovan MJ (1999) The origin of spontaneous activity in developing networks of the vertebrate nervous system. Curr Opin Neurobiol 9:94-104.
O'Leary DD (1989) Do cortical areas emerge from a protocortex? Trends Neurosci 12:400-406.
Oh JS, Manzerra P, Kennedy MB (2004) Regulation of the neuron-specific Ras GTPase-activating protein, synGAP, by Ca2+/calmodulin-dependent protein kinase II. J Biol Chem 279:17980-17988.
Okabe T, Nakamura T, Nishimura YN, Kohu K, Ohwada S, Morishita Y, Akiyama T (2003) RICS, a novel GTPase-activating protein for Cdc42 and Rac1, is involved in the beta-catenin-N-cadherin and N-methyl-D-aspartate receptor signaling. J Biol Chem 278:9920-9927.
Okamoto M, Mori S, Ichimura M, Endo H (1994) Chondroitin sulfate proteoglycans protect cultured rat's cortical and hippocampal neurons from delayed cell death induced by excitatory amino acids. Neurosci Lett 172:51-54.
Olsen O, Bredt DS (2003) Functional analysis of the nucleotide binding domain of membrane-associated guanylate kinases. J Biol Chem 278:6873-6878.
Otaki JM, Firestein S (1999) Neurestin: putative transmembrane molecule implicated in neuronal development. Dev Biol 212:165-181.
Owen EH, Logue SF, Rasmussen DL, Wehner JM (1997) Assessment of learning by the Morris water task and fear conditioning in inbred mouse strains and F1 hybrids: implications of genetic background for single gene mutations and quantitative trait loci analyses. Neuroscience 80:1087-1099.
Parker MJ, Zhao S, Bredt DS, Sanes JR, Feng G (2004) PSD93 regulates synaptic stability at neuronal cholinergic synapses. J Neurosci 24:378-388.
Parnavelas JG, Nadarajah B (2001) Radial glial cells. are they really glia? Neuron 31:881-884.
Pavlov I, Lauri S, Taira T, Rauvala H (2004) The role of ECM molecules in activity-dependent synaptic development and plasticity. Birth Defects Res C Embryo Today 72:12-24.
Pearlman AL, Sheppard AM (1996) Extracellular matrix in early cortical development. Prog Brain Res 108:117-134.
Penagarikano O, Mulle JG, Warren ST (2007) The pathophysiology of fragile x syndrome. Annu Rev Genomics Hum Genet 8:109-129.
Penn AA, Riquelme PA, Feller MB, Shatz CJ (1998) Competition in retinogeniculate patterning driven by spontaneous activity. Science 279:2108-2112.
Penny GD, Kay GF, Sheardown SA, Rastan S, Brockdorff N (1996) Requirement for Xist in X chromosome inactivation. Nature 379:131-137.
Persico AM, Baldi A, Dell'Acqua ML, Moessner R, Murphy DL, Lesch KP, Keller F (2003) Reduced programmed cell death in brains of serotonin transporter knockout mice. Neuroreport 14:341-344.

Persico AM, Mengual E, Moessner R, Hall FS, Revay RS, Sora I, Arellano J, DeFelipe J, Gimenez-Amaya JM, Conciatori M, Marino R, Baldi A, Cabib S, Pascucci T, Uhl GR, Murphy DL, Lesch KP, Keller F (2001) Barrel pattern formation requires serotonin uptake by thalamocortical afferents, and not vesicular monoamine release. J Neurosci 21:6862-6873.
Piserchio A, Salinas GD, Li T, Marshall J, Spaller MR, Mierke DF (2004) Targeting specific PDZ domains of PSD-95; structural basis for enhanced affinity and enzymatic stability of a cyclic peptide. Chem Biol 11:469-473.
Pizzorusso T, Medini P, Berardi N, Chierzi S, Fawcett JW, Maffei L (2002) Reactivation of ocular dominance plasticity in the adult visual cortex. Science 298:1248-1251.
Plenge RM, Tranebjaerg L, Jensen PK, Schwartz C, Willard HF (1999) Evidence that mutations in the X-linked DDP gene cause incompletely penetrant and variable skewed X inactivation. Am J Hum Genet 64:759-767.
Plenge RM, Hendrich BD, Schwartz C, Arena JF, Naumova A, Sapienza C, Winter RM, Willard HF (1997) A promoter mutation in the XIST gene in two unrelated families with skewed X-chromosome inactivation. Nat Genet 17:353-356.
Ponting CP, Phillips C, Davies KE, Blake DJ (1997) PDZ domains: targeting signalling molecules to sub-membranous sites. Bioessays 19:469-479.
Popp S, Andersen JS, Maurel P, Margolis RU (2003) Localization of aggrecan and versican in the developing rat central nervous system. Dev Dyn 227:143-149.
Porter K, Komiyama NH, Vitalis T, Kind PC, Grant SG (2005) Differential expression of two NMDA receptor interacting proteins, PSD-95 and SynGAP during mouse development. Eur J Neurosci 21:351-362.
Pourcho RG, Qin P, Goebel DJ (2001) Cellular and subcellular distribution of NMDA receptor subunit NR2B in the retina. J Comp Neurol 433:75-85.
Pratt T, Conway CD, Tian NM, Price DJ, Mason JO (2006) Herapan sulphation patterns generated by specific heparan sulfotransferase enzymes direct distinct aspects of retinal axon guidance at the optic chiasm. J Neurosci 28:6911-6923.
Price J (1995) Neural development. Brain stems. Curr Biol 5:232-234.
Privat A (1975) Postnatal gliogenesis in the mammalian brain. Int Rev Cytol 40:281-323.
Prusky GT, Ramoa AS (1999) Novel method of chronically blocking retinal activity. J Neurosci Methods 87:105-110.
Prydz K, Dalen KT (2000) Synthesis and sorting of proteoglycans. J Cell Sci 113 Pt 2:193-205.
Puck JM, Willard HF (1998) X inactivation in females with X-linked disease. N Engl J Med 338:325-328.
Qian X, Shen Q, Goderie SK, He W, Capela A, Davis AA, Temple S (2000) Timing of CNS cell generation: a programmed sequence of neuron and glial cell production from isolated murine cortical stem cells. Neuron 28:69-80.
Quairiaux C, Armstrong-James M, Welker E (2007) Modified sensory processing in the barrel cortex of the adult mouse after chronic whisker stimulation. J Neurophysiol 97:2130-2147.
Raedler E, Raedler A (1978) Autoradiographic study of early neurogenesis in rat neocortex. Anat Embryol (Berl) 154:267-284.

Rakic P, Hashimoto-Torii K, Sarkisian MR (2007) Genetic determinants of neuronal migration in the cerebral cortex. Novartis Found Symp 288:45-53; discussion 53-48, 96-48.
Rambourg A, Neutra M, Leblond CP (1966) Presence of a "cell coat" rich in carbohydrate at the surface of cells in the rat. Anat Rec 154:41-71.
Rastan S, Robertson EJ (1985) X-chromosome deletions in embryo-derived (EK) cell lines associated with lack of X-chromosome inactivation. J Embryol Exp Morphol 90:379-388.
Rebsam A, Seif I, Gaspar P (2002) Refinement of thalamocortical arbors and emergence of barrel domains in the primary somatosensory cortex: a study of normal and monoamine oxidase a knock-out mice. J Neurosci 22:8541-8552.
Reese BE (1988) 'Hidden lamination' in the dorsal lateral geniculate nucleus: the functional organization of this thalamic region in the rat. Brain Res 472:119-137.
Reese ML, Dakoji S, Bredt DS, Dotsch V (2007) The guanylate kinase domain of the MAGUK PSD-95 binds dynamically to a conserved motif in MAP1a. Nat Struct Mol Biol 14:155-163.
Reid CB, Liang I, Walsh C (1995) Systematic widespread clonal organization in cerebral cortex. Neuron 15:299-310.
Reuther GW, Der CJ (2000) The Ras branch of small GTPases: Ras family members don't fall far from the tree. Curr Opin Cell Biol 12:157-165.
Rice FL, Van der Loos H (1977) Development of the barrels and barrel field in the somatosensory cortex of the mouse. J Comp Neurol 171:545-560.
Rickmann M, Chronwall BM, Wolff JR (1977) On the development of non-pyramidal neurons and axons outside the cortical plate: the early marginal zone as a pallial anlage. Anat Embryol (Berl) 151:285-307.
Rizvi TA, Akunuru S, de Courten-Myers G, Switzer RC, 3rd, Nordlund ML, Ratner N (1999) Region-specific astrogliosis in brains of mice heterozygous for mutations in the neurofibromatosis type 1 (Nf1) tumor suppressor. Brain Res 816:111-123.
Ropers HH (2006) X-linked mental retardation: many genes for a complex disorder. Curr Opin Genet Dev 16:260-269.
Ropers HH, Hamel BC (2005) X-linked mental retardation. Nat Rev Genet 6:46-57.
Ropers HH, Hoeltzenbein M, Kalscheuer V, Yntema H, Hamel B, Fryns JP, Chelly J, Partington M, Gecz J, Moraine C (2003) Nonsyndromic X-linked mental retardation: where are the missing mutations? Trends Genet 19:316-320.
Ross MT et al. (2005) The DNA sequence of the human X chromosome. Nature 434:325-337.
Ross SE, Greenberg ME, Stiles CD (2003) Basic helix-loop-helix factors in cortical development. Neuron 39:13-25.
Rossi FM, Pizzorusso T, Porciatti V, Marubio LM, Maffei L, Changeux JP (2001) Requirement of the nicotinic acetylcholine receptor beta 2 subunit for the anatomical and functional development of the visual system. Proc Natl Acad Sci U S A 98:6453-6458.
Ruegg MA (2001) Molecules involved in the formation of synaptic connections in muscle and brain. Matrix Biol 20:3-12.

Rumbaugh G, Sia GM, Garner CC, Huganir RL (2003) Synapse-associated protein-97 isoform-specific regulation of surface AMPA receptors and synaptic function in cultured neurons. J Neurosci 23:4567-4576.
Rumbaugh G, Adams JP, Kim JH, Huganir RL (2006) SynGAP regulates synaptic strength and mitogen-activated protein kinases in cultured neurons. Proc Natl Acad Sci U S A 103:4344-4351.
Russwurm M, Wittau N, Koesling D (2001) Guanylyl cyclase/PSD-95 interaction: targeting of the nitric oxide-sensitive alpha2beta1 guanylyl cyclase to synaptic membranes. J Biol Chem 276:44647-44652.
Sala R, Viegi A, Rossi FM, Pizzorusso T, Bonanno G, Raiteri M, Maffei L (1998) Nerve growth factor and brain-derived neurotrophic factor increase neurotransmitter release in the rat visual cortex. Eur J Neurosci 10:2185-2191.
Salichon N, Gaspar P, Upton AL, Picaud S, Hanoun N, Hamon M, De Maeyer E, Murphy DL, Mossner R, Lesch KP, Hen R, Seif I (2001) Excessive activation of serotonin (5-HT) 1B receptors disrupts the formation of sensory maps in monoamine oxidase a and 5-ht transporter knock-out mice. J Neurosci 21:884-896.
Sanes JR, Lichtman JW (1999) Development of the vertebrate neuromuscular junction. Annu Rev Neurosci 22:389-442.
Sanes JR, Lichtman JW (2001) Induction, assembly, maturation and maintenance of a postsynaptic apparatus. Nat Rev Neurosci 2:791-805.
Sans N, Petralia RS, Wang YX, Blahos J, 2nd, Hell JW, Wenthold RJ (2000) A developmental change in NMDA receptor-associated proteins at hippocampal synapses. J Neurosci 20:1260-1271.
Sans N, Racca C, Petralia RS, Wang YX, McCallum J, Wenthold RJ (2001) Synapse-associated protein 97 selectively associates with a subset of AMPA receptors early in their biosynthetic pathway. J Neurosci 21:7506-7516.
Sans N, Prybylowski K, Petralia RS, Chang K, Wang YX, Racca C, Vicini S, Wenthold RJ (2003) NMDA receptor trafficking through an interaction between PDZ proteins and the exocyst complex. Nat Cell Biol 5:520-530.
Sawtell NB, Frenkel MY, Philpot BD, Nakazawa K, Tonegawa S, Bear MF (2003) NMDA receptor-dependent ocular dominance plasticity in adult visual cortex. Neuron 38:977-985.
Schlaggar BL, O'Leary DD (1994) Early development of the somatotopic map and barrel patterning in rat somatosensory cortex. J Comp Neurol 346:80-96.
Schlaggar BL, Fox K, O'Leary DD (1993) Postsynaptic control of plasticity in developing somatosensory cortex. Nature 364:623-626.
Sefton AJ, Dreher B, Lim WL (1991) Interactions between callosal, thalamic and associational projections to the visual cortex of the developing rat. Exp Brain Res 84:142-158.
Seidenbecher CI, Smalla KH, Fischer N, Gundelfinger ED, Kreutz MR (2002) Brevican isoforms associate with neural membranes. J Neurochem 83:738-746.
Senft SL, Woolsey TA (1991) Growth of thalamic afferents into mouse barrel cortex. Cereb Cortex 1:308-335.
Sengpiel F, Kind PC (2002) The role of activity in development of the visual system. Curr Biol 12:R818-826.

Sengpiel F, Stawinski P, Bonhoeffer T (1999) Influence of experience on orientation maps in cat visual cortex. Nat Neurosci 2:727-732.
Shah RD, Crair MC (2008) Retinocollicular synapse maturation and plasticity are regulated by correlated retinal waves. J Neurosci 28:292-303.
Shatz CJ (1996) Emergence of order in visual system development. Proc Natl Acad Sci U S A 93:602-608.
Shatz CJ, Stryker MP (1978) Ocular dominance in layer IV of the cat's visual cortex and the effects of monocular deprivation. J Physiol 281:267-283.
Shatz CJ, Stryker MP (1988) Prenatal tetrodotoxin infusion blocks segregation of retinogeniculate afferents. Science 242:87-89.
Sheng M (1996) PDZs and receptor/channel clustering: rounding up the latest suspects. Neuron 17:575-578.
Sheng M, Kim E (1996) Ion channel associated proteins. Curr Opin Neurobiol 6:602-608.
Shi J, Aamodt SM, Constantine-Paton M (1997) Temporal correlations between functional and molecular changes in NMDA receptors and GABA neurotransmission in the superior colliculus. J Neurosci 17:6264-6276.
Shimogori T, Grove EA (2005) Fibroblast growth factor 8 regulates neocortical guidance of area-specific thalamic innervation. J Neurosci 25:6550-6560.
Shulz DE, Ego-Stengel V, Ahissar E (2003) Acetylcholine-dependent potentiation of temporal frequency representation in the barrel cortex does not depend on response magnitude during conditioning. J Physiol Paris 97:431-439.
Sidman RL, Rakic P (1973) Neuronal migration, with special reference to developing human brain: a review. Brain Res 62:1-35.
Sieghart W (1995) Structure and pharmacology of gamma-aminobutyric acidA receptor subtypes. Pharmacol Rev 47:181-234.
Silbert JE, Sugumaran G (2002) Biosynthesis of chondroitin/dermatan sulfate. IUBMB Life 54:177-186.
Silva AJ, Paylor R, Wehner JM, Tonegawa S (1992a) Impaired spatial learning in alpha-calcium-calmodulin kinase II mutant mice. Science 257:206-211.
Silva AJ, Stevens CF, Tonegawa S, Wang Y (1992b) Deficient hippocampal long-term potentiation in alpha-calcium-calmodulin kinase II mutant mice. Science 257:201-206.
Simon DK, Prusky GT, O'Leary DD, Constantine-Paton M (1992) N-methyl-D-aspartate receptor antagonists disrupt the formation of a mammalian neural map. Proc Natl Acad Sci U S A 89:10593-10597.
Simons DJ, Land PW (1987) Early experience of tactile stimulation influences organization of somatic sensory cortex. Nature 326:694-697.
Skuse DH (2005) X-linked genes and mental functioning. Hum Mol Genet 14 Spec No 1:R27-32.
Sobel RA, Ahmed AS (2001) White matter extracellular matrix chondroitin sulfate/dermatan sulfate proteoglycans in multiple sclerosis. J Neuropathol Exp Neurol 60:1198-1207.
Songyang Z, Fanning AS, Fu C, Xu J, Marfatia SM, Chishti AH, Crompton A, Chan AC, Anderson JM, Cantley LC (1997) Recognition of unique carboxyl-terminal motifs by distinct PDZ domains. Science 275:73-77.
Sprengel R, Suchanek B, Amico C, Brusa R, Burnashev N, Rozov A, Hvalby O, Jensen V, Paulsen O, Andersen P, Kim JJ, Thompson RF, Sun W, Webster

LC, Grant SG, Eilers J, Konnerth A, Li J, McNamara JO, Seeburg PH (1998) Importance of the intracellular domain of NR2 subunits for NMDA receptor function in vivo. Cell 92:279-289.
Stacy RC, Demas J, Burgess RW, Sanes JR, Wong RO (2005) Disruption and recovery of patterned retinal activity in the absence of acetylcholine. J Neurosci 25:9347-9357.
Stallcup WB (2002) The NG2 proteoglycan: past insights and future prospects. J Neurocytol 31:423-435.
Stanford LE, Cuthbert PC, Grant SG (2005) In: Neuroscience. Washington DC.
Steffen H, Van der Loos H (1980) Early lesions of mouse vibrissal follicles:: their influence on dendrite orientation in the cortical barrelfield. Exp Brain Res 40:419-431.
Stein V, House DR, Bredt DS, Nicoll RA (2003) Postsynaptic density-95 mimics and occludes hippocampal long-term potentiation and enhances long-term depression. J Neurosci 23:5503-5506.
Stellwagen D, Shatz CJ, Feller MB (1999) Dynamics of retinal waves are controlled by cyclic AMP. Neuron 24:673-685.
Stephenson FA (2006) Structure and trafficking of NMDA and GABAA receptors. Biochem Soc Trans 34:877-881.
Stevenson RE, Schwartz CE (2002) Clinical and molecular contributions to the understanding of X-linked mental retardation. Cytogenet Genome Res 99:265-275.
Stewart GR, Pearlman AL (1987) Fibronectin-like immunoreactivity in the developing cerebral cortex. J Neurosci 7:3325-3333.
Streit WJ, Schulte BA, Balentine JD, Spicer SS (1986) Evidence for glycoconjugate in nociceptive primary sensory neurons and its origin from the Golgi complex. Brain Res 377:1-17.
Stryker MP, Harris WA (1986) Binocular impulse blockade prevents the formation of ocular dominance columns in cat visual cortex. J Neurosci 6:2117-2133.
Summitt RL, Tipton RE, Wilroy RS, Jr., Martens PR, Phelan JP (1978) X-autosome translocations: a review. Birth Defects Orig Artic Ser 14:219-247.
Sur M, Frost DO, Hockfield S (1988) Expression of a surface-associated antigen on Y-cells in the cat lateral geniculate nucleus is regulated by visual experience. J Neurosci 8:874-882.
Sur M, Pallas SL, Roe AW (1990) Cross-modal plasticity in cortical development: differentiation and specification of sensory neocortex. Trends Neurosci 13:227-233.
Svare B, Broida J (1982) Genotypic influences on infanticide in mice: environmental, situational and experiential determinants. Physiol Behav 28:171-175.
Svare B, Kinsley CH, Mann MA, Broida J (1984) Infanticide: accounting for genetic variation in mice. Physiol Behav 33:137-152.
Sweatt JD (2001a) The neuronal MAP kinase cascade: a biochemical signal integration system subserving synaptic plasticity and memory. J Neurochem 76:1-10.
Sweatt JD (2001b) Memory mechanisms: the yin and yang of protein phosphorylation. Curr Biol 11:R391-394.

Tada T, Sheng M (2006) Molecular mechanisms of dendritic spine morphogenesis. Curr Opin Neurobiol 16:95-101.
Takahashi N, Miner LL, Sora I, Ujike H, Revay RS, Kostic V, Jackson-Lewis V, Przedborski S, Uhl GR (1997) VMAT2 knockout mice: heterozygotes display reduced amphetamine-conditioned reward, enhanced amphetamine locomotion, and enhanced MPTP toxicity. Proc Natl Acad Sci U S A 94:9938-9943.
Takamura H, Ichisaka S, Hayashi C, Maki H, Hata Y (2007) Monocular deprivation enhances the nuclear signalling of extracellular signal-regulated kinase in the developing visual cortex. Eur J Neurosci 26:2884-2898.
Tan SS, Breen S (1993) Radial mosaicism and tangential cell dispersion both contribute to mouse neocortical development. Nature 362:638-640.
Tan SS, Williams EA, Tam PP (1993) X-chromosome inactivation occurs at different times in different tissues of the post-implantation mouse embryo. Nat Genet 3:170-174.
Tarpey P et al. (2004) Mutations in the DLG3 gene cause nonsyndromic X-linked mental retardation. Am J Hum Genet 75:318-324.
Taylor JH (1960) Nucleic acid synthesis in relation to the cell division cycle. Ann N Y Acad Sci 90:409-421.
Tekki-Kessaris N, Woodruff R, Hall AC, Gaffield W, Kimura S, Stiles CD, Rowitch DH, Richardson WD (2001) Hedgehog-dependent oligodendrocyte lineage specification in the telencephalon. Development 128:2545-2554.
Temple S (2001) The development of neural stem cells. Nature 414:112-117.
Thomas JL, Spassky N, Perez Villegas EM, Olivier C, Cobos I, Goujet-Zalc C, Martinez S, Zalc B (2000) Spatiotemporal development of oligodendrocytes in the embryonic brain. J Neurosci Res 59:471-476.
Tian N, Copenhagen DR (2003) Visual stimulation is required for refinement of ON and OFF pathways in postnatal retina. Neuron 39:85-96.
Tian N, Petersen C, Kash S, Baekkeskov S, Copenhagen D, Nicoll R (1999) The role of the synthetic enzyme GAD65 in the control of neuronal gamma-aminobutyric acid release. Proc Natl Acad Sci U S A 96:12911-12916.
Tokita Y, Bessho Y, Masu M, Nakamura K, Nakao K, Katsuki M, Nakanishi S (1996) Characterization of excitatory amino acid neurotoxicity in N-methyl-D-aspartate receptor-deficient mouse cortical neuronal cells. Eur J Neurosci 8:69-78.
Torborg CL, Feller MB (2005) Spontaneous patterned retinal activity and the refinement of retinal projections. Prog Neurobiol 76:213-235.
Torrey EF, Barci BM, Webster MJ, Bartko JJ, Meador-Woodruff JH, Knable MB (2005) Neurochemical markers for schizophrenia, bipolar disorder, and major depression in postmortem brains. Biol Psychiatry 57:252-260.
Townsend M, Yoshii A, Mishina M, Constantine-Paton M (2003) Developmental loss of miniature N-methyl-D-aspartate receptor currents in NR2A knockout mice. Proc Natl Acad Sci U S A 100:1340-1345.
Tsien JZ, Huerta PT, Tonegawa S (1996) The essential role of hippocampal CA1 NMDA receptor-dependent synaptic plasticity in spatial memory. Cell 87:1327-1338.
Upton AL, Salichon N, Lebrand C, Ravary A, Blakely R, Seif I, Gaspar P (1999) Excess of serotonin (5-HT) alters the segregation of ispilateral and

contralateral retinal projections in monoamine oxidase A knock-out mice: possible role of 5-HT uptake in retinal ganglion cells during development. J Neurosci 19:7007-7024.
Upton AL, Ravary A, Salichon N, Moessner R, Lesch KP, Hen R, Seif I, Gaspar P (2002) Lack of 5-HT(1B) receptor and of serotonin transporter have different effects on the segregation of retinal axons in the lateral geniculate nucleus compared to the superior colliculus. Neuroscience 111:597-610.
Vallender EJ, Pearson NM, Lahn BT (2005) The X chromosome: not just her brother's keeper. Nat Genet 37:343-345.
Valtschanoff JG, Weinberg RJ (2001) Laminar organization of the NMDA receptor complex within the postsynaptic density. J Neurosci 21:1211-1217.
Valtschanoff JG, Burette A, Davare MA, Leonard AS, Hell JW, Weinberg RJ (2000) SAP97 concentrates at the postsynaptic density in cerebral cortex. Eur J Neurosci 12:3605-3614.
Van der Loos H (1976a) Neuronal circuitry and its development. Prog Brain Res 45:259-278.
Van der Loos H (1976b) Barreloids in mouse somatosensory thalamus. *Neurosci Lett* 2:1-6.
Van der Loos H, Woolsey TA (1973) Somatosensory cortex: structural alterations following early injury to sense organs. Science 179:395-398.
Van Sluyters RC, Stewart DL (1974) Binocular neurons of the rabbit's visual cortex: effects of monocular sensory deprivation. Exp Brain Res 19:196-204.
Van Zundert B, Yoshii A, Constantine-Paton M (2004) Receptor compartmentalization and trafficking at glutamate synapses: a developmental proposal. Trends in Neurosciences 27:428-437.
Vanderhaeghen P, Lu Q, Prakash N, Frisen J, Walsh CA, Frostig RD, Flanagan JG (2000) A mapping label required for normal scale of body representation in the cortex. Nat Neurosci 3:358-365.
Vazquez LE, Chen HJ, Sokolova I, Knuesel I, Kennedy MB (2004) SynGAP regulates spine formation. J Neurosci 24:8862-8872.
Vickers CA, Stephens B, Bowen J, Arbuthnott GW, Grant SG, Ingham CA (2006) Neurone specific regulation of dendritic spines in vivo by post synaptic density 95 protein (PSD-95). Brain Res 1090:89-98.
Viskochil D, Buchberg AM, Xu G, Cawthon RM, Stevens J, Wolff RK, Culver M, Carey JC, Copeland NG, Jenkins NA, et al. (1990) Deletions and a translocation interrupt a cloned gene at the neurofibromatosis type 1 locus. Cell 62:187-192.
Wade CM, Daly MJ (2005) Genetic variation in laboratory mice. Nat Genet 37:1175-1180.
Waite PM, Cragg BG (1982) The peripheral and central changes resulting from cutting or crushing the afferent nerve supply to the whiskers. Proc R Soc Lond B Biol Sci 214:191-211.
Waite PM, Li L, Ashwell KW (1992) Developmental and lesion induced cell death in the rat ventrobasal complex. Neuroreport 3:485-488.
Wallace MR, Marchuk DA, Andersen LB, Letcher R, Odeh HM, Saulino AM, Fountain JW, Brereton A, Nicholson J, Mitchell AL, et al. (1990) Type 1 neurofibromatosis gene: identification of a large transcript disrupted in three NF1 patients. Science 249:181-186.

Wang JQ, Fibuch EE, Mao L (2007) Regulation of mitogen-activated protein kinases by glutamate receptors. J Neurochem 100:1-11.
Wang YM, Gainetdinov RR, Fumagalli F, Xu F, Jones SR, Bock CB, Miller GW, Wightman RM, Caron MG (1997) Knockout of the vesicular monoamine transporter 2 gene results in neonatal death and supersensitivity to cocaine and amphetamine. Neuron 19:1285-1296.
Washbourne P, Thompson PM, Carta M, Costa ET, Mathews JR, Lopez-Bendito G, Molnar Z, Becher MW, Valenzuela CF, Partridge LD, Wilson MC (2002) Genetic ablation of the t-SNARE SNAP-25 distinguishes mechanisms of neuroexocytosis. Nat Neurosci 5:19-26.
Watabe AM, Zaki PA, O'Dell TJ (2000) Coactivation of beta-adrenergic and cholinergic receptors enhances the induction of long-term potentiation and synergistically activates mitogen-activated protein kinase in the hippocampal CA1 region. J Neurosci 20:5924-5931.
Watanabe E, Fujita SC, Murakami F, Hayashi M, Matsumura M (1989) A monoclonal antibody identifies a novel epitope surrounding a subpopulation of the mammalian central neurons. Neuroscience 29:645-657.
Watson RF, Abdel-Majid RM, Barnett MW, Willis BS, Katsnelson A, Gillingwater TH, McKnight GS, Kind PC, Neumann PE (2006) Involvement of protein kinase A in patterning of the mouse somatosensory cortex. J Neurosci 26:5393-5401.
Weliky M, Katz LC (1997) Disruption of orientation tuning in visual cortex by artificially correlated neuronal activity. Nature 386:680-685.
Welker E, Armstrong-James M, Bronchti G, Ourednik W, Gheorghita-Baechler F, Dubois R, Guernsey DL, Van der Loos H, Neumann PE (1996) Altered sensory processing in the somatosensory cortex of the mouse mutant barrelless. Science 271:1864-1867.
West JD, Frels WI, Chapman VM, Papaioannou VE (1977) Preferential expression of the maternally derived X chromosome in the mouse yolk sac. Cell 12:873-882.
West JD, Papaioannou VE, Frels WI, Chapman VM (1978) Preferential expression of the maternally derived X chromosome in extraembryonic tissues of the mouse. Basic Life Sci 12:361-377.
White EL, Weinfeld L, Lev DL (1997) A survey of morphogenesis during the early postnatal period in PMBSF barrels of mouse SmI cortex with emphasis on barrel D4. Somatosens Mot Res 14:34-55.
Wiesel TN, Hubel DH (1963a) Effects of Visual Deprivation on Morphology and Physiology of Cells in the Cats Lateral Geniculate Body. J Neurophysiol 26:978-993.
Wiesel TN, Hubel DH (1963b) Single-Cell Responses in Striate Cortex of Kittens Deprived of Vision in One Eye. J Neurophysiol 26:1003-1017.
Willard HF (2000) Genomics and gene therapy. Artificial chromosomes coming to life. Science 290:1308-1309.
Willatt L, Cox J, Barber J, Cabanas ED, Collins A, Donnai D, FitzPatrick DR, Maher E, Martin H, Parnau J, Pindar L, Ramsay J, Shaw-Smith C, Sistermans EA, Tettenborn M, Trump D, de Vries BB, Walker K, Raymond FL (2005) 3q29 microdeletion syndrome: clinical and molecular characterization of a new syndrome. Am J Hum Genet 77:154-160.

Williams BP, Price J (1995) Evidence for multiple precursor cell types in the embryonic rat cerebral cortex. Neuron 14:1181-1188.
Willshaw DJ, von der Malsburg C (1976) How patterned neural connections can be set up by self-organization. Proc R Soc Lond B Biol Sci 194:431-445.
Winder DG, Martin KC, Muzzio IA, Rohrer D, Chruscinski A, Kobilka B, Kandel ER (1999) ERK plays a regulatory role in induction of LTP by theta frequency stimulation and its modulation by beta-adrenergic receptors. Neuron 24:715-726.
Wintergerst ES, Vogt Weisenhorn DM, Rathjen FG, Riederer BM, Lambert S, Celio MR (1996) Temporal and spatial appearance of the membrane cytoskeleton and perineuronal nets in the rat neocortex. Neurosci Lett 209:173-176.
Wong RO (1999) Retinal waves and visual system development. Annu Rev Neurosci 22:29-47.
Wong WT, Sanes JR, Wong RO (1998) Developmentally regulated spontaneous activity in the embryonic chick retina. J Neurosci 18:8839-8852.
Wong WT, Myhr KL, Miller ED, Wong RO (2000) Developmental changes in the neurotransmitter regulation of correlated spontaneous retinal activity. J Neurosci 20:351-360.
Woolsey TA, Van der Loos H (1970) The structural organization of layer IV in the somatosensory region (SI) of mouse cerebral cortex. The description of a cortical field composed of discrete cytoarchitectonic units. Brain Res 17:205-242.
Woolsey TA, Dierker ML, Wann DF (1975) Mouse SmI cortex: qualitative and quantitative classification of golgi-impregnated barrel neurons. Proc Natl Acad Sci U S A 72:2165-2169.
Wu YP, Siao CJ, Lu W, Sung TC, Frohman MA, Milev P, Bugge TH, Degen JL, Levine JM, Margolis RU, Tsirka SE (2000) The tissue plasminogen activator (tPA)/plasmin extracellular proteolytic system regulates seizure-induced hippocampal mossy fiber outgrowth through a proteoglycan substrate. J Cell Biol 148:1295-1304.
Xu H, Tian N (2004) Pathway-specific maturation, visual deprivation, and development of retinal pathway. Neuroscientist 10:337-346.
Xu L, Anwyl R, Rowan MJ (1998) Spatial exploration induces a persistent reversal of long-term potentiation in rat hippocampus. Nature 394:891-894.
Xu S, Furukawa T, Kanai N, Sunamura M, Horii A (2005) Abrogation of DUSP6 by hypermethylation in human pancreatic cancer. J Hum Genet 50:159-167.
Xue J, Cooper NG (2001) The modification of NMDA receptors by visual experience in the rat retina is age dependent. Brain Res Mol Brain Res 91:196-203.
Yamaguchi Y (2000) Lecticans: organizers of the brain extracellular matrix. Cell Mol Life Sci 57:276-289.
Yamakado M (1985) [Postnatal development of barreloid neuropils in the ventrobasal complex of mouse thalamus: a histochemical study for cytochrome oxidase]. No To Shinkei 37:497-506.
Yao WD, Gainetdinov RR, Arbuckle MI, Sotnikova TD, Cyr M, Beaulieu JM, Torres GE, Grant SG, Caron MG (2004) Identification of PSD-95 as a regulator of dopamine-mediated synaptic and behavioral plasticity. Neuron 41:625-638.

Yarovaya N, Schot R, Fodero L, McMahon M, Mahoney A, Williams R, Verbeek E, de Bondt A, Hampson M, van der Spek P, Stubbs A, Masters CL, Verheijen FW, Mancini GM, Venter DJ (2005) Sialin, an anion transporter defective in sialic acid storage diseases, shows highly variable expression in adult mouse brain, and is developmentally regulated. Neurobiol Dis 19:351-365.

Yoshihara Y, Kawasaki M, Tamada A, Fujita H, Hayashi H, Kagamiyama H, Mori K (1997) OCAM: A new member of the neural cell adhesion molecule family related to zone-to-zone projection of olfactory and vomeronasal axons. J Neurosci 17:5830-5842.

Zhang H, Macara IG (2008) The PAR-6 polarity protein regulates dendritic spine morphogenesis through p190 RhoGAP and the Rho GTPase. Dev Cell 14:216-226.

Zhao C, Ma H, Bossy-Wetzel E, Lipton SA, Zhang Z, Feng GS (2003) GC-GAP, a Rho family GTPase-activating protein that interacts with signaling adapters Gab1 and Gab2. J Biol Chem 278:34641-34653.

Zhou XH, Brandau O, Feng K, Oohashi T, Ninomiya Y, Rauch U, Fassler R (2003) The murine Ten-m/Odz genes show distinct but overlapping expression patterns during development and in adult brain. Gene Expr Patterns 3:397-405.

Zhou ZJ (1998) Direct participation of starburst amacrine cells in spontaneous rhythmic activities in the developing mammalian retina. J Neurosci 18:4155-4165.

Zhu X, Lee HG, Raina AK, Perry G, Smith MA (2002) The role of mitogen-activated protein kinase pathways in Alzheimer's disease. Neurosignals 11:270-281.

Zhu Y, Parada LF (2001) Neurofibromin, a tumor suppressor in the nervous system. Exp Cell Res 264:19-28.

Zhu Y, Romero MI, Ghosh P, Ye Z, Charnay P, Rushing EJ, Marth JD, Parada LF (2001) Ablation of NF1 function in neurons induces abnormal development of cerebral cortex and reactive gliosis in the brain. Genes Dev 15:859-876.

Zuccotti M, Monk M (1995) Methylation of the mouse Xist gene in sperm and eggs correlates with imprinted Xist expression and paternal X-inactivation. Nat Genet 9:316-320.

Appendices

Appendix I

Table 3 PSD proteins: MAGUKs/Adaptors/Scaffolders

PSD Proteins identified my mass spectrophotometry and antibody methods.
Adapted from Laumonnier et al., 2007. Up-to-date information is available on the G2C database (http://www.genes2cognition/org/db.html) Proteins highlighted in bold are members of the NRC/MASC. Proteins underlined are located on X-chromosome. Proteins * are DLG genes (PSD-95 family).

MAGUKs/Adaptors/Scaffolders at the PSD	
With PDZ Domain(s)	**Without PDZ-domains**
ACZONIN/PCLO	AGRIN
CASK	**AKAP5**
CHAPSYN-110/PSD-93/DLG2*	**AKAP2**
DLGH2/MPP2	APPL
DLGH3/MPP3	ARGBP2/KIAA0777
GRIP1	BAIAP2
GRIP2	BEGAIN/KIAA1446
HOMER1	CASKIN1
HOMER3	CRIPT
MAGUIN/CNKSR2	DAP4/DLGAP4
MPP6	DLGAP2
PICK1/PRKCABP	EPS15R/EPS14L1
PROSAP2/SHANK3	FLOTILLIN-1
PSD-95/DLG4*	FLOTILLIN-2
SAP102/DLG3*	**GKAP/DLGAP1**
SAP97/DLG1*	GRB10
SHANK1	**GRB1**
SHARPIN	**JIP-1/MAPK8IP1**
ZO-1/TJP1	LIME/FLJ20406
ZO-2/TJP2	KCKAP1
	NBEA
	RACK1/GNB2L1
	RC3/DMXL2
	SH3KBP1
	SHC1
	SORBS1
	SOS1
	TRAF-3
	WDR6
	YOTIAO/AKAP9

Table 4 Electrophysiological defects in *Sap102* and *Psd-95* mutants

Experiments carried out in CA1 region of hippocampus in *Psd-95* and *Sap102* mutant mice.

Data taken from Migaud et al., 1998 & Cuthbert et al., 2007.

Experiment	***PSD-95***			***SAP102***		
	-/-	***Wild-type***	***Summary***	***-/y***	***Wild-type***	***Summary***
High frequency stimulation (NMDAR dependent) (2x100Hz pulses 1 second apart, compare % fEPSPs to baseline after 60 mins)	243 % (±18%)	194 % (± 9.3%)	-/- > +/+ by 49%	230 % (±, 20%)	204 % (± 13%)	-/- = +/+
High frequency stimulation, (6 x 100Hz every 5 mins, compare saturation levels of % fEPSPs to baseline)	298 % (± 39%)	175 % (± 14%)	-/- > +/+ by 123%	Not performed as no result above		
Low frequency stimulation, 900 pulses at 5Hz (ERK dependent)(compare % fEPSPs to baseline after 45 mins)	278 % (±17%)	127 % (± 7%)	-/- > +/+ by 152%	201 % (± 4%)	150 % (± 5%)	-/- > +/+ by 51%
Low frequency stimulation, 900 pulses at 1Hz (compare % fEPSPs to baseline after 90 mins)	180 % (± 22%)	82 % (±, 20%)	-/- > +/+ by 98%	Not performed		
Pairing of presynaptic fibre pulses with a single postsynaptic action potential (100 10Hz pulses 10sec apart, record EPSP after 30 mins)	Not performed			150%	100%	-/- > +/+ by 50%

Appendix II

X-inactivation mechanism

Initially female mammalian embryos have both X-chromosomes activated, and inactivation is thought to begin at 6.5 days post-coitum (d.p.c.), at the onset of gastrulation (Monk & Harper, 1979). Different somatic tissues undergo XCI at different stages, ending with the heart, notachord, cranial mesoderm and hindgut by 10 d.p.c (Tan et al., 1993). The Xi remains inactive throughout further somatic divisions, and only becomes reactivated in female germ cells as the cells enter meiosis. During XCI Xi takes on unusual characteristics. The associated histones of the chromosome are underacetylated (Jeppesen and Turner, 1993), and the cytosines in the CpG islands become uncharacteristically methylated (Heard et al., 1997). The Xi has a condensed appearance in interphase nuclei (Barr and Bertram et al., 1949) and undergoes DNA replication late in S-phase of the cell cycle (Taylor, 1960). A macoH2A1 histone is preferentially associated with the Xi (Costanzi and Pehrson, 1998). A gene named *XIST* (X-inactivated-specific transcripts) in humans and *Xist* in mice is responsible for XCI (Brown et al., 1991a, 1991b, 1991c, Brockdorff et al., 1991). The gene is located at the Xq13 region of the human chromosome, which contains the XIC (X-inactivation centre) (Mattei et al., 1981, Summitt et al., 1978) (see diagram 18 in Chapter 3 for locus). The region is homologous to the *Xce* locus in mice, which contains alleles affecting the choice of X-chromosome to be inactivated (Johnston et al., 1981, Rastan and Robertson et al., 1985). The *Xist* gene is non-coding, has no open reading frame and codes for a 17kb RNA of which 15kb is transcribed from Xi (Brockdorff et al., 1992). Prior to XCI, FISH studies show an isolated spot marking the Xist locus on the X-chromosome. When XCI begins the RNA expands to coat the entire Xi, and on the Xa the *Xist* RNA is switched off. The mechanism of function of *XIST* is still not fully understood but mutations of the gene in mice have provided some information. If the 5' end of the gene is mutated then inactivation still occurs, but the mutated X is never inactivated (Penny et al., 1996). If the 3'end is mutated, then the mutated X always undergoes inactivation (Clerc and Avner, 1998). Therefore the 3' end is required for 'counting' of X-chromosomes and receives the signal to become active. The 5' end must be intact for it to receive the signal to become inactivated. If the *Xist* gene is translocated to an autosome then some genes on that chromosome are silenced and it adopts the heterochromatic characteristics of the Xi (Lee and Jaenisch, 1997). However the silencing on the autosome is not complete, indicating that the chromatin of a particular chromosome facilitates spread of XCI. The silencing of *XIST/Xist* on the Xa may occur by DNA methylation of the minimal promotor, causing the 'blocking' of *XIST/Xist* activity (Norris et al., 1994, Ariel et al., 1995, Zuccotti et al., 1995).

The *Xce* (X-controlling element) causes X-inactivation to be non-random. The locus of *Xce* is between two genes; tabby (*ta*) and the phosphoglycerate kinase 1 gene (*pgk1*) and maps to within the region also containing *Xist* known to contain the Xic. Three alleles have been identified; Xce^a, Xce^b, Xce^c. If double heterozygote mice are made with each combination of the three genes, the X-chromosome carrying Xce^a is more likely to be inactivated than Xce^b, Xce^b is more likely to be activated than Xce^c, and Xce^a is more likely to be inactivated than Xce^c (Cattanach et al., 1972, Johnston et al., 1981). A fourth allele Xce^d is less well characterised (Cattanach et al., 1991). In humans a cysteine to guanine mutation in the XIST minimal promotor region was found in two unrelated families where females had an unusual skew in the extent of X-inactivation (Plenge et al., 1997). This suggests that alleles in humans may function in the same way as Xce^a, Xce^b & Xce^c in mice to ensure random X-inactivation occurs.

Appendix III

Table 5 Components of ECM

The addition of GAGs to the secreted proteins forms proteoglycans or glycoproteins, which then perform functions that may be specific to that cell, tissue or organ. Table shows summary of some ECM components.

ECM Components		
Proteoglycans	Glycoproteins	Non-collagenous proteoglycans
Heparan sulphate proteoglycans Chondroitin Sulphate proteoglycans Keratan sulphate proteoglycans	Antibodies Mucins Major histocompatability complex (MHC) components Hormones (FSH, LH, TSH, HCG, AF, EPO)	Hyaluronic Acid (Hyaluron) Collagen Fibronectin Elastin Laminin Vitronectin Thrombospondins Tenascins

Table 6 Listing CSPGs by structure.

Numbers in brackets refer to size of core protein (kDa) followed by number of GAG chains that can vary from 1-100. (adapted from Galtrey & Fawcett, 2007)

CSPGs in CNS				
Leticans	Phosphacan/RPTP	Small leucine-rich Proteoglycans	Part-time proteoglycans	Others
Aggrecan (221, 100) Versican V0 (370, 17-23) Versican V1 (262, 12-15) Versican V2 (180, 5-8) Neurocan (133, 3) Brevican (97, 0-5)	RPTP (253, 3-4) Phosphacan (173, 3-4)	Decorin (36, 1) Biglycan (38, 1-2)	Neuroglycan C (56, 3-5) Thrombomodulin (58, 1) Appican(L-APP) (75-83, 1)	NG2 (248, 0-3) CD44 (37, 1-4)

Table 7 **Results from Power Analysis**

Cat-315 and Cat-316 labelling in mutants. If observed trend continues then statistical significance will be reached when 'n' = number in third column. For the purposes of this study, the required 'n' to reach significance is considered 'reasonable' if it is below 10. Any number over that is not reasonable so no result is entered in the final column.

Experiment	Current 'n'	'n' required to reach a significant result	Result reached if trend continues
Cat-315 PNN density in *Mglur5* mutants	WT n=6 KO n=4	N=15	
Cat-316 PNN density in *Mglur5* mutants	WT n=6 KO n=4	N=23	
Cat-315 PNN density in *Plc*β-1 mutants	WT n=4 KO n=5	N=64	
Cat-316 PNN density in *Plc*β-1 mutants	WT n=4 KO n=5	N=107	
Cat-315 PNN density in *Syngap* mutants	WT n=2 HET n=4	N=21	
Cat-316 PNN density in *Syngap* mutants	WT n=2 HET n=4	N=39	
Cat-315 PNN density in *Prkar2b* mutants	WT n=4 KO n=4	Reached already p=0.02	WT > KO
Cat-316 PNN density in *Prkar2b* mutants	WT n=2 KO n=4	N=71	

When entering information into the program G*Power3 certain parameters are entered in order to compute the required sample size given mean and standard deviation. The 'power' of a test (or 1- β), where β is the probability of falsely accepting H0 when H1 is true. β is therefore the probability of the test indicating that there is not a significant difference between the two data sets when there is a difference. For this study, the power parameter entered was 0.8 (β=0.2). This is considered to be an appropriate standard for adequacy and is commonly used by researchers. It is important to note that in carrying out power analysis assumptions are made about the data. First, that it is normally distributed about the mean and second that the samples collected are representative of the population. For a mutant, this is not a minor assumption as there is no way to predict that data is normally distributed. In fact, sometimes it is skewed or bimodal. If enough data were collected to prove that data is normally distributed then it is likely that a t-test would show a significant difference between mutant and wildtype, should there be a difference. Therefore Power analysis has limited use and should only be used as a guide when a reasonable amount of data has been collected and t-tests show a p-value that is close to the significance level.

Table 8 Genes expressed in different layers of hippocampus

	Layers of Hippocampus				
Layer	Molecular Layer of Dentate Gyrus	Stratum Oriens	Stratum Radiatum	Stratum Lacunosum	Stratum Pyramidale (pyramidal cell layer)
Cat-315 present?	+ (P14) ++ (P21) ++ (Ad)	+ (P14) ++ (P21) ++ (Ad)	+ (P14) ++ (P21) ++ (Ad)	+ (P14) ++ (P21) ++(Ad)	- (P14) - (P21) - (Ad)
Molecule Present	Odz 1 (PWk 6)	Cln 5 (P60) Gfap (P40) Odz 4 (PWk 6) Slc17a5 (Adult)	Gfap (P40) Slc17a5 (Adult)	Odz3 (PWk 6) Sl 17a5 (PWk 6)	Cln5 (P14 & P60) Gfap (P40) Hspa5 (p14) Sil 1 (p14) Slc17a5 (Adult)

Numbers in brackets refer to age at which expression was detected. All results are taken from immunohistochemistry studies published *and* submitted to the MGI website, and so are not exhaustive of *all* expression data published. (Information taken from MGI website)

Glossary of genes:

- *Odz 1, Odz 3, Odz 4*

  Odd Oz/ten-m homolog 1,3,4 (Drosophila) (Zhou et al., 2003)
- *Cln 5.*

  Ceroid-lipofuscinosis, neuronal 5. (Holmberg et al., 2004)
- *Gfap*

  glial fibrilary acidic protein (McCall at al., 1996)
- *Slc17a5*

  Solute carrier family 17 (anion/sugar transporter) member 5. (Yarovaya et al., 2005)
- *Hspa5*

  heat shock protein 5 (Anttonen et al., 2005)
- *Sil 1*

Endoplasmic reticulum chaperone SIL1 homolog (Anttonen et al., 2005)

Glossary

AC	Adenyl cyclase
AMPA R	AMPA receptor
β-Gal	β-Galactosidase
cAMP	Cyclic adenosine 3’, 5’-monophosphate
CNS	Central nervous system
CSPG	Chondroitin-sulphate proteoglycan
DUSP6	Dual-specific phosphatase 6
ECM	Extra-cellular matrix
ERK1	Extra-cellular regulated kinase 1
ERK2	Extra-cellular regulated kinase 2
ES	Embryonic stem
ION	Infra-orbitol nerve
KO	Knock-out
LGN	Lateral geniculate nucleus
MAGUK	Membrane-associated guanylate kinase-like domain containing protein
MAPK	Mitogen-associated protein kinase
MAPKK	Mitogen associated kinase kinase
MD	Monocular deprivation
MGluR5	Metabotropic glutamate receptor 5
MR	Mental retardation
NF1	Neurofibromin 1
NLGN	Neuroligin
NMDA	N-methyl-d-aspartate
NMDAR	N-methyl-d-aspartate receptor
NR1	NMDAR subunit 1
NR2	NMDAR subunit 2
NR3	NMDAR subunit 3
OD	Ocular dominance
PKARIIβ	Protein kinase A regulatory subunit 2

PLCβ-1	Phospho-lipase-C β-1
PrV	5th principal nuclei of brainstem
PSD-93	Post-synaptic density protein 93 kDa
PSD-95	Post-synaptic density protein 95 kDa
RICS	RhoGAP Involved in the β-Catenin-N-Cadherin and NMDAR Signalling
SAP97	Synapse-associated protein 97 kDa
SAP102	Synapse-associated protein 102 kDa
SynGAP	Synaptic Ras-GTPase activating protein
TCA	Thalamo-cortical afferent
Vpm	Ventro-Posterior Medial (thalamus)
WT	Wild-type
Xa	Active X-chromosome
XCI	X-chromosome inactivation
Xi	Inactivated X-chromosome
XIST	X-inactivated specific transcripts
XLMR	X-linked mental retardation
Xm	Maternally inherited X-chromosome
Xp	Paternally inherited X-chromosome
Xce	X controlling element